TISSUE-SPECIFIC TRANSPLANTATION ANTIGENS: STRUCTURALLY UNIQUE ISOFORMS OF MHC-RELATED PROTEINS IN IMMUNOLOGICALLY TOLERANT MILIEUS

APPROVED BY SUPERVISORY COMMITTEE

Iwona Stroynowski, Ph.D.

Michael Bennett, M.D.

Lora Hooper, Ph.D.

Edward Wakeland, Ph.D.

Joan Stein-Streilein, Ph.D.

DEDICATION

To Dave, Jake and Mom

for your unwavering love and tremendous support

TISSUE-SPECIFIC TRANSPLANTATION ANTIGENS: STRUCTURALLY UNIQUE ISOFORMS OF MHC-RELATED PROTEINS IN IMMUNOLOGICALLY TOLERANT MILIEUS

by

PAULA ANN GUIDRY

DISSERTATION

Presented to the Faculty of the Graduate School of Biomedical Sciences

The University of Texas Southwestern Medical Center at Dallas

In Partial Fulfillment of the Requirements

For the Degree of

DOCTOR OF PHILOSOPHY

The University of Texas Southwestern Medical Center at Dallas

Dallas, Texas

November, 2008

ACKNOWLEDGEMENTS

I must start by thanking my advisor Dr. Iwona Stroynowski. When I came to UT Southwestern, I knew I wanted to study the immunology of MHC, but I didn't know it would be with such a brilliant scientist and devoted mentor. Iwona's perspective on her work and that of those in her laboratory is always insightful. I am often surprised by her scientific intuition and the creative directions that it takes her. She has very high standards for the quality and rigor of her work and that of her laboratory, and her publications are flawless. Iwona pours herself into her trainees, ensuring that they have the best possible preparation for their chosen vocation, whatever it may be. If I come away with half of what she has taught me, just in these past few months, my scientific career will be off to a very good start.

Many thanks to my dissertation committee members – Drs. Lora Hooper, Mike Bennett and Ward Wakeland. Their time, input and encouragement have been invaluable. A special note of thanks to my outside committee member, Dr. Joan Stein-Streilein, who has generously given her time to review my work here and participate in my defense.

This work has been made possible by our collaborators Drs. Lora Hooper and Carla Aldrich. I also wish to thank Drs. Jim Forman, Kirsten Fischer-Lindahl, Geri Brown, Judith Head and François Bonhomme for their valuable input. Technical support was provided by Angie Mobley, Anisa Ismail, Cassie Behrendt, Charles Nguyen, Anna-Marie Fairhurst and Dr. Akira Takashima.

There are many former lab members who have contributed to my work and who I am happy to call friends. Dr. Ming Chen, Sharmila Shanmuganad, Nora Renthal, Terry

Coursey, Jennifer McLean, Neethu Kumar, Van Johnson, Omar Haddad and Lacey Bingham have all participated one aspect or another of the work described here. I have also greatly benefited from conversations with Dr. Eugene Chiang, Dr. Piotr Tabaczewski and Maile Hensen. Thanks also to my second floor neighbors in the Forman, van Oers and Sperandio labs and my many other friends on the seventh floor and beyond.

In the Immunology Graduate Program I wish to thank Drs. Richard Scheuermann, Jerry Niederkorn, Nicolai van Oers and John Schatzle for their service as Program Chair during my tenure and Karen Kazemzadeh, Renee Gugino, Nancy McKinney and Kimberly Coleman for their administrative support. I'd also like to thank Dr. Nancy Street for recruiting me to UT Southwestern and Dr. Joel Oppenheim of NYU School of Medicine for directing me to Nancy when I told him, "New York is great; I just can't stand to live here."

There are many people who participated in my training before Iwona really whipped me into shape, and I'd like to briefly thank them here: Dr. David McMurray and his laboratory at Texas A&M University, Dr. Stan Vukmanovic at NYU School of Medicine, Drs. James Chen, David Karp, Mark Siegelman and Pila Estes at UT Southwestern and Dr. Max Summers and his laboratory (particularly Drs. Sharon Braunagel, German Rosas-Acosta and Shawn Williamson) at Texas A&M University.

I'd also like to give a personal note of thanks to my friends, church family and P.E.O. sisters for their love and support.

Lastly, I thank my family. Without their support I would never have come this far. My husband Dave and son Jacob brighten my every day. The constant support and help from my mother, Mary Ann Shawver, has been invaluable. I'm also grateful for the

love and support from my dad, Paul Shawver and step-mother, Karen, my siblings Ben Shawver, Byron Smith and Dr. Darci Smith, my in-laws Jack and Judy Mayer, Drs. Erin Guidry and Ian Mangion, and Jim and Dr. Maria Guidry and their daughter Ashley. Thanks also to my extended family, grandmother Julia Williams and John R., Paula and Mallory Williams. I am so grateful to have done my doctoral studies close to home so that I might be near you all. You have been my rock, and I love you all.

TISSUE-SPECIFIC TRANSPLANTATION ANTIGENS: STRUCTURALLY UNIQUE ISOFORMS OF MHC-RELATED PROTEINS IN IMMUNOLOGICALLY TOLERANT MILIEUS

PAULA ANN GUIDRY, Ph.D.

The University of Texas Southwestern Medical Center at Dallas, 2008

IWONA TERESA STROYNOWSKI, Ph.D.

The immune network of the small intestine must maintain tolerance to an immense and diverse community of commensal microorganisms and a broad array of dietary antigens while constantly at the ready for insult from a variety of infectious agents. Situated at the front lines of intestinal immune defense are intraepithelial lymphocytes (IEL), the largest population of T cells in the body whose functions are only recently beginning to be revealed. Key to unlocking the roles of these unique immune effectors in health and disease is a better understanding of the receptor/ligand interactions

that instruct their education, maintenance and reactivity. Many lines of evidence investigating the identity and function of IEL ligands point to molecules of the nonclassical class I major histocompatibility complex (MHC). We describe here five nonclassical, or class Ib, MHC – H2-Bl, Tw5, Q1, Q2 and T3 – that are transcriptionally restricted to cells of the intestinal epithelium, in close association with IEL. Canonical and alternatively spliced transcripts of these class Ib MHC encode protein products that can be expressed at the cell surface and nonamer peptides capable of associating with the CD94/NKG2A inhibitory receptor ligand Qa-1. We and others have demonstrated that, in addition to αβ and γδ TCR, IEL are capable of expressing natural killer (NK) cell activating and inhibitory receptors including CD94/NKG2A, NKG2D, Ly49E and Ly49F. Thus, multiple products of gut-restricted class Ib MHC are positioned to associate with class I MHC-engaging T cell and NK cell receptors expressed by IEL. Since the intestine is not the only organ that must balance immune reactivity and tolerance, we wondered if tissue-specific class Ib MHC expressed in other tolerance-associated or immune privileged tissues have similar properties to gut-specific class Ib MHC. We found that liver-restricted Q10 and brain-expressed Q5, like gut-restricted class Ib MHC and human placental HLA-G, are also extensively alternatively spliced and encode nonamer peptides capable of engaging Qa-1. We postulate that these properties of tissue-specific class Ib MHC are critical to MHC-mediated tolerance induction and/or maintenance in tolerance-associated tissues.

TABLE OF CONTENTS

PRIOR PUBLICATIONS AND PRESENTATIONS

The following is list of prior publications/presentations of work presented in this dissertation:

Publications

Paula A. Guidry and Iwona Stroynowski (2005). The Murine Family of Gut-Expressed Class Ib MHC Includes Alternatively Spliced Isoforms of the Proposed HLA-G Homolog "Blastocyst MHC." *Journal of Immunology* 175: 5248-5259.

Oral Presentations

Paula Guidry and Iwona Stroynowski (2004). Nonclassical MHC Class I and Small Intestinal Mucosal Immunity. UT Southwestern Center for Immunology Retreat, Dallas, TX.

Paula Guidry and Iwona Stroynowski (2007). Poised for Interaction: Expression of Gut-Specific Class Ib MHC and T/NK Cell MHC Ligands in the Intestinal Epithelium. UT Southwestern Immunology Graduate Program Scientific Retreat, Dallas, TX.

Major Conference Presentations

Paula Guidry and Iwona Stroynowski (2004). The Murine Family of Gut-Expressed Class Ib MHC Includes Alternatively Spliced Isoforms of the Proposed HLA-G Homolog "Blastocyst MHC." 12th International Congress of Immunology, "Nonclassical MHC Recognition" Minisymposium, Montréal, Québec, Canada.

Poster Presentations

Paula Guidry and Iwona Stroynowski (2003). Nonclassical MHC Class I and Small Intestinal Mucosal Immunity. UT Southwestern Immunology Graduate Program Retreat, Parker, TX

Paula Guidry and Iwona Stroynowski (2003). Nonclassical MHC Class I and Small Intestinal Mucosal Immunity. UT Southwestern Graduate Student Poster Session, Dallas, TX

Paula Guidry and Iwona Stroynowski (2004). The Murine Family of Gut-Expressed Class Ib MHC Includes Alternatively Spliced Isoforms of the Proposed HLA-G Homolog "Blastocyst MHC." Midwinter Conference of Immunologists, Asilomar Conference Center, Monterey, CA

Paula Guidry and Iwona Stroynowski (2004). The Murine Family of Gut-Expressed Class Ib MHC Includes Alternatively Spliced Isoforms of the Proposed HLA-G Homolog "Blastocyst MHC." 12th International Congress of Immunology, Antigen Processing and Presentation II Poster Session, Montréal, Québec, Canada

Paula Guidry and Iwona Stroynowski (2005). The Murine Family of Gut-Expressed Class Ib MHC Includes Alternatively Spliced Isoforms of the Proposed HLA-G Homolog "Blastocyst MHC." UT Southwestern Immunology Graduate Program Retreat, Dallas, TX

LIST OF FIGURES

LIST OF TABLES

LIST OF APPENDICES

LIST OF DEFINITIONS

The following list does not include standard abbreviations published in the first issues of each volume of The Journal of Immunology.

α-MSH	α-melanocyte stimulating hormone
aLAK	adherent lymphokine activated killers
APC	antigen presenting cell; allophycocyanin
ARP	apolipoprotein repressor protein
ATF	activating transcription factor
β_2m	beta$_2$-microglobulin
Bl	blastocyst
CHO	Chinese hamster ovary
COUP	chicken ovalbulin upstream promoter
CYT	cytoplasmic tail
DC	dendritic cell
DETC	dendritic epithelial T cell
dNK	decidual natural killer
diH_2O	deionized water
ΔRn	change in normalized reporter signal
EF2	elongation factor 2
EGFR	epidermal growth factor receptor
EM	extraction medium
EnhA	Enhancer A

EnhB	Enhancer B
EPCR	endothelial protein C receptor
ER	endoplasmic reticulum; estrogen receptor
ETF	EGFR-specific transcription factor
ex	exon
fabpi	intestinal fatty acid binding protein gene
FcRn	neonatal Fc receptor
GATA	GATA-binding protein
GM	GM-CSF-transduced B78H1 melanoma
GR	glucocorticoid receptor
H1	B78H1 melanoma
H60	minor histocompatibility antigen 60
HFE	hemochromatosis gene
hsp	heat shock protein
Id2	inhibitor of DNA binding 2
IEC	intestinal epithelial cell
IEL	intraepithelial lymphocyte
ILT	immunoglobulin-like transcript
iNKT	invariant natural killer T
int	intron
IRES	internal ribosomal entry site
IRF	interferon regulatory factor
ISRE	interferon-stimulated response element

KIR	killer cell immunoglobulin-like receptor
L	leader peptide
LAK	lymphokine activated killer
LB	Luria-Bertani
LMP	low molecular weight protein
LSM	lymphocyte separation medium
MAIT	mucosal associated invariant T
MBP	MHC binding protein
MCS	multiple cloning site
mdr	multi-drug resistance gene
MICA	MHC class I-related sequence A
MICB	MHC class I-related sequence B
MID	mean internal density
MIF	migration inhibitory factor
MLN	mesenteric lymph node
MR1	MHC class I-related sequence 1
MRP	multidrug resistance-associated protein
MULT	murine ULBP-like transcript
PIR	paired immunoglobulin-like receptor
pMHC	peptide/MHC complex
PU.1	purine-box binding factor 1
PVDF	polyvinylidene fluoride
Qdm	Qa-1 determinant modifier

qPCR	quantitative polymerase chain reaction
RA	retinoic acid
RAET	retinoic acid early transcript
RAR	retinoic acid receptor
RXR	retinoid X receptor
SAGE	serial analysis of gene expression
SOEing	“splicing” by overlap extension
SRF	serum response factor
T3R	thyroid hormone receptor
TL	thymus leukemia
TM	transmembrane
ULBP	UL binding protein
USF	upstream stimulatory factor
UTR	untranslated region
VIP	vasoactive intestinal peptide
WT	Wilms tumor
Znα2gp	zinc-binding α2 glycoprotein

CHAPTER ONE

Introduction

The primary organ responsible for digestion and nutrient absorption in mammals is the small intestine. Populated with an immense and diverse community of commensal microorganisms and under a constant barrage of dietary antigens, the intestine must maintain a state of immune tolerance while always on the alert for pathogenic infection. To achieve this critical balance, the small intestine is home to a vast, complex immune network whose many functions have only recently begun to be explored. Here we will review the current understanding of a major component of the intestinal immune system, the intraepithelial lymphocytes (IEL), highlighting potential receptor/ligand interactions that may contribute to their function in the gut, the main focus of this thesis.

Anatomy and Immunological Functions of the Mammalian Intestine

The small intestine is a coiled tube that extends from the pylorus at the distal end of the stomach to the ileocaecal valve at the proximal end of the large intestine (Figure 1.1A). It is composed of three sections: (from the pylorus) the duodenum, the jejunum, and the ileum. The short, curved duodenum encircles the head of the pancreas as it extends from the stomach to the jejunum. From here, the remainder of the small intestine, the jejunum and the ileum, winds through the abdomen until it joins with the large intestine at the ileocaecal valve. Though functionally and macroscopically distinct,

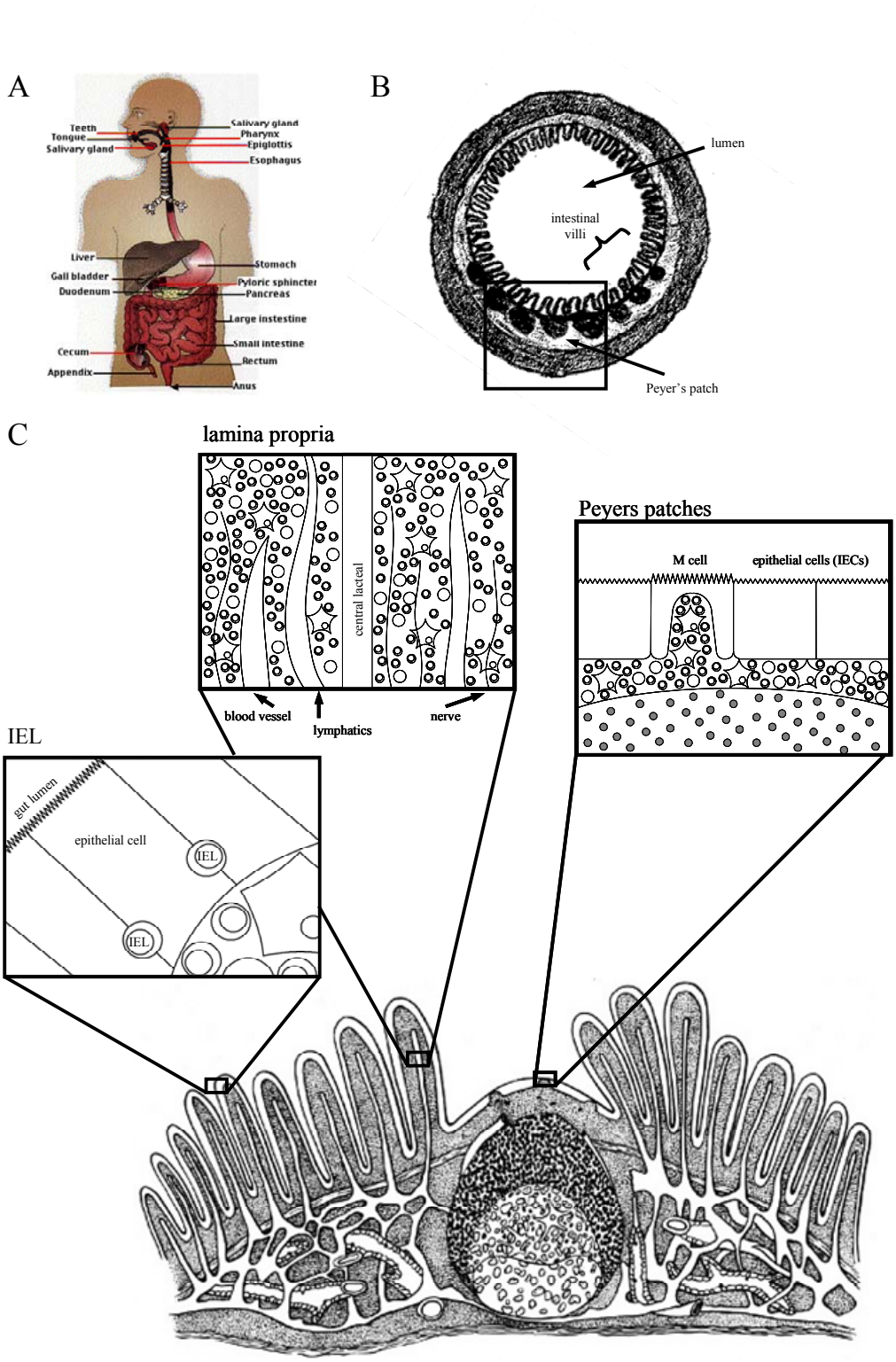
A
Teeth
Tongue
Salivary gland
Salivary gland
Pharynx
Epiglottis
Esophagus
Liver
Gall bladder
Duodenum
Stomach
Pyloric sphincter
Pancreas
Large instestine
Small intestine
Cecum
Rectum
Appendix
Anus
B
lumen
intestinal villi
Peyer's patch
C
lamina propria
central lacteal
blood vessel
lymphatics
nerve
Peyers patches
M cell
epithelial cells (IECs)
IEL
gut lumen
epithelial cell
IEL
IEL

Figure 1.1 Immunological architecture of the small intestine. A. Organs of the human digestive tract. Image from Kimball's Biology Pages (1). B. Cross-sectional view of the small intestine. The luminal surface of the gut is comprised of crypt/villus units which are overlaid by a single cell layer of absorptive epithelium. Peyer's patches (left) are unencapsulated lymphoid follicles that resemble lymph nodes. These structures extend from just beneath the epithelium through the submucosa. C. Immunological compartments of the small intestine. Peyer's patches are overlaid by specialized follicle-associated epithelium containing M cells, which transcytose intact antigens to basolateral DC. The lamina propria forms the cores of the villi and is densely populated by $CD4^+$ IL-10/TGF-β-secreting plasma cells and DC, which can extend their dendrites through the epithelial monolayer to sample luminal antigens. The intestinal epithelium is populated by predominantly $CD8^+$ intraepithelial lymphocytes (IEL) which are tethered to intestinal epithelial cells (IEC) by $\alpha_E\beta_7$ integrin interaction with IEC-expressed E-cadherin (CD103). Modified from Dr. Art Anderson (2).

the jejunum and ileum have no definite boundary relative to one another, instead gradually transitioning from one into the other. The winding small intestine is joined to the back abdominal wall by the mesentery, which houses intestinal nerves, vasculature and lymphatics (3).

A cross-sectional view of the small intestine reveals a luminal architecture of crypt/villus units overlaid by a single cell layer of absorptive epithelium (Figures 1.1B and C) (3). Intestinal epithelial cells (IEC) consist predominantly of villus-associated enterocytes, interspersed with mucus-secreting goblet cells and neuropeptide-producing enteroendocrine cells, and crypt-associated paneth cells, which synthesize an array of antimicrobial, digestive and growth factors (3). Originating from multipotent stem cells situated four to five cell strata beneath the crypt base, epithelial progenitors differentiate into one of the three villus lineages as they migrate apically and into paneth cells as they travel to the crypt base (4). This migration/differentiation program is rapid and continuous, generating a constant supply of new enterocytes at the villus base which migrate to the apex and are shed in a matter of 2-5 days (5). Directly underneath the

intestinal epithelium lies the lamina propria, a compact, elastin-rich layer of connective tissue that provides mechanical support for the barrier cells above and forms the cores of the villi. Beneath this lie several vascularized, innervated layers of connective tissue and smooth muscle which form the remaining architecture of the small intestine (3).

The intestine is the most evolutionarily ancient organ, having arisen with the first multicellular animals. Situated directly under the intestinal epithelium in the primordial gut, macrophage-like lymphoid cells developed to defend against foreign invaders (6). Today, a diverse and complex gut-associated immune network functions in both intestinal defense against pathogens and tolerance to a co-evolved luminal microflora and dietary antigens. Key immunological players in the mammalian intestine include dendritic cells (DC) (7), professional antigen presenting cells (APC) that initiate the adaptive immune response, plasma cells, B cells that secrete immunoglobulins (Igs), predominantly IgA (7, 8), $CD4^+$ T cells, lymphocytes (7) that respond to antigenic challenge by producing pro- or anti-inflammatory cytokines, and $CD8^+$ T cells that express either the αβ or the γδ T cell receptor (TCR) and either the CD8αβ heterodimeric co-receptor or the CD8αα homodimer (7, 9) and whose proposed functions will be addressed in detail below. The tolerance-dominated environment of the gut is established, maintained, and, when necessary, breached by innate and adaptive immune effectors in four major immunological compartments that are specific to the gut: Peyer's patches – unencapsulated lymph node-like structures that are overlaid by specialized follicle-associated epithelium which samples luminal contents for recognition by underlying immune effectors; mesenteric lymph nodes (MLN) – regional lymph nodes of the intestine housed within the connective mesentery; lamina propria – home to

immunoregulatory $CD4^+$ T cells and IgA-secreting plasma cells; and intestinal intraepithelial lymphocytes (IEL) – a pool of predominantly $CD8^+$ T cells that is interdigitated between cells of the absorptive epithelium (7) (Figure 1.1C).

Residing in the lamina propria and Peyer's patches intestinal DC are a key player in intestinal immune tolerance and reactivity (10, 11). These cells sample regional intestinal commensals both by accepting intact microorganisms from Peyer's patch associated epithelium (12) and by extending dendritic processes from the lamina propria directly into the lumen of the gut (13). Loaded with non-pathogenic, non-invasive commensal bacteria, DC migrate either to Peyer's patch germinal centers and/or to the MLN without undergoing full maturation (7, 14). Here, these DC present antigen to naïve T and B cells, inducing their maturation into interleukin-10 (IL-10) and transforming growth factor-β (TGF-β)-secreting $CD4^+$ T cells and IgA-producing plasma cells (15-17). Instructed by the DC, these lymphocytes then follow the efferent lymphatics where they enter the blood supply at the thoracic duct and make their way back to the lamina propria where they help maintain a tolerogenic milieu (18-21). Under inflammatory conditions, regional DC arrive in the MLN as mature APC, inducing the activation of, among other effectors, $CD8^+$ cytotoxic T lymphocytes (CTL) which traffic back to the lamina propria and interdigitate into the epithelial monolayer (22, 23). Here these effector memory T cells join a resident natural memory T cell population that is present from birth (24). Together these enigmatic lymphocytes are the IEL.

Intestinal Intraepithelial Lymphocyes

IEL are predominantly $CD8^+$ T cells that reside at the basolateral junctions of IEC in the epithelial monolayer (25). Relatively long-lived with respect to their associated epithelial cells, IEL can have a half-life of three weeks or longer (26). This suggests that the same IELs survey many passing IEC in their lifetimes. IEL constitute 1 in 10 to 1 in 5 of the cells in the intestinal epithelium (27) and account for about half of peripheral lymphocytes in the body (50 to 100 million cells in the mouse) (28). Still, little is known about the function of this immense population of immune effectors.

All IEL have a unique "partially activated" phenotype, displaying a subset of effector/memory markers, including the T cell early activation marker CD69 (29-31), yet they do not express other activation markers, like OX40, Ly-6C or the costimulatory molecule ICOS, unless stimulated through the TCR subunit CD3 (32). Even IEL from gnotobiotic mice express CD69 (33), despite the absence of antigen priming. Thus, IEL acquire an antigen-experienced phenotype without encountering foreign antigen.

IEL constitutively synthesize large cytolytic granules and are directly cytotoxic *ex vivo* (34-37). This and their close association with epithelial cells, which are frequently targeted for infection by intestinal pathogens, has led to the hypothesis that IEL provide the first line of defense against infected or transformed cells. When stimulated through CD3, IEL elaborate cytokines but do not proliferate (38), a phenotype that likely protects the integrity of the epithelial barrier but renders IEL difficult to study *in vitro*. Because they are cytotoxic *ex vivo* but do not normally kill *in situ*, and because they produce cytokines in response to proinflammatory stimuli but do not proliferate, IEL have been characterized as "activated but resting." The acquisition and maintenance of this unusual phenotype, however, are not well understood. Like other innate T cell

effectors in the intestine (iNKT [invariant natural killer T] cells (39) and MAIT [mucosal associated invariant T] cells (40)), IEL express an oligoclonal set of TCRs (41). Importantly, the nature of the antigen(s) that propagate this restricted IEL repertoire are not currently known. In order to address this and many other questions we turn to the mouse model.

Major Subsets of IEL in Mice

While individual IEL share many common phenotypical characteristics with one another, the IEL population is actually quite diverse. IEL can be broadly characterized into two types (25, 42): conventional, effector memory TCR$\alpha\beta^+$ CD8$\alpha\beta^+$ T cells, sharing many features with peripheral, thymically educated T cells that recirculate through the blood and lymph and orchestrate immune responses against pathogens (41, 43), and unconventional, gut-specific, natural memory TCR$\alpha\beta^+$ or TCR$\gamma\delta^+$ lymphocytes (25, 41), which are CD8$\alpha\alpha^+$ or CD8$^-$ (44) and whose function is poorly understood. While the populations of these cells vary from species to species (25, 45) and along the cephalocaudal axis of the gastrointestinal tract (46, 47), IEL of the rodent small intestine are ~80-90% CD8$\alpha\alpha^+$ or CD8$\alpha\beta^+$. The remaining cells are CD4$^-$ CD8$^-$, CD4$^+$ CD8$^+$ or CD4$^+$ CD8$^-$ (32). Each of these subpopulations of IEL is thought to contribute to unique functions in the epithelial monolayer, including immunotolerance, pathogen response, wound repair and both propagation and control of autoimmunity (25).

Conventional TCR$\alpha\beta^+$ CD8$\alpha\beta^+$ IEL

Conventional TCR$\alpha\beta^+$ CD8$\alpha\beta^+$ IEL are descendents of naïve T cells that have undergone positive and negative selection program in the thymus and are found in many peripheral organs (24, 43). The TCR ligands for these conventional IEL are class Ia or "classical" members of the major histocompatibility complex (MHC), highly polymorphic molecules that bind a diverse array of endogenous self and non-self peptides for presentation to CD8$^+$ T cells. Upon antigenic challenge in the Peyer's patches or mesenteric lymph nodes, resident DC activate and instruct CD8$^+$ and CD4$^+$ T cells to upregulate integrins, including LFA-1 (leukocyte function-associated antigen-1), VLA-1 (very late antigen-1) and $\alpha_4\beta_7$ integrin, and chemokine receptors like CCR9, CCR6, CCR5 and CXCR3 (48-53) and thus direct these nascent IEL to the lamina propria. Expressing $\alpha_E\beta_7$ integrin, conventional IEL can cross the intestinal basement membrane and bind E-cadherin, tethering these effectors to the intestinal epithelium (54). Here, they demonstrate potent and immediate antigen-specific reactivity against an array of pathogens, including dsDNA, dsRNA and ssRNA viruses, gram positive bacteria and various parasitic protozoa (55-66).

Unlike peripheral CD8$^+$ T cells, conventional IEL have an oligoclonal TCR repertoire that is thought to be progressively reshaped by repeated antigen stimulation (25, 41, 67-69). While the small intestinal epithelium is the main residence of conventional TCR$\alpha\beta^+$ CD8$\alpha\beta^+$ IEL, cells with similar TCRβ clonotypes can be found in the lamina propria and in circulation (43). Conventional IEL are similarly found in the large intestine, where they are more numerous than unconventional IEL and include a higher percentage of CD4$^+$ cells than in the small intestine (25, 70).

Unconventional IEL

TCRαβ$^+$ CD8αα$^+$ and TCRγδ$^+$ IEL are the two most abundant populations of T cells in mice (6, 41, 42) yet their functions are little understood. These cells constitute the majority of the IEL population from birth through young adulthood (71, 72) (while conventional IEL arrive at the epithelial monolayer as they encounter foreign antigen and are directed to the intestine (25)). Permanent residents of the intestine, unconventional IEL are not found outside of the IEL compartment and are the most concentrated in the small intestine, with far fewer in the colon (25, 70). Intriguingly, TCRαβ$^+$ CD8αα$^+$ and TCRγδ$^+$ IEL share more in common with each other than either does with TCRαβ$^+$ CD8αβ$^+$ IEL (73), yet their lineage relationship remains unknown.

Unconventional IEL are thought to be predominantly educated in the thymus (22), though a low level of extrathymic education also occurs in normal mouse cryptopatches, aggregates of c-kit$^+$ IL-7R$^+$ Thy$^+$ CD3$^-$ B220$^-$ lymphoid cells in the crypt lamina propria (6). Thymic selection of unconventional IEL is believed to generate self-reactive, oligoclonal T cells with a memory phenotype that is imprinted on them during their selection/education in early development, and does not reflect an encounter with foreign antigen as with conventional IEL (25). Unconventional IEL lack or have low expression levels of many common T cell markers, including Thy-1, CD28 and CD2 and utilize FcεRγ as part of their CD3 signal transduction pathway (74-80). These cells elaborate a paradoxical transcriptome, including both activating and inhibitory-associated gene activity (81). This “activated but resting” phenotype includes transcription of

granzymes A and B and Fas ligand, involved in cell-mediated cytolysis, and lymphotactin and macrophage migration inhibitory factor (MIF), soluble factors that regulate CTL activity (81, 82).

Conditioned by the unique gut milieu, which, in the normal, healthy intestine includes abundant retinoic acid, produced by resident DC (83), and tolerogenic TGF-β and IL-10, produced by IEC, DC, $CD4^+$ lamina propria T cells and the IEL themselves (84), unconventional IEL remain quiescent in the antigen-rich environment of the gut (25). Though they are capable of cytotoxicity, exhibiting NK cell-like antigen independent killing and antibody-dependent cell mediated cytotoxicity directly *ex vivo* (85), it appears that these cells promote tolerance in the gut by suppressing their own cytotoxicity and the activation of conventional IEL (25). The mechanisms by which they develop, mature, are activated and/or induce/maintain tolerance, however, are still largely unknown. Importantly, the self ligands responsible for their thymic/extrathymic education and for their maintenance and reactivity in the epithelial monolayer remain unidentified.

TCRγδ$^+$ IEL

A major, but still enigmatic population of unconventional IEL is the γδ T cell. TCRγδ$^+$ IEL, which constitute 35-65% of all IEL in the small intestine of healthy mice (42), can serve a cytotoxic and/or regulatory role in different immunological contexts (25). Under conditions of stress, human γδ IEL can mediate the destruction of IEC expressing MICA (MHC class I-related sequence A) and MICB (86), *Mhc*-encoded class I-like molecules in the human that do not bind peptides or the class I light chain, β_2-

microglobulin (β_2m) (87, 88). Acting in a regulatory capacity, TCR$\gamma\delta^+$ IEL can limit the pathology of conventional IEL-mediated inflammation by controlling conventional IEL activity in response to infection (89) and in celiac disease (44). γδ IEL also participate in the tissue repair response by elaborating growth factors in response to damage (25, 89, 90).

It has often been speculated that, functionally and developmentally, γδ IEL resemble invariant innate immune effectors like iNKT and MAIT cells. iNKT cells mediate immune activation and regulation via the class I-like molecule CD1d (91) while MAIT recognize the MHC class I-related (MR1) molecule in the presence of B cells and an intestinal flora (40). Like these innate T cells, γδ IEL have a restricted TCR repertoire and elaborate cytokines upon induction (25). Like iNKT and MAIT cells, it is thought that γδ IEL may undergo strong agonist selection in the thymus, though this concept is still controversial as no evidence has been presented in its support (25). Rare subpopulations of TCR$\gamma\delta^+$ IEL undergo expansion under activating conditions. In one example of this, a TCR$\gamma\delta^+$ CD8$\alpha\beta^+$ IEL population in the mouse has been shown to expand in response to *Salmonella* infection (92), though whether this response is inflammatory or regulatory remains to be determined. Unlike MAIT cells, however, which require commensal flora for their selection and maintenance, γδ IEL are present in the germ-free intestine (93) and are thought to bind self-ligands on infected, diseased or stressed cells to initiate their physiological (cytotoxic, regulatory and/or repair) responses (25). While it is known that MAIT and iNKT cells are restricted by evolutionarily conserved class I related molecules (MR1 and CD1d, respectively), the natural ligand(s)

for γδ IEL remain unknown. The parallels between γδ and iNKT/MAIT cells suggest that as yet unidentified class I MHC may also serve as their restricting elements.

The thymic differentiation program of tissue-specific γδ IEL is sequential, with skin dendritic epithelial T cells (DETC) emerging earliest in fetal development, lung, reproductive tract and tongue γδ T cells arising next in the early fetus, and IEL and peripheral γδ cells differentiating in the late (mouse embryonic day 15-16) fetus and young adult (94). Despite their concurrent education with peripheral, polyclonal γδ T cells, γδ IEL have a highly restricted repertoire, preferentially using Vγ5 and Vγ1.1 with diverse junctional sequences and multiple Vδ. This is similar to other tissue-specific γδ IEL, like DETCs, though γδ IEL utilize a less restricted TCR than DETCs, suggesting that they are selected by and can interact with more ligands (95).

Only one case of a γδ TCR interacting ligand has been characterized in detail, the murine class Ib MHC protein T10/T22, which is recognized by a very small sub-population of peripheral γδ T cells (0.1-1%) (96). Class Ib, or "nonclassical" class I MHC, differ from class Ia, or classical class I MHC, in that they are minimally polymorphic and are rarely involved in presentation of pathogens to conventional $CD8^+$ T cells. T10/T22 is a ubiquitously expressed, interferon-γ (IFN-γ)-inducible class Ib MHC that has an occluded antigen binding cleft and does not bind peptides (97). Unlike the αβ TCR, which recognizes the peptide binding surface of MHC, the γδ TCR that is specific for T10/T22 engages these class Ib ligands in a manner similar to antibody recognition of antigen, focusing on the exposed β sheet floor and α1 helix (98, 99). It is not known currently if other class I-like structures serve as recognition elements for the γδ TCR and if the recognition mode of the T10/T22-specific γδ TCR is typical of this class of T cell

receptors. γδ T cell clones that directly recognize foreign, stress-induced or tumor-expressed antigens have also been identified (100-105), but it is not clear if the γδTCR or another receptor engages these ligands. Thus, the dominant ligand(s) of the oligoclonal γδ T cell population, either in the periphery or in the IEL compartment, remain unknown.

The T10/T22 model and the class I-related restricting elements for iNKT and MAIT cells suggest that other class Ib MHC expressed in the intestinal epithelium might serve as ligands for the γδ TCR on IEL. Interestingly, γδ IEL are present in $\beta_2m^{-/-}$ mice (106), suggesting that, if one or more class Ib MHC is recognized by the γδ IEL TCR, it/they assume MIC-like, β_2m-free structures. Particular class I MHC candidates, however, have yet to be identified. Are they inducible? Do they complex with pathogenic and/or self peptides? Do they convey stress signals or something else? These are key questions in γδ IEL immunology today.

TCRαβ$^+$ CD8αα$^+$ IEL

The other major unconventional IEL population, which constitutes ~20-30% of all IEL in the small intestine of healthy mice (about half of all TCRαβ$^+$ IEL), is composed of TCRαβ$^+$ CD8αα$^+$ T cells (41). Like γδ IEL, little is known about this abundant component of the IEL repertoire. They are similarly directly cytotoxic *ex vivo* and seed the gut early in life (34-37, 107, 108). Like Foxp3$^+$ regulatory T cells and iNKT cells, TCRαβ$^+$ CD8αα$^+$ IEL are thought to require strong agonist interaction for positive selection in the thymus and are autoreactive (22, 25, 109). As a consequence of their thymic selection, these unconventional IEL upregulate CD8αα, a marker of their mature phenotype (25). As touched upon before, TCRαβ$^+$ CD8αα$^+$ IEL also express a mixture of

inhibitory and activating genes, including those supportive of cytotoxic functions and others supporting regulatory/tolerizing functions.

TCRαβ$^+$ CD8αα$^+$ IEL express an oligoclonal TCR repertoire that is non-overlapping with that of conventional IEL (41, 43). The TCR ligands for TCRαβ$^+$ CD8αα$^+$ IEL remain largely unknown, but important evidence suggests that they belong to the class I MHC family. TCRαβ$^+$ CD8αα$^+$ IEL are absent in the intestines of $\beta_2m^{-/-}$ mice (110, 111), but are present in class Ia MHC deficient $K^{b-/-}D^{b-/-}$ and in class I-related $CD1^{-/-}$ animals (112), Hence, one or more β_2m-associating class Ib MHC is/are required for their presence in the gut. This population of IEL are present in $TAP^{-/-}$ mice, but at substantially lower numbers than in wild type animals (111, 112). (TAP is the transporter associated with antigen processing, the molecule responsible for trafficking cytosolic peptides into the lumen of the endoplasmic reticulum [ER] where they can be loaded into the class I MHC peptide binding groove (113-116).) The reduced presence of TCRαβ$^+$ CD8αα$^+$ IEL in $TAP^{-/-}$ mice suggests that both TAP-independent and TAP-dependent recognition elements contribute to the selection and maintenance of these cells. All gut-expressed class Ib MHC are potential ligands for the TCRs of TCRαβ$^+$ CD8αα$^+$ IEL. Two have been extensively studied in this context: TL and Qa-2. TL (encoded by the murine T-region genes *H2-T3* and *H2-T18*) does not bind peptides (117), is expressed by IEC (118), and is a known ligand for CD8αα (38) but not for the IEL TCR. Qa-2 is a ubiquitously expressed, peptide binding class Ib MHC (119) found on IEC (120), whose presence in the genome augments TCRαβ$^+$ CD8αα$^+$ IEL counts in the intestines of mice (121). To date neither TL nor Qa-2 has been demonstrated to directly associate with any IEL TCR. Thus, in addition to TL and Qa-2 it is likely that other, as yet undetermined,

TAP-dependent as well as TAP-independent, gut-expressed class Ib MHC restrict the oligoclonal repertoire of TCR$\alpha\beta^+$ CD8$\alpha\alpha^+$ IEL TCR. The quest to identify the natural self ligand restricting these T cells is seen as the key to unlocking their role in the immune system.

NK Cell Receptors and Their MHC Ligands

NK Cell Receptors that Engage MHC Class I and Class I-Like Ligands

In addition to TCR-mediated signaling, lymphocytes, such as NK cells and T cells, can respond to immunological stimuli through the expression of various NK cell receptors which engage class I MHC and class I-like proteins. Under normal conditions, in healthy organisms, these NK cell receptors serve to maintain self-tolerance of circulating lymphocytes, while under pathological conditions, they allow activated NK or T cells to eliminate diseased cells. Nearly all NK cells and some T cells carry two classes of inhibitory receptors (the murine Ly49 family and CD94/NKG2A) that sense overall expression levels of class I MHC. During many viral infections and malignant transformations, class I MHC are downregulated, and inhibitory signals mediated by these receptors are lost, rendering class I MHC^{low} cells susceptible to cytolysis (122). In contrast, activating NK cell receptors (such as NKG2D, CD94/NKG2C/E and some members of the Ly49 family) bind class I MHC-like molecules induced during the stress response/viral infections/neoplasia/autoimmunity, targeting these cells for destruction (44, 123-125).

Below is a brief introduction to major NK cell receptor families which engage class I MHC or class I-like proteins, regulating evolutionarily conserved innate immunity in vertebrates. Probably the most important mechanism that monitors cell health by sensing class I MHC expression involves the NK cell receptor CD94 that can heterodimerize with the inhibitory C-type lectin-like NKG2A or its activating variants, NKG2C or NKG2E (126). These receptors engage the nonclassical class I MHC protein Qa-1 (which will be described in detail below), or its human homolog human leukocyte antigen (HLA)-E, associated with leader peptides of class I MHC (127). When CD94 is coupled to NKG2A, phosphorylation through the NKG2A cytoplasmic immune tyrosine inhibitory motifs (ITIMs) overrides NK cell activation, inhibiting target cell cytolysis (128). In contrast, the CD94/NKG2C and CD94/NKG2E activating receptors activate NK cells through association with the immune tyrosine activation motif (ITAM)-bearing DAP12 accessory molecule (129). Factors influencing CD94 choice of NKG2A v NKG2C are: a six fold higher affinity of NKG2A over NKG2C for HLA-E coupled with its class I leader peptide ligand (130); increased association with NKG2C upon DAP12 cell surface expression(131); and differential expression of NKG2A and NKG2C by different $CD8^+$ T cells (132).

NKG2D, distantly related to NKG2A/C/E family receptors, is a C-type lectin-like activating receptor expressed on NK cells and most $CD8^+$ T cells and γδ T cells in humans (123). When this homodimer engages stress-inducible, MHC class I-like ligands, it associates with the DAP10 co-receptor and triggers a proinflammatory signaling cascade through phosphorylation of the DAP10 cytoplasmic ITAMs (133).

Also conserved in the mouse and humans are the PIR (paired immunoglobulin receptor)/ILT (immunoglobulin-like transcript) family of activating and inhibitory receptors. Through a variable number of immunoglobulin-like domains these receptors recognize multiple class I MHC proteins. Different PIR/ILT family members are expressed by different cell types, but they can be broadly characterized as expressed by monocytes, B cells, DC, NK cells and T cells (134).

Found only in the mouse, Ly49 family members are C-type lectin-like molecules expressed on nearly all NK cells and a subset of CTL, where they appear to be induced by chronic antigen exposure (135). Expressed in a variegated fashion on NK cells, they engage different canonically folded, β_2m-associated class I MHC structures (136). Most Ly49 family members characterized to date are inhibitory (Ly49A, Ly49C, Ly49G and Ly49I), Ly49D and Ly49H being the only known activating Ly49s (137). In addition to engaging host class I MHC, these homodimers recognize some viral proteins that mimic class I, leading to inhibition of killing or direct cytotoxicity, depending on the nature of the receptor (activating or inhibitory). While humans do not carry functional Ly49 genes, they utilize structurally unrelated functional homologs, KIRs (killer cell immunoglobulin-like receptors). Comprised of both activating and inhibitory family members, individual KIRs, like Ly49s, recognize different class I MHC molecules and alleles of these molecules and are expressed in a variegated fashion on NK cells and a small subset of $CD8^+$ T cells (138, 139).

Structural Properties and Receptor Interaction Sites of MHC Class I Molecules

Since the focus of this thesis includes class I-like molecules related to classical (or class Ia) MHC, we will describe here the hallmarks of the "class I MHC fold" and the means by which they engage TCR and NK cell receptors. Class I MHC molecules are heterodimers consisting of a heavy chain, encoded by several *Mhc* loci, and a non-covalently associated invariant light chain, β_2m. X-ray crystallography of class I MHC molecules reveals α1 and α2 domains comprised of an anti-parallel β-sheet overlaid with two α-helices (140) (Figure 1.2). The α1 and α2 N-terminal β-strands align in an anti-parallel orientation, non-covalently associate via hydrogen bonds and together form an 8 stranded β-sheet. This comprises the floor of the peptide binding domain, with the α-helices of each domain forming parallel walls that are hydrogen bonded to the β-sheet below. These α-helical walls are closed off at the ends, accommodating only short (8-10 aa) peptides (141).

C-terminal to the α2 domain is the α3 domain, an Ig-like, β-sandwich structure comprised of two anti-parallel β-sheets. Structurally similar, the β_2m light chain non-covalently associates with the α3 heavy chain domain (though α1/α2 contacts are also apparent) (141). From the α3 domain, the class I heavy chain forms a ~19 aa transmembrane region followed by a cytoplasmic tail of variable length.

Receptors for class I MHC and class I-related molecules include αβ and γδ T cell receptors, the CD8 co-receptor, and the diverse array of NK cell receptors mentioned above (CD94/NKG2A/C/E, NKG2D, Ly49, KIR and PIR/ILT), each of which interacts in its own manner with the peptide/MHC (pMHC) fold (Figure 1.3). The αβ TCR

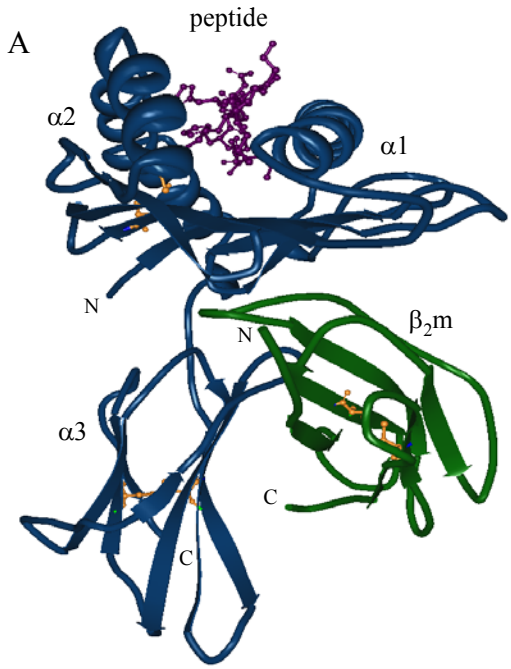
A
peptide
α2
α1
N
N
β2m
α3
C
C

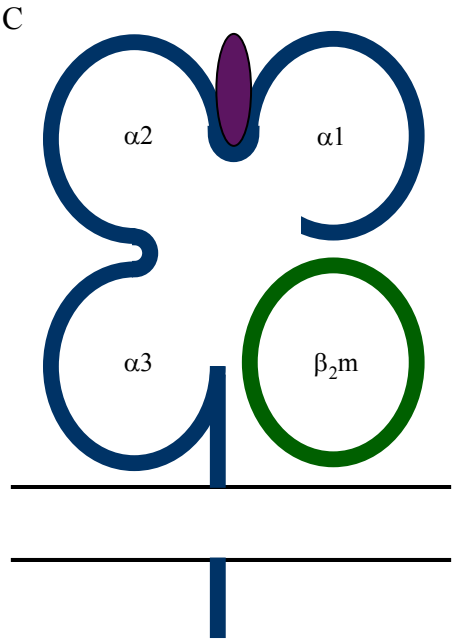
C
α2
α1
α3
β2m

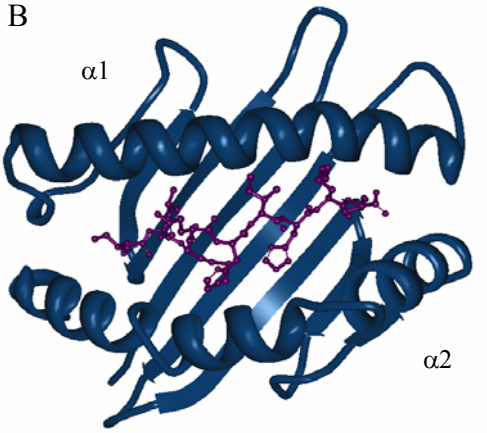
B
α1
α2

Figure 1.2 General structure of class I MHC. Canonical class I MHC heavy chain associates with the β_2m light chain through its α3 domain, while its α1 and α2 domains cooperate to bind endogenous peptide. Crystal structure of H2-Q9 in association with a self peptide (PDB: 1K8D, (142)). Class I MHC heavy chain is blue, the β_2m light chain is green, disulfide bonds are orange and the peptide is purple. A. Ribbon diagram of the class I MHC crystal structure with the self-peptide depicted in ball-and-stick mode. Orientation is such that the four globular domains are easily distinguished, while the peptide binding groove is in the plane of the observer. B. Ribbon diagram of the class I MHC peptide binding groove in complex with the ball-and-stick self peptide. Orientation is that of (A) turned counterclockwise 90° and forward 90°. C. Generic cartoon diagram of class I MHC in association with a peptide ligand. This diagram will be used in further figures to represent class I MHC and its derivatives.

interacts with pMHC in a diagonal orientation, recognizing conserved features of the class I MHC peptide binding fold while mediating specificity by engaging polymorphic class I MHC residues and contacts on the associated peptide (143). The only identified class I MHC ligand for the γδ TCR, T10/T22, has a unique fold that lacks portions of the peptide binding groove α helices, exposing the anti-parallel β-sheets below (97). The associating γδ TCR interacts with the exposed floor of the peptide binding domain on the side of the class I structure (rather than the top as with the αβ TCR) (143).

CD8 is a T cell co-receptor that can be expressed either as a heterodimer of CD8α and CD8β subunits (CD8αβ) or a CD8α homodimer (CD8αα). The crystal structure of CD8αα in association with pMHC indicates that the major interaction site with the MHC heavy chain involves a protruding α3 loop with additional contacts in the β_2m light chain and, to a lesser extent, α1/α2 (144). Though the structure of CD8αβ has not been solved, it is believed that the β chain would replace the CD8α chain with the highest pMHC association (144).

Interaction surfaces of class I MHC with their NK cell receptors are also diverse. CD94/NKG2A recognizes peptide/HLA-E complexes with contacts on HLA-E and

αβTCR
HLA-A2

γδTCR
T22

KIR2DL2
HLA-Cw3

CD94/NKG2A
HLA-E

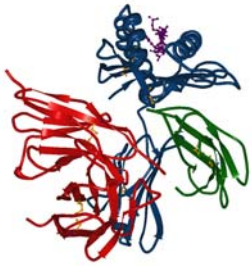

CD8αα
K^b

LIR-1
HLA-A2

Ly49A
D^d
site 1

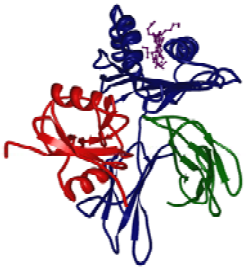

Ly49C
K^b
site 2

Figure 1.3 Receptor/ligand interactions of class I MHC. Receptors for class I MHC interact with their ligand on various surfaces. The αβTCR binds class I MHC across the peptide binding groove (PDB: 1AO7 (143)). The γδTCR binds the class I MHC T22 on the side of the abrogated peptide binding groove (PDB: 1YPZ (98)). KIR2DL2 associates with class I MHC in the same manner as the αβTCR (PDB: 1EFX (145)). The CD94/NKG2A heterodimer binds HLA-E through its peptide binding groove (PDB: 3CII (146)). CD8αα associates primarily with the α3 domain of class I MHC (PDB: 1BQH (144)). LIR1 makes contact with both the α3 domain and β_2m light chain of class I MHC (PDB: 1P7Q (147)). Ly49 molecules can interact with two sites on class I MHC (Ly49A – PDB: 1QO3 (148); Ly49C – PDB: 1P4L (149)). The class I MHC heavy chain is blue, the β_2m light chain is green, disulfide bonds are orange, the peptide is purple and the receptor is red.

several on the associated peptide (146). NKG2D binds a broad array of structures that all bear resemblance to the α1α2 peptide binding domain of class I MHC (150-152). Ly49 family members engage class I MHC on two sites. Site 1 is the N-terminal end of the α1 helix; site 2 is comprised of a cavity beneath the peptide binding groove which involves residues in the α1 and α2 domains and β_2m (153). KIRs interact with the α1α2 domain of class I MHC in a manner reminiscent of TCR (145). Finally, PIR/ILT bind an array of class I MHC molecules through the minimally polymorphic α3 domain and β_2m light chain (134).

As touched upon before, class I MHC can be roughly divided into three types: class Ia, class Ib and class I-related (Figure 1.4). Class Ia MHC are highly polymorphic, ubiquitously expressed molecules that bind a diverse array of peptides and include murine H2-K, -D and -L and human HLA-A, -B and -C. Class Ib and class I-related MHC are a broad group of molecules that share the basic class Ia MHC fold, but in general are only moderately polymorphic and expressed differentially in individual tissues or cell types. Genes encoding class Ib MHC are human *HLA-E*, *-F* and *-G* and large clusters of genes in the mouse *Mhc* known as the *H2-Q*, *H2-T* and *H2-M* regions.

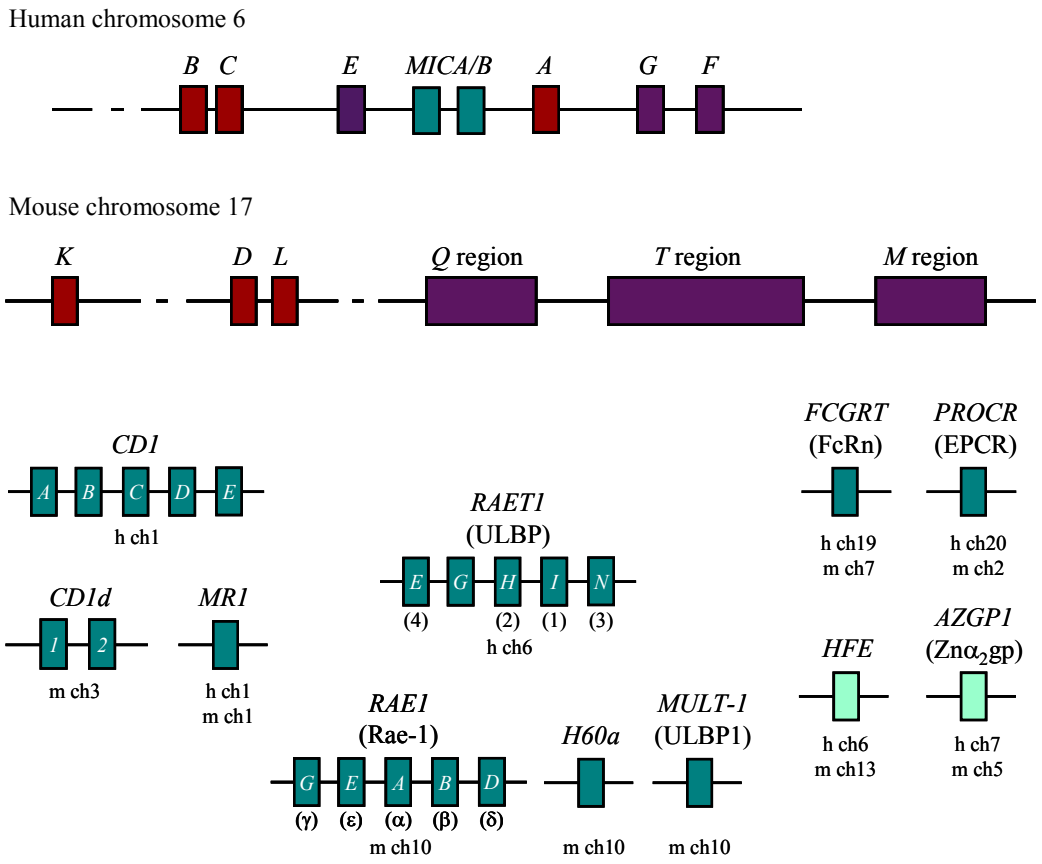

Figure 1.4 The human and mouse *Mhc* regions contain many classical and non-classical class I heavy chain genes. Cartoon representation of class I and class I-like *Mhc* loci in mouse and man. Class Ia genes are colored red, class Ib genes are purple, and class I-like genes are turquoise. Class I-like *Mhc* that serve no demonstrated immunological role are shaded light turquoise. Gene names are italicized above the representative rectangle. Protein names (where appropriate) are in parenthesis below the gene name. If multiple genes are present in the gene family, they are annotated within the rectangle (and below, for the protein name). Chromosomal location is indicated for mouse and human underneath the locus.

Class I-related molecules are further differentiated by their location in or outside of the *Mhc*, their distant evolutionary relationship to class Ia and class Ib MHC, their conservation between species and/or their roles outside of antigen presentation. Class I-related molecules that perform antigen presentation functions are MR1 and the CD1

family (154). NKG2D ligands include MICA and MICB in humans (123), minor histocompatibility antigen 60 (H60) in mice (155) and UL binding protein (ULBP) proteins, encoded by the retinoic acid early transcript-1 (*RAET*)-*l* gene family (155-157). Other class I-related family members that share the overall class I fold but primarily perform functions unrelated to antigen presentation include endothelial protein C receptor (EPCR), the neonatal Fc receptor (FcRn), the hemochromatosis gene (*HFE*) and zinc-binding α2 glycoprotein 1 ($Zn\alpha_2gp1$), encoded by *AZGP1* (127).

In the following sections we provide an overview of two major families of NK cell receptors – CD94/NKG2 and NKG2D – and their interactions with class Ib and class I-related ligands.

NK Cell Receptors and Their Functions

CD94/NKG2A and its Evolutionarily Conserved Ligands

Expressed on ~50% of NK cells (158) and induced by IL-15 and TGF-β on activated $CD8^+$ T cells (159-162), the evolutionarily conserved CD94/NKG2A receptor inhibits cell mediated cytotoxicity by engaging ubiquitously expressed mouse Qa-1 and human HLA-E on target cells (127). Importantly it is thought to override most of the activating signals delivered via other receptors except, in some cases, NKG2D (123, 133, 163, 164).

Believed to have arisen independently by convergent evolution, Qa-1 and HLA-E are functional homologues that bind a selected peptide pool of hydrophobic, mainly

nonameric sequences, with identical anchor residues and very similar primary amino acid sequences (127). These peptides are predominantly derived from the leader sequences of class I MHC, and can be delivered to the HLA-E/Qa-1 groove by TAP-dependent and TAP-independent pathways (165, 166). In addition to class I leader peptides, HLA-E and Qa-1 ligands include peptides derived from proteins induced during heat shock (hsp60 [heat shock protein 60] and MRP7 [multidrug resistance-associated protein 7]) (167, 168).

The TAP-dependence of Qa-1/HLA-E association with class I-derived leader peptides is a consequence of the co-translational cleavage of class I leader sequences in the ER, followed by retrograde transfer into the cytosol (169). There, these leader sequences (called Qdm [Qa-1 determinant modifier] in the mouse) are processed by the proteasome, transported back into the ER lumen by TAP, and loaded into the peptide binding groove of Qa-1 or HLA-E (127). On the cell surface, Qdm-bound Qa-1/HLA-E complexes can be engaged by CD94/NKG2A (170). Possibly due to the substitution of two critical F pocket residues with serines (171), the association of Qa-1/HLA-E with Qdm is quite weak (with a $t_{½}$ of about 1.5 hours at 37°C for Qa-1) (172), and a constant supply of Qdm is needed to protect cells from possible NK/T cell lysis.

Qdm (AMAPRTLLL) associates with Qa-1 via major anchors at positions P2 and P9 and a series of minor anchors at the P7 lysine and possibly the P5 arginine and P6 threonine (173-176). While the identity of the P1 residue seems to be of little consequence to Qa-1 binding (176), data placing the Qdm N-terminus at the P1 alanine (177) suggest that P1, like for class Ia MHC (141, 178), serves as the amino terminal

pocket A binding element. The P3 alanine, P4 proline and P8 leucine have been shown to have little to no role in Qa-1 binding (174-176).

While useful as a predictive measure of Qa-1 association, primary amino acid sequence alone does not determine whether a peptide will bind Qa-1. Diverse peptides have been shown to associate with the Qa-1 peptide binding groove. The dominant peptide associated with Qa-1 in the absence of Qdm is derived from the heat shock protein hsp60 (GMKFDRGYI) (167). Additional Qa-1 ligands include peptides from the mycobacterial hsp60 homolog GroEL (GMQFDRGYL) (167), the preproinsulin leader peptide (ALWMRFLPL) (179) and a peptide derived from the TCR of autoreactive $CD4^+$ T cells in experimental autoimmune encephalomyelitis (180).

In addition to the amino acid requirements for loading into the peptide binding groove of Qa-1/HLA-E, interaction with CD94/NKG2A is also peptide-dependent. Murine CD94/NKG2A can discriminate between Qdm substitutions at non-anchor P4, P5 and P8 (176). Human CD94/NKG2A discerns subtle changes in overall peptide conformation induced by substitutions in non-anchor positions (181). Most of this interaction is mediated through CD94 contacts with the HLA-E-associated leader peptide. CD94 interacts with the side chains of the P5 arginine and the P8 phenylalanine, while binding the peptide backbone of the P6 threonine. The only contact mediated by NKG2A is a relatively weak van der Waal's interaction with the P5 arginine, which falls into the groove at the interface between CD94 and NKG2A (182). Thus CD94 is thought to mediate HLA-E/peptide binding while the NKG2 subunit (inhibitory NKG2A or activating NKG2C) determines the outcome of the interaction. NKG2C has a 6-fold lower affinity for CD94 than NKG2A, as mediated by the interface between the

individual subunits (130). Interestingly, a conservative P5 substitution of lysine for arginine increases the affinity of NKG2C for CD94 to approximately that of NKG2A (146). Thus, Qa-1 association with the inhibitory NKG2A or the activating NKG2C subunit has some indirect peptide dependence.

NKG2D and its Ligands

NKG2D is a C-type lectin-like activating receptor expressed by all NK cells, virtually all human $CD8^+$ peripheral blood lymphocytes (PBL) (123) and activated mouse $CD8^+$ T cells (155). This homodimeric receptor monitors its environment for conditions of cell stress, including pathogenic infection, genotoxic stress, heat shock and tumorigenesis. It responds by eliminating damaged cells predominantly through the upregulation/recognition of NKG2D ligands, all of which are structurally related to class I MHC (Figure 1.5).

While all NKG2D ligands share significant homology with the α1α2 domains of class I MHC ligands, they are actually quite diverse with as little as 30% homology at the amino acid level. Having undergone independent evolutionary diversification, each ligand has its own pattern of tissue-specific constitutive expression and is upregulated in response to unique cell stressors. Thus, individual NKG2D ligands may have tissue-specific and/or stress-specific roles in innate immunity. Human NKG2D ligands include MICA and MICB, encoded within the *Hla*-locus, and the ULBP (*RAET-1*) family members, which are encoded on human chromosome 6. MICA, which encodes a class I MHC heavy chain-like protein, is constitutively expressed in the gut and airway

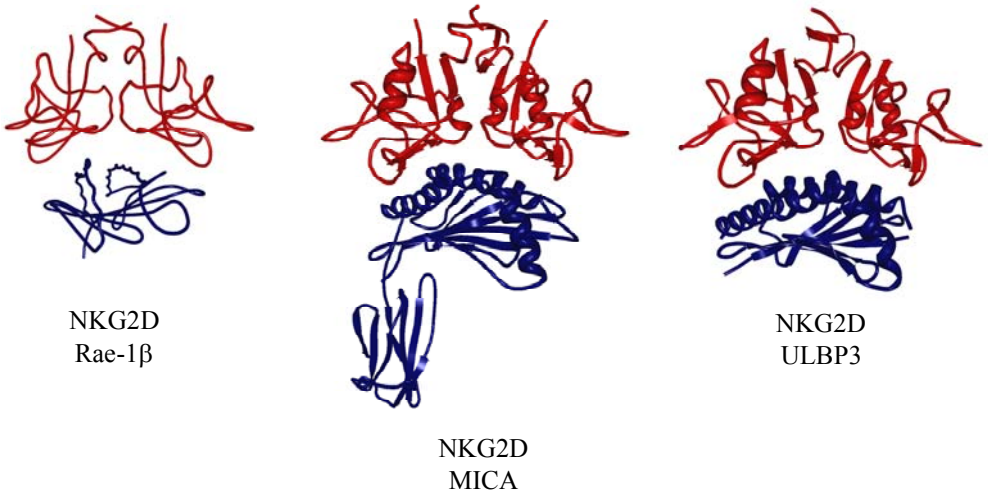

Figure 1.5 Receptor/ligand interactions of NKG2D. NKG2D interacts with the basic α1α2 architecture on different ligands despite their low overall homology. Rae-1β (PDB: 1JSK (150)); MICA (PDB: 1HYR (152)); ULBP3 (PDB: 1KCG (151)). The class I-like heavy chain is blue and NKG2D is red.

epithelium. Largely intracellular under steady state conditions, MICA is trafficked to the basolateral surface of epithelial cells under conditions of stress, where it can interact with NKG2D-expressing effector cells (183, 184). There is no known genetic homolog to the MIC ligand in mice. ULBP family member transcripts can be found in many normal tissues, and cell surface expression is upregulated in tumor lines and in healthy cells in response to genotoxic stress (185).

Mice have homologs to ULBPs – retinoic acid inducible Rae-1α, β, γ, δ and ε – but also have independently evolved H60 and MULT1 (murine ULBP-like transcript) NKG2D ligands. Rae-1s are not expressed in normal tissues (186) but, like ULBPs, can be upregulated in tumor lines (155). MULT1 is transcribed in a variety of adult mouse tissues (187, 188), but its regulation in response to cell stress has not been explored. H60

is differentially expressed in inbred mouse strains (155) and transcripts can be found in many tissues (189). Recently, two H60 homologs, H60b and H60c were discovered in the mouse. While H60b, expressed in various tissues, can be upregulated in response to infection, H60c, expressed predominantly in the skin, cannot (189). Thus, as in humans, each murine NKG2D ligand has its own unique tissue distribution, can be upregulated in response to different stressors and has a different affinity for NKG2D (190), significantly diversifying the spectrum of NKG2D responses in the mouse.

Structurally, all NKG2D ligands retain the basic class I-like α1α2 domain configuration and, except for MICA/B, lack the α3-like domain. None described to date binds peptides or β_2m due to genetic features that occlude the groove and eliminate the β_2m binding site. Both human and mouse NKG2D broadly recognize the class I MHC fold, interacting with the pre-conformed Rae-1 α1α2-like structure and stabilizing the class I MHC architecture of MICA. Though NKG2D is a homodimer, each domain interacts with its ligand differently. These interactions are mediated through a key tyrosine at the receptor/ligand interface (one on each member of the homodimer) that interacts with six distinct surfaces on the α1α2 domains of MICA, Rae-1β and ULBP3. Thus, the NKG2D receptor is highly promiscuous, making contact with structurally distinct surfaces on a variety of ligands.

Expression of NK Cell Receptors on IEL

IEL and NK Cell Receptors in Human Disease

Perhaps the best understood example of the involvement of IEL and their NK cell receptors is the role of the NKG2 family of receptors in human celiac disease, a small bowel disorder brought about by a $CD4^+$ T cell antigen-specific response to wheat gliadin that is propagated by antigen-nonspecific IEL (191). Mucosal damage in this illness is thought to be mediated primarily by $TCR\alpha\beta^+$ $CD8^+$ IEL which, in the presence of IL-15, are reprogrammed into NK-like effectors (called lymphokine activated killers, or LAK) that exhibit cytolytic activity independent of TCR (192, 193). These IEL are characterized by increased expression of NKG2D, which mediates cytolysis of IL-15-induced MIC-expressing IEC (194), and CD94/NKG2C, which engages HLA-E on diseased IEC, inducing IEL cytokine secretion and proliferation (193). Paradoxically, $TCR\gamma\delta^+$ $CD8^{+/-}$ IEL expressing CD94/NKG2A release anti-inflammatory TGF-β when stimulated by HLA-E, suppressing the HLA-E and MICA-mediated autoreactivity of conventional IEL. Thus, the multiple, often mutually conflicting outcomes of IEL function appear at least in part to be mediated by activating and inhibitory NK cell receptors recognizing class I MHC and class I-like ligands.

Basic research of these interactions is hindered, in humans, by selective sampling of IEL from the colon and restricted access to samples from healthy individuals. Hence, to address key questions in this field, it is necessary to identify and characterize ligands of murine IEL of the small intestine.

NK Cell Receptors on Mouse IEL

Little is known about the expression of NK cell receptors by mouse IEL and the functional significance of their presence or absence. Transcriptional analysis of TCRαβ$^+$ CD8αβ$^+$, TCRαβ$^+$ CD8αα$^+$ and TCRγδ$^+$ IEL has revealed preferential expression of immunosuppressive genes, including inhibitory NK cell receptors, by the TCRαβ$^+$ CD8αα$^+$ subset. Strikingly, 40% of this IEL population express either the Ly49E or Ly49F inhibitory NK cell receptor (195), but the ligand(s) for these receptors and their function upon engagement in IEL remain unknown. Serial analysis of gene expression (SAGE) from αβ and γδ IEL detected rare to low expression of CD94, NKG2A and NKG2D (81). Interestingly, the transcript for Ly49E was also found to be rare in this analysis, yet 23% of TCRαβ$^+$ CD8αα$^+$ IEL are Ly49E$^+$ by flow cytometry (195). Another report found that 14% of CD8$^+$ IEL express cell surface NKG2A (196). Therefore the abundance of transcript may not reflect the amount of NK cell receptor protein present on IEL, and the expression of CD94 and NKG2D by murine IEL subsets remain undefined.

Class Ib MHC in Immunologically Privileged Sites

Immunological Privilege

Because of their propensity for limited immune-mediated inflammation, tissues such as the brain, testes, pregnant uterus, anterior chamber of the eye and cornea are considered to be immune privileged. These are tissues that have limited regenerative capacity or are of critical importance for reproductive success and can tolerate little "bystander" immune damage but still require protection from pathogenic infection (197,

198). Thus, the immune privileged environment offers limited reactivity of effectors that would cause the most peripheral damage, like NK cells and CTL, while less destructive antibody responses are preserved (199).

This privileged immunological environment is established and maintained in various ways (198). Several immune privileged tissues have limited lymphatic drainage (200) and express reduced levels of class Ia MHC (201-203), making them less visible to adaptive immune effectors. Instead, these tissues often express tolerogenic class Ib MHC like HLA-E, described above, and HLA-G, described below. They also typically express pro-apoptotic membrane factors like FasL (204-210) and TRAIL (tumor necrosis factor [TNF]-related apoptosis-inducing ligand) (211-213) and complement regulatory proteins that inhibit the complement cascade (214-223). Immunologically privileged tissues also elaborate a variety of anti-inflammatory soluble factors, including the immunoregulatory cytokine, TGF-β, VIP (vasoactive intestinal peptide) which inhibits T cell activation, α-MSH (α-melanocyte stimulating hormone), which induces $CD4^+$ $CD25^+$ regulatory T cells, somatostatin, which suppresses IFN-γ production by activated T cells, and MIF, which suppresses NK cell activity. Interestingly, the human NKG2D ligand, MICA, is expressed in the trophoblast in normal pregnancy, and the murine NKG2D ligand, Rae-1, was first described in the brain. Thus, NKG2D and its ligands may not always function to induce cytotoxicity and may be associated with tolerogenic function in tissues of immune privilege.

Similar to the placenta, which must maintain tolerance to paternal antigens, the small intestine and liver must remain immunologically quiescent to a diverse array of commensal and dietary antigens. In contrast to immunologically privileged tissues, the

small intestine and liver, which we refer to as tolerance-dominated, are highly regenerative and, when necessary, can mount a robust immune response. Under normal, healthy conditions, however, tolerance dominates. The intestinal tolerogenic milieu is established by some of the same cytokines/factors as are employed by immune privileged tissues, including TGF-β, αMSH and MIF (81, 224). It has not been determined if tissue-specific class Ib MHC, like HLA-G, best described in the placenta, cornea and retina, play a role in establishing/maintaining the tolerance-dominated atmosphere of the gut and liver.

HLA-G

During placentation, semiallogeneic fetal trophoblast cells invade the maternal decidua. These trophoblasts cells are class Ia MHC negative, expressing instead the immunoregulatory class Ib MHC molecule HLA-G (225). Found only in humans, HLA-G is a minimally polymorphic class Ib MHC molecule that tolerizes NK cells, APC and $CD8^+$ T cells in the placenta (225). HLA-G encodes multiple alternatively spliced isoforms, including canonical, α1α3, α3, ULBP-like α1α2 and soluble versions of the canonical, α1α3 and ULBP-like isoforms (226-230). Additionally, membrane-bound forms of HLA-G can become soluble by cell surface cleavage (225). Several of these molecules, in addition to the HLA-G leader peptide bound by HLA-E, have been implicated in HLA-G-mediated tolerogenic function.

The HLA-G/HLA-E pMHC complex is believed to tolerize decidual NK (dNK) cells (231, 232). This unique population of NK cells is characterized by its $CD56^{bright}$

phenotype, a marker for immunoregulatory NK activity, and high surface expression of CD94/NKG2A (233-235). Engagement of these NK cell inhibitory receptors by fetal trophoblast-expressed HLA-G/HLA-E pMHC inhibits dNK mediated cytotoxicity (232).

Known receptors for canonical HLA-G are ILT2, ILT4 and KIR3DL4, though the latter's function in HLA-G mediated tolerance has come into question as of late (225, 236-238). As described earlier, ILTs are inhibitory receptors expressed on T cells, B cells, NK cells, macrophages and DC. ILT2 and ILT4 bind all class I MHC, but have the highest affinity interaction with HLA-G (239). Very little is understood, however, about how engagement of these receptors translates into inhibitory function by immune cells.

HLA-G and its many isoforms affect each of the ILT-expressive immune effectors. All four membrane-bound forms of HLA-G can overcome activating MICA/NKG2D stimulation (225, 240). Intriguingly, the only common feature of these molecules, outside of their cell surface association, is expression of the α1 domain. Soluble canonical HLA-G regulates $CD8^+$ T cells by inducing them to express Fas/FasL and undergo apoptotic cell death (241). APC expressing HLA-G are prevalent in pregnancy, transplantation and cancer, the latter co-opting pregnancy-mediated tolerance mechanisms (225). *In vitro*, these APC have been shown to decrease $CD4^+$ T cell proliferation and induce them to follow a regulatory T cell program (225). HLA-G mediates decidual macrophage suppression and suppresses DC maturation (242-244), and recombinant soluble canonical HLA-G and soluble α1α3 have been shown to induce APC to make the immunoregulatory cytokine TGF-β (245).

Murine Class Ib MHC in Immunologically Privileged Sites

While the immunotolerizing role of the human class Ib MHC HLA-G has been extensively studied, little is known about murine class Ib MHC expression in immunologically privileged sites. This is particularly important, as the mouse is the most widely used model for studying immunotolerance. As a group, class Ib MHC are characterized by their generally restricted tissue distribution and limited polymorphism. Among these are liver-restricted Q10 (246, 247), Q5, which is highly expressed in the brain (unpublished observations by Nora Renthal of our laboratory), and gut-restricted TL, Q1 and Q2 (248-250).

Q10 is a nonpolymorphic class Ib MHC with a truncated transmembrane domain that renders it soluble (246, 247). Highly transcribed in the liver, Q10 is found in large molecular weight multivalent complexes at concentrations of 20-60 μg/mL in serum (251). Q10 binds a heterogeneous peptide repertoire and is only partially TAP-dependent (252), suggesting it follows both classical and non-classical antigen presentation pathways. Transcripts for Q10 include three alternatively spliced isoforms, which encode canonical, α1α3 and α3 variants (unpublished observations by Dr. Ming Chen of our laboratory), but the function of these molecules remains undefined. The leader peptide of Q10 encodes the Qdm sequence, but it is unknown if this leader can be processed in such a manner as to provide Qdm for Qa-1 association.

Q5 is a class Ib MHC that is ubiquitously transcribed and, unlike class Ia MHC, highly expressed in the brain. Like Q10, Q5 is alternatively spliced (unpublished observations by Nora Renthal of our laboratory) and encodes Qdm in its leader peptide, but the functional implications of this splicing and the ability of the Q5 leader to provide

Qdm to Qa-1 remain undefined. Intriguingly, the Q5 protein variants (canonical, α1α3 and α1) are the same as the predominant alternatively spliced products of tolerogenic HLA-G, which also encodes a leader peptide capable of binding to the Qa-1 homolog, HLA-E. While at least one allele of Q5 has been designated as a pseudogene due to a stop codon mutation in one of the major exons (253), studies in our laboratory have determined that the alternatively spliced messages are expressed at similar levels as in animals with an intact Q5 allele. Q5 is currently under study by Nora Renthal of our laboratory.

TL, encoded by *H2-T3*^{b} and/or *H2-T18*^{d} depending upon the mouse strain, is a class Ib MHC that is transcriptionally restricted to epithelial cells of the small intestine (248). With an abrogated peptide binding groove, TL does not bind peptides (254), nor has it been shown to interact with the TCR. Instead, TL binds the CD8αα co-receptor, altering T cell responses to TCR-mediated signaling. This includes increased cytokine production, decreased cytotoxicity and decreased proliferation (38). Q1 and Q2 have similarly been determined to be restricted to the intestinal epithelium (249, 250), but little else is known about these tissue-restricted molecules.

While it is clear that the tissue-restricted class Ib MHC in humans studied to date play important roles in establishing/maintaining immune privilege, the expression and function of tissue-specific class Ib MHC in mice, the predominant model organism for the study of immune tolerance, remain largely undefined. In the intestine, class Ib MHC are the best candidates for the elusive TCRαβ^{+} CD8αα^{+} and TCRγδ^{+} IEL TCRs, but particular class Ib MHC have not been identified. Additionally, human IEL have been

demonstrated to respond to stimuli through activating and inhibitory NK cell receptors that recognize class I and class I-like proteins, but their expression on murine IEL and the ligands that they engage have not been extensively characterized. Addressing the receptor/ligand interactions of IEL is paramount in the quest to understand IEL function in health and disease.

Rationale

Despite 20 years of intense studies of IEL, little is known about the pathways that they regulate. The key to understanding their functions is identification of the self-ligands that regulate their selection/differentiation and that are recognized in the gut during "tolerance- dominated" and "activated" states. We describe here our experiments to address these important questions.

We first analyzed known class Ib MHC for specific expression in the gastrointestinal tract, identifying two novel gut-restricted class Ib MHC including H2-Bl, previously reported to be expressed only at the maternal/fetal interface. We described H2-Bl alternatively spliced products and polymorphisms and next characterized H2-Bl's transcriptional regulation, demonstrating a much higher expression of this tissue-specific class Ib MHC in the intestine than the placenta. We localized the transcription of gut-specific class Ib MHC to IEC and determined the expression of their putative TCR and NK cell receptor ligands on IEL. Noticing the similarities of the gut-specific class Ib MHC leader peptides to Qdm, we assayed these molecules for their ability to bind Qa-1, the ligand for the inhibitory receptor CD94/NKG2A, finding that the H2-Bl, Q5 and Q10

nonamer peptides can be generated by the antigen processing machinery and presented by Qa-1. Additionally, the exogenously applied H2-Bl nonamer is capable of mediating NK cell inhibition, presumably via CD94/NKG2A. Finally, we characterized the expression of protein products from canonical and alternatively spliced transcripts of gut-specific, liver-specific and brain-expressed class Ib MHC in the context of the classical class I MHC antigen presentation pathway, identifying many cell surface expressed molecules. Thus, we report the identification and characterization of several novel class Ib MHC products that represent candidates for receptors displayed on TCR$\gamma\delta^+$ and TCR$\alpha\beta^+$ CD8$\alpha\alpha^+$ unconventional IEL and putative effectors in the liver and brain.

CHAPTER TWO

Materials and Methods

Mice

129/SvJ, C57BL/6J and B6.*RAG1*$^{-/-}$ mice were obtained from The Jackson Laboratory (Bar Harbor, ME). CD1 (ICR)BR (henceforth referred to as ICR) mice were obtained from Charles River Laboratories (Wilmington, MA). C57BL/6NCr mice used for DNA sequence analysis were obtained from the National Cancer Institute Animal Production Program (Frederick, MD). B6.$K^{b-/-}D^{b-/-}$ mice (255) were generously provided by Dr. J. Forman (UT Southwestern, Dallas, TX). C3H/HeJ, FVB/NJ and BALB/cJ mice were generously provided by Dr. M. Bennett (UT Southwestern, Dallas, TX). 129 x B6 F1 mice were generated by crossing a 129/SvJ male with a C57BL/6J female. 129/SvJ, C57BL/6J, 129 x B6 F1, ICR, B6.*RAG1*$^{-/-}$ and B6.$K^{b-/-}D^{b-/-}$ mice were housed under specific pathogen-free conditions at the University of Texas Southwestern Medical Center (Dallas, TX); C3H/HeJ, FVB/NJ, BALB/cJ and C57BL/6NCr mice were housed in the UT Southwestern conventional mouse facility (Dallas, TX). All animals of both sexes were 2-5 months old unless otherwise noted. All experiments involving animals were performed according to institutional review board guidelines.

Cell Lines and Culture Conditions

The B16-derived B78H1 (H1) melanoma line and GM-CSF transduced B78H1 (GM) melanoma (256) were provided by Dr. H. I. Levitsky (The Johns Hopkins School of Medicine, Baltimore, MD). Qa-1^b transfected B78H1 ((257), clones LS and HeS) were provided by Dr. C. Aldrich (Indiana University School of Medicine, Evansville, IN). The Hepa1 murine hepatoma was originally provided by Dr. O. Hankinson (UCLA, Los Angeles, CA) (258). NK-resistant P815 mastocytoma (259) and NK-sensitive YAC-1 lymphoma (260) lines were the gift of Dr. J. Schatzle (UT Southwestern, Dallas, TX). The murine T cell lymphoma RMA-S (261) and a J1, T23-transfected variant of the human lymphoblastoid C1R (177), were maintained at the Indiana University School of Medicine by Dr. C. Aldrich. B78H1, B78H1 derivatives and Hepa1 cell lines were propagated in a 1:1 mixture of high glucose DMEM and RPMI 1640 (Mediatech, Inc., Manassas, VA; final concentration of 3.25 mg/mL L-glucose) with 1X essential and nonessential amino acids (as recommended by the vendor), 4 mM L-glutamine, 1 mM sodium pyruvate and 10 mM HEPES (Mediatech) and 10% FBS (Atlanta Biologicals, Norcross, GA) (cDR10N). P815 and YAC cell lines were cultured in RPMI (Mediatech), supplemented as above (cRPMI). All cell lines were cultured at 37°C in 5% CO_2. G418 (Mediatech) was used at 0.8 mg/mL for selection and 0.4 mg/mL for maintenance. Hyrgomycin B (Mediatech) was used at 0.6 mg/mL and puromycin (Sigma-Aldrich, St. Louis, MO) was used at 6 µg/mL. Adherent cells were passaged by washing flasks with cold PBS, applying 0.25% trypsin (Mediatech) at 37°C for 1 minute and resuspending in culture medium.

CTL clones D5D2 (177), 39.1D7x (262) and 52.4D11c (262), specific for Qdm-loaded Qa-1^b, were the kind gift of Dr. C. Aldrich. CTL were cultured in MEM Eagle

(Sigma-Aldrich) supplemented with 10% FBS, 10 mM HEPES, 1 mM sodium pyruvate, 5 mM L-glutamine, 50 μM 2-ME, 1.5X non-essential amino acids, 0.5X essential amino acids, 1 mg/mL dextrose and 0.15% sodium bicarbonate (Sigma-Aldrich). This mixture (sMEM) was supplemented with EL4-derived IL-2, a gift of Dr. C. Aldrich. $H2^b$ (C57BL/6J) splenocytes were depleted of red blood cells using Tris-buffered ammonium chloride (17 mM Tris-HCl, 144 mM NH_4Cl @ pH 7.2), γ-irradiated (1500 rad) and plated at $0.27x10^6$ cells per well of a 24 well plate in 1 mL sMEM + IL-2 for use as CTL feeder cells the day before CTL passage. Day 7 CTL were collected from their plates by gentle pipetting and reseeded atop the feeder cells at approximately $0.1x10^6$ cells per well in a final culture volume of 2 mL.

RNA and DNA Isolation

Tissues were harvested from mice for RNA and DNA isolation as follows. Adult mice were euthanized by CO_2 asphyxiation, and neonatal mice were CO_2 asphyxiated and decapitated prior to tissue harvest. Spleen, thymus, kidneys, lungs, heart, testes, ovaries, virgin uterus, brain, eyes, foot pad, ear, abdominal skin (shaved), whole embryo and embryonic and neonatal intestine and liver were harvested as whole organs. Pregnancy associated tissues were harvested from CO_2 asphyxiated late term pregnant mice (embryonic day 16-19). Each lobe of the uterus was cut longitudinally, and embryos were removed from the uterus and immediately decapitated. Placentas (with attached umbilical cord) were tweezed from the uterus, and both were harvested as whole organs. A single lobe of the adult liver and hind leg skeletal muscle were taken as representative

samples of those tissues. Gastrointestinal tissues were washed of luminal contents. To enrich for intestinal epithelial cell populations in small intestine samples, visible Peyer's patches with associated epithelium were removed. All tissues were then flash frozen in liquid nitrogen, pulverized and solubilized in Tri® Reagent (Molecular Research Center, Inc,, Cincinnati, OH).

In some cases, small intestinal samples were further fractionated into IEL, IEC and lamina propria samples. Once the intestine had been flushed and visible Peyer's patches had been removed, the intestine was opened longitudinally to expose the luminal surface and cut into 1 cm lengths. These tissue fragments were then washed with vigorous shaking four times in 40 mL ice cold 1X PBS. Washed intestinal segments (from a single mouse) were placed in a clean 50 mL conical centrifuge tube with 25 mL 1 mM DTT, 1mM EDTA, 3% FBS in 1X PBS (extraction medium [EM]) and incubated rotating at 100 rpm, 37°C for 30 minutes to extract the epithelial monolayer from the intestinal basement membrane. This mixture was then vortexed on a setting of 3 for 10 seconds to dissociate any residual epithelium from the basement membrane. Epithelial cells in suspension were decanted from the remaining intestinal pieces, which were subjected to another three rounds of epithelial removal to enrich for lamina propria. These lamina propria/intestinal substructure segments were then washed twice in 1X PBS and dissolved in Tri® Reagent.

Epithelial cells from the first extraction were passaged through a 70 micron filter to filter out any remaining intact intestinal tissue. This mixture of IEC and IEL was then underlaid with 20 mL lymphocyte separation medium (LSM, Sigma-Aldrich) and centrifuged at 400 x g, 4°C for 20 minutes without braking. Cells at the LSM/EM

interface were collected, pelleted by centrifugation at 400 x g, 4°C for 15 minutes and resuspended in 3 mL cold 1% BSA (Sigma-Aldrich) in PBS (FACS Buffer) for staining or 1 mL Tri® reagent for RNA isolation.

Cells from the epithelial monolayer in FACS buffer were treated with a 1:1000 dilution of anti-mouse CD16/CD32 (clone 2.4G2, BD Biosciences, San Jose, CA) to block non-specific Fc receptor antibody binding, then stained with a 1:80 dilution of PE-conjugated anti-CD3 (BD Biosciences) to detect IEL. These stained, mixed IEL/IEC were then subjected to FACS on a MoFlo Cytometer (Beckman Coulter, Inc, Fullerton, CA). IEL were selected based on their low forward and side scatter (FSC/SSC) profile and FL2 channel fluorescence. IEC were selected based on their high FCS/SSC profile and confirmed by their autofluorescence in both FL1 and FL2 channels. Both sorted IEL and IEC were reexamined by flow cytometry to determine the purity of the populations. IEL and IEC were then collected by centrifugation at 400 x g for 6 minutes and resuspended in an appropriate volume of Tri® Reagent.

Total RNA and genomic DNA were individually isolated from flash frozen/pulverized tissues, single-cell suspensions of cells removed directly *ex vivo* and cultured cells, tissues and cell lines, using Tri® Reagent according to the manufacturer's protocols. The concentrations of RNA and DNA samples were quantitated spectrophotometrically. Additionally, RNA quality was evaluated by visualizing rRNA bands on a 1% agarose gel containing ethidium bromide.

Analysis of gut-restricted class Ib genes from wild-derived mouse strains (263) was performed on DNA samples provided by Drs. A. Orth and F. Bonhomme from mice held at the genetic repository of Laboritoire GPIA (Génome, Populations, Interactions,

Adaptation, Université de Montpellier, France, http://www.univ-montp2.fr/~genetix/souris.htm). Jejunal RNA from germ free and conventionalized germ free C57BL/6J mice was the kind gift of Dr. L. Hooper (Washington University, St. Louis, MO). Dr. Hooper also supplied cDNA from the small intestines of conventional NMRI mice at various ages in early postnatal development.

DNA Primers

The sequences of the primers used in this study are listed in Tables 2.1-2.4. Oligonucleotide primers were synthesized by Integrated DNA Technologies, Inc. (Coralville, IA) or Invitrogen (Carlsbad, CA). Primer specificity was determined by BLASTN analysis (National Center for Biomedical Information [NCBI], http://www.ncbi.nlm.nih.gov/BLAST/) and verified experimentally by sequencing the amplification products.

Transcriptional Analysis by Northern

Northerns were performed according to standard procedures. 20 µg whole tissue RNA was denatured in 2-5 volumes RNA loading buffer without ethidium bromide (Sigma-Aldrich), heated at 65°C for 10 minutes, chilled on ice and immediately loaded on an RNase free 1.67% agarose gel in 1X MES buffer (Sigma-Aldrich) and 2.2 M formaldehyde (Fisher Scientific, Pittsburg, PA) along with 5-10 µg 0.24-9.5 kb RNA ladder (Invitrogen). The sample-loaded agarose gel was run at 50 V at 4°C for 3-4 hours

Table 2.1 *Primers used for the PCR detection and cloning of class Ib MHC*[a]

Primer Name	Sequence (5' to 3')
cyclophilin F	CCA TCG TGT CAT CAA GGA CTT CAT
cyclophilin R	TTG CCA TCC AGC CAG GAG GTC T
GAPDH F	TGA AGG TCG GTG TGA ACG GAT TTG
GAPDH R	GGC CTT CTC CAT GGT GGT GAA GAC
TAP1 F	GTC CAG ATG CCT TCG CTA TCA G
TAP1 R	GTT GCC TGT GTC CTC AGT CAC
TAP2 F	CAC CAT GTC CAG GAT CAA CC
TAP2 R	CGC AGT TCA GAA TCA GCA CC
Tapasin F	GAA GTG GGC TAG AAG TCT GAG
Tapasin R	CAC AAC GGG TGC TGG TGT TAG
$\beta_2 m$ F	ATG GCT CGC TCG GTG ACC CTG
$\beta_2 m$ R	ATT GCT CAG CTA TCT AGG ATA
K^b ex2 F	GAG CCC CGG TAC ATG GAA
K^b ex3 R	CAG GTA GGC CCT GAG TCT
D^b ex2 F	GAG CCC CGG TAC ATC TCT
D^b ex3 R	CAG GTA GGC CTT GTA ATG
Xho I/$Q1^b$ ex1 F	TGG CAG CTC GAG TGA CCC TGA CCA AAA CCG GA
EcoR I/$Q1^b$ ex3 R	ACC CCA GAA TTC AGC CAG ACA ACT TCT GGA AG
$Q1^b$/$Q2^b$ 5'UTR/ex1 F	GCC TCA GAT GCC CTG TAT TCC
$Q1^b$/$Q2^b$ 3'UTR R	CTC AGT CTA CTC CAG GCA GCT GTC
$Q2^b$ 5'UTR/ex1 F	TCA GAT GCC CTG TAT CCC AGA TGG
Xho I/$Q2^b$ ex2 F	CCT GGC CTC GAG AGG AGC CCC GGT TCA TTA TC
EcoR I/$Q2^b$ ex3 R	GTA ATC GAA TTC ATC GTA GGC AGA CTG CTC A
$Q2^b$ 3'UTR R	CAC CAG AGT GTC ACC TTT ACA ATT C
$Q4^b$ ex2/ex3 F	AGA ATC CTC GAG GGG AGC AAT GGC GTC
$Q4^b$ ex4 R	GCA CGC GAA TTC CCT CCA GGT AGG CCT TGCT
$Q6^b$/$Q8^b$ ex4 F	CAT GTG CTC GAG CAC CCC AGG TCT TAT GGT GC
$Q6^b$/$Q8^b$ ex5 R	CAA GCG AAT TCG ACA ACC AGA ATA GCT ACG T
$Q7^b$/$Q9^b$ ex2 F	CTC TTC GTG TGA AAG TAT GGA GCT GGA GC
$Q7^b$/$Q9^b$ 5'UTR R	ACT ACA ACC AGA GCA AGG G
$Q10^b$ ex3 F	CGT GGA CTC GAG CGG ACG TGG CGG CGA TT
$Q10^b$ ex5 R	CCA CCA GAA TTC TAA TGA TGG CCA CAG CAG AT
$T3^b$ 5'UTR/ex1 F	CTT CAG ATT TCC CTA ACA TGA GG
$T3^b$ ex2 F	GTA CAT AGC TGT GGG CTA CC
$T3^b$ ex3 R	CCA TCA TAG CCA TGC TGC TC
$T3^b$ 3'UTR R	GAA GAA GTA ACA AGA CAT TGT CAG G
$T22^b$ ex2 F	GGA GCA GGA GGA AGC AGA TA
$T22^b$ ex3 R	GAG CAG TGG CTC TTC AGG TC
$T23^b$ ex2 F	CAG AGT AAA CCT GAG GAC CC
$T23^b$ ex3 R	AGG CCT CCT GAC AAT ACC CG

Table 2.1 *Primers used for the PCR detection and cloning of class Ib MHC, cont.*

Primer Name	Sequence (5' to 3')
H2-Bl ^{bc} 5'UTR F	GCG CCG CTC GAG TCT CCT GCA GTT CAG CTC CT
H2-Bl ^{bc} 5'UTR/ex1 F1	CAG ATG CCC TGT ATT CCA AAT GG
H2-Bl ^{bc} 5'UTR/ex1 F2	TAT TCC AAA TGG GGC AAT GGC GCA
H2-Bl ^{bc} int3 F	GCA GTC GGG TGC TCT TAC C
H2-Bl ^{bc} ex3 R1	CGC TAC CAG ATC CGC CGC CA
H2-Bl ^{bc} ex3 R2^{b}	CGC ACT CGC CCT CTA GGT AGA A
H2-Bl ^{bc} ex5 R^{b}	CTC TTC AAC ACA AAA GCC AC
H2-Bl ^{bc} 3'UTR R	ACT CCA CTA ATC AAC CCT CAG
H2-Bl ^{bc} 3'UTR R2	AGA GGC GAA TTC TCT AGA TAG GCA TGA CCA CAA
Tw5 ^{bc} 5'UTR F	TCA GAC ATC CAG GAT CCC AG
Tw5 ^{bc} 5'UTR/ex1 F	ACA TCC AGG ATC CCA GAT GG
Tw5 ^{bc} ex3 F	GTT TGC TTA CGA AGG CCA AG
Tw5 ^{bc} ex3 R	CGT GAT CAG AGC TGC CAT G
Tw5 ^{bc} 3'UTR R	CTT AAC TTC TGA GCC ATC TCT CC

[a] "b" or "bc" superscripts in primer names indicate that the primers were designed from DNA sequences of the H2^{b} (C57BL/6) or H2^{bc} (129/SvJ) haplotypes, but this designation does not preclude cross-reactivity on the same or very similar genes in other haplotypes.
[b] Primers designated H2-Bl^{bc} ex3 R2 and H2-Bl^{bc} ex5 R were first described in Sipes et al (264) under the designations E3R and E5R, respectively.

Table 2.2 *Primers used for the PCR detection of T cell and NK cell receptors on IEL*

Primer Name	Sequence (5' to 3')
NaPi IIb F	CCT GGG ACC TGC CTG AAC T
NaPi IIb R	AAT GCA GAG CGT CTT CCC TTT
sprr-2a F	CTG GGC CTT GTC GTC CTG TCA T
sprr-2a R	CCT GTT GTG CTT CCC CTG GTG TA
CD3 ε F	ACT TTC TGG GGC ATC CTG TG
CD3 ε R	GCC GCT CCT TGT TTT GCC CTC TG
CD3 ζ F	TCA GCG CCT CCT TTT CTC CTC A
CD3 ζ R	TCT CCG CCT CTC GCC TTT TGT
CD103 F	CTG TGT CCG GTG GGT TAG ATT TCA
CD103 R	CAG GGT GGG GTT GGG GTA GTC
CD8 α F	CAC CGC CAG GAA GCT ACA ACT ACT
CD8 α R	CAG GGG ATG GGG GTG AGA T
CD8 β F	CCC CAC CCA GAG ACC CAG AAG
CD8 β R	CCA AGG CCC AGT CCA AGA AGA GTA
CD4 F	AAC TGG TTC GGC ATG ACA CTC TC
CD4 R	CAG GGG CCA CCA CTT GAA CTA C
TCR α*C* F[a]	TAC CCC AGT TCA GAC GTT CC
TCR α*C* R[a]	CAG CGT CAT GAG CAG GTT AA
TCR β*C* F[b]	ACA TCA GTG CAG ACC GGT G
TCR β*C* R[b]	CAC AGC ATA TAG GGT GGC CT
TCR γ*C* F	GGG CTT GAT TGC TGT CTT TG
TCR γ*C* R	CTG CTA GAG GGG CTG AGA GA
NK1.1 F	CTG GGC TCA TCC TCC TTG TCC T
NK1.1 R	CTC GGG GTT TCA TGG TTT AGT TCC
Ly49 univ F[c]	CTC TTG GAA TCT TCT GTT TCC TTC
Ly49 univ R[c]	TTC AGT TCA TCT TCA TCT TCT ATC TTC
Ly49 univ R2[c]	GAA ATA ATA ACA TTT AGT ACC ATA GCA GAA CC
Ly49A/B/G/Q F	GGA GGT CAC TTA TTC AAC TGT GAG ATT TC
Ly49A/B/C/E/F/G/J/Q R	TGA GCT GCC AGG GTA CTG AAC AC
Ly49C/E/F/J F	GAG GTC ACT TAC TCA ACT GTG AGA CTT C
Ly49D/H F	CAC TTT CCC AAC TAT GAG ATT CC
Ly49D/H R	CAA TGA GCT GCC AAG GAA CTC
CD94 F	GGC AGT TTC TAG GAT CAC TCG
CD94 R	CTT CCT GGA ATT CTA CAG TGG T
NKG2A F	ACT CAT TGC TGG TAC CCT GGG
NKG2A R	GAG GAC AAG GCT GTG CTG AAG
NKG2C/E F	ACC TGC TTG GAA CTG AAC AGG
NKG2C/E R	GCA AAA TTT TTG CAG TAG CCA TG
NKG2D F	ATT CGA TTC ACC CTT AAC ACA TTG
NKG2D R	CTT GAG CCA TAG ACA GCA CAG G

[a] NCBI UniSTS 144577

[a] NCBI UniSTS 144580

[c] univ - universal; specific for all known Ly49 sequences

Table 2.3 *Primers used for the real-time PCR detection of class Ib MHC*

Targeted cDNA	Primer Name	Sequence (5' to 3')
GAPDH [a]	*GAPDH* F2	AGG TCG GTG TGA ACG GAT TTG
	GAPDH R2	TGT AGA CCA TGT AGT TGA GGT CA
$\beta_2 m$	$\beta_2 m$ ex1 F2	CTC GGT GAC CCT GGT CTT TCT GG
	$\beta_2 m$ ex2 R2	GCG GGT GGA ACT GTG TTA CGT AGC
T23	*T23* [b] ex2 F	CAG AGT AAA CCT GAG GAC CC
	T23 [b] ex3 R	AGG CCT CCT GAC AAT ACC CG
Q1 canonical isoform	*Q1* ex2 F	GGC AGT GAG AAG AGA TTC CAA GAG AGC
	Q1 ex3 R	GCA GGT ACC CGC TTT GAA GGC
Q2	*Q2* ex2 F	GGA ACA CAC AGG TCT CCA AGG AAA ATG
	Q2 ex3 R	CCT CGG AGT AGG CTT CCG TCT GG
H2-Bl all isoforms	*H2-Bl* [bc] ex5 F	GTG ATC ATC ATT GAA GCT ATG GTG GC
	H2-Bl [bc] ex6 R	GGA GCT GTC AGG ATG CAG ATG ATC C
H2-Bl canonical isoform	*H2-Bl* ex3 F2	GGT GCT GCA GAG CTA TAC AAG TTC TAC C
	H2-Bl ex4 R	CTG GGA TGA TGG GTC ACA TGT GC
H2-Bl -33nt isoforms	*H2-Bl* -33nt ex1-2 F	GAG ACT CGC GCG GTG TTC CG
	H2-Bl ex2 R2	CCG GTC CCT CCT GTT CCA TCC
H2-Bl +33nt isoforms	*H2-Bl* [bc] 5'UTR/ex1 F1	CAG ATG CCC TGT ATT CCA AAT GG
	H2-Bl 3' ex1-2	CAT CGA GTG TGG GCC CGC GCG AG
H2-Bl $\alpha 1/\alpha 2$ isoforms	*H2-Bl* ex3 F2	GGT GCT GCA GAG CTA TAC AAG TTC TAC C
	H2-Bl ex3-5 R3	GGT TGA TGG AGG AGG CTC TGT GC
H2-Bl $\alpha 1/\alpha 3$ isoforms	*H2-Bl* ex2 F2	GGG AGC GGG AAA CAC AGA TCG
	H2-Bl ex2-4 R	CCT TTG GGG GAT CGC CCT TG
Tw5	*Tw5* ex5-6 F	GAA GAG CAA GAG AAA AAT AGG TGG AAA AGG
	Tw5 ex7 R	GAA GGC CTC CAG AAA CAA GGC AG
T3	*T3* ex5 F	ATG AGC GGA AGT GTT ATG ATG TGG ATG
	T3 ex6 R	GAC CCT CGG GCT GAA TCT GAC G

[a] Courtesy of William Renthal

Table 2.4 *Primers used for the FLAG epitope tagging of class Ib MHC*

Construct	Primer Name	Sequence (5' to 3')
flagQ1^{bc}	Q1^{b} 5'UTR/ex1 F	GGC CTC AGA TGC CCT GTA TTC
	flagQ1^{b} ex1 R	CTT GTC GTC GTC GTC CTT GTA GTC CGC TCC GGT TTT GGT CAG GG
	flagQ1^{b} ex2 F	GAC TAC AAG GAC GAC GAC GAC AAG GGC TCA CAC TCG CTG CGG TAT TTC
	Q1^{b}/Q2^{b} 3'UTR R	CTC AGT CTA CTC CAG GCA GCT GTC
flagQ1^{bc} α3	Q1^{b} 5'UTR/ex1 F	GGC CTC AGA TGC CCT GTA TTC
	flagQ1^{b} ex1 R	CTT GTC GTC GTC GTC CTT GTA GTC CGC TCC GGT TTT GGT CAG GG
	flagQ1^{b} ex4 F	GAC TAC AAG GAC GAC GAC GAC AAG GAC CCC CCA AAG GCA CAT G
	Q1^{b}/Q2^{b} 3'UTR R	CTC AGT CTA CTC CAG GCA GCT GTC
flagQ2^{bc}	Q2^{b} 5'UTR/ex1 F	TCA GAT GCC CTG TAT CCC AGA TGG
	flagQ2^{b} ex1 R	CTT GTC GTC GTC GTC CTT GTA GTC CGC GCG TGT CTC AGT CAG TTT C
	flagQ2^{b} ex2 F	GAC TAC AAG GAC GAC GAC GAC AAG GGC TCA CAC TCG CTG CGG TAT TTC
	Q2^{b} 3'UTR R	CAC CAG AGT GTC ACC TTT ACA ATT C
flagTw5^{bc}	Tw5^{bc} 5'UTR F	TCA GAC ATC CAG GAT CCC AG
	flagTw5^{bc} ex1 R	CTT GTC GTC GTC GTC CTT GTA GTC CGC GAG GGT TTC GGT CAG G
	flagTw5^{bc} ex2 F	GAC TAC AAG GAC GAC GAC GAC AAG GGC TCA CAC TCG ATG CGG TAT TTT G
	Tw5^{bc} 3'UTR R	CTT AAC TTC TGA GCC ATC TCT CC
flagH2-Bl^{q}	H2-Bl^{bc} 5'UTR/ex1 F1	CAG ATG CCC TGT ATT CCA AAT GG
	flagH2-Bl^{q} ex1 R	CTT GTC GTC GTC GTC CTT GTA GTC CGC GCG AGT CTG GAT CAT G
	flagH2-Bl^{bc} ex2 F	GAC TAC AAG GAC GAC GAC GAC AAG GGC CCA CAC TCG ATG CGA TAT TTC
	H2-Bl^{bc} 3'UTR R	ACT CCA CTA ATC AAC CCT CAG
flagH2-Bl^{bc}	H2-Bl^{bc} 5'UTR/ex1 F1	CAG ATG CCC TGT ATT CCA AAT GG
	flagH2-Bl^{bc} ex1 R	CTT GTC GTC GTC GTC CTT GTA GTC CGC GCG AGT CTC GAT CAT AGT C
	flagH2-Bl^{bc} ex2 F	GAC TAC AAG GAC GAC GAC GAC AAG GGC CCA CAC TCG ATG CGA TAT TTC
	H2-Bl^{bc} 3'UTR R	ACT CCA CTA ATC AAC CCT CAG
flagH2-Bl^{bc} -33nt	H2-Bl^{bc} 5'UTR/ex1 F1	CAG ATG CCC TGT ATT CCA AAT GG
	flagH2-Bl^{bc} ex1 R	CTT GTC GTC GTC GTC CTT GTA GTC CGC GCG AGT CTC GAT CAT AGT C
	flagH2-Bl^{bc} -33nt ex2 F	GAC TAC AAG GAC GAC GAC GAC AAG GTG TTC CGG CCC GGC C
	H2-Bl^{bc} 3'UTR R	ACT CCA CTA ATC AAC CCT CAG

Table 2.4 *Primers used for the FLAG epitope tagging of class Ib MHC, cont*

Construct	Primer Name	Sequence (5' to 3')
flagH2-Bl^{bc} α1/α3	H2-Bl^{bc} 5'UTR/ex1 F1	CAG ATG CCC TGT ATT CCA AAT GG
	flagH2-Bl^{bc} ex1 R	CTT GTC GTC GTC GTC CTT GTA GTC CGC GCG AGT CTC GAT CAT AGT C
	flagH2-Bl^{bc} ex2 F	GAC TAC AAG GAC GAC GAC GAC AAG GGC CCA CAC TCG ATG CGA TAT TTC
	H2-Bl^{bc} 3'UTR R	ACT CCA CTA ATC AAC CCT CAG
flagH2-Bl^{bc} α1/α3 - 33nt	H2-Bl^{bc} 5'UTR/ex1 F1	CAG ATG CCC TGT ATT CCA AAT GG
	flagH2-Bl^{bc} ex1 R	CTT GTC GTC GTC GTC CTT GTA GTC CGC GCG AGT CTC GAT CAT AGT C
	flagH2-Bl^{bc} -33nt ex2 F	GAC TAC AAG GAC GAC GAC GAC AAG GTG TTC CGG CCC GGC C
	H2-Bl^{bc} 3'UTR R	ACT CCA CTA ATC AAC CCT CAG
flagH2-Bl^{b} α1/α2	H2-Bl^{bc} 5'UTR/ex1 F1	CAG ATG CCC TGT ATT CCA AAT GG
	flagH2-Bl^{bc} ex1 R	CTT GTC GTC GTC GTC CTT GTA GTC CGC GCG AGT CTC GAT CAT AGT C
	flagH2-Bl^{bc} ex2 F	GAC TAC AAG GAC GAC GAC GAC AAG GGC CCA CAC TCG ATG CGA TAT TTC
	H2-Bl^{bc} 3'UTR R	ACT CCA CTA ATC AAC CCT CAG

or until the dye front traveled about 2/3 of the length of the gel. It was then stained with 5 μg/mL ethidium bromide in RNase free water with gentle agitation at room temperature for 20-30 minutes, destained in RNase free water under the same conditions as the staining, and visualized for 18S and 28S rRNA under UV light to ensure uniform sample loading and RNA quality. To remove the formaldehyde, the gel was soaked in RNase-free water for 1 hour with agitation, changing the water every 20 minutes. It was then equilibrated in 20X SSC (3 M sodium choloride, 0.3 M sodium citrate in RNase-free water) for 15 minutes with gentle agitation.

The Schleicher & Schuell Turboblotter® downward transfer system (Whatman, Kent, UK) was used according to the manufacturer's protocols to transfer RNA from the gel to the included NYTRAN® SuPerCharge membrane. After transfer, the membrane was gently rocked in a washing solution of 2X SSC for 5 minutes. It was then placed on a fresh sheet of dry GB002 blotting paper to remove any excess 2X SSC buffer. The RNA was crosslinked to the nylon membrane using a Stratalinker UV Crosslinker (Stratagene, La Jolla, CA) set to 120 mJ/cm^2 for 5 minutes. The efficiency of the transfer was checked by placing the gel under UV light and comparing with the pretransfer picture.

While crosslinking was in progress, one of three radiolabeled probes (H2-Bl 3' UTR, H2-Bl ex1-ex2 or β-actin) was generated by PCR. Plasmid DNA containing the 3' UTR of H2-Bl (pCR II_H2-Bl 3'UTR, see below) or small intestinal cDNA from a 129/SvJ mouse (H2-Bl exon 2 and β-actin probes) was used as the template in a PCR reaction containing 40 μM dGTP, 40 μM dTTP, 40 μM dCTP, 3 μM dATP and 1 μM α^{32}P-dATP. Primers used to amplify the 3' UTR H2-Bl probe were forward 5'-AAT

CTT TGA GCT GAG GGT TGA TTA G-3' and reverse 5'-TGT TGC CAT TTA TTT CTG CTT CAG C-3', designed by J. McLean (UT Southwestern, Dallas, TX). Primers used to amplify the H2-Bl ex1-ex2 probe were forward 5'-CAG ATG CCC TGT ATT CCA AAT GG-3' and reverse 5'-CCT TGC TCT GGT TGT AGT AGT G-3'. Primers used to amplify the β-actin probe were forward 5'-AGC CAT GTA CGT AGC CAT CC-3' and reverse 5'-ACT CAT CGT ACT CCT GCT TGC T-3', a suggestion of C. Nguyen and gift of Dr. W. Wakeland (UT Southwestern, Dallas, TX). PCRs were performed with HotStarTaq® DNA Polymerase (Qiagen, Valencia, CA) according to the manufacturer's protocols. Thermocycling was performed using a PTC-200 Peltier Thermal Cycler (MJ Research, Waltham, MA) with an initial 15 minute 95°C step followed by 30 cycles with a 30 second 94°C denaturing step, a 30 second 52°C annealing step and a 60 second 72°C extension step. After a final 7 minute 72°C extension, the PCR was brought to 4°C until ready to purify from free dNTPs.

Probe purification was performed using Bio-Spin columns with Bio-Gel P-6 in SSC (BioRad, Hercules, CA) according to the manufacturer's recommendations. The incorporation of radionucleotides into the probe was measured by scintillation counting on an LS 6500 Multi-Purpose Scintillation Counter (Beckman Coulter, Fullerton, CA). 0.5 µL 100 mM sodium hydroxide was added to 49.5 µL of the probe for a final concentration of 1 mM, and the double-stranded DNA probe was denatured by boiling for 10 minutes and placed immediately on ice.

Following crosslinking, the membrane was prehybridized at 42˚C for 30 minutes with enough Ultrahyb buffer (Ambion) to keep the membrane uniformly wet (about 6-10 mL depending on the size of the membrane and the hybridization bottle) plus 100 µL pre-

boiled herring sperm DNA at 10 mg/mL (Invitrogen) to reduce non-specific binding of the probe to the membrane. Due to the usually low radioactivity of the purified probe, all 50 μL was added to the hybridization tube and allowed to hybridize to the RNA-crosslinked membrane overnight in a GeneMate™ H06000V Autoblot Mini Hybridization Oven (Bellco Glass, Inc., Vineland, NJ) at 48˚C.

Before detection of the hybridized probe, the membrane was washed repeatedly to reduce non-specific hybridization. The membrane was first rinsed in approximately 40 mL preheated low stringency wash buffer (2X SSC in 0.1% SDS at 48°C). It was then washed in the hybridization oven twice for 5 minutes at 48°C in approximately 25 mL low stringency wash buffer, followed by two further washes for 15 minutes in high stringency wash buffer (0.1X SSC in 0.1% SDS). The fully washed membrane was placed on a piece of filter paper dampened with high stringency wash buffer, covered with plastic wrap, placed in a developing cassette with X-Omat AR film (Kodak, Rochester, NY) and exposed at -80°C for various amounts of time. The film was then developed using a SRX-101A Medical Film Processor (Konika, Tokyo, Japan).

For hybridization with another probe, the RNA-conjugated membrane was stripped of its first probe in a 50 mL conical centrifuge tube. The membrane was first rinsed once with room temperature water. It was then boiled for 5 minutes in 1% SDS, then in 0.5% SDS for another 5 minutes. The membrane was washed two final times for 5 minutes in boiling water. All wash volumes were approximately 40 mL. Finally, the membrane was wet with room temperature water, checked for residual radioactivity with a Geiger counter and placed in a cassette with film as before to ensure no residual probe remained. The membrane was then treated as above with a second probe.

Reverse Transcription and PCR

Semi-quantitative RT-PCR was performed as follows. 2 μg total mRNA was reverse transcribed to cDNA using an Omniscript® RT kit (Qiagen, Valencia, CA) and oligo-dT primers. 2 μL of this 20 μL cDNA reaction was used in each RT-PCR requiring primers in the 3' UTR and 5' UTR of the transcript. 1 μL cDNA was used in all other RT-PCR reactions unless otherwise noted. Where genomic DNA was PCR amplified, 90 ng DNA was used as the template. All PCR amplification was performed using either HotStarTaq® DNA Polymerase (Qiagen) or Platinum® Taq DNA Polymerase High Fidelity (Invitrogen) according to the manufacturer's protocols on a PTC-200 Peltier Thermal Cycler (MJ Research) or a GeneAmp® PCR System 9700 (Applied Biosystems, Foster City, CA). Primer pairs for all MHC genes used in RT-PCR reactions spanned at least one intron, and PCRs controlling for genomic DNA contamination of RNA samples were performed using a 10-fold excess of total RNA as a template. All PCR reactions were performed at an annealing temperature of 55°C with a 90 second extension time. The number of cycles was adjusted individually for each experiment and is described in the accompanying figure legend.

Less than 2 μg of RNA was used to generate cDNA for RT-PCR analysis of IEL and IEC transcription due to the small number of IEL recovered from the FACS sort (see RNA and DNA Isolation, above). IEC RNA was diluted to the approximate concentration of the IEL RNA sample by comparing volume-corrected cell equivalents of RNA (volume of IEC ≈ 1.84 x volume IEL; see Appendix A) and titrating cDNA for

similar glyceraldehyde-3-phosphate dehydrogenase (GAPDH) PCR amplification. The number of cycles used for PCR was then recalibrated for each primer set to ensure signal intensity in the linear range of an agarose gel.

PCR Quantitation by Densitometry

RT-PCR reactions were resolved on a 1 – 1.2% agarose gel containing ethidium bromide with 1kb DNA or 1kb DNA Plus molecular weight standards (Invitrogen). DNA bands were visualized under UV light and photographed using a Gel Doc 1000 and MultiAnalyst imaging software (BioRad). Tiff images were inverted in ImageJ software (NIH, http://rsb.info.nih.gov/ij/) and background was subtracted with a rolling ball radius of 50. Measurements of internal pixel density were taken over a given area to obtain mean internal density (MID). MID for each band was subtracted from the gel background MID. Background-subtracted MIDs from each sample were then divided by the background-subtracted MID of the GAPDH band amplified from the same cDNA to obtain signal/GAPDH quantities, the y-axis value in all densitometry plots unless otherwise stated. In RT-PCR experiments analyzing cephalocaudal expression of class Ib MHC and NK and T cell markers, linear regression was performed on signal/GAPDH densitometric values using the Pearson's correlation coefficient.

Real-time PCR

Quantitative PCR (qPCR) was performed as follows. 2 μg total mRNA was reverse transcribed to cDNA using an Omniscript® RT kit (Qiagen) and oligo-dT primers. cDNA was diluted 1:5 to 1:25 in autoclaved deionized (di)H_2O, and 5 μL was used in each qPCR reaction with forward and reverse primers (Table 2.3) at a final concentration of 70 nM. Primers were chosen based upon their amplification of a single species by RT-PCR, specificity, as determined by sequencing amplification products, and uniform dissociation curve. Isoform-specific primers were further vetted by checking their cross-reactivity in an RT-PCR reaction with pCR II cloned cDNA of other isoforms. $K^{b-/-}D^{b-/-}$ small intestinal and splenic cDNAs were used as positive and negative controls for gut-specific class Ib MHC, respectively. A 1:5 serial dilution of $K^{b-/-}D^{b-/-}$ small intestinal cDNA containing 50 ng RNA was used to establish a standard curve for quantitation. All qPCR reactions were performed in triplicate with ABsolute™ qPCR SYBR® Green ROX Mix (Thermo Fisher Scientific, Inc., Waltham, MA) or iTaq™ SYBR® Green Supermix with ROX (BioRad) on a 7300 Real Time PCR System (Applied Biosystems) according to the manufacturer's protocols.

The relative standard curve method, as described in Bookout et al (265), was used to analyze qPCR data. Briefly, a threshold was chosen in the linear range of the product amplification plot (cycle number versus the change in normalized reporter signal [ΔRn]) for all reactions performed with a given primer. The average and standard deviation message quantities for each triplicate reaction (as interpolated from the standard curve by the 7300 System SDS Software [Applied Biosystems]) were exported in a tab-delimited text file for analysis in Microsoft® Excel (Microsoft, Redmond, WA). Outliers (with a coefficient of variation [standard deviation/average] > 17%) were

removed, and the message quantity for each sample was normalized to the GAPDH message quantity for that cDNA (signal/GAPDH). Finally, the standard deviation of the normalized value was calculated, and the data was reported in bar graph format.

Molecular Cloning

PCR products were separated on an agarose gel, and individual bands were extracted using a QIAquick® Gel Extraction Kit (Qiagen). This purified DNA was then integrated into the pCR II vector using the TA Cloning® Kit (Invitrogen) according to the manufacturer's protocols. Plasmid DNA was isolated using a QIAfilter® Plasmid Midi Kit (Qiagen).

N-Terminal FLAG Epitope Tagging of Class Ib MHC

Due to the lack of antibodies that will recognize gut-specific class Ib MHC, constructs were created to insert an N-terminal FLAG epitope tag (DYKDDDDK) between the co-translationally cleaved leader peptide and α1 domain of the class Ib MHC transcripts under study according to a strategy reported in Fulton et al (266). For each individual class Ib MHC, pCR II-cloned cDNA was used as the template in two separate PCR reactions. In the first PCR, the forward primer originally used to clone the cDNA and a reverse primer encoding the reverse complement of the FLAG epitope followed by the 3' end of exon 1 were used to amplify the 5' fragment of the FLAG construct (5' UTR-exon 1-FLAG) (Figure 2.1). In the second PCR, a forward primer encoding the

A

1st PCR

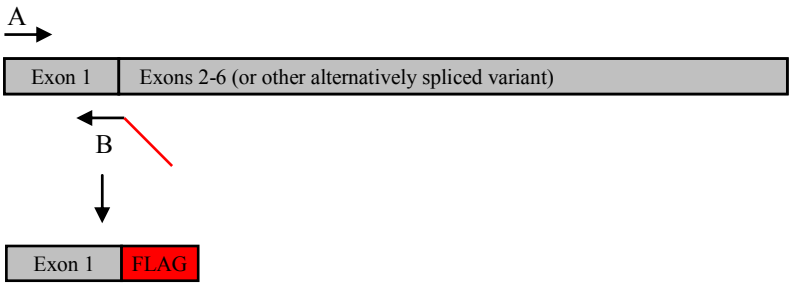

2nd PCR

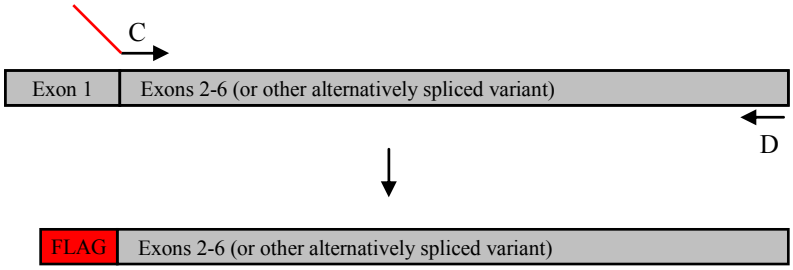

3rd PCR

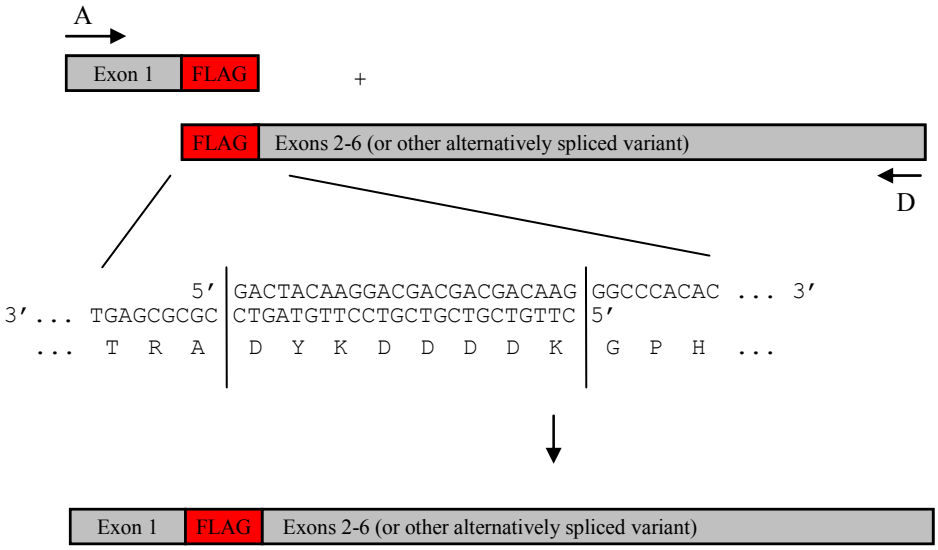

B

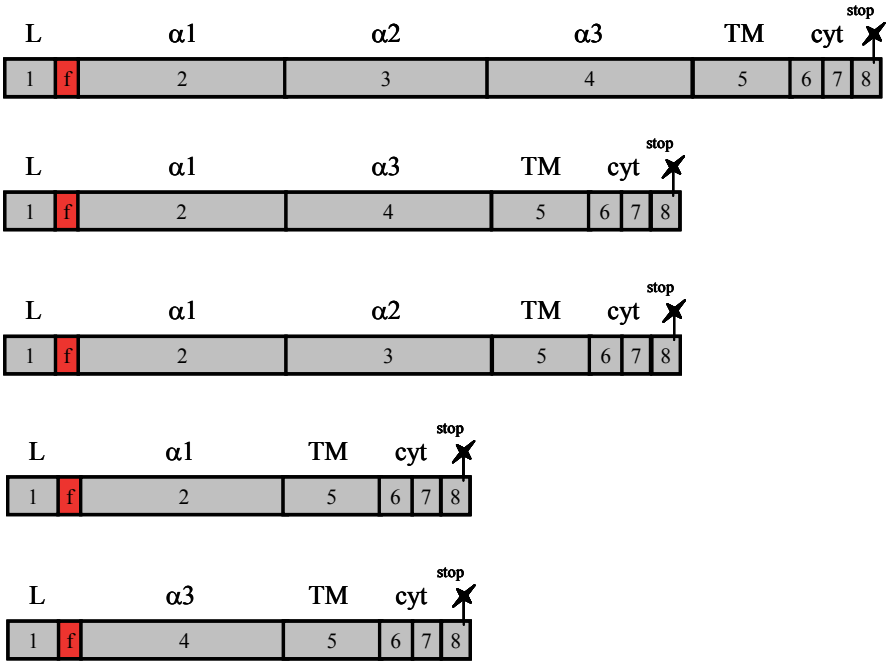
L
α1
α2
α3
TM
cyt
stop
1
f
2
3
4
5
6
7
8
L
α1
α3
TM
cyt
stop
1
f
2
4
5
6
7
8
L
α1
α2
TM
cyt
stop
1
f
2
3
5
6
7
8
L
α1
TM
cyt
stop
1
f
2
5
6
7
8
L
α3
TM
cyt
stop
1
f
4
5
6
7
8

C

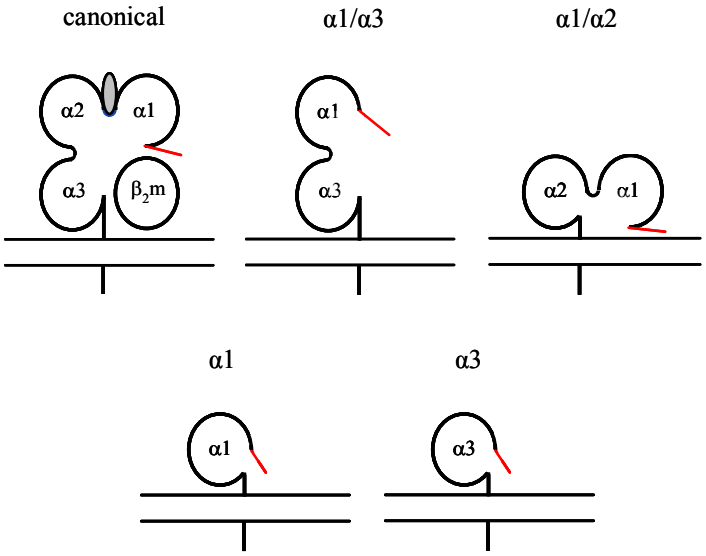
canonical
α1/α3
α1/α2
α2
α1
α3
β2m
α1
α3
α2
α1
α1
α3
α1
α3

Figure 2.1 N-terminally FLAG-tagged class Ib MHC. A. Generation of FLAG-tagged class Ib MHC by PCR. In the first and second PCRs, primers complementary to the 5'UTR (A) and 3'UTR (D) of the class Ib MHC of interest were paired with primers specific for the exon 1-2 (or exon 1-4) junction with a 5' end encoding the FLAG epitope (B & C, see Table 2.4 for a listing of primers). In a third, SOEing PCR reaction, the complementary regions of the FLAG-tagged DNAs generated in the previous reactions acted as primers to "splice" together the two segments into a single, FLAG-tagged construct (see text for details). B. Schematic representation of mRNAs generated from FLAG-tagged constructs. The FLAG epitope is positioned between exons 1 and 2 (or 4) of the class Ib MHC cDNA. C. Putative N-terminally FLAG-tagged class Ib MHC proteins. Upon co-translational cleavage of the leader peptide, it is expected that the hydrophilic N-terminal FLAG tag will be solvent-exposed and detectable using anti-FLAG antibodies.

FLAG epitope followed by the 5' end of exon 2 and the reverse primer originally used in cloning the cDNA were used to generate the 3' end of the construct (FLAG-exon2-…-3' UTR) (see Figure 2.1). Both PCRs were amplified over 26 cycles using Platinum® Taq DNA Polymerase High Fidelity (Invitrogen). These two PCR products were purified by gel electrophoresis on a 1% agarose gel and isolated from the gel using a QIAquick® Gel Extraction Kit (Qiagen). In a third, SOEing ("splicing" by overlap extension) PCR reaction (267), equal molar ratios of the fragments generated in the first two PCRs were combined with 5 μM of the forward and reverse primers originally used in cloning the wild type cDNA. After PCR amplification with Platinum® Taq (Invitrogen) for 26 cycles, the final epitope-tagged construct was cloned into pCR II, sequenced and subcloned into expression vectors as described below.

Generation of Mammalian Expression Constructs

For transient expression in mammalian cells, cDNAs (each containing its own stop codon) were placed under the CMV promoter of pcDNA™ 3.1/*myc*-His (-) A (pcDNA3.1N; Invitrogen, Carlsbad, CA), without expression of the C-terminal epitope tag. For generating stable cell lines, cDNAs were cloned into pEFIRES-P, an expression vector in which the multiple cloning site (MCS) is 5' to an internal ribosomal entry site (IRES) that precedes a puromycin resistance gene. The bicistronic message created by cloning the cDNA of interest into the MCS is driven by the elongation factor 2 (EF2) promoter. This pEFIRES-P vector was the kind gift of Dr. V. Garcia (UT Southwestern, Dallas, TX).

cDNA for both pcDNA3.1N and pEFIRES-P expression vectors were excised from pCR II constructs (described above) using pCR II EcoR I sites flanking the insert. pcDNA3.1N and pEFIRES-P MCS were digested with EcoR I and dephosphorylated with shrimp alkaline phosphatase (Roche, Basel, Switzerland). EcoR I-digested vectors and inserts were then purified by agarose gel electrophoresis, extracted from the gel using a QIAquick® Gel Extraction Kit (Qiagen) and ligated with one another at a 1:1 molar ratio using T4 DNA ligase (Invitrogen) overnight at 15°C. Electrically or chemically competent DH5α *Escherichia coli* (Invitrogen) were then transformed with the DNA constructs according to the manufacturer's instructions. Transformants were plated on Luria-Bertani (LB) agar plates (268) with 50 µg/mL ampicillin (Sigma-Aldrich) and cultured overnight at 37°C. Ampicillin resistant colonies were cultured overnight in 1 mL Terrific Broth (268) on a 225 rpm shaker at 37°C, and plasmid DNA was isolated the following day as follows. Bacteria were pelleted from culture media by centrifugation at 6000 x g for 5 minutes, resuspended in a solution of 0.1 M NaCl, 10 mM Tris-HCl, pH

8.0, 1 mM EDTA, pH 8.0, 5% Triton x-100 (STET) with 0.625 mg/mL lysozyme and 62.5 µg/mL RNase A and boiled for 45 seconds. Cell debris was pelleted by centrifugation at 24,000 x g for 10 minutes at room temperature and removed from the microfuge tube using a toothpick. Plasmid DNA was precipitated from the lysate by adding 1/10 volume of 5M sodium acetate, pH 5.2 and ½ volume 100% isopropanol and centrifuging at 24,000 x g for 30 minutes at room temperature. After decanting the acid/alcohol mixture, the DNA preparation was incubated at 37°C for 20 minutes to dry the pellet, then resuspended in 10 mM Tris-HCl, pH 8.0. 1/5 of this preparation was digested with EcoR I to confirm insertion of the cDNA and one of several restriction endonucleases to determine orientation (Table 2.5). Constructs were further examined for identity and orientation by sequencing using T7 (5'-TAA TAC GAC TCA CTA TAG GG-3') and BGH (5'-TAG AAG GCA CAG TCG AGG-3') primers for pcDNA3.1N constructs and pEF F (5'-TCT CAA GCC TCA GAC AGT GGT TC-3') and pEFIRES R (5'-GGC CGC CCG GGT CG-3') primers for pEFIRES-P. Finally, pcDNA3.1N constructs were isolated from 25 mL overnight LB/ampicillin cultures using Plasmid Midi Kits (Qiagen). pEFIRES-P constructs were isolated from 3 mL overnight LB/ampicillin cultures using E.Z.N.A.® Plasmid Mini Kits (Omega Bio-Tek, Norcross, GA).

DNA Sequence Analysis

DNA sequences were generated using BigDye® Terminator v3.0 Cycle Sequencing and 3100 and 3730 capillary analyzers (Applied Biosystems). Where PCR-

Table 2.5 *pEFIRES-P mammalian expression vector orientation determination by restriction endonuclease digestion.*

Construct Name (vector_insert)	cDNA Splicing Variant	Insert Length (bp)	Restriction Enzyme	Insert Cut Sites (bp)	pEFIRES-P[a] Cut Sites (bp)	Construct Size (bp)	Orientation-Specific Bands (bp)				Clone Number
							Forward Orientation		Reverse Orientation		
pEFIRES-P_D[bc]	n.a.	1185	Not I	68	1457	6874	1124	5750	75	6799	1-1
pEFIRES-P_T3[bc]	n.a.	1215	Pst I	342	1200	6904	592	6312	1123	5781	3-1
pEFIRES-P_Q1[bc]	Q1.1	1105	Apa I	721	1440	6794	721	6073	384	6410	4-3
pEFIRES-P_Q1[bc] α3	Q1.2	559	Apa I	175	1440	6248	175	6073	384	5864	11-22
pEFIRES-P_Q2[bc]	n.a.	1150	Apa I	717	1440	6839	717	6122	433	6406	5-10
pEFIRES-P_Tw5[bc]	n.a.	1262	BamH I	23	3020	6951	2809	4142	1593	5358	12-1
pEFIRES-P_H2-Bl[bc]	H2-Bl.1	1209	Not I	70	1457	6898	1146	5752	77	6821	11-2
pEFIRES-P_H2-Bl[q]	H2-Bl.1	1209	Apa I	106, 146, 717	1440	6898	106	6181	492	5795	9-1
pEFIRES-P_H2-Bl[bc] -33nt	H2-Bl.1a	1176	Not I	70	1457	6865	1113	5752	77	6788	13-2
pEFIRES-P_H2-Bl[bc] α1/α3	H2-Bl.2	932	Not I	70	1457	6621	869	5752	77	6544	15-5
pEFIRES-P_H2-Bl[bc] α1/α3 -33nt	H2-Bl.2a	899	Not I	70	1457	6588	836	5752	77	6511	13-2
pEFIRES-P_H2-Bl[b] α1/α2	H2-Bl/B6.2	933	Not I	70	1457	6622	870	5752	77	6545	7-1
pEFIRES-P_Q10[b] (1st ATG)	Q10.1 (1st ATG)	1472	BamH I	19	3020	7161	3023	4138	1589	5572	19-2
pEFIRES-P_Q10[b] α3 (1st ATG)	Q10.3 (1st ATG)	913	Apa I	155	1440	6602	155	6447	758	5844	21-7
pEFIRES-P_Q10[b] α3 (2nd ATG)	Q10.3 (2nd ATG)	904	Apa I	146	1440	6593	146	6447	758	5835	22-1
pEFIRES-P_Q10.GPI[b]	n.a.	1050	BamH I	19	3020	6739	2601	4138	1589	5150	23-1
pEFIRES-P_Q5[k]	Q5.1	1050	Apa I	687	1440	6739	687	6052	363	6376	8-4
pEFIRES-P_Q5[k] α1/α3	Q5.2	774	Pst I	504	1200	6463	754	5709	520	5943	29-2
pEFIRES-P_Q5[k] α1	Q5.3	474	Xho I/Acc I	155	1445	6163	155	6008	319	5844	30-4
pEFIRES-P_flagQ1[bc]	Q1.1	1129	Apa I	745	1440	6818	745	6073	384	6434	4-2
pEFIRES-P_flagQ1[bc] α3	Q1.2	583	Apa I	175	1440	6272	175	6097	408	5864	5-1
pEFIRES-P_flagQ2[bc]	n.a.	1174	Apa I	741	1440	6863	741	6122	433	6430	6-3
pEFIRES-P_flagTw5[bc]	n.a.	1286	BamH I	47	3020	6975	2809	4166	1617	5358	8-1
pEFIRES-P_flagH2-Bl[q]	H2-Bl.1	1233	Apa I	130, 170, 741	1440	6922	130	6181	492	5819	1-1
pEFIRES-P_flagH2-Bl[bc]	H2-Bl.1	1233	Not I	70	1457	6922	1170	5752	77	6845	10-4
pEFIRES-P_flagH2-Bl[bc] -33nt	H2-Bl.1a	1200	Not I	70	1457	6889	1137	5752	77	6812	2-3
pEFIRES-P_flagH2-Bl[bc] α1/α3	H2-Bl.2	956	Not I	70	1457	6645	893	5752	77	6568	16-3
pEFIRES-P_flagH2-Bl[bc] α1/α3 -33nt	H2-Bl.2a	923	Not I	70	1457	6612	860	5752	77	6535	3-3
pEFIRES-P_flagH2-Bl[b] α1/α2	H2-Bl/B6.2	957	Not I	70	1457	6646	894	5752	77	6569	18-3
pEFIRES-P_flagQ10[b] (1st ATG)	Q10.1 (1st ATG)	1496	BamH I	43	3020	7185	3023	4162	1613	5572	20-1
pEFIRES-P_flagQ10.GPI	n.a.	1074	BamH I	43	3020	6763	2601	4162	1613	5150	24-1
pEFIRES-P_flagQ5[k] α1/α3	Q5.2	798	Pst I	528	1200	6487	778	5709	520	5967	9-9
pEFIRES-P_flagQ5[k] α1	Q5.3	498	Xho I/Acc I	179	1445	6187	179	6008	319	5868	10-5

Table 2.5 *pEFIRES-P mammalian expression vector orientation determination by restriction endonuclease digestion, cont.*

Construct Name (vector_insert)	cDNA Splicing Variant	Insert Length (bp)	Restriction Enzyme	Insert Cut Sites (bp)	pEFIRES-P[a] Cut Sites (bp)	Construct Size (bp)	Orientation-Specific Bands (bp)				Clone Number
							Forward Orientation		Reverse Orientation		
pEFIRES-P_flag mQ9[b]	Q9.1	1020	Not I	32	1457	6709	995	5714	39	6670	15-3
pEFIRES-P_flag mQ9[b] α1/α2	Q9.3	744	Not I	32	1457	6433	719	5714	39	6394	16-1
pEFIRES-P_flag mQ9[b] α3	Q9.7	474	Not I	32	1457	6163	449	5714	39	6124	18-1

[a] The EcoR I site used for insertion is positioned at ~1450 bp in the pEFIRES-P sequence. Vector cut sites are approximate.

[b] Q10.GPI is an artifical, membrane-bound hybrid of Q10 exons 1-4 and Q9 exons 5-6.

amplified cDNA was sequenced, the primers used in the amplification were also used for sequencing. Where cloned PCR products were sequenced, M13 (-20) (5'-GTA AAA CGA CGG CCA G-3') and M13 reverse (5'-CAG GAA ACA GCT ATG AC-3') primers were used. Sequence alignments were performed using the ClustalV function (269) in Lasergene® v5 MegAlign™ software (DNASTAR, Inc., Madison, WI). Amino acid and molecular weight predictions were performed with Lasergene® v5 EditSeq™ software. Similarity searches were performed by BLASTN analysis (NCBI, http://blast.ncbi.nlm.nih.gov/Blast.cgi). DNA sequences of class I MHC cloned cDNAs were submitted to GenBank (AY989821-AY989882; Table 2.6).

Transfections

Transient transfections were performed as follows. B78H1 and its derivatives were plated on 6 well plates (9.5 cm^2) at $0.2x10^6$ cells per well in 1 mL culture media the day before the transfection. Transfections were performed with Fugene 6 (Roche) according to the manufacturer's protocols approximately 16 hours after plating (when the cells were 50-70% confluent). In brief, the Fugene 6 transfection reagent and GIBCO™ OptiMEM I (Invitrogen) media were removed from storage at 4^oC and allowed to come to room temperature for 30 minutes to 2 hours. 2 µg plasmid DNA (2 µg pcDNA3.1_X or 1 µg pcDNA3.1_X + 1 µg pcDNA1_TAP2 [X indicating the cDNA under study]) was aliquoted to a sterile 1.5 mL microcentrifuge tube. 200 µL OptiMEM I was added to a separate microcentrifuge tube, and 10 µL Fugene 6 was added to the center of the media. The OptiMEM I/Fugene 6 was tapped to mix and allowed to incubate at room

Table 2.6 *Detailed listing of sequences from gut-restricted class Ib MHC in wild-derived and inbred strains of mice by GenBank Accession Number*

Gene Name	Splicing Variant	Inclusive Regions[a]	Molecule Type	Sequence Type	Mouse	GenBank Name	Accession Number
H2-Bl^{b}	H2-Bl.1	ex1-2-3-4-5-6	cDNA	clone combined	C57BL/6J	Mus musculus blastocyst MHC (H2-Bl.1) C57BL/6J mRNA, complete cds.	AY989821
	H2-Bl.1a	ex1-p2-3-4-5-6	cDNA	clone combined	C57BL/6J	Mus musculus blastocyst MHC (H2-Bl.1a) C57BL/6J mRNA, complete cds.	AY989822
	H2-Bl/B6.1	ex1-2-p3-4-5-6	cDNA	clone combined	C57BL/6J	Mus musculus blastocyst MHC (H2-Bl/B6.1) C57BL/6J mRNA, complete cds.	AY989823
	H2-Bl.2	ex1-2-4-5-6	cDNA	clone combined	C57BL/6J	Mus musculus blastocyst MHC (H2-Bl.2) C57BL/6J mRNA, complete cds.	AY989824
	H2-Bl.2a	ex1-p2-4-5-6	cDNA	clone combined	C57BL/6J	Mus musculus blastocyst MHC (H2-Bl.2a) C57BL/6J mRNA, complete cds.	AY989825
	H2-Bl/B6.2	ex1-2-3-5-6	cDNA	clone combined	C57BL/6J	Mus musculus blastocyst MHC (H2-Bl/B6.2) C57BL/6J mRNA, complete cds.	AY989826
	H2-Bl/B6.2a	ex1-p2-4-5-6	cDNA	clone combined	C57BL/6J	Mus musculus blastocyst MHC (H2-Bl/B6.2a) C57BL/6J mRNA, complete cds.	AY989827
	H2-Bl/B6.3a	ex1-p2-p4-3'UTR	cDNA	clone combined	C57BL/6J	Mus musculus blastocyst MHC (H2-Bl/B6.3a) C57BL/6J mRNA, complete cds.	AY989828
	H2-Bl/B6.4a	ex1-p2-p5-6	cDNA	clone combined	C57BL/6J	Mus musculus blastocyst MHC (H2-Bl/B6.4a) C57BL/6J mRNA, complete cds.	AY989829
	H2-Bl/B6.5a	ex1-p2-3'UTR	cDNA	clone combined	C57BL/6J	Mus musculus blastocyst MHC (H2-Bl/B6.5a) C57BL/6J mRNA, complete cds.	AY989830
	H2-Bl/B6.5b	ex1-p2-3'UTR	cDNA	clone combined	C57BL/6J	Mus musculus blastocyst MHC (H2-Bl/B6.5b) C57BL/6J mRNA, complete cds.	AY989831
	H2-Bl/B6.6a	ex1-p4-5-6	cDNA	clone combined	C57BL/6J	Mus musculus blastocyst MHC (H2-Bl/B6.6a) C57BL/6J mRNA, complete cds.	AY989832
	H2-Bl/B6.7	ex1-5-6	cDNA	clone combined	C57BL/6J	Mus musculus blastocyst MHC (H2-Bl/B6.7) C57BL/6J mRNA, complete cds.	AY989833
	H2-Bl/B6.7a	pex1-p5-6	cDNA	clone combined	C57BL/6J	Mus musculus blastocyst MHC (H2-Bl/B6.7a) C57BL/6J mRNA, complete cds.	AY989834
	H2-Bl/B6.7b	pex1-p5-6	cDNA	clone combined	C57BL/6J	Mus musculus blastocyst MHC (H2-Bl/B6.7b) C57BL/6J mRNA, complete cds.	AY989835
	H2-Bl/B6.8a	pex1-3'UTR	cDNA	clone combined	C57BL/6J	Mus musculus blastocyst MHC (H2-Bl/B6.8a) C57BL/6J mRNA, complete cds.	AY989836
	H2-Bl/B6.8b	pex1-3'UTR	cDNA	clone combined	C57BL/6J	Mus musculus blastocyst MHC (H2-Bl/B6.8b) C57BL/6J mRNA, complete cds.	AY989837
H2-Bl^{bc}	H2-Bl.1	ex1-2-3-4-5-6	cDNA	clone combined	129/SvJ	Mus musculus blastocyst MHC (H2-Bl.1) 129/SvJ mRNA, complete cds.	AY989838
	H2-Bl.1a	ex1-p2-3-4-5-6	cDNA	clone combined	129/SvJ	Mus musculus blastocyst MHC (H2-Bl.1a) 129/SvJ mRNA, complete cds.	AY989839
	H2-Bl.2	ex1-2-4-5-6	cDNA	clone combined	129/SvJ	Mus musculus blastocyst MHC (H2-Bl.2) 129/SvJ mRNA, complete cds.	AY989840
	H2-Bl.2a	ex1-p2-4-5-6	cDNA	clone combined	129/SvJ	Mus musculus blastocyst MHC (H2-Bl.2a) 129/SvJ mRNA, complete cds.	AY989841
	H2-Bl.1	ex1-2-3-4-5-6	cDNA	clone combined	ICR 5	Mus musculus blastocyst MHC (H2-Bl.1) ICR5 mRNA, complete cds.	AY989842
	H2-Bl.1a	ex1-p2-3-4-5-6	cDNA	clone combined	ICR 5	Mus musculus blastocyst MHC (H2-Bl.1a) ICR5 mRNA, complete cds.	AY989843
	H2-Bl.1	ex1-2-3-4-5-6	cDNA	clone combined	ICR 7	Mus musculus blastocyst MHC (H2-Bl.1) ICR7 mRNA, complete cds.	AY989844
	H2-Bl.1a	ex1-p2-3-4-5-6	cDNA	clone combined	ICR 7	Mus musculus blastocyst MHC (H2-Bl.1a) ICR7 mRNA, complete cds.	AY989845
	H2-Bl.2	ex1-2-4-5-6	cDNA	clone combined	ICR 5	Mus musculus blastocyst MHC (H2-Bl.2) ICR5 mRNA, complete cds.	AY989846
	H2-Bl.2a	ex1-p2-4-5-6	cDNA	clone combined	ICR 8	Mus musculus blastocyst MHC (H2-Bl.2a) ICR8 mRNA, complete cds.	AY989847
	H2-Bl.2a	ex1-p2-4-5-6	cDNA	clone combined	$K^{b-/-}D^{b-/-}$	Mus musculus blastocyst MHC (H2-Bl.2a) B6.Kb-/-Db-/- mRNA, complete cds.	AY989848
	n.a.	ex1-int1-ex2-int2-pex3	genomic DNA	direct	129/SvJ	Mus musculus blastocyst MHC (H2-Bl) 129/SvJ exons 1 - 3 and partial cds.	AY989849
H2-Bl^{q}	H2-Bl.1	ex1-2-3-4-5-6	cDNA	clone combined	ICR 3	Mus musculus blastocyst MHC (H2-Bl.1) ICR3 mRNA, complete cds.	AY989850
	H2-Bl.1	ex1-2-3-4-5-6	cDNA	clone combined	ICR 6	Mus musculus blastocyst MHC (H2-Bl.1) ICR6 mRNA, complete cds.	AY989851
	H2-Bl.1	ex1-2-3-4-5-6	cDNA	clone combined	ICR 8	Mus musculus blastocyst MHC (H2-Bl.1) ICR8 mRNA, complete cds.	AY989852
	H2-Bl.1a	ex1-p2-3-4-5-6	cDNA	clone combined	ICR 3	Mus musculus blastocyst MHC (H2-Bl.1a) ICR3 mRNA, complete cds.	AY989853
	H2-Bl.1a	ex1-p2-3-4-5-6	cDNA	clone combined	FVB/NJ	Mus musculus blastocyst MHC (H2-Bl.1a) FVB/NJ mRNA, complete cds.	AY989854
	n.a.	ex1-int1-ex2-int2-pex3	genomic DNA	direct	FVB/NJ	Mus musculus blastocyst MHC (H2-Bl) FVB/NJ exons 1 - 3 and partial cds.	AY989855
H2-Bl^{k}	H2-Bl.2	ex1-2-4-5-6	cDNA	clone combined	C3H/HeJ	Mus musculus blastocyst MHC (H2-Bl.2) C3H/HeJ mRNA, complete cds.	AY989856
	H2-Bl.2a	ex1-p2-4-5-6	cDNA	clone combined	C3H/HeJ	Mus musculus blastocyst MHC (H2-Bl.2a) C3H/HeJ mRNA, complete cds.	AY989857
H2-Bl BIK	n.a.	ex2-int2-ex3	genomic DNA	direct	BIK/g	Mus musculus domesticus blastocyst MHC (H2-Bl) BIK/g exons 2 - 3 and partial cds.	AY989858
H2-Bl BZO	n.a.	ex2-int2-ex3	genomic DNA	direct	BZO	Mus musculus domesticus blastocyst MHC (H2-Bl) BZO exons 2 - 3 and partial cds.	AY989859
H2-Bl BID	n.a.	ex1-int1-ex2-int2-pex3	genomic DNA	direct	BID	Mus musculus spp. blastocyst MHC (H2-Bl) BID exons 1 - 3 and partial cds.	AY989860
H2-Bl DEB	n.a.	ex1-int1-ex2-int2-pex3	genomic DNA	direct	DEB	Mus musculus domesticus blastocyst MHC (H2-Bl) DEB exons 1 - 3 and partial cds.	AY989861
H2-Bl DIK	n.a.	ex1-int1-ex2-int2-pex3	genomic DNA	direct	DIK	Mus musculus domesticus blastocyst MHC (H2-Bl) DIK exons 1 - 3 and partial cds.	AY989862
H2-Bl MGA	n.a.	ex1-int1-ex2-int2-pex3	genomic DNA	direct	MGA	Mus musculus musculus blastocyst MHC (H2-Bl) MGA exons 1 - 3 and partial cds.	AY989863

Table 2.6 *Detailed listing of sequences from gut-restricted class Ib MHC in wild-derived and inbred strains of mice by GenBank Accession Number, cont.*

Gene Name	Splicing Variant	Inclusive Regions[a]	Molecule Type	Sequence Type	Mouse	GenBank Name	Accession Number
H2-Bl MPR	n.a.	ex1-int1-ex2-int2-pex3	genomic DNA	direct	MPR	Mus musculus spp. blastocyst MHC (H2-Bl) MPR exons 1 - 3 and partial cds.	AY989864
H2-Bl SMZ	n.a.	ex1-int1-ex2-int2-pex3	genomic DNA	direct	SMZ	Mus spretus blastocyst MHC (H2-Bl) SMZ exons 1 - 3 and partial cds.	AY989865
H2-Bl SEB	n.a.	pex1-int1-ex2-int2-pex3	genomic DNA	direct	SEB	Mus spretus blastocyst MHC (H2-Bl) SEB exons 1 - 3 and partial cds.	AY989866
H2-Bl like	canonical	ex1-2-3-4-5-6	cDNA	clone	ICR 8	Mus musculus similar to blastocyst MHC (H2-Bl-like 1) ICR8 mRNA, partial cds.	AY989867
	n.a.	pex1-int1-ex2-int2-pex3	genomic DNA	direct	CTA	Mus musculus similar to blastocyst MHC (H2-Bl-like 2) CTA exons 1 - 3 and partial cds.	AY989868
$Tw5^{bc}$	canonical	ex1-2-3-4-5-6-7-8	cDNA	clone combined	129/SvJ	Mus musculus MHC class Ib Tw5 129/SvJ mRNA, complete cds.	AY989869
Tw5 SEB	n.a.	pex3	genomic DNA	direct	SEB	Mus musculus MHC class Ib Tw5 SEB exon 3 and partial cds.	AY989870
$T3^{bc}$	canonical	ex1-2-3-4-5-6	cDNA	clone combined	129/SvJ	Mus musculus MHC class Ib similar to T3 (TL) 129/SvJ mRNA, complete cds.	AY989871
T3 SEB	n.a.	pex2-int2-pex3	genomic DNA	direct	SEB	Mus musculus MHC class Ib similar to T3 (TL) SEB exons 2 - 3 and partial cds.	AY989872
$T3^{bc}$ like	canonical	ex1-2-3-4-5-6	cDNA	clone	129/SvJ	Mus musculus MHC class Ib similar to T3 (2) (TL) 129/SvJ mRNA, complete cds.	AY989873
$Tw3^{bc}$	Tw3.1a	ex1-2-3-pint3-ex4-5-6	cDNA	clone combined	$K^{b-/-}D^{b-/-}$	Mus musculus MHC class Ib Tw3 (Tw3.1a) 129/SvJ mRNA, complete cds.	AY989874
	Tw3.1b	ex1-2-p3-pint3-ex4-5-6	cDNA	clone combined	$K^{b-/-}D^{b-/-}$	Mus musculus MHC class Ib Tw3 (Tw3.1b) 129/SvJ mRNA, complete cds.	AY989875
	Tw3.2a	ex1-pint3-ex4-5-6	cDNA	clone combined	$K^{b-/-}D^{b-/-}$	Mus musculus MHC class Ib Tw3 (Tw3.2a) 129/SvJ mRNA, complete cds.	AY989876
	Tw3.2b	ex1-pint3-ex4-5-6	cDNA	clone combined	$K^{b-/-}D^{b-/-}$	Mus musculus MHC class Ib Tw3 (Tw3.2b) 129/SvJ mRNA, complete cds.	AY989877
	Tw3.3	ex1-6	cDNA	clone combined	$K^{b-/-}D^{b-/-}$	Mus musculus MHC class Ib Tw3 (Tw3.3) 129/SvJ mRNA, complete cds.	AY989878
Q1 SEB	n.a.	pex1-int1-ex2-int2-pex3	genomic DNA	direct	SEB	Mus spretus MHC class Ib Q1 SEB exons 1 - 3 and partial cds.	AY989879
Q2	canonical	ex1-2-3-4-5-6-7-8	cDNA	clone combined	$K^{b-/-}D^{b-/-}$	Mus musculus MHC class Ib Q2 129/SvJ mRNA, complete cds.	AY989880
Q2 SEB	n.a.	pex2-int2-pex3	genomic DNA	direct	SEB	Mus spretus MHC class Ib Q2 SEB exons 2 - 3 and partial cds.	AY989881

[a] The designation "p" as in "pint3" or "pex2" indicates the presence of only a portion of the corresponding intron or exon.

temperature for 5 minutes. This mixture was then added dropwise to the aliquoted DNA, mixed by tapping and allowed to incubate at room temperature for 15-45 minutes. The OptiMEM containing Fugene 6-complexed DNA was then added dropwise, in a counterclockwise fashion, to the 16 hour culture of cells. After 48 hours of culture with the Fugene 6/DNA-containing media, the cells were assayed for cDNA expression by RT-PCR and/or by Western or flow cytometry for translation products. For transfections performed in 24 well plates (1.9 cm^2), all volumes and DNA concentrations were quartered.

Stable transfections were performed in the same manner as transient transfections with the following modifications. H1 and GM cells were transfected in 6 well plates with 10 ng pcDNA3.1N +/- 40 ng pcDNA 1_TAP2, selected in media containing 0.8 mg/mL G418 and cloned by limiting dilution to produce H13.1N (PG1-1.1), H1TAP (PG1-2.5), GM3.1N (PG1-3.3) and GMTAP (PG1-4.4). LS cells were transfected in 6 well plates with 10 ng pcDNA/Hygro (+) (pcDNA3.1H, Invitrogen) +/- 40 ng pcDNA 1_TAP2, selected in media containing 0.8 mg/mL G418, 0.6 mg/mL hygromycin B and cloned by limiting dilution to produce LS 3.1H (PG7-5.1) and LS TAP (PG7-6.11). These clones were then transfected in 24 well plates with 10 ng pEFIRES-P_X and selected in media containing 0.4 mg/mL G418 and 6 µg/mL puromycin +/- 0.6 mg/mL hygromycin B. Alternatively, LS cells were transfected with 10 ng pEFIRES-P_X +/- 40 ng pcDNA1_TAP2 and selected in 6 µg/mL puromycin. G418/puromycin-resistant cell lines are listed in Table 2.7. Hepa1 cells were transfected in the same manner as the G418-resistant B78H1 derivatives except that the cells were plated at a 2X density to allow for a slower rate of division than the H1 clones. Antibiotic selection of stably

Table 2.7 *Generation, Designation and Propagation of Cell Lines and Clones*

Transfected Cell Line/Clone	Transfected Construct(s) (vector_insert)	Line/Clone Name	Line/Clone Designation[a]	Culture Media[b]
H1	pcDNA3.1N	H13.1N	PG1-1.1	cDR10N0.4G
H1	pcDNA3.1N + pcDNA1_TAP2	H1TAP	PG1-2.5	cDR10N0.4G
GM	pcDNA3.1N	GM3.1N	PG1-3.3	cDR10N0.4G
GM	pcDNA3.1N + pcDNA1_TAP2	GMTAP	PG1-4.4	cDR10N0.4G
LS	pcDNA3.1H	LS 3.1H	PG7-5.1	cDR10N0.4G0.6H
LS	pcDNA3.1H + pcDNA1_TAP2	LS TAP	PG7-6.11	cDR10N0.4G0.6H
H13.1N	pEFIRES-P_D^{bc}	H1 D^{bc}	PG9-1P, PG8-7P	cDR10N0.4G6P
H1TAP	pEFIRES-P_D^{bc}	H1TAP D^{bc}	PG9-2P	cDR10N0.4G6P
GM3.1N	pEFIRES-P_D^{bc}	GM D^{bc}	PG9-3P, PG8-9P	cDR10N0.4G6P
GMTAP	pEFIRES-P_D^{bc}	GMTAP D^{bc}	PG9-4P, PG9-10P	cDR10N0.4G6P
H13.1N	pEFIRES-P_T3^{bc}	H1 T3^{bc}	PG9-5P, PG8-13P	cDR10N0.4G6P
H1TAP	pEFIRES-P_T3^{bc}	H1TAP T3^{bc}	PG9-6P	cDR10N0.4G6P
GM3.1N	pEFIRES-P_T3^{bc}	GM T3^{bc}	PG9-7P, PG8-15P	cDR10N0.4G6P
GMTAP	pEFIRES-P_T3^{bc}	GMTAP T3^{bc}	PG9-8P, PG8-16P	cDR10N0.4G6P
H13.1N	pEFIRES-P_Q1^{bc}	H1 Q1^{bc}	PG9-9P, PG8-19P	cDR10N0.4G6P
H1TAP	pEFIRES-P_Q1^{bc}	H1TAP Q1^{bc}	PG9-10P	cDR10N0.4G6P
GM3.1N	pEFIRES-P_Q1^{bc}	GM Q1^{bc}	PG9-11P, PG8-21P	cDR10N0.4G6P
GMTAP	pEFIRES-P_Q1^{bc}	GMTAP Q1^{bc}	PG9-12P, PG8-22P	cDR10N0.4G6P
H13.1N	pEFIRES-P_Q1^{bc} α3	H1 Q1^{bc} α3	PG9-13P	cDR10N0.4G6P
H1TAP	pEFIRES-P_Q1^{bc} α3	H1TAP Q1^{bc} α3	PG9-14P	cDR10N0.4G6P
GM3.1N	pEFIRES-P_Q1^{bc} α3	GM Q1^{bc} α3	PG9-15P	cDR10N0.4G6P
GMTAP	pEFIRES-P_Q1^{bc} α3	GMTAP Q1^{bc} α3	PG9-16P	cDR10N0.4G6P
H13.1N	pEFIRES-P_Q2^{bc}	H1 Q2^{bc}	PG9-17P, PG8-25P	cDR10N0.4G6P
H1TAP	pEFIRES-P_Q2^{bc}	H1TAP Q2^{bc}	PG9-18P	cDR10N0.4G6P
GM3.1N	pEFIRES-P_Q2^{bc}	GM Q2^{bc}	PG9-19P, PG8-27P	cDR10N0.4G6P
GMTAP	pEFIRES-P_Q2^{bc}	GMTAP Q2^{bc}	PG9-20P, PG8-28P	cDR10N0.4G6P
H13.1N	pEFIRES-P_Tw5^{bc}	H1 Tw5^{bc}	PG9-21P	cDR10N0.4G6P
H1TAP	pEFIRES-P_Tw5^{bc}	H1TAP Tw5^{bc}	PG9-22P	cDR10N0.4G6P
GM3.1N	pEFIRES-P_Tw5^{bc}	GM Tw5^{bc}	PG9-23P	cDR10N0.4G6P
GMTAP	pEFIRES-P_Tw5^{bc}	GMTAP Tw5^{bc}	PG9-24P	cDR10N0.4G6P
H13.1N	pEFIRES-P_H2-Bl^{q}	H1 H2-Bl^{q}	PG9-25P, PG8-49P	cDR10N0.4G6P
H1TAP	pEFIRES-P_H2-Bl^{q}	H1TAP H2-Bl^{q}	PG9-26P	cDR10N0.4G6P
GM3.1N	pEFIRES-P_H2-Bl^{q}	GM H2-Bl^{q}	PG9-27P, PG8-51P	cDR10N0.4G6P

Table 2.7 *Generation, Designation and Propagation of Cell Lines and Clones, cont.*

Transfected Cell Line/Clone	Transfected Construct(s) (vector_insert)	Line/Clone Name	Line/Clone Designation[a]	Culture Media[b]
GMTAP	pEFIRES-P_H2-Bl^{q}	GMTAP H2-Bl^{q}	PG9-28P, PG8-52P	cDR10N0.4G6P
H13.1N	pEFIRES-P_H2-Bl^{bc}	H1 H2-Bl^{bc}	PG9-29P, PG8-37P	cDR10N0.4G6P
H1TAP	pEFIRES-P_H2-Bl^{bc}	H1TAP H2-Bl^{bc}	PG9-30P	cDR10N0.4G6P
GM3.1N	pEFIRES-P_H2-Bl^{bc}	GM H2-Bl^{bc}	PG9-31P, PG8-39P	cDR10N0.4G6P
GMTAP	pEFIRES-P_H2-Bl^{bc}	GMTAP H2-Bl^{bc}	PG9-32P, PG8-40P	cDR10N0.4G6P
H13.1N	pEFIRES-P_H2-Bl^{bc} -33nt	H1 H2-Bl^{bc} -33nt	PG9-33P, PG8-55P	cDR10N0.4G6P
H1TAP	pEFIRES-P_H2-Bl^{bc} -33nt	H1TAP H2-Bl^{bc} -33nt	PG9-34P	cDR10N0.4G6P
GM3.1N	pEFIRES-P_H2-Bl^{bc} -33nt	GM H2-Bl^{bc} -33nt	PG9-35P, PG8-57P	cDR10N0.4G6P
GMTAP	pEFIRES-P_H2-Bl^{bc} -33nt	GMTAP H2-Bl^{bc} -33nt	PG9-36P, PG8-58P	cDR10N0.4G6P
H13.1N	pEFIRES-P_H2-Bl^{bc} α1/α3	H1 H2-Bl^{bc} α1/α3	PG9-37P, PG8-61P	cDR10N0.4G6P
H1TAP	pEFIRES-P_H2-Bl^{bc} α1/α3	H1TAP H2-Bl^{bc} α1/α3	PG9-38P	cDR10N0.4G6P
GM3.1N	pEFIRES-P_H2-Bl^{bc} α1/α3	GM H2-Bl^{bc} α1/α3	PG9-39P, PG8-63P	cDR10N0.4G6P
GMTAP	pEFIRES-P_H2-Bl^{bc} α1/α3	GMTAP H2-Bl^{bc} α1/α3	PG9-40P, PG8-64P	cDR10N0.4G6P
H13.1N	pEFIRES-P_H2-Bl^{bc} α1/α3 -33nt	H1 H2-Bl^{bc} α1/α3 -33nt	PG9-41P	cDR10N0.4G6P
H1TAP	pEFIRES-P_H2-Bl^{bc} α1/α3 -33nt	H1TAP H2-Bl^{bc} α1/α3 -33nt	PG9-42P	cDR10N0.4G6P
GM3.1N	pEFIRES-P_H2-Bl^{bc} α1/α3 -33nt	GM H2-Bl^{bc} α1/α3 -33nt	PG9-43P	cDR10N0.4G6P
GMTAP	pEFIRES-P_H2-Bl^{bc} α1/α3 -33nt	GMTAP H2-Bl^{bc} α1/α3 -33nt	PG9-44P	cDR10N0.4G6P
H13.1N	pEFIRES-P_H2-Bl^{b} α1/α2	H1 H2-Bl^{b} α1/α2	PG9-45P	cDR10N0.4G6P
H1TAP	pEFIRES-P_H2-Bl^{b} α1/α2	H1TAP H2-Bl^{b} α1/α2	PG9-46P	cDR10N0.4G6P
GM3.1N	pEFIRES-P_H2-Bl^{b} α1/α2	GM H2-Bl^{b} α1/α2	PG9-47P	cDR10N0.4G6P
GMTAP	pEFIRES-P_H2-Bl^{b} α1/α2	GMTAP H2-Bl^{b} α1/α2	PG9-48P	cDR10N0.4G6P
H13.1N	pEFIRES-P_Q10^{b} (1st ATG)	H1 Q10^{b} (1st ATG)	PG9-49P, PG8-79P	cDR10N0.4G6P
H1TAP	pEFIRES-P_Q10^{b} (1st ATG)	H1TAP Q10^{b} (1st ATG)	PG9-50P	cDR10N0.4G6P
GM3.1N	pEFIRES-P_Q10^{b} (1st ATG)	GM Q10^{b} (1st ATG)	PG9-51P, PG8-81P	cDR10N0.4G6P
GMTAP	pEFIRES-P_Q10^{b} (1st ATG)	GMTAP Q10^{b} (1st ATG)	PG9-52P, PG8-82P	cDR10N0.4G6P
H13.1N	pEFIRES-P_Q10^{b} α3 (1st ATG)	H1 Q10^{b} α3 (1st ATG)	PG9-53P, PG8-91P	cDR10N0.4G6P
H1TAP	pEFIRES-P_Q10^{b} α3 (1st ATG)	H1TAP Q10^{b} α3 (1st ATG)	PG9-54P	cDR10N0.4G6P
GM3.1N	pEFIRES-P_Q10^{b} α3 (1st ATG)	GM Q10^{b} α3 (1st ATG)	PG9-55P, PG8-93P	cDR10N0.4G6P
GMTAP	pEFIRES-P_Q10^{b} α3 (1st ATG)	GMTAP Q10^{b} α3 (1st ATG)	PG9-56P, PG8-94P	cDR10N0.4G6P
H13.1N	pEFIRES-P_Q10^{b} α3 (2nd ATG)	H1 Q10^{b} α3 (2nd ATG)	PG9-57P, PG8-97P	cDR10N0.4G6P
H1TAP	pEFIRES-P_Q10^{b} α3 (2nd ATG)	H1TAP Q10^{b} α3 (2nd ATG)	PG9-58P	cDR10N0.4G6P
GM3.1N	pEFIRES-P_Q10^{b} α3 (2nd ATG)	GM Q10^{b} α3 (2nd ATG)	PG9-59P, PG8-99P	cDR10N0.4G6P
GMTAP	pEFIRES-P_Q10^{b} α3 (2nd ATG)	GMTAP Q10^{b} α3 (2nd ATG)	PG9-60P, PG8-100P	cDR10N0.4G6P

Table 2.7 *Generation, Designation and Propagation of Cell Lines and Clones, cont.*

Transfected Cell Line/Clone	Transfected Construct(s) (vector_insert)	Line/Clone Name	Line/Clone Designation[a]	Culture Media[b]
H13.1N	pEFIRES-P_Q10.GPI	H1 Q10.GPI	PG9-61P, PG8-103P	cDR10N0.4G6P
H1TAP	pEFIRES-P_Q10.GPI	H1TAP Q10.GPI	PG9-62P	cDR10N0.4G6P
GM3.1N	pEFIRES-P_Q10.GPI	GM Q10.GPI	PG9-63P, PG8-105P	cDR10N0.4G6P
GMTAP	pEFIRES-P_Q10.GPI	GMTAP Q10.GPI	PG9-64P, PG8-106P	cDR10N0.4G6P
H13.1N	pEFIRES-P_Q5^{k}	H1 Q5^{k}	PG9-65P	cDR10N0.4G6P
H1TAP	pEFIRES-P_Q5^{k}	H1TAP Q5^{k}	PG9-66P	cDR10N0.4G6P
GM3.1N	pEFIRES-P_Q5^{k}	GM Q5^{k}	PG9-67P	cDR10N0.4G6P
GMTAP	pEFIRES-P_Q5^{k}	GMTAP Q5^{k}	PG9-68P	cDR10N0.4G6P
H13.1N	pEFIRES-P_Q5^{k} α1/α3	H1 Q5^{k} α1/α3	PG9-69P, PG8-115P	cDR10N0.4G6P
H1TAP	pEFIRES-P_Q5^{k} α1/α3	H1TAP Q5^{k} α1/α3	PG9-70P	cDR10N0.4G6P
GM3.1N	pEFIRES-P_Q5^{k} α1/α3	GM Q5^{k} α1/α3	PG9-71P, PG8-117P	cDR10N0.4G6P
GMTAP	pEFIRES-P_Q5^{k} α1/α3	GMTAP Q5^{k} α1/α3	PG9-72P, PG8-118P	cDR10N0.4G6P
H13.1N	pEFIRES-P_Q5^{k} α1	H1 Q5^{k} α1	PG9-73P, PG8-121P	cDR10N0.4G6P
H1TAP	pEFIRES-P_Q5^{k} α1	H1TAP Q5^{k} α1	PG9-74P	cDR10N0.4G6P
GM3.1N	pEFIRES-P_Q5^{k} α1	GM Q5^{k} α1	PG9-75P, PG8-123P	cDR10N0.4G6P
GMTAP	pEFIRES-P_Q5^{k} α1	GMTAP Q5^{k} α1	PG9-76P, PG8-124P	cDR10N0.4G6P
H13.1N	pEFIRES-P_flagQ1^{bc}	H1 flagQ1^{bc}	PG9-77P	cDR10N0.4G6P
H1TAP	pEFIRES-P_flagQ1^{bc}	H1TAP flagQ1^{bc}	PG9-78P	cDR10N0.4G6P
GM3.1N	pEFIRES-P_flagQ1^{bc}	GM flagQ1^{bc}	PG9-79P	cDR10N0.4G6P
GMTAP	pEFIRES-P_flagQ1^{bc}	GMTAP flagQ1^{bc}	PG9-80P	cDR10N0.4G6P
H13.1N	pEFIRES-P_flagQ1^{bc} α3	H1 flagQ1^{bc} α3	PG9-81P, PG13-17P, PG13-37P	cDR10N0.4G6P
H1TAP	pEFIRES-P_flagQ1^{bc} α3	H1TAP flagQ1^{bc} α3	PG9-82P, PG13-18P, PG13-38P	cDR10N0.4G6P
GM3.1N	pEFIRES-P_flagQ1^{bc} α3	GM flagQ1^{bc} α3	PG9-83P, PG13-19P, PG13-39P	cDR10N0.4G6P
GMTAP	pEFIRES-P_flagQ1^{bc} α3	GMTAP flagQ1^{bc} α3	PG9-84P, PG13-20P, PG13-40P	cDR10N0.4G6P
H13.1N	pEFIRES-P_flagQ2^{bc}	H1 flagQ2^{bc}	PG9-85P	cDR10N0.4G6P
H1TAP	pEFIRES-P_flagQ2^{bc}	H1TAP flagQ2^{bc}	PG9-86P	cDR10N0.4G6P
GM3.1N	pEFIRES-P_flagQ2^{bc}	GM flagQ2^{bc}	PG9-87P	cDR10N0.4G6P
GMTAP	pEFIRES-P_flagQ2^{bc}	GMTAP flagQ2^{bc}	PG9-88P	cDR10N0.4G6P
H13.1N	pEFIRES-P_flagTw5^{bc}	H1 flagTw5^{bc}	PG9-89P, PG8-31P	cDR10N0.4G6P
H1TAP	pEFIRES-P_flagTw5^{bc}	H1TAP flagTw5^{bc}	PG9-90P	cDR10N0.4G6P
GM3.1N	pEFIRES-P_flagTw5^{bc}	GM flagTw5^{bc}	PG9-91P, PG8-33P	cDR10N0.4G6P
GMTAP	pEFIRES-P_flagTw5^{bc}	GMTAP flagTw5^{bc}	PG9-92P, PG8-34P	cDR10N0.4G6P
H13.1N	pEFIRES-P_flagH2-Bl^{q}	H1 flagH2-Bl^{q}	PG9-93P	cDR10N0.4G6P

Table 2.7 *Generation, Designation and Propagation of Cell Lines and Clones, cont.*

Transfected Cell Line/Clone	Transfected Construct(s) (vector_insert)	Line/Clone Name	Line/Clone Designation[a]	Culture Media[b]
H1TAP	pEFIRES-P_flagH2-Bl^{q}	H1TAP flagH2-Bl^{q}	PG9-94P	cDR10N0.4G6P
GM3.1N	pEFIRES-P_flagH2-Bl^{q}	GM flagH2-Bl^{q}	PG9-95P	cDR10N0.4G6P
GMTAP	pEFIRES-P_flagH2-Bl^{q}	GMTAP flagH2-Bl^{q}	PG9-96P	cDR10N0.4G6P
H13.1N	pEFIRES-P_flagH2-Bl^{bc}	H1 flagH2-Bl^{bc}	PG9-97P, PG8-43P	cDR10N0.4G6P
H1TAP	pEFIRES-P_flagH2-Bl^{bc}	H1TAP flagH2-Bl^{bc}	PG9-98P	cDR10N0.4G6P
GM3.1N	pEFIRES-P_flagH2-Bl^{bc}	GM flagH2-Bl^{bc}	PG9-99P, PG8-45P	cDR10N0.4G6P
GMTAP	pEFIRES-P_flagH2-Bl^{bc}	GMTAP flagH2-Bl^{bc}	PG9-100P, PG8-46P	cDR10N0.4G6P
H13.1N	pEFIRES-P_flagH2-Bl^{bc} -33nt	H1 flagH2-Bl^{bc} -33nt	PG9-101P	cDR10N0.4G6P
H1TAP	pEFIRES-P_flagH2-Bl^{bc} -33nt	H1TAP flagH2-Bl^{bc} -33nt	PG9-102P	cDR10N0.4G6P
GM3.1N	pEFIRES-P_flagH2-Bl^{bc} -33nt	GM flagH2-Bl^{bc} -33nt	PG9-103P	cDR10N0.4G6P
GMTAP	pEFIRES-P_flagH2-Bl^{bc} -33nt	GMTAP flagH2-Bl^{bc} -33nt	PG9-104P	cDR10N0.4G6P
H13.1N	pEFIRES-P_flagH2-Bl^{bc} $\alpha1/\alpha3$	H1 flagH2-Bl^{bc} $\alpha1/\alpha3$	PG9-105P, PG8-67P, PG13-9P, PG13-29P	cDR10N0.4G6P
H1TAP	pEFIRES-P_flagH2-Bl^{bc} $\alpha1/\alpha3$	H1TAP flagH2-Bl^{bc} $\alpha1/\alpha3$	PG9-106P, PG13-10P, PG13-30P	cDR10N0.4G6P
GM3.1N	pEFIRES-P_flagH2-Bl^{bc} $\alpha1/\alpha3$	GM flagH2-Bl^{bc} $\alpha1/\alpha3$	PG9-107P, PG8-69P, PG13-11P, PG13-31P	cDR10N0.4G6P
GMTAP	pEFIRES-P_flagH2-Bl^{bc} $\alpha1/\alpha3$	GMTAP flagH2-Bl^{bc} $\alpha1/\alpha3$	PG9-108P, PG8-70P, PG13-12P, PG13-32P	cDR10N0.4G6P
H13.1N	pEFIRES-P_flagH2-Bl^{bc} $\alpha1/\alpha3$ -33nt	H1 flagH2-Bl^{bc} $\alpha1/\alpha3$ -33nt	PG9-109P	cDR10N0.4G6P
H1TAP	pEFIRES-P_flagH2-Bl^{bc} $\alpha1/\alpha3$ -33nt	H1TAP flagH2-Bl^{bc} $\alpha1/\alpha3$ -33nt	PG9-110P	cDR10N0.4G6P
GM3.1N	pEFIRES-P_flagH2-Bl^{bc} $\alpha1/\alpha3$ -33nt	GM flagH2-Bl^{bc} $\alpha1/\alpha3$ -33nt	PG9-111P	cDR10N0.4G6P
GMTAP	pEFIRES-P_flagH2-Bl^{bc} $\alpha1/\alpha3$ -33nt	GMTAP flagH2-Bl^{bc} $\alpha1/\alpha3$ -33nt	PG9-112P	cDR10N0.4G6P
H13.1N	pEFIRES-P_flagH2-Bl^{b} $\alpha1/\alpha2$	H1 flagH2-Bl^{b} $\alpha1/\alpha2$	PG9-113P, PG8-73P	cDR10N0.4G6P
H1TAP	pEFIRES-P_flagH2-Bl^{b} $\alpha1/\alpha2$	H1TAP flagH2-Bl^{b} $\alpha1/\alpha2$	PG9-114P	cDR10N0.4G6P
GM3.1N	pEFIRES-P_flagH2-Bl^{b} $\alpha1/\alpha2$	GM flagH2-Bl^{b} $\alpha1/\alpha2$	PG9-115P, PG8-75P	cDR10N0.4G6P
GMTAP	pEFIRES-P_flagH2-Bl^{b} $\alpha1/\alpha2$	GMTAP flagH2-Bl^{b} $\alpha1/\alpha2$	PG9-116P, PG8-76P	cDR10N0.4G6P
H13.1N	pEFIRES-P_flagQ10^{b} (1st ATG)	H1 flagQ10^{b} (1st ATG)	PG9-117P, PG8-85P	cDR10N0.4G6P
H1TAP	pEFIRES-P_flagQ10^{b} (1st ATG)	H1TAP flagQ10^{b} (1st ATG)	PG9-118P	cDR10N0.4G6P
GM3.1N	pEFIRES-P_flagQ10^{b} (1st ATG)	GM flagQ10^{b} (1st ATG)	PG9-119P, PG8-87P	cDR10N0.4G6P
GMTAP	pEFIRES-P_flagQ10^{b} (1st ATG)	GMTAP flagQ10^{b} (1st ATG)	PG9-120P, PG8-88P	cDR10N0.4G6P
H13.1N	pEFIRES-P_flagQ10.GPI	H1 flagQ10.GPI	PG9-121P, PG8-109P	cDR10N0.4G6P
H1TAP	pEFIRES-P_flagQ10.GPI	H1TAP flagQ10.GPI	PG9-122P	cDR10N0.4G6P
GM3.1N	pEFIRES-P_flagQ10.GPI	GM flagQ10.GPI	PG9-123P, PG8-111P	cDR10N0.4G6P
GMTAP	pEFIRES-P_flagQ10.GPI	GMTAP flagQ10.GPI	PG9-124P, PG8-112P	cDR10N0.4G6P
H13.1N	pEFIRES-P_flagQ5^{k} $\alpha1/\alpha3$	H1 flagQ5^{k} $\alpha1/\alpha3$	PG9-125P, PG13-5P, PG13-25P	cDR10N0.4G6P
H1TAP	pEFIRES-P_flagQ5^{k} $\alpha1/\alpha3$	H1TAP flagQ5^{k} $\alpha1/\alpha3$	PG9-126P, PG13-6P, PG13-26P	cDR10N0.4G6P

Table 2.7 *Generation, Designation and Propagation of Cell Lines and Clones, cont.*

Transfected Cell Line/Clone	Transfected Construct(s) (vector_insert)	Line/Clone Name	Line/Clone Designation[a]	Culture Media[b]
GM3.1N	pEFIRES-P_flagQ5^{k} α1/α3	GM flagQ5^{k} α1/α3	PG9-127P, PG13-7P, PG13-27P	cDR10N0.4G6P
GMTAP	pEFIRES-P_flagQ5^{k} α1/α3	GMTAP flagQ5^{k} α1/α3	PG9-128P, PG13-8P, PG13-28P	cDR10N0.4G6P
H13.1N	pEFIRES-P_flagQ5^{k} α1	H1 flagQ5^{k} α1	PG9-129P	cDR10N0.4G6P
H1TAP	pEFIRES-P_flagQ5^{k} α1	H1TAP flagQ5^{k} α1	PG9-130P	cDR10N0.4G6P
GM3.1N	pEFIRES-P_flagQ5^{k} α1	GM flagQ5^{k} α1	PG9-131P	cDR10N0.4G6P
GMTAP	pEFIRES-P_flagQ5^{k} α1	GMTAP flagQ5^{k} α1	PG9-132P	cDR10N0.4G6P
H13.1N	pEFIRES-P_flag mQ9^{b}	H1 flag mQ9^{b}	PG9-133P	cDR10N0.4G6P
H1TAP	pEFIRES-P_flag mQ9^{b}	H1TAP flag mQ9^{b}	PG9-134P	cDR10N0.4G6P
GM3.1N	pEFIRES-P_flag mQ9^{b}	GM flag mQ9^{b}	PG9-135P	cDR10N0.4G6P
GMTAP	pEFIRES-P_flag mQ9^{b}	GMTAP flag mQ9^{b}	PG9-136P	cDR10N0.4G6P
H13.1N	pEFIRES-P_flag mQ9^{b} α1/α2	H1 flag mQ9^{b} α1/α2	PG9-137P	cDR10N0.4G6P
H1TAP	pEFIRES-P_flag mQ9^{b} α1/α2	H1TAP mQ9^{b} α1/α2	PG9-138P	cDR10N0.4G6P
GM3.1N	pEFIRES-P_flag mQ9^{b} α1/α2	GM flag mQ9^{b} α1/α2	PG9-139P	cDR10N0.4G6P
GMTAP	pEFIRES-P_flag mQ9^{b} α1/α2	GMTAP flag mQ9^{b} α1/α2	PG9-140P	cDR10N0.4G6P
H13.1N	pEFIRES-P	H1 IRES-P	PG9-145P, PG8-1P	cDR10N0.4G6P
H1TAP	pEFIRES-P	H1TAP IRES-P	PG9-146P	cDR10N0.4G6P
GM3.1N	pEFIRES-P	GM IRES-P	PG9-147P, PG8-3P	cDR10N0.4G6P
GMTAP	pEFIRES-P	GMTAP IRES-P	PG9-148P, PG8-4P	cDR10N0.4G6P
LS 3.1H	pEFIRES-P_D^{bc}	H1Qa-1^{b}D^{bc}	PG10-1P	cDR10N0.4G0.6H6P
LS TAP	pEFIRES-P_D^{bc}	H1TAPQa-1^{b}D^{bc}	PG10-2P	cDR10N0.4G0.6H6P
LS	pEFIRES-P_D^{bc}	H1Qa-1^{b}D^{bc}	PG10-3P	cDR10N0.4G0.6H6P
LS	pEFIRES-P_D^{bc} + pcDNA1_TAP2	H1Qa-1^{b}D^{bc} + TAP2	PG10-4P	cDR10N0.4G0.6H6P
LS 3.1H	pEFIRES-P_T3^{bc}	H1Qa-1^{b}T3^{bc}	PG10-5P	cDR10N0.4G0.6H6P
LS TAP	pEFIRES-P_T3^{bc}	H1TAPQa-1bT3^{bc}	PG10-6P	cDR10N0.4G0.6H6P
LS	pEFIRES-P_T3^{bc}	H1Qa-1^{b}T3^{bc}	PG10-7P	cDR10N0.4G0.6H6P
LS	pEFIRES-P_T3^{bc} + pcDNA1_TAP2	H1Qa-1^{b}T3^{bc} + TAP2	PG10-8P	cDR10N0.4G0.6H6P
LS 3.1H	pEFIRES-P_Q1^{bc}	H1Qa-1^{b}Q1^{bc}	PG10-9P	cDR10N0.4G0.6H6P
LS TAP	pEFIRES-P_Q1^{bc}	H1TAPQa-1^{b}Q1^{bc}	PG10-10P	cDR10N0.4G0.6H6P
LS	pEFIRES-P_Q1^{bc}	H1Qa-1^{b}Q1^{bc}	PG10-11P	cDR10N0.4G0.6H6P
LS	pEFIRES-P_Q1^{bc} + pcDNA1_TAP2	H1Qa-1^{b}Q1^{bc} + TAP2	PG10-12P	cDR10N0.4G0.6H6P
LS 3.1H	pEFIRES-P_Q1^{bc} α3	H1Qa-1^{b}Q1^{bc} α3	PG10-13P	cDR10N0.4G0.6H6P
LS TAP	pEFIRES-P_Q1^{bc} α3	H1TAPQa-1^{b}Q1^{bc} α3	PG10-14P	cDR10N0.4G0.6H6P
LS	pEFIRES-P_Q1^{bc} α3	H1Qa-1^{b}Q1^{bc} α3	PG10-15P	cDR10N0.4G0.6H6P

Table 2.7 *Generation, Designation and Propagation of Cell Lines and Clones, cont.*

Transfected Cell Line/Clone	Transfected Construct(s) (vector_insert)	Line/Clone Name	Line/Clone Designation[a]	Culture Media[b]
LS	pEFIRES-P_Q1^{bc} α3 + pcDNA1_TAP2	H1Qa-1^{b}Q1^{bc} α3 + TAP2	PG10-16P	cDR10N0.4G0.6H6P
LS 3.1H	pEFIRES-P_Q2^{bc}	H1Qa-1^{b}Q2^{bc}	PG10-17P	cDR10N0.4G0.6H6P
LS TAP	pEFIRES-P_Q2^{bc}	H1TAPQa-1^{b}Q2^{bc}	PG10-18P	cDR10N0.4G0.6H6P
LS	pEFIRES-P_Q2^{bc}	H1Qa-1^{b}Q2^{bc}	PG10-19P	cDR10N0.4G0.6H6P
LS	pEFIRES-P_Q2^{bc} + pcDNA1_TAP2	H1Qa-1^{b}Q2^{bc} + TAP2	PG10-20P	cDR10N0.4G0.6H6P
LS 3.1H	pEFIRES-P_Tw5^{bc}	H1Qa-1^{b}Tw5^{bc}	PG10-21P	cDR10N0.4G0.6H6P
LS TAP	pEFIRES-P_Tw5^{bc}	H1TAPQa-1^{b}Tw5^{bc}	PG10-22P	cDR10N0.4G0.6H6P
LS	pEFIRES-P_Tw5^{bc}	H1Qa-1^{b}Tw5^{bc}	PG10-23P	cDR10N0.4G0.6H6P
LS	pEFIRES-P_Tw5^{bc} + pcDNA1_TAP2	H1Qa-1^{b}Tw5^{bc} + TAP2	PG10-24P	cDR10N0.4G0.6H6P
LS 3.1H	pEFIRES-P_H2-Bl^{q}	H1Qa-1^{b}H2-Bl^{q}	PG10-25P	cDR10N0.4G0.6H6P
LS TAP	pEFIRES-P_H2-Bl^{q}	H1TAPQa-1^{b}H2-Bl^{q}	PG10-26P	cDR10N0.4G0.6H6P
LS	pEFIRES-P_H2-Bl^{q}	H1Qa-1^{b}H2-Bl^{q}	PG10-27P	cDR10N0.4G0.6H6P
LS	pEFIRES-P_H2-Bl^{q} + pcDNA1_TAP2	H1Qa-1^{b}H2-Bl^{q} + TAP2	PG10-28P	cDR10N0.4G0.6H6P
LS 3.1H	pEFIRES-P_H2-Bl^{bc}	H1Qa-1^{b}H2-Bl^{bc}	PG10-29P	cDR10N0.4G0.6H6P
LS TAP	pEFIRES-P_H2-Bl^{bc}	H1TAPQa-1^{b}H2-Bl^{bc}	PG10-30P	cDR10N0.4G0.6H6P
LS	pEFIRES-P_H2-Bl^{bc}	H1Qa-1^{b}H2-Bl^{bc}	PG10-31P	cDR10N0.4G0.6H6P
LS	pEFIRES-P_H2-Bl^{bc} + pcDNA1_TAP2	H1Qa-1^{b}H2-Bl^{bc} + TAP2	PG10-32P	cDR10N0.4G0.6H6P
LS 3.1H	pEFIRES-P_H2-Bl^{bc} -33nt	H1Qa-1^{b}H2-Bl^{bc} -33nt	PG10-33P	cDR10N0.4G0.6H6P
LS TAP	pEFIRES-P_H2-Bl^{bc} -33nt	H1TAPQa-1^{b}H2-Bl^{bc} -33nt	PG10-34P	cDR10N0.4G0.6H6P
LS	pEFIRES-P_H2-Bl^{bc} -33nt	H1Qa-1^{b}H2-Bl^{bc} -33nt	PG10-35P	cDR10N0.4G0.6H6P
LS	pEFIRES-P_H2-Bl^{bc} -33nt + pcDNA1_TAP2	H1Qa-1^{b}H2-Bl^{bc} -33nt + TAP2	PG10-36P	cDR10N0.4G0.6H6P
LS 3.1H	pEFIRES-P_H2-Bl^{bc} α1/α3	H1Qa-1^{b}H2-Bl^{bc} α1/α3	PG10-37P	cDR10N0.4G0.6H6P
LS TAP	pEFIRES-P_H2-Bl^{bc} α1/α3	H1TAPQa-1^{b}H2-Bl^{bc} α1/α3	PG10-38P	cDR10N0.4G0.6H6P
LS	pEFIRES-P_H2-Bl^{bc} α1/α3	H1Qa-1^{b}H2-Bl^{bc} α1/α3	PG10-39P	cDR10N0.4G0.6H6P
LS	pEFIRES-P_H2-Bl^{bc} α1/α3 + pcDNA1_TAP2	H1Qa-1^{b}H2-Bl^{bc} α1/α3 + TAP2	PG10-40P	cDR10N0.4G0.6H6P
LS 3.1H	pEFIRES-P_H2-Bl^{bc} α1/α3 -33nt	H1Qa-1^{b}H2-Bl^{bc} α1/α3 -33nt	PG10-41P	cDR10N0.4G0.6H6P
LS TAP	pEFIRES-P_H2-Bl^{bc} α1/α3 -33nt	H1TAPQa-1^{b}H2-Bl^{bc} α1/α3 -33nt	PG10-42P	cDR10N0.4G0.6H6P
LS	pEFIRES-P_H2-Bl^{bc} α1/α3 -33nt	H1Qa-1^{b}H2-Bl^{bc} α1/α3 -33nt	PG10-43P	cDR10N0.4G0.6H6P
LS	pEFIRES-P_H2-Bl^{bc} α1/α3 -33nt + pcDNA1_TAP2	H1Qa-1^{b}H2-Bl^{bc} α1/α3 -33nt + TAP2	PG10-44P	cDR10N0.4G0.6H6P
LS 3.1H	pEFIRES-P_H2-Bl^{b} α1/α2	H1Qa-1^{b}H2-Bl^{b} α1/α2	PG10-45P	cDR10N0.4G0.6H6P
LS TAP	pEFIRES-P_H2-Bl^{b} α1/α2	H1TAPQa-1^{b}H2-Bl^{b} α1/α2	PG10-46P	cDR10N0.4G0.6H6P
LS	pEFIRES-P_H2-Bl^{b} α1/α2	H1Qa-1^{b}H2-Bl^{b} α1/α2	PG10-47P	cDR10N0.4G0.6H6P
LS	pEFIRES-P_H2-Bl^{b} α1/α2 + pcDNA1_TAP2	H1Qa-1^{b}H2-Bl^{b} α1/α2 + TAP2	PG10-48P	cDR10N0.4G0.6H6P

Table 2.7 *Generation, Designation and Propagation of Cell Lines and Clones, cont.*

Transfected Cell Line/Clone	Transfected Construct(s) (vector_insert)	Line/Clone Name	Line/Clone Designation[a]	Culture Media[b]
LS 3.1H	pEFIRES-P_Q10^{b} (1st ATG)	H1Qa-1^{b}Q10^{b} (1st ATG)	PG10-49P	cDR10N0.4G0.6H6P
LS TAP	pEFIRES-P_Q10^{b} (1st ATG)	H1TAPQa-1^{b}Q10^{b} (1st ATG)	PG10-50P	cDR10N0.4G0.6H6P
LS	pEFIRES-P_Q10^{b} (1st ATG)	H1Qa-1^{b}Q10^{b} (1st ATG)	PG10-51P	cDR10N0.4G0.6H6P
LS	pEFIRES-P_Q10^{b} (1st ATG) + pcDNA1_TAP2	H1Qa-1^{b}Q10^{b} (1st ATG) + TAP2	PG10-52P	cDR10N0.4G0.6H6P
LS 3.1H	pEFIRES-P_Q10^{b} α3 (1st ATG)	H1Qa-1^{b}Q10^{b} α3 (1st ATG)	PG10-53P	cDR10N0.4G0.6H6P
LS TAP	pEFIRES-P_Q10^{b} α3 (1st ATG)	H1TAPQa-1^{b}Q10^{b} α3 (1st ATG)	PG10-54P	cDR10N0.4G0.6H6P
LS	pEFIRES-P_Q10^{b} α3 (1st ATG)	H1Qa-1^{b}Q10^{b} α3 (1st ATG)	PG10-55P	cDR10N0.4G0.6H6P
LS	pEFIRES-P_Q10^{b} α3 (1st ATG) + pcDNA1_TAP2	H1Qa-1^{b}Q10^{b} α3 (1st ATG) + TAP2	PG10-56P	cDR10N0.4G0.6H6P
LS 3.1H	pEFIRES-P_Q10^{b} α3 (2nd ATG)	H1Qa-1^{b}Q10^{b} α3 (2nd ATG)	PG10-57P	cDR10N0.4G0.6H6P
LS TAP	pEFIRES-P_Q10^{b} α3 (2nd ATG)	H1TAPQa-1^{b}Q10^{b} α3 (2nd ATG)	PG10-58P	cDR10N0.4G0.6H6P
LS	pEFIRES-P_Q10^{b} α3 (2nd ATG)	H1Qa-1^{b}Q10^{b} α3 (2nd ATG)	PG10-59P	cDR10N0.4G0.6H6P
LS	pEFIRES-P_Q10^{b} α3 (2nd ATG) + pcDNA1_TAP2	H1Qa-1^{b}Q10^{b} α3 (2nd ATG) + TAP2	PG10-60P	cDR10N0.4G0.6H6P
LS 3.1H	pEFIRES-P_Q10.GPI	H1Qa-1^{b}Q10.GPI	PG10-61P	cDR10N0.4G0.6H6P
LS TAP	pEFIRES-P_Q10.GPI	H1TAPQa-1^{b}Q10.GPI	PG10-62P	cDR10N0.4G0.6H6P
LS	pEFIRES-P_Q10.GPI	H1Qa-1^{b}Q10.GPI	PG10-63P	cDR10N0.4G0.6H6P
LS	pEFIRES-P_Q10.GPI + pcDNA1_TAP2	H1Qa-1^{b}Q10.GPI + TAP2	PG10-64P	cDR10N0.4G0.6H6P
LS 3.1H	pEFIRES-P_Q5^{k}	H1Qa-1^{b}Q5^{k}	PG10-65P	cDR10N0.4G0.6H6P
LS TAP	pEFIRES-P_Q5^{k}	H1TAPQa-1^{b}Q5^{k}	PG10-66P	cDR10N0.4G0.6H6P
LS	pEFIRES-P_Q5^{k}	H1Qa-1^{b}Q5^{k}	PG10-67P	cDR10N0.4G0.6H6P
LS	pEFIRES-P_Q5^{k} + pcDNA1_TAP2	H1Qa-1^{b}Q5^{k} + TAP2	PG10-68P	cDR10N0.4G0.6H6P
LS 3.1H	pEFIRES-P_Q5^{k} α1/α3	H1Qa-1^{b}Q5^{k} α1/α3	PG10-69P	cDR10N0.4G0.6H6P
LS TAP	pEFIRES-P_Q5^{k} α1/α3	H1TAPQa-1^{b}Q5^{k} α1/α3	PG10-70P	cDR10N0.4G0.6H6P
LS	pEFIRES-P_Q5^{k} α1/α3	H1Qa-1^{b}Q5^{k} α1/α3	PG10-71P	cDR10N0.4G0.6H6P
LS	pEFIRES-P_Q5^{k} α1/α3 + pcDNA1_TAP2	H1Qa-1^{b}Q5^{k} α1/α3 + TAP2	PG10-72P	cDR10N0.4G0.6H6P
LS 3.1H	pEFIRES-P_Q5^{k} α1	H1Qa-1^{b}Q5^{k} α1	PG10-73P	cDR10N0.4G0.6H6P
LS TAP	pEFIRES-P_Q5^{k} α1	H1TAPQa-1^{b}Q5^{k} α1	PG10-74P	cDR10N0.4G0.6H6P
LS	pEFIRES-P_Q5^{k} α1	H1Qa-1^{b}Q5^{k} α1	PG10-75P	cDR10N0.4G0.6H6P
LS	pEFIRES-P_Q5^{k} α1 + pcDNA1_TAP2	H1Qa-1^{b}Q5^{k} α1 + TAP2	PG10-76P	cDR10N0.4G0.6H6P
LS 3.1H	pEFIRES-P	H1Qa-1^{b}	PG10-77P	cDR10N0.4G0.6H6P
LS TAP	pEFIRES-P	H1TAPQa-1^{b}	PG10-78P	cDR10N0.4G0.6H6P
LS	pEFIRES-P	H1Qa-1^{b}	PG10-79P	cDR10N0.4G0.6H6P
LS	pEFIRES-P + pcDNA1_TAP2	H1Qa-1^{b} + TAP2	PG10-80P	cDR10N0.4G0.6H6P
Hepa1	pEFIRES-P_H2-Bl^{bc} α1/α3	Hepa1 H2-Bl^{bc} α1/α3	PG12-10P	cDR10N6P

[a] Designations for clones and lines are coded as in the following examples, respectively: PG1-1.1 - creator's initials and transfection number - well number . Clone number; PG8-7P - creator's initals and transfection number - well number and line resistance (P = puromycin).

[b] cDR10N - see Cell Lines and Culture Conditions in Materials and Methods; 0.4G = 0.4 mg/mL G418; 0.6H = 0.6 mg/mL hygromycin B; 6P = 6 μg/mL puromycin

transfected cells was begun 24 hours post transfection for B78H1 and its derivatives and 36 hours post transfection for Hepa1.

SDS-PAGE, Western Transfer and Immunoblotting

For the detection of FLAG-tagged class Ib MHC, SDS-PAGE and Westerns were performed as follows. Transiently transfected cells in 6 well plates were trypsinized 24 hours post transfection and pelleted by centrifugation at 400 x g for 6 minutes. After aspirating off the culture medium cells were frozen at -20°C until ready to use. Frozen cells were resuspended in 0.1% SDS, passed repeatedly through an 18 gauge syringe to shear genomic DNA and boiled for 5 minutes. 10 µL of 3X SDS-PAGE loading buffer (240 mM Tris-HCl, pH 6.8, 6% SDS, 16% 2-ME, 30% glycerol, 0.6 mg/mL bromophenol blue) was added to 20 µL cell lysate, which was then loaded onto a 12% SDS-PAGE gel and run at 100 V until the dye front was ~0.5 cm from the bottom of the gel. Low range, biotinylated molecular weight standards (BioRad) were run alongside the lysate samples.

For Western transfer, the gel was rinsed with diH_2O for 15 minutes with mild agitation, then again with transfer buffer (3.03 mg/mL Tris-HCl, 14.4 mg/mL glycine, 15% methanol). A BioTrace™ polyvinylidene fluoride (PVDF) membrane (Pall Corporation, East Hills, NY) was pre-wet with 100% methanol for 1 minute then equilibrated in transfer buffer for 15 minutes. The transfer was performed at 100 V, 4°C for 1 hour, after which the membrane was washed with gentle agitation for 5 minutes in diH_2O. To reduce non-specific antibody association, the membrane was blocked in a

solution of 5% non-fat powdered milk in TBST (100 mM Tris-HCl, pH 7.5, 0.9% NaCl, 0.05% Tween 20) at room temperature for 1 hour. It was then washed twice for 5 minutes in TBST. Immunoblotting was performed with a 1:1000 dilution of HRP-conjugated anti-FLAG antibody (clone M2, Sigma-Aldrich) in TBST at room temperature for 1 hour with mild agitation. The immunoblotted membrane was washed 6 times for 5 minutes each in TBST, after which it was incubated for 2 minutes in ECL™ Western Blotting System HRP substrate (GE Healthcare Life Sciences, Piscataway, NJ) and exposed to Kodak ™ X-OMAT Blue film for 15 seconds to 1 minute (Kodak). Film was developed using a SRX-101A Medical Film Processor (Konika).

To ensure equal sample loading, the membrane was stained with Coomassie blue. Briefly, the membrane was washed twice in TBST for 5 minutes, then transferred to a solution of 40% methanol, 10% acetic acid with 0.1% Coomassie blue R-250. After 5 minutes incubation with mild agitation, the membrane was destained in 40% methanol, 10% acetic acid until the protein bands were visible.

Peptide Stabilization of Qa-1

Qdm and Qdm-like peptides were synthesized by the Protein Chemistry Technology Center at UT Southwestern on an ABI 433A Peptide Synthesizer (Applied Biosystems) using fmoc chemistry. Their purity and identity were confirmed by reversed-phase HPLC and mass spectrometry. Sequences of the peptides used in these studies were as follows: Qdm – AMAPRTLLL, H2-Bl^{q} – AMAQRTLLL, H2-Bl^{bc} 9-mer – AMAQRTLFL, H2-Bl^{bc} 8-mer – MAQRTLFL, Q1^{bc} – AMALGRLLL, Q2^{bc} –

AMALRRLLL, Tw5^{bc} – NMRLRRVFR, 2Q3L – AQLAAAAAA, Ala 9-mer – AAAAAAAAA. All of the synthesized peptides were of the correct mass except for Q1^{bc}, which contained a glycine-deleted contaminant, and Q2^{bc}, which contained an arginine-deleted contaminant. Lyophilized peptides were reconstituted in 0-15% DMSO, depending upon the hydrophobicity of the peptide. Stock peptides were further diluted in culture medium to a final concentration of 500 μM to 1 nM peptide in 3.4% to 4.7% DMSO, depending upon the application. In accordance with the findings of Aldrich et al, DMSO concentrations were maintained at the same level for each peptide under study (177).

Peptide stabilization of cell surface Qa-1 was performed as follows. Trypsinized LS or HeS cells were brought to $5x10^4$ cells in 50 μL media containing peptide and incubated overnight in a 15 mL conical tube @ 5% CO_2, room temperature on a rocker. Cells were then treated with ^{51}Cr and used as targets in CTL or aLAK (adherent lymphokine-activated killer) assays (see below). For antibody staining, cells were incubated overnight with media containing peptide in a humidified incubator at 27-29°C, 5% CO_2, trypsinized and stained with anti-Qa-1^{b} antibody or with anti-β_2m antibody to detect β_2m-associated, peptide stabilized Qa-1 by flow cytometry. Peptide stabilization of Qa-1 expressed on J1 and RMA-S cells was performed at Indiana University School of Medicine by Dr. C. Aldrich.

Flow Cytometric Analysis of Transfectants

Individual B78H1-derived cell lines and clones grown in 24 well plates were trypsinized, collected into 200 µL culture media and transferred to a single well of a 96 well U-bottom plate. Cells grown in larger cultures were resuspended in larger volumes of media and used in multiple staining conditions on several 96 well plates. Once transferred to U-bottom plates, cells were collected by centrifugation at 400 x g, 4°C for 3 minutes. The media was either decanted with a quick flip of the wrist or aspirated. For fixing and permeabilizing, cells were washed by resuspending in 200 µL ice cold 1X PBS. Cells were collected by centrifugation as before and washed once again in cold 1X PBS. These washed cells were then fixed and permeabilized by resuspending in ice cold 70% ethanol and incubating at -20°C for 1 hour to several days. They were then washed once with cold 1X PBS and once with either 1% BSA or 1% FBS in cold 1X PBS (FACS buffer) and stained.

Fixed and permeabilized cells were stained with anti-FLAG antibodies to detect intracellular and cell surface (total cellular) FLAG-tagged class Ib MHC. Cells taken directly from culture were stained with anti-FLAG, anti-Qa-1^{b} or anti-β_2m antibodies to detect cell surface FLAG-tagged class Ib MHC, Qa-1^{b} and β_2m-associated class Ib MHC, respectively. Between each staining step and before flow analysis cells were washed 1X in FACS buffer. All antibody incubations were performed at 4°C for approximately 30 minutes. FLAG detection was achieved with a primary incubation in a 1:500 dilution of an affinity purified rabbit anti-FLAG polyclonal antibody (Sigma-Aldrich), a secondary incubation with a 1:100 dilution of biotinylated goat anti-rabbit Ig (BD Biosciences) and a ternary incubation with a 1:100 dilution of PE-conjugated streptavidin (Biosource, Camarillo, CA). Qa-1 detection was performed with a primary incubation in a 1:100

dilution of biotinylated anti-Qa-1^b (6A8.6F10.1A6, BD Biosciences) and a secondary incubation with a 1:100 dilution of PE-conjugated streptavidin. β_2m detection was performed with a primary incubation in a 1:500 dilution of biotinylated anti-β_2m (S19.8) and a secondary incubation with a 1:100 dilution of PE-conjugated streptavidin. Detection of fluorescence was performed on a FACScan™ cytometer using CellQuest™ Pro software for acquisition and analysis (BD Biosciences).

Flow Cytometric Analysis of IEL

Preparation of small intestinal mixed IEL/IEC samples in FACS buffer was performed as described in the RNA and DNA Isolation section above. Splenocytes, used as positive controls for T and NK cell receptor expression, were generated by crushing a spleen in Tris-buffered ammonium chloride with a glass homogenizer. After a 10 minute room temperature incubation, splenocytes were isolated from lysed red blood cells by centrifugation at 400 x g for 6 minutes, then resuspended in 3 mL cold FACS buffer (1% BSA in PBS). Mixed IEL/IEC and splenocytes were counted by hemocytometer and brought to $20x10^6$ cells/mL and $2x10^6$ cells/mL, respectively. Splenocytes and IEL/IEC were combined at a 1:1 ratio for spiked IEL/IEC samples, used to help define positive populations and set compensations. To inhibit non-specific antibody binding, 5 µL anti-mouse CD16/CD32 (clone 2.4G2, BD Biosciences) was added per mL cells, which were then incubated on ice for 30 minutes. Cells were collected by centrifugation at 400 x g, 4^oC for 10 minutes, washed twice with 10 mL FACS buffer and finally resuspended at a concentration of $20x10^6$ cells/mL in FACS buffer. Fluorophore conjugated antibodies

(Table 2.8) were diluted to 2X in FACS buffer, and 100 µL of this 2X stain was plated per well of a 96 well U-bottom plate. 100 µL concentrated cells ($2x10^6$ cells total) were mixed with the antibodies on the 96 well plate and allowed to incubate on ice for 30 minutes. Stained cells were then washed twice with 200 µL FACS buffer per well, resuspended in 1% formaldehyde in 1X PBS and left, foiled, at 4^oC overnight or analyzed immediately. Flow acquisition was performed with a CyAn cytometer using Summit software (DakoCytomation, Glostrup, Denmark). Data analysis was performed using FloJo v8.7.1 software (Tree Star, Inc, Ashland, OR).

Generation and Culture of aLAK Cells

Adherent lymphokine activated killers (aLAK) were generated as follows. A spleen was harvested from a 8-12 week old C57BL/6J mouse under sterile conditions. Splenocytes were isolated by crushing the spleen in Tris-buffered ammonium chloride with a glass homogenizer. After a 10 minute room temperature incubation, splenocytes were isolated from lysed red blood cells by centrifugation at 400 x g for 6 minutes, then resuspended in 3 mL cDMEM (DMEM supplemented with 1X essential and nonessential amino acids, 4 mM L-glutamine, 1 mM sodium pyruvate, 10 mM HEPES, 100 IU penicillin/mL, 100 µg/mL streptomycin (Mediatech), 0.1 mM 2-ME and 10% FBS). Live splenocytes were counted by hemocytometer, diluted to $3x10^6$ cells per mL in 50 mL cDMEM + 500 IU recombinant human IL-2 per mL (TECIN™ [Teceleukin], NCI Biological Resources Branch, Fredrick, MD) and plated at 2 mL per well on a 24 well plate. LAK were cultured for 3 days in a humidified incubator at 37^oC, 10% CO_2. Non-

Table 2.8 *Antibodies used for the Detection of NK and T Cell Receptors on IEL*

Specificity	Fluorophore[c]	Clone Name	Supplier	Catalog Number	Lot #	Dilution Factor[d]
CD3	PE	17A2	BD PharMingen	28005B	M050014	80
CD3ε	APC	145-2C11	eBioscience	17-0031	E016736	80
CD3ε	APC	145-2C11	BD PharMingen	553066	37592	250
CD4	FITC	H129.19	BD PharMingen	553631	49463	100
CD4	PE	GK1.5	BD PharMingen	553730	38683	400
CD8α	PE	53-6.7	BD PharMingen	553032	60109	300
CD8α	APC-Cy7	53-6.7	eBioscience	10-0081	E017088	10
CD8α	APC-Alexa 750	53-6.7	eBioscience	27-0081	E021296	40
CD8α	PE-Alexa 610	5H10	Caltag	MCD0822	0202	1200
CD8α	PerCP	53-6.7	BD PharMingen	553036	39842	ND
CD8β	APC	CT-CD8b	eBioscience	17-0031-81	E016736	320
CD8β	PE-Cy5	CT-CD8b	eBioscience	15-0082	E015618	1200
CD8β.2	FITC	53-5.8	BD PharMingen	01054D	M046025	640
CD44	PE	IM7	BD PharMingen	553134	M075858	80
CD94	FITC	18d3	eBioscience	11-0941	E014444	400
CD94[a]	PE	18d3	BioLegend	105508	B100354	480
NK1.1	PE	PK136	BD PharMingen	553165	M053937	50
NK1.1	PE-Cy7	PK136	eBioscience	25-5941	E015088	75
NKG2A	PE	16a11	eBioscience	12-5897	E010863	7.5
NKG2A	PE	16a11	eBioscience	12-5897	E006897	40
NKG2A/C/E	FITC	20d5	eBioscience	11-5896	E010856	80
NKG2A/C/E	FITC	20d5	eBioscience	11-5896	E007097	40
NKG2D	PE	CX5	eBioscience	12-5882	E010864	30
NKG2D	PE	CX5	eBioscience	12-5882	E018564	30
NKG2D	PE-Cy7	CX5	eBioscience	25-5882	E015892	80
Ly49A[b]	FITC	A1	BD PharMingen	553677	unknown	300
Ly49A[a]	FITC	A1	BD PharMingen	553677	M065465	100
Ly49C/I[b]	PE	1F8	BD PharMingen	553277	unknown	80
Ly49D[b]	FITC	4E5	BD PharMingen	555313	unknown	240
Ly49G2[a]	FITC	4D11	BD PharMingen	555315	M068466	160
Ly49I/J[b]	FITC	8H7	unknown	unknown	unknown	80
TCRβ	FITC	H57-597	BD PharMingen	553171	M059469	640
TCRβ	APC	H57-597	BD PharMingen	553174	M065189	10
TCRβ	APC	H57-597	eBioscience	17-5961	E015611	60
γδTCR	FITC	GL3	eBioscience	11-5711	E018109	50
γδTCR	PE	GL3	eBioscience	12-5711	E018110	100
Qa-1	PE	C49-4	unknown	P002654	P002938-C02	20

[a] The gift of Dr. J. Forman

[b] The gift of Dr. M. Bennett

[c] APC - allophycocyanin, Cy - cyanine dye family, FITC - fluorescein isothiocyanate, PE - phycoerythrin, PerCP - peridinin chlorophyll protein; X-Y = tandem dye

[d] IEL/IEC @ $2x10^6$ cells in 200 μL final volume

adherent cells were then aspirated off the culture, after which fresh cDMEM + IL-2 was added. These aLAK were then cultured as before for a further 2 days to be used as effectors in ^{51}Cr-release assays.

^{51}Cr-Release Assays

Day 5 cultures of CTL clones or day 5-7 cultures of aLAK were used as effectors in ^{51}Cr-release assays on targets expressing peptide stabilized Qa-1^{b} as follows. Qa-1-bearing LS cells were cultured overnight in a humidified incubator at 27-29°C, 5% CO_2 with various concentrations of peptide. In blocking assays performed with CTL (data generated by Dr. C. Aldrich), 1 nM Qdm was added to the overnight peptide stabilization culture 1 hour prior to target harvest. YAC and P815 positive and negative controls for aLAK assays were brought to 5x10^{4} cells in 50 µL of their overnight culture media. 25 µL of $Na^{51}CrO_4$ at 1 mCi/mL (Amersham, Arlington Heights, IL) + 25 µL cRPMI was added to the control cells. 25 µL of $Na^{51}CrO_4$ at 1 mCi/mL (Amersham, Arlington Heights, IL) + 25 µL 2X peptide was added to the overnight peptide stabilized targets. All cells were then incubated at 37°C, 5% CO_2 for 1 hour, tapping to mix every 15 minutes. After chromium uptake, targets were washed twice with 10 mL cDMEM, centrifuging at 400 x g for 6 minutes to collect. They were then resuspended in a final volume of 5 mL cDMEM, and 100 µL (2000 targets) was plated per well of a 96 well U-bottom plate in enough wells to analyze triplicate assays at the desired effector to target (E:T) ratios.

CTL or aLAK cultures were harvested off 24 well plates by gentle pipetting and transferred to 50 mL conical tubes. They were then collected by centrifugation at 400 x g for 10 minutes, brought to $2x10^6$ cells/mL in cDMEM and serially diluted to the desired E:T ratio. Diluted effectors and 1% SDS and cDMEM maximal and spontaneous release controls were plated in 100 µL per well atop the targets, and the plates were centrifuged at 400 x g for a few seconds to bring the effectors in close proximity to their targets. The effectors were allowed to lyse their targets at 37°C 10% CO_2 for 4 hours, releasing ^{51}Cr into the culture media. The plate was centrifuged as before, and 100 µL of the medium from the top of the wells was pipetted into 1.2 mL Skatron tubes (Skatron Instruments AS, Leir, Norway) for gamma counting on a ME Plus Automatic Gamma Counter (Micromedic Systems, Huntsville, AL). ^{51}Cr-release data is reported as percent specific release ([experimental release - spontaneous release]/[maximum release - spontaneous release] x 100%). All CTL data shown was generated by Dr. C. Aldrich with RMA-S or J1 targets.

CHAPTER THREE

Identification of Class Ib MHC Isoforms Expressed in the Gut

BACKGROUND AND RATIONALE

The balance between immune tolerance to harmless commensal flora and dietary products and immune response to harmful pathogens is highly regulated in the mammalian gastrointestinal tract. Although the relevant, gut-specific pathways of the innate and adaptive immune system are not yet fully understood, they likely depend on the immune effectors residing in, or migrating into, the intestinal tissues. Many gut-localized effector cells, including IEL, T cells and/or NK cells, express TCR, NKG2D, CD94/NKG2 and other receptors which, *in vitro* or in the context of systemic immunity, engage MHC class I antigens or related proteins and signal change in cytotoxicity, cytokine secretion or other immune effector functions (270, 271). To date, only a handful of class I MHC antigens and class I-like proteins has been implicated in the regulation of mucosal immunity in the gastrointestinal tract (38, 40, 92, 192, 272).

In the mouse, the extended family of MHC class I-related proteins is very large and includes two to three highly polymorphic "classical" class I MHC antigens (class Ia) encoded by *H2-K*, *D* and *L* loci, multiple oligomorphic "non-classical" MHC proteins (class Ib) mapping to *H2-Q*, *T* and *M* regions, and additional, structurally divergent class I-like proteins found outside of the *Mhc* (273-275). Although most mouse strains encode dozens of *Q*, *T* and *M* class I genes, only a few of these genes have been studied in any detail. (For a full review on mouse class Ib *Mhc* organization see Kumanovics, et al

(273).) We performed a survey of the known mouse class Ib *Mhc* genes and identified those that are preferentially expressed in gut tissues and may therefore impact immune regulation in this tolerance-dominated milieu. Unexpectedly, we found that *T* region-encoded "blastocyst MHC" (264), the class I MHC that was previously proposed to be a homolog of tolerance-inducing, trophoblast-restricted human HLA-G (225), as well as its putative paralog, *Tw5* (276), are abundantly transcribed in the gastrointestinal tract of many mouse strains. "Blastocyst *Mhc*," designated as *H2-Bl*, has been shown recently to give rise to two alternatively spliced mRNAs in mouse placenta and a teratocarcinoma cell line, F9 (277). Furthermore, in a model system of a transfected RMA-S tumor and in the presence of Qa-1 class Ib MHC (278), the two H2-Bl isoforms acted to protect target cells from NK cell-mediated lysis (277). The mechanism responsible for this pathway was hypothesized to involve binding of *H2-Bl* encoded leader peptides to Qa-1 molecules and their presentation to CD94/NKG2A inhibitory receptors on NK cells. This pathway was proposed to play an important role in enhancing reproductive success of the species by maintaining NK cell tolerance at the maternal/fetal interface in a manner reminiscent of human HLA-G (225).

We find that in intestinal tissues *H2-Bl* is alternatively spliced into multiple, truncated isoforms, in addition to the two detected in the mouse placenta (277). Furthermore, analysis of *H2-Bl* sequences from several inbred, outbred and wild mouse strains revealed that the putative antigen-binding contact sites and the residues required for maintenance of class I structure are generally conserved. Intriguingly, in some cases, the limited polymorphism of the *H2-Bl* locus is associated with pronounced differences in the gut-expressed profile of mRNA isoforms. This observation suggests that allelic

variation of *H2-Bl* genes controls the potential impact of its leader peptide-containing products during H2-Bl/NK cell receptor interactions in the gut. The findings are discussed in the context of the proposed relationship of *H2-Bl* to trophoblast-restricted *HLA-G* and other class Ib genes active in immune-tolerance dominated tissues.

RESULTS

Transcription of Multiple Class Ib *Mhc* Genes in Intestinal Tissues of C57BL/6J Mice

One of the difficulties in studying the multigene family of class I MHC antigens is their close sequence homology and the inherent difficulty in distinguishing individual members by standard Northern blot hybridizations or antibody-based approaches. To overcome this limitation we relied on a sensitive RT-PCR assay to survey body-wide expression patterns of selected class I genes. A panel of highly specific primers, diagnostic for 18 sequenced, or partially sequenced, class I MHC genes from $H2^{b}$ and $H2^{bc}$ mice (Table 2.1) was used to examine C57BL/6J tissues (Figure 3.1 and data not shown). Transcription of class Ia (K^{b} and D^{b}), β_2m, as well as the majority of the tested class Ib was detected in all sampled organs: the small and large intestine, stomach, thymus, spleen, liver, kidney, brain, heart, lung, testes and ovaries/uterus. The ubiquitously transcribed class Ib included *T23*, encoding the Qa-1 antigen (279, 280), *Q6-Q9*, encoding Qa-2 antigens (281, 282), *Q4* (283), *T10/22* (284) and *M3/M4* (285). The transcripts of *Q10* (247) were detected only in liver, while transcripts of *M9* (286)

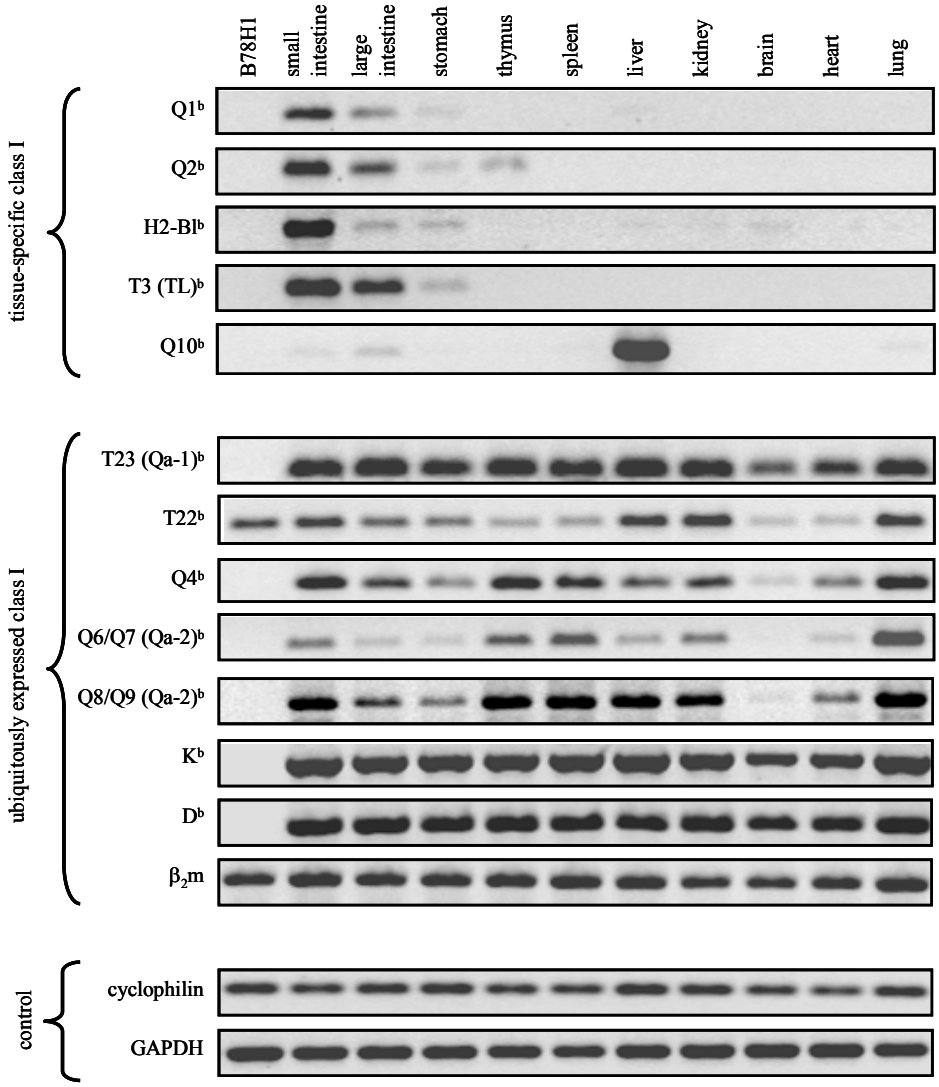
B78H1
small intestine
large intestine
stomach
thymus
spleen
liver
kidney
brain
heart
lung
tissue-specific class I
Q1b
Q2b
H2-Blb
T3 (TL)b
Q10b
ubiquitously expressed class I
T23 (Qa-1)b
T22b
Q4b
Q6/Q7 (Qa-2)b
Q8/Q9 (Qa-2)b
Kb
Db
β2m
control
cyclophilin
GAPDH

Figure 3.1 Multiple class Ib MHC are selectively expressed in the gastrointestinal tract of a C57BL/6J mouse. RT-PCR analysis of transcriptional activity of *Q1*^{b}, *Q2*^{b}, *T3*^{b}, *H2-Bl*^{b} and *Q10*^{b} class Ib was performed on total mRNA isolated from tissues of C57BL/6J mice. The "b" superscript denotes the *H2*^{b} haplotype. For comparison, I display the expression profile of ubiquitously expressed class Ia, *K*^{b} and *D*^{b}, b_2m and class Ib molecules *T23*^{b}, *T22*^{b}, *Q4*^{b} and the Qa-2 transcripts, *Q7/Q9*^{b} and *Q6/Q8*^{b}. *Cyclophilin* and *GAPDH* transcript levels served as cDNA quality controls. B78H1 is a B16-derived melanoma devoid of class I heavy chain transcription (256) and serves as a negative control. Primers used in this analysis included Xho I/*Q1*^{b} ex1 F, EcoR I/*Q1*^{b} ex3 R, Xho I/*Q2*^{b} ex2 F, EcoR I/*Q2*^{b} ex3 R, *T3*^{b} ex2 F, *T3*^{b} ex3 R, *H2-Bl*^{bc} 5'UTR/ex1 F2, *H2-Bl*^{bc} ex3 R1, *Q10*^{b} ex3 F, *Q10*^{b} ex5 R, *T23*^{b} ex2 F, *T23*^{b} ex3 R, *T22*^{b} ex2 F, *T22*^{b} ex3 R, *Q4*^{b} ex2/ex3 F, *Q4*^{b} ex4 R, *Q6*^{b}/*Q8*^{b} ex4 F, *Q6*^{b}/*Q8*^{b} ex5 R, *Q7*^{b}/*Q9*^{b} ex2 F, *Q7*^{b}/*Q9*^{b} 5' UTR R, *K*^{b} ex2 F, *K*^{b} ex3 R, *D*^{b} ex2 F, *D*^{b} ex3 R, b_2m F, b_2m R, *cyclophilin* F, *cyclophilin* R, *GAPDH* F and *GAPDH* R. All PCR reactions were performed with HotStarTaq® over 32 reaction cycles. All bands were of the expected size, and their identities were confirmed by sequencing.

were absent from all tested tissues (data not shown). Specificity of RT-PCR signals was confirmed for each gene by sizing and sequencing of amplified bands from small intestinal samples.

Class Ib MHC genes *Q1* (249, 287), *Q2* (250, 287), *T3* (118, 248) and, unexpectedly, *H2-Bl*, were found to be transcribed predominantly in the gastrointestinal tract (top panel of Figure 3.1). Transcription of *Q1*, *Q2* and *T3*-related genes was previously observed in gastrointestinal tissues (248, 250). In contrast, *H2-Bl* was thought to be silent in adult tissues and expressed only in embryonic blastocyst and placenta, in a manner reminiscent of human *HLA-G*. The original study reporting absence of *H2-Bl* transcripts in adult tissues did not examine samples from the gastrointestinal tract thus explaining the seeming discrepancy between our conclusions and those reached by Sipes et al. (264).

Single Residue Polymorphisms of *H2-Bl* Alleles in Inbred Mouse Strains

Sipes et al. (264) generated the complete sequence of the *H2-Bl* gene from cosmids of 129/SvJ DNA and identified an open reading frame spanning six exons. The exon-intron organization of *H2-Bl* was found to be similar to other class I MHC genes, with individual exons encoding distinct protein domains. The three extracellular domains of the H2-Bl protein, α1, α2 and α3, were most closely related to class Ia sequences, the transmembrane (TM) domain was class Ib-like, and the truncated cytoplasmic (CYT) domain was unique. Accordingly, the 129/SvJ H2-Bl molecule was predicted to have a structure similar to class Ia proteins. Partial sequencing of *H2-Bl* from C57BL/6J suggested also that this allele encodes a full size molecule identical to the 129/SvJ protein. Although the gene was found to have null alleles (BALB/c and DBA/2), it appeared to be highly conserved in a subset of the analyzed inbred, *H2-Bl* positive strains.

Since the pattern of substitutions in MHC exons is often indicative of functional adaptations (288, 289), we sought to identify the polymorphisms occurring within the entire coding region of *H2-Bl* and to extend the scope of the *H2-Bl* sequence analysis to additional strains/genetic backgrounds.

Initially we examined contiguous coding regions of *H2-Bl* alleles partially sequenced by Sipes et al. (264): from C57BL/6J, FVB/NJ and, as a reference, from 129/SvJ inbred strains. Small intestinal *H2-Bl* transcripts containing six exons were amplified with *H2-Bl* specific primers derived from the 5' and 3' untranslated regions (UTR) of the gene (Table 2.1). The RT-PCR conditions were optimized for each strain to correct for differences in the transcriptional levels of gut-synthesized, canonical *H2-Bl*

mRNA. Full size, ~1200 bp cDNA products were subcloned and sequenced. To correct for errors in PCR amplification, multiple clones were sequenced from each reaction.

The DNA sequence and conceptual translation of the region corresponding to the mature H2-Bl protein (exon 2-exon 6) confirmed the original nucleotide and amino acid predictions for the 129/SvJ allele made by Sipes et al. (Figure 3.2, AY989383).

Canonically spliced *H2-Bl* from FVB/NJ mice differed from its 129/SvJ counterpart in 22 nucleotide positions (AY989854-55). Exon 2 contained four synonymous substitutions (GAT→GAC at Asp_{39}, CCG→CCC at Pro_{50}, GAA→GAG at Glu_{53} and GGC→GGT at Gly_{90}) and two nonsynonymous substitutions (CGG→GGG, Arg_{14}→Gly_{14}, GCG→TCG, Ala_{49}→Ser_{49}). Exon 3 contained three synonymous polymorphisms (GAT→GAC at Asp_{137}, GAG→GAA, at Glu_{163} and CTC→CTT at Leu_{168}) and one nonsynonymous substitution (ACC→GCC, Thr_{125}→Ala_{125}). In exon 4, five synonymous (GCA→GCC at Ala_{187}, ACT→ACC at Thr_{225}, AAG→AAA at Lys_{253}, TAC→TAT at Tyr_{257} and CCC→CCA at Pro_{269}) and three nonsynonymous polymorphisms (CAT→CGT, His_{191}→Arg_{191}, CAT→CGT, His_{260}→Arg_{260} and TAC→CAC, Tyr_{262}→His_{262}) were detected. Finally, exon 5 contained one synonymous (TCC→TCA at Ser_{279}) and two nonsynonymous substitutions (GTG→GCG, Val_{306}→Ala_{306} and AGC→AGG, Ser_{310}→Arg_{310}) and exon 6 contained one nonsynonymous polymorphism (AAG→AGG, Lys_{323}→Arg_{323}).

Comparison of the intact canonical alleles from 129/SvJ and FVB/NJ strains revealed strong conservation of class I structure and peptide-binding residues in particular. The synonymous *H2-Bl* substitutions predominated over the nonsynonymous ones in the three extracellular domains (12 vs. 6) while the reverse was true in the buried,

```
α1 (exon 2)                 10        20        30        40        50        60        70        80        90
                            :         :         :         :         :         :         :         :         :
H2 Consensus        GPHSLRYFETAVSRPGLGEPRYISVGYVDNTEFVRFDSDAENPRYEPRARWMEQEGPEYWERETQIAKGNEQSFRVDLRTLLRYYNQSAG

H2-Bl (129/SvJ)     GPHSMRYFETAVFRPGLGEPRFISVGYVDNTQFVSFDSDAENPRSEPRAPWMEQEGPEYWERETQIAKDNEQSFGWSLRNLIHYYNQSKG
H2-Bl (FVB/NJ)      -------------G------------------------*---------S*--*-----------------------------------*
H2-Bl (C57BL/6J)    ----------------------------------------------------------------------------------------

Tw5 (129/SvJ)       -S----------S----------------D----R--G------Y--W----------------------V---RG-----LL-----E-
Q1 (C57BL/6J)       -S--L-----S-S---F-K----------D----R-----K---Y------------------N-RRV-GS-KR-QE--ST-LS-------
Q2 (Kb-/-Db-/-)     -S--L---T---S----------I-----D----R---------M-----------------N--VS-E-----RV--GTALS-------
T3-like (129/SvJ)   -S--L---YA-LS--AIS--WY-A---L-D----R---TG-TGTYKLS---V--------A---E-VTS-A-F-REN-QTMLE---L-QN
HLA-G*01011         -S------SA--S---R------AM----D----R----SAC--M------V---------E--RNT-AHA-TDRMN-QT-RG-----EA

α2 (exon 3)                 100       110       120       130       140       150       160       170       180
                            :         :         :         :         :         :         :         :         :
H2 Consensus        GSHTLQRMYGCDVGSDWRLLRGYEQFAYDGCDYIALNEDLKTWTAADMAAQITRRKWEQAGAAERYRAYLEGECVEWLRRYLKNGNATLLRT

H2-Bl (129/SvJ)     GFHTFQRLSGCDMGLDGRLLRGYLQFAYDGRDYITLNEDLKTWMAADLVALITRRKWEQAGAAELYKFYLEGECVEWLRRYLELGNETLLRT
H2-Bl (FVB/NJ)      ---------------------------------A-----------*-------------------------*----*--------------
H2-Bl (C57BL/6J)    ------------------------------------------------------------------------*-A----------Q--K------

Tw5 (129/SvJ)       -S----------L-S--------------E-Q---A--------T---MA-------------------A----------------R-K------
Q1 (C57BL/6J)       -I----K-----L-S----QS---------L---A-----E--T---VA-QE-------------KHRT----K-IM--H------K-M----
Q2 (Kb-/-Db-/-)     -S--L-W-V---L-P--S-----E-S-------LA-----I--T----A--K--S-L----L--KRRA---VD-LT---------K----H-
T3-like (129/SvJ)   -S--I-VMY--EVEFF-S-F-A-E-HG---Q---A--------T---MA-E---S------YT--RRT----P-KDS-L----NRKK-QEC-
HLA-G*01011         SS--L-WMI---L-S--------E-Y----K--LA-----RS-T---TA-Q-SK--C-A-NV--QRRA----T-----H----N-K-M-Q-A

α3 (exon 4)                 190       200       210       220       230       240       250       260       270
                            :         :         :         :         :         :         :         :         :
H2 Consensus        DSPKAHVTHHPRSEGKVTLRCWALGFYPADITLTWQLNGEELTQDMELVETRPAGDGTFQKWAAVVVPLGKEQNYTCHVYHEGLPEPLTLRW

H2-Bl (129/SvJ)     DPPKAHVTHHPRPAGDVTLRCWALGFYPADITLTWQLNGEELTQDMELVETRPAGDGTFQKWAAVVVPLGKEQNYTCHVYHEGLPEPLTLRW
H2-Bl (FVB/NJ)      ----*---R-----------------------------------*---------------------------*---*--R-H------*-----
H2-Bl (C57BL/6J)    ------------------------------------------------------------.-----------------------------

Tw5 (129/SvJ)       --------------E-------------------------------------------------S---------K-----H------------
Q1 (C57BL/6J)       -------------SQ-------------------------------------------------S-----------------------------
Q2 (Kb-/-Db-/-)     -----------SSQ--------------------------D------------S---------S-M--F-E-PR-----E------------
T3-like (129/SvJ)   ----T-----A--E----------------H-------------I--T-------T---------------S-E--K-----------------
HLA-G*01011         ----T------VFDYEA------------E-I----RD--DQ---V----------------------S-E--R-----Q--------M---

Transmembrane (exon 5)                                          Cytoplasmic tail (exons 6-7/8)

H2-Bl (129/SvJ)     EPPPSTGSNMVNIAVLVVLGAVIIIEA·····MVAFVLKSSRKI   ·······------------------------AILPGPAGTKG·····SSAS.
H2-Bl (FVB/NJ)      ----*------------------------·····-----A---R---   ···------------------------------R-·····----.
H2-Bl (C57BL/6J)    ---------------------------·····-------------   ···------------------------------·····----.

Tw5 (129/SvJ)       ------V---II-E--I------N-G-·····---------K---   GGKGGVYALAGGSNSIHGSALFLEAFK---------R-HLHPDS-MLP.
Q1 (C57BL/6J)       ----Y-V----I-----------V-G-VVIIGV--S--M-RR-NK   GG···QGEDCALAPSRD····SAQSSDIS--·LDCKA.
Q2 (Kb-/-Db-/-)     ------D-Y--I-------------G-VV·------M-RG-NT   GG···KVRDYAQDPGRD····SPQSSDIS--·LE··L.
T3-like (129/SvJ)   ---Q-SMP-RTTVRA-L·------G-MIILGF-SGS-MMMM--N   NGGNGDDNTAAYQNEREHLSLSPRAESEA-GVE--M-D·LPSAPPLVS.
HLA-G*01011         ·····KQ-SLPT-PIMGIVAGLVVLA-VVT·GAA--A--WRKKSS   D.
```

Figure 3.2 Comparison of the predicted class Ib products selectively expressed in the gut and HLA-G, the putative human homolog of H2-Bl. MHC class Ib transcripts were PCR amplified from small intestinal cDNA of the indicated mice and separated on an agarose gel. Canonically spliced isoforms were gel extracted, cloned into pCR II and sequenced (AY989821, AY989838, AY989854-55, AY989869, AY989871 and AY989880). Primers and conditions for the PCR amplifications were as follows: H2-Bl (129/SvJ): *H2-Bl*^{bc} 5'UTR/ex1 F1 and *H2-Bl*^{bc} 3'UTR R, HotStarTaq®, 35 cycles; H2-Bl (FVB/NJ): *H2-Bl*^{bc} 5'UTR/ex1 F1 and *H2-Bl*^{bc} 3'UTR R, HotStarTaq®, 35 cycles; H2-Bl (C57BL/6J): *H2-Bl*^{bc} 5'UTR/ex1 F1 and *H2-Bl*^{bc} 3'UTR R, HotStarTaq®, 35 cycles, 18 reactions pooled and acid/ethanol precipitated; Tw5: *Tw5*^{bc} 5'UTR F and *Tw5*^{bc} 3'UTR R, Platinum® Taq, 32 cycles; Q2: *Q2*^{b} 5'UTR/ex1 F and *Q2*^{b} 3'UTR R, HotStarTaq®, 35 cycles; T3-like: *T3*^{b} 5'UTR/ex1 F and *T3*^{b} 3'UTR R, Platinum® Taq, 32 cycles. Q1 (U96752, predicted protein) and HLA-G (AAM74993) sequences were collected from the NCBI database. H2 consensus is as reported in Stroynowski (290). Dots above the H2 consensus indicate residues conserved across H2 and HLA-A proteins. Residues underlined in the H2 consensus are involved in peptide binding. Dashes in the class Ib sequences indicate identity to the predicted amino acid sequence of H2-Bl from 129/SvJ. Asterisks in FVB/NJ and C57BL/6J H2-Bl sequences denote synonymous polymorphisms in *H2-Bl* with respect to the 129/SvJ allele. Dots represent gaps in the alignment. Periods signify stop codons.

TM and CYT, regions (1 vs. 3). More significantly, all six nonsynonymous polymorphisms fell outside of the peptide-binding region defined by Bjorkman (141) (Figure 3.2 and Figure 3.3). Five of the six nonsynonymous substitutions occurred in residues that are variable in murine and human class I MHC (290) and the one exception (in the conserved Ala_{125} position) did not interfere with any known structural properties of class I proteins. Furthermore, none of the nonsynonymous polymorphisms changed the β_2m-interacting residues in the HLA-A2 model (141) or affected the CD8 binding site (291). Interestingly, while the majority of the synonymous substitutions occurred at random locations, two of them may have functional significance. One is in the Gly_{90} codon, at the junction of exon 2 and intron 2, and may therefore be responsible for splicing choices of *H2-Bl* mRNA in the parental strains (see below). The other is located at a codon corresponding to residue 163, predicted to face into the groove and towards

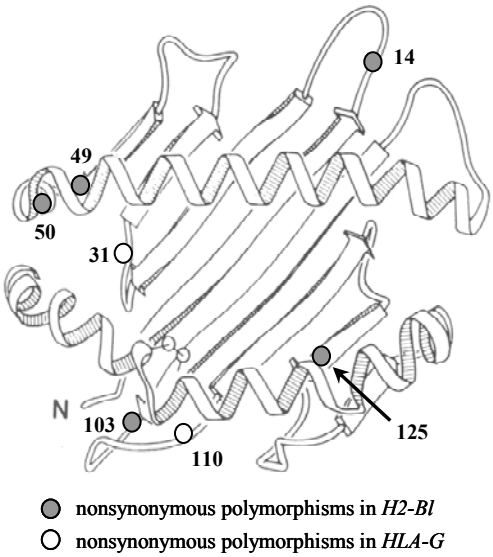

Figure 3.3 *H2-Bl* polymorphisms do not affect the peptide binding groove and affect different loci than *HLA-G* polymorphisms. The peptide binding α1 and α2 domains of a classical class I molecule is shown (from Bjorkman et al (141)). α1 and α2 domain nucleotide sequences were PCR amplified with Platinum® Taq over 32 cycles, using primers specific for exon 1 and exon 3 of 129/SvJ-derived *H2-Bl* (*H2-Bl*^{bc} 5'UTR/ex1 F1 and *H2-Bl*^{bc} ex3 R2). Positions of *HLA-G* polymorphisms were obtained from Arnaiz-Villena et al (292). Polymorphisms in *H2-Bl* and *HLA-G* resulting in frame shifts or premature stop codons are not pictured.

the TCR (141). This position is highly variable in class Ia molecules, and its variation is known to alter recognition by CTL. Its conservation in H2-Bl may be indicative of functional selection for binding of invariant ligands, such as peptides and/or T/NK cell receptors.

In contrast to the 129/SvJ and FVB/NJ alleles, we found that C57BL/6J *H2-Bl* encodes a truncated protein (AY989821). The *H2-Bl* cDNAs from C57BL/6J differed from their 129/SvJ counterparts by five nucleotides in the exon 2-exon 6 coding region (Figure 3.2). These included four nucleotides in exon 3 (one synonymous substitution CTA→CTG at Leu_{160} and three nonsynonymous substitutions GGC→GCC [Gly_{162}→Ala_{162}], GAG→CAG [Glu_{173}→Gln_{173}] and AAT→AAG [Asn_{176}→Lys_{176}] and one nonsynonymous substitution in exon 4, (CAG→TAG). The latter polymorphism converts Glu_{235} into a stop codon and was independently confirmed by sequencing of *H2-*

Bl genomic DNA from a C57BL/6NCr mouse. Thus, if translated, *H2-Bl* from C57BL/6 mice would generate a truncated, secreted protein, lacking the cysteine bridge (Cys_{195}:Cys_{246}) in the β_2m-binding domain. Since such a product is unlikely to perform classical antigen-presenting functions, the nonsynonymous polymorphism in the position corresponding to the putative peptide contact residue (Gly_{162}→Ala_{162}) appears to be of little predictive value.

In summary, our data indicate that two of the three sequenced cDNA alleles of *H2-Bl* (129/SvJ H2-Bl^{bc} and FVB/NJ H2-Bl^{q}) encode canonical, membrane bound class I proteins with highly conserved peptide binding sites. The third allele (C57BL/6J H2-Bl^{b}) is truncated and predicted to be secreted and lacking in class I protein features.

***H2-Bl* Sequences in Wild-Derived Mice**

To gain further knowledge of the diversity of *H2-Bl* we analyzed 5' segments of this gene from 8 *H2-Bl* positive wild-derived mouse strains of various *Mus* species and subspecies further characterized in a following section. The nucleotide compositions were established by direct sequencing of uncloned PCR products amplified from genomic DNA (Figure 3.4, AY989849, AY989855, AY989858-66 and AY989868). All but one of the strains (*Mus m. spp.*, MPR/Pakistan) appeared homozygous at the *H2-Bl* locus (or had a null allele on the other chromosome). Interestingly, their polymorphism patterns showed that the wild alleles are either identical to FVB/NJ *H2-Bl^{q}* (BIK/Israel and SMZ/Morocco), or to129/SvJ *H2-Bl^{bc}* (BZO/Algeria), or are exact, or nearly exact,

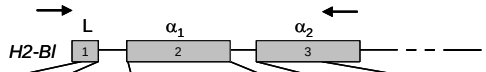

amino acid position			Ala -11	Thr -7	Glu -4	Thr -3	-	-	-	-	Arg 14	Asp 36	Ala 49	Pro 50	Glu 53	Gly 90	-	-	-	Met 103	Thr 125	Asp 137	Leu 141
Inbred	129/B6	prototype	GCG	ACT	GAG	ACT	C	A	G	-----	CGG	GAT	GCG	CCG	GAA	GGC	A	G	T	ATG	ACC	GAT	CTG
	FVB		GCA	ACC	CAG	ACT	C	G	G	AGACC	GGG	GAC	TCG	CCC	GAG	GGT	G	G	G	ATG	GCC	GAC	CTG
Mus m. dom.	BIK	Israel	ND	ND	ND	ND	ND	ND	ND	ND	GGG	GAC	TCG	CCC	GAG	GGT	G	G	G	ATG	GCC	GAC	CTG
	BZO	Algeria	ND	ND	ND	ND	ND	ND	ND	ND	CGG	GAT	GCG	CCG	GAA	GGC	A	G	T	ATG	ACC	GAT	CTG
	DIK	Israel	GCG	ACT	GAG	ACT	C	A	G	-----	CGG	GAT	GCG	CCG	GAA	GGC	A	G	T	ATG	ACC	GAC	CTG
	DEB	Spain	GCG	ACT	GAG	ACT	C	A	G	-----	CGG	GAT	GCG	CCG	GAA	GGC	A	G	T	ATG	ACC	GAC	CTG
Mus m. spp.	BID	Iran	GCG	ACT	GAG	ACT	C	A	G	-----	CGG	GAT	GCG	CCG	GAA	GGT	A	G	G	GTG	ACC	GAC	CTG
	MPR	Pakistan	GCG	ACT	GAG	AC$^{T}/_{C}$	$^{C}/_{A}$	A	$^{G}/_{T}$	-----	CGG	GAT	GCG	C$^{C}/_{A}$G	GAA	GGT	A	$^{G}/_{A}$	G	ATG	ACC	GAC	CTG
Mus m. mus.	MGA	Georgia	GCG	ACT	GAG	ACT	C	A	G	-----	CGG	GAT	GCG	CCG	GAA	GGC	A	G	T	ATG	ACC	GAT	CTT
Mus spretus	SMZ	Morocco	GCA	ACC	CAG	ACT	C	G	G	AGACC	GGG	GAC	TCG	CCC	GAG	GGT	G	G	G	ATG	GCC	GAC	CTG
nucleotide position			-233	-221	-214	-209	-162	-143	-138	-120 to -115	39	116	144	148-9	158	269	289	374	396	512	578	616	628

Figure 3.4 Two dominant alleles of *H2-Bl* and *H2-Bl* alleles with subtle variations thereon predominate among *H2-Bl*-positive wild-derived mice from multiple *Mus musculus* subspecies and *Mus spretus*. *H2-Bl* from genomic DNA of eight wild-derived and three inbred strains of mice that contain the *H2-Bl* gene was PCR amplified as in Figure 3 using primers specific for exon 1 and exon 3 of 129/SvJ-derived *H2-Bl* (*H2-Bl*^{bc} 5'UTR/ex1 F1 and *H2-Bl*^{bc} ex3 R2, arrows) (AY989849, AY989855, AY989858-62 and AY989864-66). Wild mouse strains are listed by a three letter designation, species and subspecies, where appropriate, and country of origin. Polymorphic nucleotides detected across the sequenced region are shown with the affected codon when in an exon and alone when in an intron. The amino acid translation of the 129/SvJ prototype sequence resides above the appropriate codon. Amino acid 1 is the first amino acid of α1, as is traditional of MHC class I sequences. Nucleotide position 1 is the first nucleotide of exon 2 (i.e. the second nucleotide of the first composite codon of the α1 domain). There is no zero position in the nucleotide or amino acid sequence. Darkened codons indicate those in which a nonsynonymous substitution has occurred (GAG→CAG, Glu_{-4}→Gln_{-4}; CGG→GGG, Arg_{14}→Gly_{14}; GCG→TCG, Ala_{49}→Ser_{49}; CCG/C→CAG/C, Pro_{50}→Gln_{50}; ATG→GTG, Met_{103}→Val_{103}; ACC→GCC, Thr_{125}→Ala_{125}). Only one of these nonsynonymous substitutions (Thr_{125}→Ala_{125}) affects a residue which is conserved in the H2 consensus (290), and this residue has no particular ascribed role in class I structure or function. BIK and BZO *H2-Bl* sequences were preformed at a separate time than the rest and did not have the same resolution in the 5' end of the sequence.

chimeric versions of these two alleles. DIK/Israel and DEB/Spain differed from 129/SvJ by one silent FVB/NJ-like substitution at the Asp_{137} codon. MGA/Georgia differed from the prototype 129/SvJ *H2-Bl*^{bc} by one silent substitution at Leu_{141}. The most divergent alleles (*Mus m. spp.*, BID/Iran and MPR/Pakistan) carried a more extensive "microchimerism" of 129/SvJ and FVB/NJ sequences. In addition, each of these alleles

contained one unique (not found in the two major alleles) nonsynonymous substitution in the predicted mature protein sequences: $Pro_{50} \rightarrow Gln_{50}$ (MPR/Pakistan) and $Met_{103} \rightarrow Val_{103}$ (BID/Iran). Both these polymorphisms are located outside of the highly conserved class I MHC regions and the predicted peptide-binding residues of the groove (Figure 3.3).

Strain-Dependent Alternative Splicing of *H2-Bl* Genes

During our experiments seeking to identify the canonical *H2-Bl* gut transcripts we detected strain-dependent variation in length and in relative abundance of *H2-Bl*-specific cDNAs (Figure 3.5, H2-Bl panel). The *H2-Bl* cDNA amplified from 129/SvJ with primers specific for the 5' and 3' UTR of *H2-Bl* migrated as two major bands in agarose gels (~1200 bp and ~900 bp). cDNA from FVB/NJ migrated as a single band (~1200 bp) as did the C3H/HeJ cDNA (~900 bp). Interestingly, the *H2-Bl*-positive C57BL/6J mice, like the control BALB/cJ *H2-Bl*-negative mice, typed negative in this semi-quantitative assay, suggesting that the steady state gut $H2\text{-}Bl^b$ mRNA levels in C57BL/6J strain are too low to be detected under the standard RT-PCR conditions used in this set of experiments (legend to Figure 3.5). Similar results were observed by Northern blot analysis (data not shown), thus confirming overall low transcript abundance of the C57BL/6J $H2\text{-}Bl^b$ allele.

After changing experimental conditions to enhance detection of C57BL/6J mRNAs (Figure 3.6), two major *H2-Bl* cDNA species were visualized by gel electrophoresis. The relative intensities of the upper, ~1200 bp, and the lower, ~900 bp, bands were reproducibly altered in C57BL/6J compared to 129/SvJ lanes (Figure 3.6A and B).

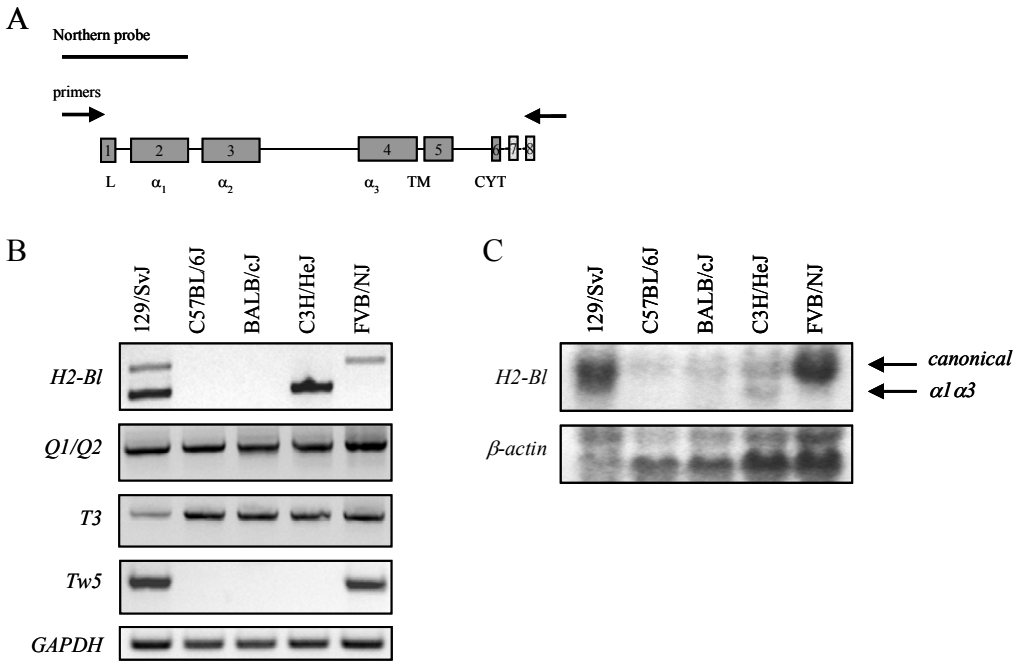

Figure 3.5 Transcriptional activity and alternative splicing of gut class Ib differ among inbred mouse strains. A) Diagram of MHC class Ib transcripts (exons depicted as blocks). PCR primers specific for the 5' and 3' UTR of the indicated class Ib genes are depicted as arrows. The Northern probe specific for the leader and α1 domain of H2-Bl is depicted as a line. B) PCR amplificatation of MHC class Ib transcripts from small intestinal cDNA of inbred mice. Primers and conditions for the PCR reactions were as follows: *H2-Bl*: HotStarTaq®, 30 cycles with *H2-Bl*^{bc} 5'UTR/ex1 F1 and *H2-Bl*^{bc} 3'UTR R; *Q1*/*Q2*: Platinum® Taq, 32 cycles with *Q1*^{b}/*Q2*^{b} 5'UTR/ex1 F and *Q1*^{b}/*Q2*^{b} 3' UTR R, dually specific for *Q1* and *Q2*; *T3*: Platinum® Taq, 32 cycles with *T3*^{b} 5'UTR/ex1 F and *T3*^{b} 3'UTR R; *Tw5*: HotStarTaq®, 32 cycles with *Tw5*^{bc} 5'UTR F and *Tw5*^{bc} 3'UTR R. The *GAPDH* control reaction was performed as in Figure 1. The upper band of *H2-Bl* corresponds to canonically spliced H2-Bl while the lower band lacks exon 3. All other gut-restricted class Ib bands correspond to canonically spliced isoforms. The identities of *H2-Bl* isoforms and all other gut-restricted class Ib transcripts were confirmed by cloning and sequencing or sequencing directly from PCR amplifications (AY989821-41, AY989854, AY989856-57, AY989869, AY989871 and AY989873). Exon/exon junctions were determined by aligning band sequences with genomic DNA fragments from the NCBI database. C) Northern of small intestinal total RNA from the indicated mice. The RNA-crosslinked membrane was first hybridized with the H2-Bl probe, then stripped and re-probed for β-actin. Based on the position of the lower band in the C3H sample, is it likely that the upper band of *H2-Bl* corresponds to canonically spliced H2-Bl while the lower band lacks exon 3.

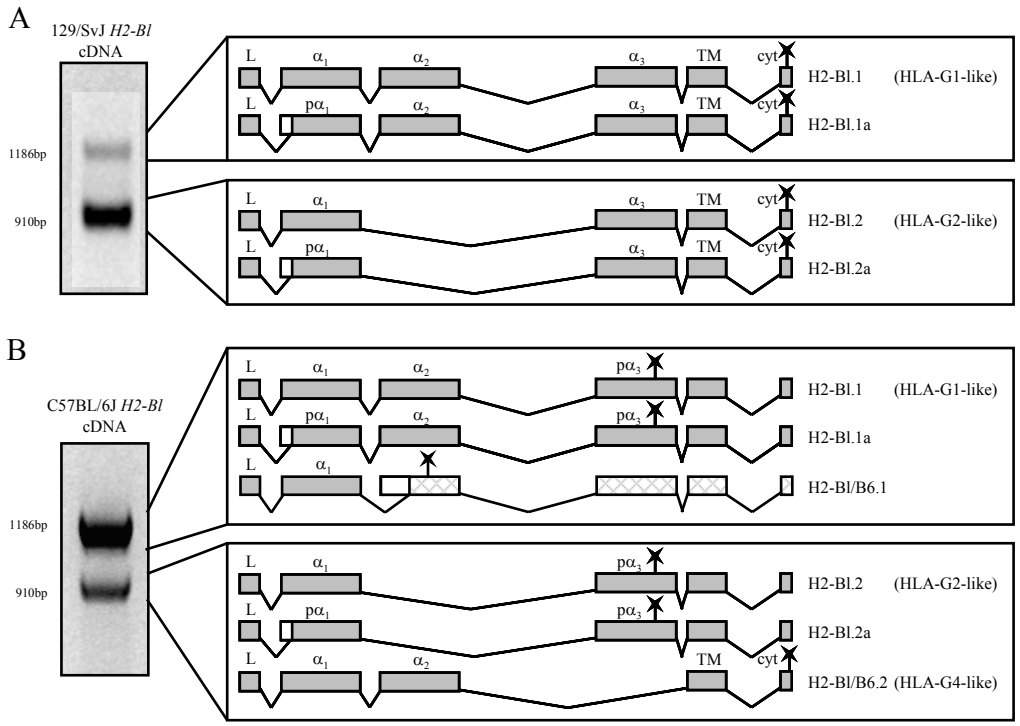
A
129/SvJ H2-Bl
cDNA
1186bp
910bp
L
α1
α2
α3
TM
cyt
pα1
H2-Bl.1
(HLA-G1-like)
H2-Bl.1a
H2-Bl.2
(HLA-G2-like)
H2-Bl.2a
B
C57BL/6J H2-Bl
cDNA
pα3
H2-Bl/B6.1
H2-Bl/B6.2
(HLA-G4-like)

Figure 3.6 *H2-Bl* is transcribed into multiple alternatively spliced isoforms which differ in exon composition and abundance between 129/SvJ and C57BL/6J inbred mice. A) *H2-Bl* isoforms in 129/SvJ small intestinal mRNA. The 129/SvJ *H2-Bl* allele has an intact open reading frame with 6 possible exons. Canonical isoforms (H2-Bl.1 and .1a, lacking the first 33 nt of exon 2) and those lacking exon 3 (H2-Bl.2 and .2a, lacking the first 33 nt of exon 2) are the predominant species in the 129/SvJ small intestine (AY989838-41). B) The C57BL/6J *H2-Bl* allele is truncated due to a premature stop codon in exon 4. Like 129/SvJ, the C57BL/6J mouse produces H2-Bl.1, .1a, .2 and .2a, but C57BL/6J *H2-Bl* also splices into a variant missing exon 4 (H2-Bl/B6.2) and another that utilizes a cryptic splice site 26 nt into exon 3, shifting the reading frame to produce a stop codon 36 aa into the altered reading frame of exon 3 (H2-Bl/B6.1) (AY989821-26). Many other smaller alternatively spliced isoforms of *H2-Bl* can also be detected at low levels in the C57BL/6J mouse (not pictured, AY989827-37). These isoforms were generated by use of cryptic splicing sites or by alternative splicing of multiple exons, and frequently gave rise to transcripts with an altered reading frame. The common feature of these isoforms is their retention of an intact leader peptide. In both 129/SvJ and C57BL/6J *H2-Bl* cDNA pools, the H2-Bl.1:H2-Bl.1a and H2-Bl.2:H2-Bl.2a ratios were approximately 1:1. The designation "p" preceding a domain name (as in "pa1") indicates that, upon mRNA translation, a "portion" of the canonical domain will be present. 129/SvJ small intestinal *H2-Bl* was amplified using HotStarTaq® over 30 reaction cycles and applied directly to an agarose gel. 18 HotStarTaq® PCR reactions of C57BL/6J small intestinal *H2-Bl* at 35 cycles were combined, concentrated by acid/ethanol precipitation and run on an agarose gel. Both 129/SvJ and C57BL/6J *H2-Bl* alleles were amplified using *H2-Bl*^{bc} 5'UTR/ex1 F1 and *H2-Bl*^{bc} 3'UTR R primers. DNA from the bands shown was extracted from the agarose gel, cloned into pcDNA II and sequenced to determine the identities of the isoforms. Presence of the stop codon in C57BL/6 *H2-Bl* was confirmed by sequencing of the relevant gene fragment from PCR-amplified genomic C57BL/6NCr DNA using *H2-Bl*^{bc} int3 F and *H2-Bl*^{bc} ex5 R primers (data not shown).

The *H2-Bl* RT-PCR products amplified from small intestinal RNA of each of the studied strains were eluted from an agarose gel, cloned and sequenced (Figure 3.5 and Figure 3.6, AY989821-71, AY989854 and AY989856-57). Multiple clones were analyzed to correct for possible PCR errors. The ~1200 bp cDNA bands from 129/SvJ and C57BL/6J mice contained two common species, H2-Bl.1 and H2-Bl.1a, present in ~1:1 ratio. The first corresponds to the 1186 bp canonical isoform encoding leader (L), α1, α2, α3, TM, and CYT regions, and the second one is a differentially spliced, 1153 bp product, lacking the first 33 nucleotides of exon 2. The ~900 bp bands in both strains

also contained two common products: a 910 bp isoform, H2-Bl.2, lacking exon 3, and its 877 bp truncation variant, H2-Bl.2a, lacking 33 nucleotides in the 5' end of exon 2. In addition, C57BL/6J gave rise to at least two other isoforms. The first of them, H2-Bl/B6.1, is generated by splicing at a cryptic site in exon 3, which leads to an alternative reading frame ending with a premature stop codon in the α2 domain. The second, H2-Bl/B6.2, skips exon 4. Since removal of this coding region deletes the stop codon, the H2-Bl/B6.2 transcript from the C57BL/6J allele may give rise to a protein structurally reminiscent of NKG2D-ligands such as α3-domain lacking, class I-related Rae-1 polypeptides (156). H2-Bl.1, H2-Bl.2 and H2-Bl/B6.2 isoforms correspond in exon/exon organization to *HLA-G* isoforms designated as HLA-G1 (canonical) , HLA-G2 (α1α3) and HLA-G4 (α1α2), respectively (225, 293).

In many genes a premature stop codon leads to stop-codon mediated mRNA degradation (294) and alternative splicing of the transcripts (295). We suggest that the nonsense mutation, CAG→TAG in exon 4 of C57BL/6J *H2-Bl*^{b}, is responsible for drastically reduced *H2-Bl* transcript levels and the synthesis of unique H2-Bl/B6.1 and H2-Bl/B6.2 isoforms detected in this strain. This polymorphism may also contribute to the generation of additional short *H2-Bl* splicing variants observed preferentially in this strain (legend to Figure 3.6).

The *H2-Bl* cDNAs from FVB/NJ (~1200 bp band) contained the canonical, H2-Bl.1, and the truncated canonical, H2-Bl.1a, isoforms in 1:1 ratio, but lacked detectable H2-Bl.2/2a isoforms (data not shown). Since one of the polymorphisms between FVB/NJ and 129/SvJ alleles occurs at the junction of exon 2 and intron 2 (Figure 3.2) it is

likely that this silent substitution, CAG→TAG, is responsible for differential splicing of exon 3.

The exon/exon organization of the C3H/HeJ *H2-Bl* cDNAs corresponded to H2-Bl.2/2a isoforms (data not shown). The H2-Bl.1/1a isoforms were not detected in this strain. Since the sequences of the C3H/HeJ H2-Bl.2/2a were identical to the corresponding isoforms from 129/SvJ, the polymorphism regulating differential splicing of exon 3 in this allele may be located outside of the sequenced regions, possibly in introns 2, 3 or in the spliced out exon 3.

Unapparent Contribution of Non-*Mhc* Genes to *H2-Bl* Allele-Specific Expression Profiles

To test if non-MHC genes contribute to the observed low expression of *H2-Bl* mRNA in C57BL/6J mice we took advantage of $K^{b-/-}D^{b-/-}$ mice (255) derived from the 129/SvJ strain and backcrossed for six generations to C57BL/6J. Presence of 129/SvJ loci in the *Mhc* was confirmed by showing that $K^{b-/-}D^{b-/-}$ gut transcripts contain sequences unique to *Tw5*, a gene related to *H2-Bl* and shown to exist in 129/SvJ but not in C57BL/6J MHC (276). The RT-PCR analysis of *Tw5* transcripts in several tissues revealed that this gene, proposed to be a paralog of *H2-Bl* on the basis of sequence homology (276), has a restricted expression pattern, identical to the *H2-Bl* allele of the $K^{b-/-}D^{b-/-}$ strain (Figure 3.7). *H2-Bl* transcript levels in gut tissues from C57BL/6J mice were reproducibly reduced compared to $K^{b-/-}D^{b-/-}$ control, indicating that the background genes in C57BL/6J do not influence this phenotype. Other gut-restricted genes, *Q1*, *Q2*

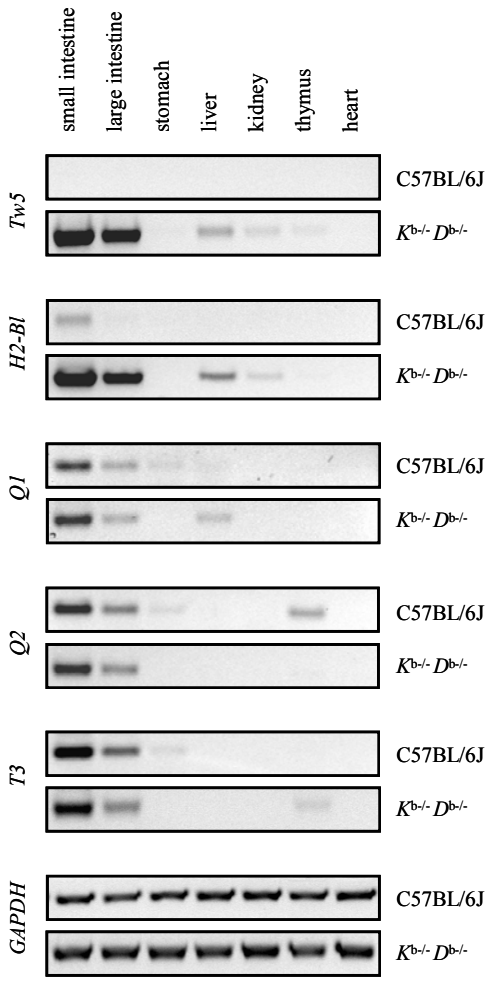

Figure 3.7 Genes outside of the C57BL/6J *Mhc* are not responsible for the low abundance of *H2-Bl* transcript in the C57BL/6J mouse, nor do they impact the abundance of other gut-restricted class Ib MHC. RT-PCR analysis of transcriptional activity of gut-restricted MHC class Ib was performed in selected tissues of C57BL/6J and $K^{b-/-}$ $D^{b-/-}$ mice. Results for individual class I transcripts in tissues of both mice are boxed for mouse-to-mouse comparison. Primers used to amplify *Q1*, *Q2*, *T3*, *H2-Bl* and *GAPDH* were identical to those used in Figure 1. Amplification of *Tw5*, the putative paralog of *H2-Bl* (276), was performed with $Tw5^{bc}$ 5'UTR/ex1 F and $Tw5^{bc}$ ex3 R. All bands were of the expected size, and their identities were confirmed by sequencing. Half of the *GAPDH* reaction was loaded on the agarose gel to ensure the signal was within the linear detection range of the gel. PCR results were generated with 30 reaction cycles using HotStarTaq®.

and *T3*, identified in the initial survey of C57BL/6J, had similar expression profiles in the two strains. Minor, strain-dependent differences in the mRNA levels were detected in a few of the secondary organs (*Q2* and *T3* in thymus, *Q1* in liver) suggesting that *Q1*, *Q2* and *T3* alleles, or their paralogs from C57BL/6J and $K^{b-/-}D^{b-/-}$, may have slightly different tissue distributions in the two strains.

We also considered the possibility that alternative splicing of *H2-Bl* is imposed by the gut milieu and controlled by non-*Mhc* genes expressed in this tissue. To address this possibility we tested transcriptional profiles of K^b and D^b genes (data not shown) as well as gut-restricted class I genes, *Q1*, *Q2*, *T3* and *Tw5* (Figure 3.5). In each case, only a

single species of class I cDNA, with a molecular weight predicted for the relevant canonical isoform, was amplified.

Taken together, the data support the conclusion that the alternative splicing pattern and the polymorphism in expression levels of *H2-Bl* transcripts are allele specific and are not modulated by strain-dependent variation in non-*Mhc* genes.

Comparison of Gut-Restricted Class Ib Genes in Wild-Derived Mouse Strains

We demonstrated here that two *T* region genes, *H2-Bl* and *Tw5*, are preferentially transcribed in the gut tissues of adult mice. Exon-intron organization of *Tw5* was originally deduced from the genomic sequence of 129/SvJ mice (276). It predicted six translated exons for this gene of which one, exon 6, was postulated to encode a 19 amino acid long cytoplasmic tail. Our analysis of *Tw5* cDNAs revealed that *Tw5* transcripts contain eight exons, of which the last three encode a 48 amino acid long cytoplasmic tail (AY989869). Interestingly, the comparison of amino acid sequences of Tw5 to other gut-restricted class Ib studied here showed that in the C-terminus Tw5 is more related to Q1, Q2 and T3 than to its proposed paralog, H2-Bl (Figure 3.2). *Tw5*, unlike *H2-Bl*, encodes a tyrosine residue (at position 230) implicated in the endocytic signaling in class Ia antigens (296). Tyrosine residues with potentially similar functions are also found in the cytoplasmic tails of Q2 and T3 (Figure 3.2). Divergence in the predicted amino acid composition is also seen within exon 1 of *Tw5* and *H2-Bl* (264, 276). The putative leader peptide of Tw5, unlike the leader peptide of H2-Bl, bears no substantial homology to the prototype class Ia leader, Qdm (176), and is not predicted to bind to Qa-1 or interact with

CD94/NKG2 receptors. The remainder of the Tw5 protein, particularly the α1, α2 and α3 domains, is closely related to H2-Bl (85.8% identity at the amino acid level). Unexpectedly, *T* region encoded Tw5 is more closely related to *Q* region Q1 and Q2 in α1, α2 and α3 (83.2% and 80.7% identity, respectively) than to *T* region encoded T3 (70.8%). Both H2-Bl and Tw5 are only distantly related to their proposed human homolog, HLA-G (68.2% and 72.3% identity, respectively) and share only one variable residue (Met_5) that distinguishes these three proteins from all other gut-restricted class Ib studied here.

Finally, since *H2-Bl* is believed to represent a murine homolog of *HLA-G*, we investigated if these two proteins share a common pattern of polymorphism. Figure 3.3 shows that the nonsynonymous polymorphic substitutions in the predicted H2-Bl and HLA-G α1/α2 domains affect distinct structural regions, but in both cases, are located outside of the putative peptide-contact residues.

Distribution of Gut-Specific Class Ib Genes in Wild-Derived Mouse Strains

Since *H2-Bl* and *Tw5* have null alleles among inbred strains (264, 276) we wondered if these genes and *Q1*-, *Q2*- and *T3*-like, gut-specific loci have been maintained in the genomes of wild mice under pathogen-imposed and breeding-dependent selections.

DNA from 32 specimens of mice from distinct locations in Europe, Africa, Asia and the Pacific were typed by PCR for *Q1*-, *Q2*-, *H2-Bl*-, *Tw5*- and *T3*-like genes with class Ib specific primers (Table 3.1). The identity of each type of gut-specific gene was confirmed by sequencing of PCR products amplified from SEB (Spain) *Mus spretus*

Table 3.1 *Detection of gut-restricted class Ib MHC in the genomes of inbred and wild-derived mouse strains* [a]

Mouse Type	Strain Name	Country of Origin	MHC Class Ib Gene [b]				
			Q1	*Q2*	*H2-Bl*	*Tw5*	*T3* (TL)
Inbred Strain	C57BL/6NCr		+	+	+	-	+
	129/SvJ		+	+	+	+	+
	FVB/NJ		+	+	+	+	+
Mus m. domesticus	BIK	Israel	+	+	+	+	+
	BZO	Algeria	+	+/-	+	-	+
	DIK	Israel	+	+	+	+	+
	DJO	Italy	+	+	-	-	+
	DMZ	Morocco	+	+	+	-	+
	DOT	Tahiti	+	+	+	-	+
	ZZMO	Tunisia	+	+	+	-	+
	DDO	Denmark	+	-	+	-	+
	DEB	Spain	+	+	+	+	+
	DGA	Georgia	-	-	+	+	+
Mus m. musculus	MAM	Armenia	-	-	+	+	+
	MGA	Georgia	+	+	+	-	+
	MBK	Bulgaria	+	-	+	-	+
	MBS	Bulgaria	+	-	+	+	+
	MDH	Denmark	+	-	+/-	-	+
	MPB	Poland	-	-	+	-	+
Mus m. castaneus	CIM	India	+	+	-	-	+
	CTA	Taiwan	-	+	+	+	+
	CTP	Thailand	+	+	+/-	-	+
Mus m. molossinus	MOL	Japan	-	-	+	+	+
Mus m. spp.	TEH	Iran	+	-	+	+	+
	BID	Iran	-	-	+	-	+
	MAC	Iran	+	-	+	+	+
	KAK	Iran	+	+	+	+	+
	DHA	India	+	+	-	+	+
	MPR	Pakistan	+	+	+	+	+
Mus spretus	SFM	France	-	-	-	-	+
	SMZ	Morocco	+	+	+	-	+
	STF	Tunisia	+	+	-	+	+
	SEB	Spain	+	+	+	+	+
Mus macedonicus	XBS	Bulgaria	+	-	+/-	-	+
Mus spicilegus	ZRU	Ukraine	+	-	+	-	+

[a] Genomic DNA from the indicated mice was tested by PCR with Platinum® Taq over 30 cycles using the following primers: Xho I/*Q1* [b] ex1 F and EcoR I/*Q1* [b] ex3 R; Xho I/*Q2* [b] ex2 F and EcoR I/*Q2* [b] ex3 R; *H2-Bl* [bc] 5'UTR/ex1 F2 and *H2-Bl* [bc] ex3 R1; *Tw5* [bc] ex3 F and *Tw5* [bc] ex3 R; *T3* [b] ex2 F and *T3* [b] ex3 R. Primers are specific to C57BL/6J alleles (*Q1* , *Q2* and *T3*) or 129/SvJ alleles (*H2-Bl* and *Tw5*) but cross-react with other alleles. Since modern inbred strains of mice are predominantly descendants of the *Mus musculus* subspecies, sequence confirmation of PCR products from all five genes was performed in the distantly related *Mus spretus* mouse, SEB.

[b] Reactions yielding a band at the expected size were scored as positive, "+." Those with a very faint band at the appropriate size were scored as ambiguously positive, "+/-." Those with no visible band or a band of the incorrect size were scored as negative, "-." Mice positive for a particular gene are considered to have that gene or a highly homologous gene.

mouse DNA (AY989866, AY898970, AY989872, AY989879 and AY989881) and scoring for the presence of PCR bands with the predicted size in all other cases. We assume that negative typing is indicative of homozygous null alleles, though some genes that diverged in their sequences may have been missed due to the polymorphism in the sequences corresponding to primer locations. Only one of the gut-restricted genes, *T3*-like, was present in all studied mice, while other genes were detected with variable frequency. *Q1*-like genes were found in 25 mice, *Q2*-like in 17, *H2-Bl*-like in 24 and *Tw5*-like in 15 out of 32 mice tested. In addition, one mouse scored as "ambiguously positive" for *Q2* (footnote to Table 3.1), and three similar determinations were made for *H2-Bl*.

Only one mouse scored negative for four (*Q1*, *Q2*, *H2-Bl* and *Tw5*) of the gut-specific genes, and two mice lacked three of the gut-specific genes (*Q1*, *Q2* and *Tw5* in both cases). *H2-Bl* was absent in three cases along with its paralog *Tw5*, and in two cases its loss was accompanied by the presence of all other gut-specific class Ib.

Judging from this data, it appears that gut-specific class Ib are inherited and maintained independently of each other, as there is no clear correlation between presence/absence of these genes and the genetic classification/geographical origin of the tested mice. Thus we conclude that the gut-expressed class Ib may be selectively maintained in the environments in which they contribute to their host's fitness.

Inheritance of *H2-Bl* Alleles Selected for Reproductive Success

The *H2-Bl* cDNA clones described in Sipes et al. (264) were derived from a library made from ~2000 blastocysts of outbred ICR mice. All three independently identified clones were identical in their regions of overlap and corresponded to the 129/SvJ allele. Since ICR mice originated from a heterogeneous pool of mice encoding different MHC and were bred for fecundity (297), we wondered if the 129/SvJ allele has been selectively passed on because it contributed to the reproductive success of the ICR stock.

To address this issue, 9 ICR mice from at least two different litters were examined here. All expressed *H2-Bl* in gut tissues as judged by RT-PCR (data not shown). Full size (5' UTR - 3' UTR) RT-PCR products from 5 of these 9 ICR mice were analyzed by cloning/DNA sequencing (AY989842-47, AY989850-53 and AY989867). Two of the mice appeared homozygous for the 129/SvJ allele of *H2-Bl* (100% identity) and gave rise to the predicted alternatively spliced isoforms. Two other mice were consistent with homozygosity for the FVB/NJ allele and did not express the truncated, exon 3-deleted products (H2-Bl.2/2a). An alternative interpretation of the data is that the putative homozygotes carried a null allele on one of the sister chromosomes. The fifth mouse gave rise to a mixture of 129/SvJ and FVB/NJ cDNA products, suggesting that it is a heterozygote for the *H2-Bl* locus.

We thus conclude that the selection for fecundity in ICR mice did not eliminate either of the two major alleles of *H2-Bl* from the breeding pool.

SUMMARY AND DISCUSSION

Recent advances in the understanding of the complex immunological roles played by the members of the extended family of class I and class I-like proteins revived our interest in class I genes encoded by the *Q* and *T* regions of the mouse *Mhc*. Specifically we were interested in re-examining those MHC class Ib genes that were previously sequenced, or partially sequenced, but whose functions remain unknown. To address if any of them represent candidates for NK/IEL receptor ligands, we surveyed their body-wide expression patterns, emphasizing tissues enriched for epithelial cells, particularly the intestines.

Unexpectedly, in addition to the class Ib genes identified earlier as gut-restricted, *Q1* (249, 287), *Q2* (250, 287) and *T3* (248), we discovered that *H2-Bl*, a gene so far detected only in blastocyst and placenta (264) and proposed to play a role in inducing NK cell tolerance at the maternal-fetal interface (277), is selectively expressed in the intestinal tissues enriched for epithelial cells. We generated a series of complete, contiguous sequences of *H2-Bl* cDNAs corresponding to mature, canonical class Ib H2-Bl proteins from several inbred and outbred mice. In addition, we sequenced 5' DNA sequences of *H2-Bl* genes from wild-derived mouse strains originating from different locations in Europe, Asia, Africa and the Pacific. Two predominant alleles were identified among the studied mice, typified by *H2-Bl* from 129/SvJ and FVB/NJ strains. They differed from each other at 22 nt positions, 9 of which resulted in amino acid replacements. This degree of divergence between the two "prototype" *H2-Bl* alleles is larger than in most stringently conserved class Ib (247, 282) but is similar to that observed in *T23* and *Q2* genes (280, 287). While we favor the interpretation that the *H2-*

Bl sequences from 129/SvJ and FVB/NJ correspond to true alleles, we cannot formally exclude the possibility that they were amplified from distinct genomic loci.

Past studies demonstrated that extensive polymorphism in the classical class I MHC genes affects predominantly the residues of the groove and correlates with the ability to bind peptides with different sequence motifs (298, 299). It is also thought that the polymorphism patterns represent, at least to some degree, a record of past pathogen-driven selections and are predictive of functionally important locations in the studied proteins (34, 35). The pattern of amino acid substitutions in the major *H2-Bl* alleles and in closely related sequences from wild-derived mice appears to be non-randomly distributed in relation to the functionally important protein regions. The conceptual translation of each *H2-Bl* allele, with the exception of the C57BL/6J allele, is expected to give rise to a canonical protein with 3 extracellular domains, TM and CYT regions. Remarkably, the residues that are highly conserved between mouse and human class I proteins, as well as those that are universally present in class I chains throughout vertebrate evolution (298) remain invariant among different *H2-Bl* alleles. Since the conservation of these residues is thought to be critical for structural integrity of class I MHC, the allelic variants of H2-Bl proteins are likely to fold into class Ia-like structures.

The repertoire of nucleotide substitutions in the variants of the canonical *H2-Bl* outside of the class I "framework" residues also appears non-random. Even though the polymorphisms are spread throughout the coding regions (6 in exon 2, 4 in exon 3, 8 in exon 4, 3 in exon 5 and 1 in exon 6 for the two major alleles), none affect residues in the putative peptide-contact sites. Furthermore, none of the residues that are highly polymorphic in class Ia is substituted in *H2-Bl* variants. In one case, where nucleotide

substitution occurred at such a position, at Glu_{163} (a residue that is predicted to face into the groove and toward the T cell receptor), the change is synonymous. In general, the synonymous substitutions in *H2-Bl* alleles predominate over the nonsynonymous in the three extracellular domains, while the reverse correlation is observed in the TM and CYT regions. This suggests that selective conservation of the H2-Bl N-terminus might have indeed occurred during evolutionary history of this gene in *Mus* species. Since the side chains involved in peptide binding in typical class I ($Tyr_{7,}$ $Tyr_{59,}$ $Tyr_{159,}$ Tyr_{171} for the N-terminus and Thr_{143}, Tyr_{84}, Lys_{146} and Trp_{147} for the C-terminus (300)) are strictly conserved in the H2-Bl sequences analyzed here, it is most likely that this class Ib molecule binds peptides. Alternatively, the observed pattern of substitutions may be indicative of selection for binding of conserved, non-peptidic short ligands or a necessity to interact with invariant receptors, such as specific members of the TCR, NKG2D, Ly49 or CD94/NKG2 families.

The most striking feature of the strain-dependent variation of *H2-Bl* alleles is the diversity of their alternatively spliced transcripts. We identified here at least 4 different repertoires of transcriptional isoforms generated in the gut of 129/SvJ, FVB/NJ, C3H/HeJ and C57BL/6J mice. The 129/SvJ allele gives rise to at least four major isoforms: the canonical transcript (H2-Bl.1), its truncated variant lacking codons for 11 aa at the N-terminus (H2-Bl.1a), α2-domain lacking isoform (H2-Bl.2) and its N-terminal truncated variant (H2-Bl.2a). The FVB/NJ mice express only H2-Bl.1 and H2-Bl.1a, while C3H/HeJ express only detectable levels of H2-Bl.2 and H2-Bl.2a. Most interestingly of all, a polymorphic substitution of Glu_{235} into a premature stop codon not only converts canonical $H2\text{-}Bl^{b}$ into a potentially secreted, truncated protein, but also alters

qualitatively and quantitatively its profile of isoforms. The relative proportions of H2-Bl.1/1a to H2-Bl.2/2a are reversed compared to 129/SvJ, new isoforms are synthesized, including an α1 and α2 domain-encoding, Rae-1-like transcript (H2-Bl/B6.2), and the overall level of *H2-Bl* transcripts from this allele is severely depressed. We propose that the reduction in the steady state levels of *H2-Bl* mRNA in C57BL/6J and the change in the profile of alternative splicing is due to the presence of the stop codon since the nonsense-mediated effects on RNA degradation and splicing patterns have been reported in other systems (294, 295). The differential splicing between 129/SvJ and FVB/NJ alleles may also be attributed to a specific polymorphism; in this case one possible candidate is a synonymous substitution at the Gly_{90} codon near the junction of exon 2/intron 2.

To the best of our knowledge, this is the first reported case of a class I MHC gene in which polymorphism affects alternative splicing of exons encoding extracellular domains. Its direct consequence is the expression of variant sets of canonical and non-canonical products that may be shaped by balancing evolution (301). Interestingly, the truncated, non-canonical isoform found thus far only in H2-Bl, H2-Bl.1a, is theoretically compatible with a class I-like structure, despite the predicted displacement/rearrangement of β strands (302). The H2-Bl isoform lacking the α2 domain, H2-Bl.2, resembles similar truncated polypeptides encoded by human and mouse class I MHC and non-MHC genes, including *HLA-G* (225), *MICA/B* (303) and *MR1* (304). H2-Bl/B6.2, lacking the α3 domain, is in turn structurally similar to the HLA-G4 isoform (225) and several members of the mouse family of NKG2D ligands, such as Rae-1 (156, 274).

One feature common to all *H2-Bl* isoforms studied here is the presence of exon 1, encoding the leader peptide. The N-terminal leaders of class I MHC are co-translationally cleaved before the mature protein leaves the ER. Many of these leaders bind to Qa-1 (or its human homolog, HLA-E). When the complexes are presented at the cell surface they engage inhibitory or activating NKG2 receptors on NK cells or T cells and either potentiate or downregulate effector functions (176). It has been recently shown that H2-Bl.1 and H2-Bl.2 isoforms can provide leader peptides for binding to Qa-1 molecules (277). The leader/Qa-1 complexes expressed on the surface of tumor cells were able to attenuate NK activity *in vitro* and *in vivo* (277). By extension, we propose that the polymorphism affecting the profiles of *H2-Bl* transcripts impacts effector functions of gut-localized cells expressing CD94/NKG2. In addition to NK cells, these might include IEL and other populations of immune cells in the lamina propria or the epithelial layer of the intestines.

It is of interest to note that *Tw5*, shown here to be gut-specific and earlier proposed to be a paralog of *H2-Bl* on the basis of sequence homology (276), does not give rise to alternatively spliced transcripts. This feature, as well as the differences in the length and the composition of the cytoplasmic domains, may be indicative of their distinct roles in the mucosal immune system.

H2-Bl was originally postulated to be the murine homolog of human *HLA-G* (264). Finding that *H2-Bl* is highly expressed in adult gut tissues may not necessarily contradict this hypothesis, since the intestinal milieu, like the maternal/fetal interface, is dominated by immunological tolerance. *H2-Bl* encodes leader peptides that provide protection from NK cytolysis (277) as does *HLA-G* (305), and both class I encode similar

alternatively spliced isoforms that may perform homologous functions. On the other hand, the two class Ib molecules do not share overlapping patterns of nonsynonymous polymorphism that would indicate similar evolutionary pressures. They also direct synthesis of a non-overlapping set of truncated transcripts. It is thus possible that detection of *H2-Bl* in the blastocyst is related to genome-wide epigenetic reprogramming that allows expression of a multitude of otherwise tissue-specific genes at this stage of embryonic development (306). Indeed, we detected a CpG island (307) in the 5' region of the *H2-Bl* gene (data not shown) which, upon demethylation, could give rise to transcription of *H2-Bl* in blastocysts.

Little is currently known about the roles of other class Ib proteins expressed selectively in the gut tissues. The best characterized member of this family in the mouse, TL, encoded by *T3* and related genes, is thought to modulate cytokine production by IEL upon binding to CD8αα receptors (38). The Q1 and Q2 proteins have not yet been studied. While the *Q1* gene is highly conserved among different mouse strains (287), *Q2*, like *H2-Bl* described here, has divergent alleles. *Q2* sequences from $H2^b$ and $H2^k$ differ at 97 nucleotides in exons 2 and 3, resulting in 46 amino acid replacements. Strikingly, this diversity, unlike the diversity of *H2-Bl* alleles but similar to polymorphisms in classical class I *Mhc* or *MICA/B* genes (308), appears to result from selection for diversification of the peptide-binding site.

Given the distinctive structural properties of the gut-specific class Ib examined here, we wondered if they are all essential for survival in the wild. Our results demonstrated that only *T3*-like genes are maintained in all genomes of wild-derived mouse strains, while other gut-specific class Ib genes have null loci and are inherited

independently of each other. This diversity of class Ib functions in the gut is probably magnified by contributions of MHC products with a broad tissue distribution. We have shown here that at least 11 ubiquitously transcribed class I MHC are co-expressed in epithelial cell-enriched tissues, along with the gut-specific class Ib genes. Two of the widely expressed class I-like proteins, MR1 and Qa-1, were shown to have local effects in the gut and to regulate expression of unique, gastrointestinal T cell subsets (40, 92).

Taken together, our data suggest that a large number of class I MHC and class I-like genes are active in the tolerance-dominated, pathogen-reactive milieu of the gut. The complexity of their canonical product functions may be potentiated by expression of multiple alternatively spliced isoforms.

CHAPTER FOUR

Localization of Gut-Specific Class Ib MHC and their Putative Ligands within Small Intestinal Immunological Sub-compartments

BACKGROUND AND RATIONALE

In the previous chapter we characterized several novel class Ib MHC genes and demonstrated their selective transcription in adult tissues of the gastrointestinal tract. Among them was *H2-Bl*, initially reported to be transcriptionally active solely during embryonic life (264) and proposed on this basis to represent a functional homolog of human *HLA-G*. The latter is a class Ib MHC antigen that resides on the trophoblasts of the developing embryo, where it engages in tolerance inducing interactions with a variety of inhibitory lymphocyte receptors (CD94/NKG2A, ILT-2) that protect the fetus from maternal immune attack (309). The similarities between the tolerance dominated environments of the small intestine and the placental tissues prompted us to focus on intestinal compartments where tissue-specific class Ib MHC may encounter immune cells with class I-reactive NK and T cell receptors. We have also reexamined their developmental expression and analyzed promoter regions for elements responsive to known transcription factors. Contrary to previous reports (277), we find that *H2-Bl*, like other gut-specific *Q1*, *Q2*, *T3* and *Tw5* genes studied here, is expressed at appreciable levels only during adult life and is developmentally regulated similarly to class Ia *Mhc* and to many other ubiquitously expressed class Ib *Mhc*, which reach their peak expression level several weeks after birth (249, 310). We find that all gut-specific class

Ib are selectively transcribed in epithelial cells of the gut monolayer, where they may come in contact with IEL expressing αβ or γδ TCR as well as unusual combinations of inhibitory and activating NK cell receptors. Our flow cytometry experiments identified these putative NK class Ib MHC-reactive receptors as NKG2D, NKG2A and/or CD94 displayed constitutively on small subsets of conventional (TCR$\alpha\beta^+$ CD8$\alpha\beta^+$) and unconventional (TCR$\gamma\delta^+$ and/or TCR$\alpha\beta^+$ CD8$\alpha\alpha^+$ or TCR$\alpha\beta^+$ CD8$^-$) IEL. The promoter regions of *H2-Bl*, *Tw5*, *Q1* and *Q2* share striking similarities with each other and contain many transcription factor elements that were previously shown to restrict other gut-specific, non-*Mhc* genes to the enterocyte lineage and impart crypt-to-villus and duodenal-to-colonic gradients of gene expression in the gut (311, 312). Consistent with this analysis, we find that *H2-Bl*, *Tw5*, *Q1* and *Q2* are most highly transcribed in the duodenal-proximal segments of the small intestine. Their expression diminishes along the cephalocaudal axis until it drops precipitously in the large intestine. Expression of rare but detectable gut class Ib MHC transcripts in the thymus, where most IEL are educated, and the presence of IFN-γ responsive elements in their promoters are consistent with their proposed functions as specialized antigen presenting or inflammation signaling molecules in the gut. Taken together, the results of our studies suggest that the class Ib MHC described here help to regulate proximal IEL immune effectors with which they come in contact in the small intestinal epithelial layer.

RESULTS

Gut-Specific Class Ib *Mhc* Are Predominantly Expressed in IEC

In the previous chapter we reported that two novel class Ib MHC genes, *H2-Bl* and *Tw5*, are selectively transcribed in unfractionated gut tissues. To localize their expression to specific compartments of the small intestine, gut cells from a 129/SvJ mouse were fractionated into lamina propria and epithelial monolayer using standard purification procedures (Materials and Methods). The expression of several class I MHC and control genes was examined by semi-quantitative RT-PCR (Figure 4.1). All gut-specific class Ib *Mhc*, *Q1*, *Q2*, *Tw5* and *H2-Bl* were detected in the epithelial monolayer but not in the lamina propria or spleen, while ubiquitously expressed *H2-D*^{b} and *T23* (Qa-1 gene) were detected in all samples (Figure 4.1A). The epithelial monolayer contains two major cell populations: IEL, expressing the CD103 integrin (313), and IEC, expressing sprr2a, a small proline-rich protein characteristic of these cells (314, 315). We sorted these two cell types by flow cytometry according to size (IEL gate and IEC gate in Figure 4.1C) and surface CD3 expression (CD3ε gate in Figure 4.1C) to yield purified populations of IEL (~93% CD3 positive) and IEC (>99% CD3 negative). The purity of the samples was further verified by RT-PCR of sprr2a and CD103 markers (Figure 4.1B bottom). Semi-quantitative RT-PCR on pure IEL and IEC samples demonstrated that gut-specific class Ib (*H2-Bl*, *Tw5*, *Q1* and *Q2*) are exclusively transcribed in IEC, while ubiquitous class I MHC, *H2-D*^{b} and *T23* are expressed in both cell types.

Cephalocaudal Regulation of Gut-Specific Class Ib *Mhc* Resembles that of Enterocyte-Restricted Genes

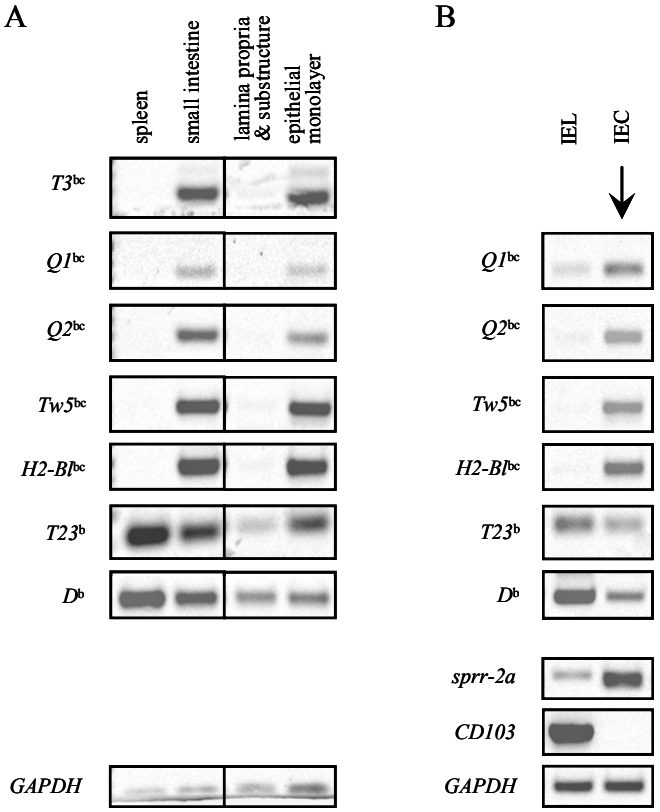
A
spleen
small intestine
lamina propria & substructure
epithelial monolayer
T3bc
Q1bc
Q2bc
Tw5bc
H2-Blbc
T23b
Db
GAPDH
B
IEL
IEC
Q1bc
Q2bc
Tw5bc
H2-Blbc
T23b
Db
sprr-2a
CD103
GAPDH

C

Pre-Sort IEL/IEC

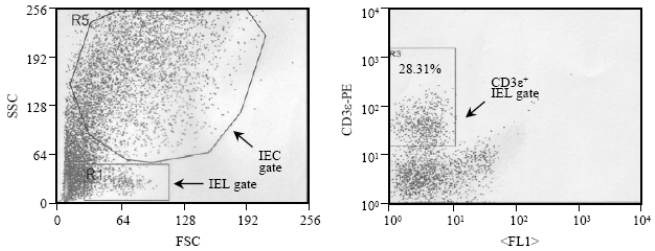

Post-Sort IEL

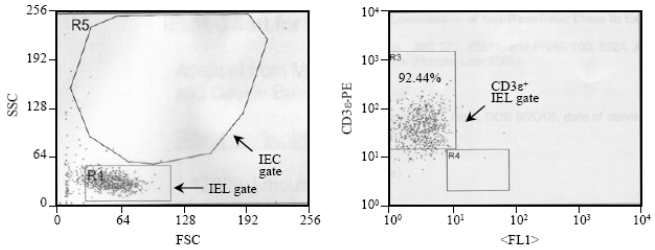

Post-Sort IEC

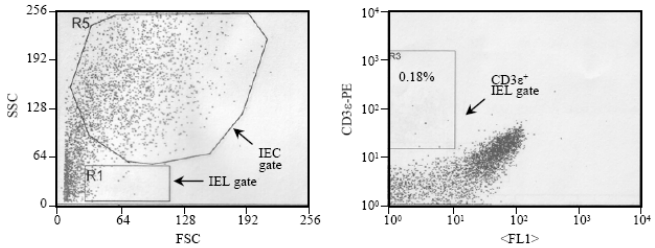

Figure 4.1 Gut-specific class Ib MHC are expressed predominantly in the small intestinal epithelial monolayer and can be further localized to IECs. A. Detection of gut-specific class Ib MHC expression in intestinal substructures by semi-quantitative RT-PCR. The epithelial monolayer and lamina propria/intestinal substructure were isolated as described in Materials and Methods. Spleen cDNA was used as a negative control for gut-specific class Ib MHC. *GAPDH* transcript levels served as a cDNA quality control. Class I MHC primers and *GAPDH* primers were the same as those in Figures 3.1 and 3.7. Other primers used were as follows: *CD103* – *CD103* F and *CD103* R; *sprr2a* – *sprr2a* F and *sprr2a* R. RT-PCR reactions were run for 26 cycles for $T23^{bc}$, D^{bc}, *CD103*, *sprr2a* and *GAPDH* and 30 cycles for the remaining reactions. B. Expression of gut-specific class Ib MHC in IEL and IEC by semi-quantitative RT-PCR. IEL and IEC were isolated from the epithelial monolayer by FACS according to size and CD3 expression (see Figure 4.1C). Due to the small number of IEL recovered from the sort (~0.25×10^6), IEC RNA was diluted to the approximate concentration of the IEL RNA sample (by comparing volume-corrected cell equivalents of RNA [see Appendix B] and titrating the cDNA for similar *GAPDH* PCR amplification). The number of cycles used for PCR was then recalibrated for each primer set to ensure signal intensity in the linear range of an agarose gel. *CD103* served as a control for IEL contamination of the IEC sample, and *sprr2a* served as a control for IEC enrichment. Cycling conditions were as follows: 32 cycles: $T23^{bc}$ and *sprr2a*; 34 cycles: $Tw5^{bc}$, $H2\text{-}Bl^{bc}$, D^{b} and *GAPDH*; 38 cycles: $Q1^{bc}$, $Q2^{bc}$ and *CD103*. C. Purification of IEL and IEC populations by FACS. Pre- and post-sort flow cytometric profiles of IEL and IEC are shown. In the first row (left side) FSC^{hi} SSC^{hi} IEC were sorted on the R5 gate. To sort IEL, the R1 gate was applied to the FL1 v PE dot plot (right side), and IEL were collected based on their CD3ε-PE^{+} $FL1^{-}$ profile. In the second row, FACS profiles of post-sort IEL reveal a > 92% pure population of cells by CD3ε-PE fluorescence. FACS profiles of FSC^{hi} SSC^{hi} autofluorescent (PE^{+} $FL1^{+}$) IEC in the third row indicate > 99% purity for this cell population. The RT-PCR experiments described above were performed once for one animal.

A number of genes transcriptionally restricted to the enterocyte lineage (such as *mdr3* [multi-drug resistance 3] and *fabpi* [intestinal fatty acid binding protein]) have a distinct duodenal-ileal expression pattern that relates to their function along the cephalocaudal axis (311, 312). It has also been reported that type and number of IEL differ along the same axis (46, 47). To determine if gut-restricted class Ib MHC are similarly regulated, we performed semi-quantitative RT-PCR on equally sized segments of the gastrointestinal tract of a 129 x B6 F1 mouse (Figure 4.2). Small intestinal segment 1 corresponded roughly to the duodenum, segments 2-4 to the jejunum and

segments 5-8 to the ileum. Large intestinal segments 1, 2 and 3 correspond roughly to the ascending, transverse and descending colon, respectively. All gut-specific class Ib MHC displayed a similar cephalocaudal expression pattern with limited to undetectable expression in the duodenum, high expression in the jejunum and trailing expression from the ileum to the colon (Figure 4.2). Linear regression analysis of the *GAPDH*-normalized band intensities (see Materials and Methods) of *Q1*, *Q2*, *H2-Bl*, *Tw5* and *T3* RT-PCR products revealed a close correlation among gut-restricted class Ib cephalocaudal profiles ($p<0.01$ for each two-way comparison). Based on these observations we conclude that transcription of gut-specific class Ib MHC is highest in the jejunum, where most unconventional IEL reside (46), whereas ubiquitously transcribed class Ia MHC are distributed more uniformly along gut sections.

Expression Gradients of NK and T Cell Receptors on IEL Correlate with Class Ib *Mhc* in the Small Intestine

To ask if expression of putative class Ib MHC-reactive NK and TCR receptors on IEL also changes along the cephalocaudal axis of the gut, we performed additional experiments. The small intestine of a 129 x B6 F1 mouse was divided into segments as in Figure 4.2, and the epithelial monolayer containing IEL was isolated from each segment. The distribution of IEL along the cephalocaudal axis was examined by RT-PCR of *CD103* and confirmed that IEL are most numerous in the jejunum and that their numbers (as judged by CD103 expression), are correlated with expression levels of the neighboring class Ib MHC in IEC (Figure 4.3; $p<0.01$ for H2-Bl; $p<0.05$ for Tw5).

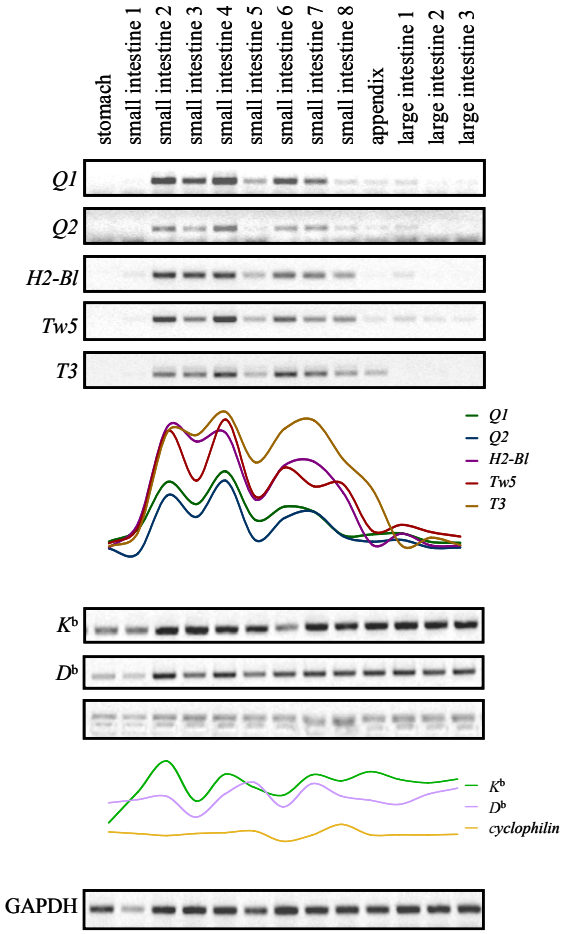

Figure 4.2 *H2-Bl* and other gut-restricted class Ib MHC are expressed throughout the small intestine of *H2*^{bc} haplotype mice. Semi-quantitative RT-PCR was performed on equally sized sections of the gastrointestinal tract of a 129 x B6 F1 mouse. Densitometric representations of RT-PCR results are depicted below the corresponding agarose gel resolved products. Intestinal sections roughly correspond to the following: small intestine 1 – duodenum; small intestine 2-4 – jejunum; small intestine 5-8 – ileum; large intestine 1 – ascending colon; large intestine 2 – transverse colon; large intestine 3 – descending colon (Grey's Anatomy). Primers and RT-PCR conditions were the same as in Figure 4.1A (see Table 2.1). *GAPDH* and *cyclophilin* transcripts served as cDNA quality controls. For densitometry plots, each intestinal segment was plotted against its normalized class Ib MHC signal/*GAPDH* signal in smoothed line graphs. This data is representative of three RT-PCR experiments run on the same templates (made from two pooled 129 x B6 F1 animals). Similar data (with less pronounced variation of class Ib MHC transcription along the cephalocaudal axis) was collected on samples generated from $K^{b-/-}D^{b-/-}$ and B6 mice (data not shown).

Consistent with this, we observed that other genes of interest, such as NK receptors NKG2D ($p<0.01$), CD94 ($p<0.01$) and NKG2A (visually similar, but statistically not significant) colocalized with CD103 and class Ib MHC. Similar trends were observed with T cell receptor chains γ and β and CD8α and β, (though no statistically significant correlation was noted). NKG2C/E was detected, but its expression was too low to quantitate reliably. No appreciable NK1.1 transcription was detected despite the use of approximately four times as much cDNA in the intestinal samples as in the spleen positive control, suggesting that the observed NK cell receptor transcripts originate from intestinal T cells rather than from contaminating NK or NKT cells. RT-PCR on cDNA isolated from CD3ε-sorted IEL indicated further that NK cell receptors CD94 and NKG2A are transcribed by epithelial T cells and not by the neighboring IEC (Figure 4.3B).

In an effort to determine the consistency of class I MHC ligand expression across different strains of mice and to examine assay-dependent variability, we performed the same semi-quantitative RT-PCR experiment on intestinal segments from $K^{b-/-}D^{b-/-}$ ($H2^{bc}$ on the C57BL/6J background) and C57BL/6J ($H2^{b}$) mice and compared the results to those from the 129 x B6 F1 ($H2^{b/bc}$) mouse. As in the first experiment, CD103 signal correlated with NKG2D ($p<0.01$ and $p<0.05$), NKG2A ($p<0.05$ and $p<0.01$) and CD94 (visually similar) in $K^{b-/-}D^{b-/-}$ and C57BL/6J intestinal segments, respectively (data not shown). To approximate the level of transcription of T and NK cell receptors for each of the three mice, we quantitated the agarose-resolved RT-PCR bands from a representative segment (segment 4) by densitometry and normalized the results to *GAPDH* (Figure 4.3A, right panel). This analysis revealed similar levels of T cell receptor expression

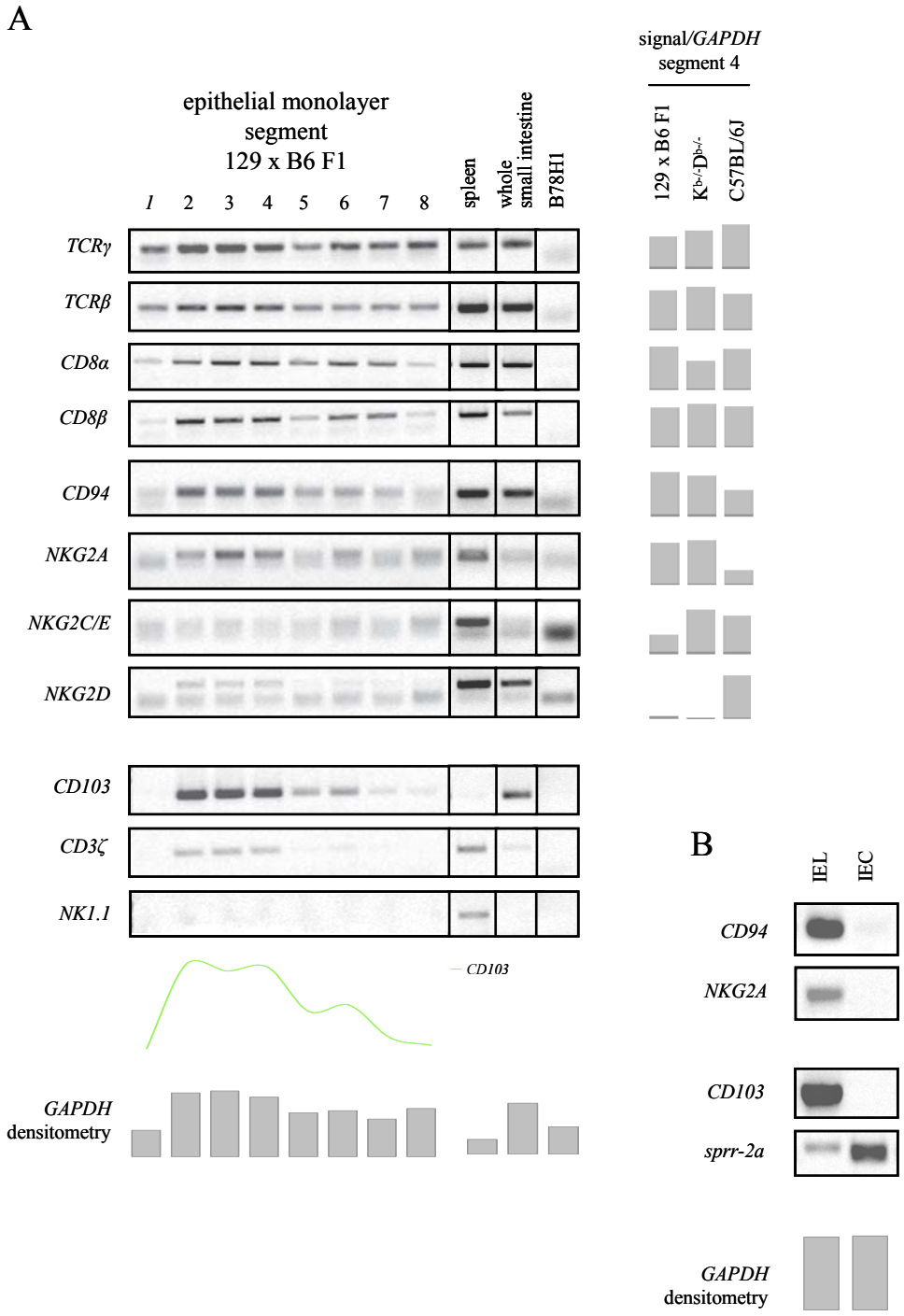
A
epithelial monolayer segment 129 x B6 F1
1 2 3 4 5 6 7 8
spleen
whole small intestine
B78H1
signal/GAPDH segment 4
129 x B6 F1
Kb-/-Db-/-
C57BL/6J
TCRγ
TCRβ
CD8α
CD8β
CD94
NKG2A
NKG2C/E
NKG2D
CD103
CD3ζ
NK1.1
CD103
GAPDH densitometry
B
IEL
IEC
CD94
NKG2A
CD103
sprr-2a
GAPDH densitometry

Figure 4.3 Putative ligands of class Ib MHC are expressed in gut fractions enriched for IEL. A. IEL receptor transcripts co-localize with those of gut-specific class Ib MHC along the cephalocaudal axis. At left, epithelial monolayer cDNA from the indicated intestinal sections of a 129 x B6 F1 mouse was subjected to semiquantitative RT-PCR using HotStarTaq® under the following conditions: *GAPDH* – 26 cycles; *CD103*, *CD3ζ*, *NK1.1*, *TCRγ* and *CD94* – 32 cycles; *TCRβ* and *CD8α* – 34 cycles; *CD8β*, *NKG2A*, *NKG2C/E* and *NKG2D* – 36 cycles. *GAPDH*, *CD103* and *CD3ζ* PCRs were performed with 1 µL cDNA in a 25 µL reaction, while all others were performed with 2 µL. Primers used are listed in Tables 2.1 and 2.2. Spleen and whole small intestine from a $K^{b-/-}D^{b-/-}$ mouse and B78H1 tumor served as positive and negative controls. Densitometric representations of RT-PCR results are depicted below gel-resolved PCR products. At right, RT-PCR bands from segment 4 of three different strains of mice were quantitated by densitometry. Each bar corresponds to the ratio of RT-PCR signal/GAPDH for the indicated segment. B. The IEL fraction of the intestinal epithelial monolayer transcribes both CD94 and NKG2A heterodimer partners. cDNA was generated and diluted as in Figure 4.1. Semiquantitative RT-PCRs were performed using HotStarTaq® with the primers listed in Table 2.2 under the following conditions: *sprr-2a* – 32 cycles; *GAPDH* – 34 cycles; *CD94*, *NKG2A* and *CD103* – 38 cycles. *CD103* and *sprr-2a* data are copied from Figure 4.1A for the purposes of illustration.

across all three strains. NK cell receptor expression was much more variable, and this variation was not correlated with NK cell receptor genotype or expression levels/nature of MHC class Ib antigens expressed in each of the strains.

Previously published studies of mouse IEL have revealed low but detectable expression of the MHC-binding C-type lectin-like Ly49 members of the NK cell receptor family in some IEL populations (81, 195). Consistent with these reports, but subject to the limitations of our assay, we found that transcription of various Ly49 family members, can be observed in the small intestine of a C57BL/6J mouse, but is diminished in an IEL-deficient B6.*RAG1*$^{-/-}$ animal (Figure 4.4A; 16-43% reduction in signal across five Ly49-specific primer sets). These results suggest that Ly49 receptors are present on intestinal T cells of a healthy animal but are absent when IEL fail to develop normally in *RAG*$^{-/-}$ animals.

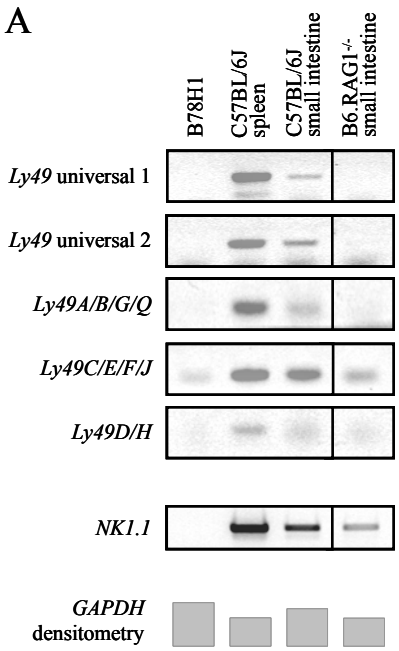
A
B78H1
C57BL/6J spleen
C57BL/6J small intestine
B6.RAG1-/- small intestine
Ly49 universal 1
Ly49 universal 2
Ly49A/B/G/Q
Ly49C/E/F/J
Ly49D/H
NK1.1
GAPDH densitometry

B

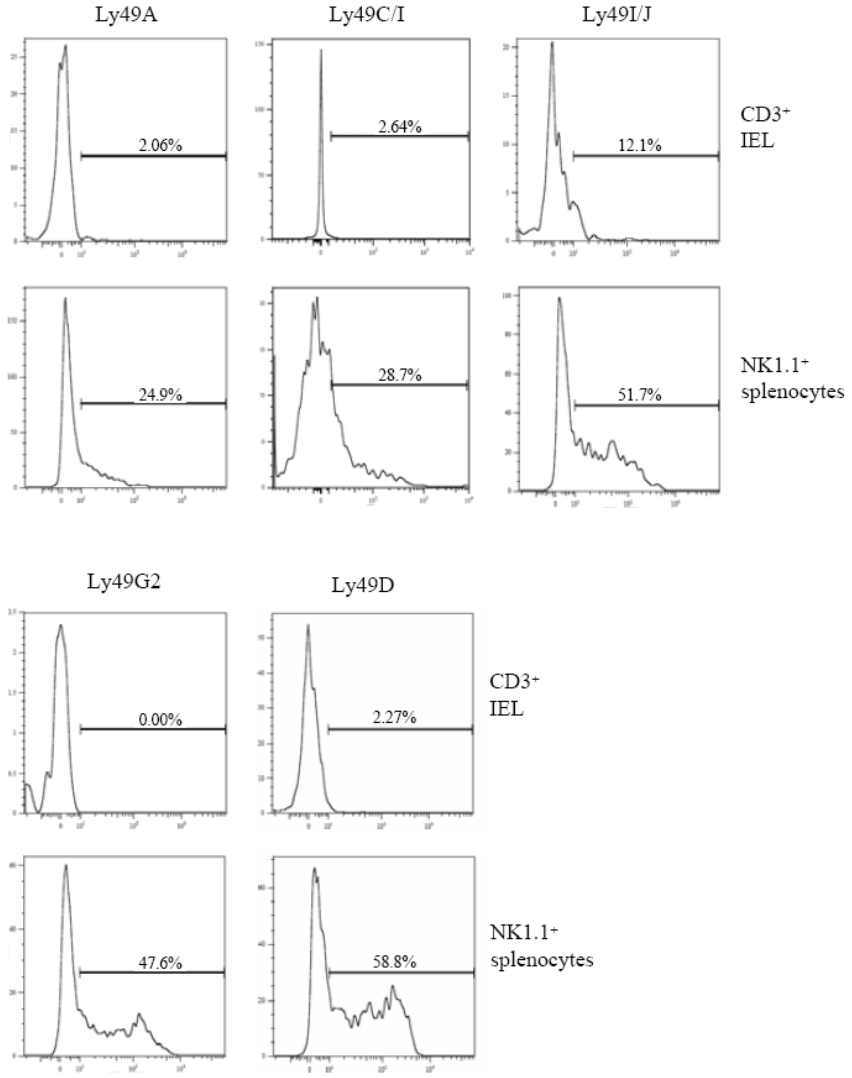
Ly49A
Ly49C/I
Ly49I/J
2.06%
2.64%
12.1%
CD3+
IEL
24.9%
28.7%
51.7%
NK1.1+
splenocytes
Ly49G2
Ly49D
0.00%
2.27%
CD3+
IEL
47.6%
58.8%
NK1.1+
splenocytes

Figure 4.4 Expression of Ly49 family members by intestinal T cells is detectable, but very few IEL express Ly49s. A. Intestinal T cells express low levels of *Ly49* NK cell receptors. Transcription of the indicated NK cell receptors in C57BL/6J and B6.*RAG1*$^{-/-}$ whole small intestine was evaluated by semiquantitative RT-PCR using HotStarTaq®. Primers and conditions for the PCR reactions were as follows: *Ly49* universal 1: 32 cycles with *Ly49* univ F and *Ly49* univ R; *Ly49* universal 2: 32 cycles with *Ly49* univ F and *Ly49* univ R2; *Ly49A/B/G/Q*: 32 cycles with *Ly49A/B/G/Q* F and *Ly49A/B/C/E/F/G/J/Q* R; *Ly49C/E/F/J*: 32 cycles with *Ly49C/E/F/J* F and *Ly49A/B/C/E/F/G/J/Q* R; *Ly49D/H*: 32 cycles with *Ly49D/H* F and *Ly49D/H* R; *GAPDH*: 26 cycles with *GAPDH* F and *GAPDH* R. B78H1 and C57BL/6J small intestine cDNAs served as negative and positive controls, respectively. All RT-PCR bands were of the expected size and were sequenced from the C57BL/6J spleen positive control to confirm specificity. Because these primers were designed to detect multiple *Ly49*s, cDNA species detected in the intestine may be different from those identified in the spleen. B. Expression profiles of Ly49 family members on IEL. Mixed IEL/IEC and splenocytes from 5 C57BL/6J mice were stained with anti-CD3-APC (IEL/IEC) or anti-NK1.1-PE-Cy7 (splenocytes) and the indicated anti-Ly49 antibody and analyzed by flow cytometry.

In summary we find that, in addition to T lineage receptors, bulk IEL transcribe low levels of NK cell receptors capable of engaging class I MHC. The cephalocaudal distribution of NK cell receptor-expressing αβ and γδ IEL mirrors that of gut-restricted class Ib *Mhc* expression by IEC. Thus T/NK cell receptors on IEL may be poised to engage protein products of these unique class Ib *Mhc*.

NK Cell Receptors Are Expressed on Small Subsets of IEL

The RT-PCR studies of gene expression in bulk IEL preparations do not discriminate between low level transcription in the majority of cells and selective, but high expression of NK cell receptors in rare IEL subsets. To distinguish between these possibilities and to identify the putative IEL expressing CD94, NKG2A and/or NKG2D markers, we have performed six color flow cytometry on IEL cells extracted from the

epithelial monolayer of the small intestine of healthy adult C57BL/6J mice. The main conventional (TCRαβ$^+$ CD8αβ$^+$) and unconventional (all TCRγδ$^+$ and CD8$^-$ or CD8αα$^+$ TCRαβ$^+$) IEL populations were identified by staining with fluorophore-conjugated anti-CD8α, anti-CD8β and either anti-TCRβ or anti-TCRγδ antibodies. The NK markers were probed with anti-NKG2A, anti-CD94 and anti-NKG2D labeled antibodies. Rigorous preliminary experiments were performed to establish the optimal concentrations of the reagents and the most appropriate settings of the flow cytometer for this analysis. The ratio of IEL subsets observed in our experiments (~50% TCRαβ cells and ~40% TCRγδ cells of the IEL gated population) was fairly typical for healthy, adult C57BL/6J mice, as were the proportions of different conventional and unconventional IEL subpopulations (in TCRγδ cells: ~80% were CD8αα$^+$, ~15% were CD8$^-$ and ~5% were CD8αβ$^+$ [data not shown]; in TCRαβ cells: 40% were classical CD8αβ$^+$, 40% were CD8αα$^+$ and ~20% were CD8$^-$) (41, 42). The initial analysis performed by single color flow cytometery revealed that small fractions of bulk IEL expressed CD94 (< 4%), NKG2A (< 17%) and NKG2D (< 10%) (Figure 4.5A). Subsequent analysis determined the identity of these subsets

A

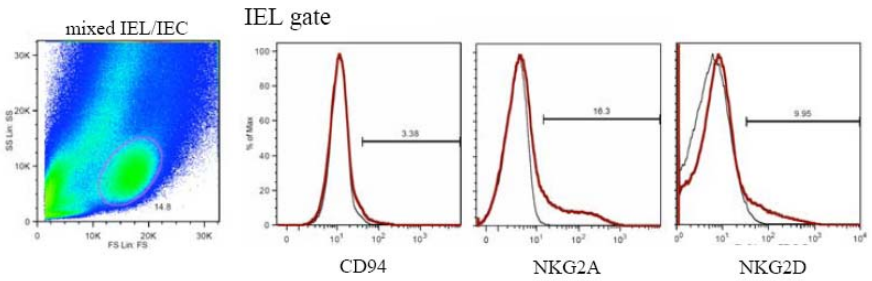

B

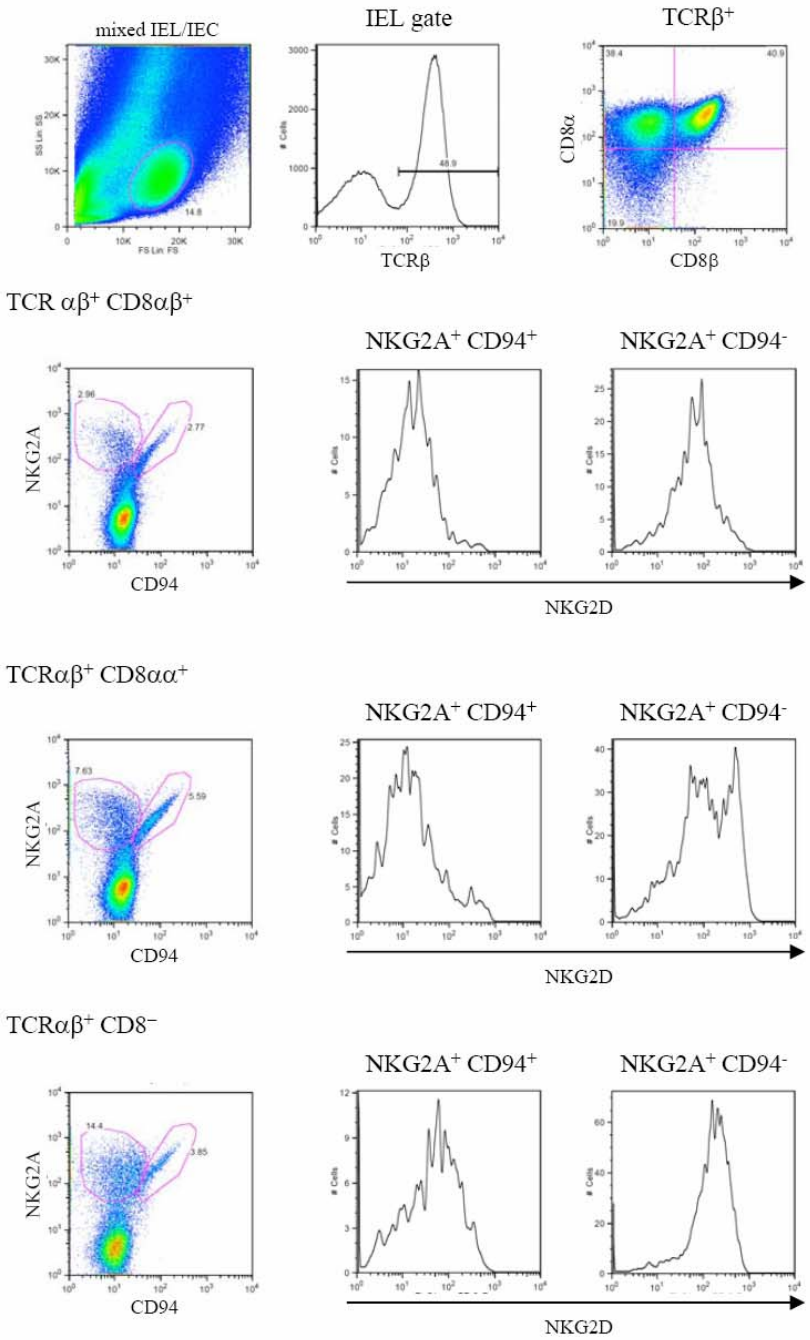
mixed IEL/IEC
IEL gate
TCRβ+
CD8α
TCRβ
CD8β
TCR αβ+ CD8αβ+
NKG2A+ CD94+
NKG2A+ CD94-
NKG2A
CD94
NKG2D
TCRαβ+ CD8αα+
NKG2A+ CD94+
NKG2A+ CD94-
NKG2A
CD94
NKG2D
TCRαβ+ CD8−
NKG2A+ CD94+
NKG2A+ CD94-
NKG2A
CD94
NKG2D

C

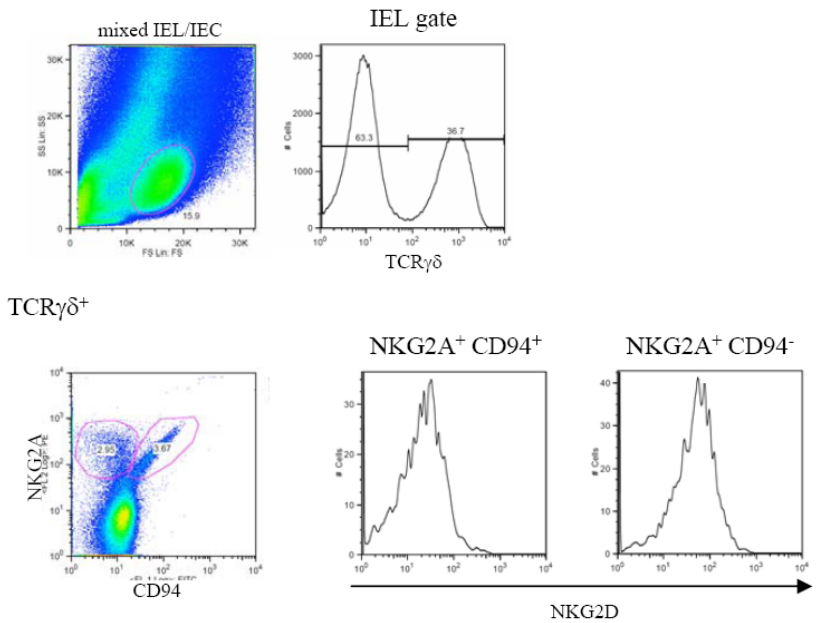

Figure 4.5 A newly identified population of NKG2A$^+$ CD94$^-$ IEL expresses NKG2D. A. Expression of CD94, NKG2A and NKG2D by IEL. Mixed IEL/IEC from 5 C57BL/6J mice were stained with anti-CD94-FITC, anti-NKG2A-PE or anti-NKG2D-PE-Cy7 fluorophore-conjugated antibodies (Table 2.8) and subjected to flow cytometry. IEL were selected by their FSC^{int}/SSC^{lo} profile (left panel) and were then examined for NK cell receptor expression (right panels). Black – unstained IEL; red – stained IEL. B. CD94, NKG2A and NKG2D expression profiles of TCRαβ$^+$ CD8αβ$^+$, TCRαβ$^+$ CD8αα$^+$ and TCRαβ$^+$ CD8$^-$ IEL. Mixed IEL/IEC from the mice in A were stained with anti-TCRβ-APC, anti-CD8α-APC-Alexa 750, anti-CD8β-PE-Cy5, anti-CD94-FITC, anti-NKG2A-PE and anti-NKG2D-PE-Cy7 (Table 2.8) and subjected to flow cytometry. TCRβ$^+$ IEL (as determined by their FSC^{int}/SSC^{lo} [top left panel] and TCRβ [top middle panel] profiles) were gated based on their expression of CD8α and CD8β (top right panel). CD8αβ$^+$, CD8αα$^+$ and CD8$^-$ populations were then analyzed for their CD94 and NKG2A receptor expression. CD94$^+$ NKG2A$^+$ and CD94$^-$ NKG2A$^+$ IELs were then examined for their expression of NKG2D. C. CD94, NKG2A and NKG2D expression profiles of γδTCR$^+$ IEL. Mixed IEL/IEC from the mice in A were stained with anti-TCRγδ-PE-Cy5, CD8α-APC-Alexa 750, anti-CD8β-APC, anti-CD94-FITC, anti-NKG2A-PE and anti-NKG2D-PE-Cy7 (Table 2.8) IEL were selected and analyzed as in B. Due to the homogeneity of γδ IEL CD8α and CD8β expression profiles (data not shown), CD8αβ$^+$, CD8αα$^+$ and CD8$^-$ TCRγδ$^+$ IEL were not individually analyzed for NK cell receptor expression. The CD94$^+$ NKG2A$^+$ and CD94$^-$ NKG2A$^+$ populations of IEL were seen in 3 separate experiments with 3 different groups of C57BL/6J mice (data not shown).

(Figure 4.5B & C). Thus, we observed that all conventional and unconventional IEL, defined by their TCR and CD8 expression, contained populations co-expressing CD94 and NKG2A (ranging from 2-5%). In addition, we detected a phenotypically new fraction of IEL (ranging in γδ and αβ TCR cells from 3-17%), which expressed NKG2A but not CD94. This subpopulation was most elevated in the unconventional TCRαβ IEL (>10% positive). Interestingly, the NKG2A$^+$ cells, but not the double positive NKG2A$^+$ CD94$^+$ cells, co-expressed activating NKG2D receptors. While NKG2D was detected on all NKG2A$^+$ CD94$^-$ IEL, it was highest in the two unconventional subpopulations of TCRαβ cells: CD8αα$^+$ and CD8$^-$ cells. We believe that it is highly unlikely that the observed data could be attributed to the presence of NK/NKT cells in our IEL preparations, because this scenario would predict a strong bias toward CD8$^-$ populations, which we do not see. In addition, the analyzed cells have been gated to select specifically for TCR-expressing IEL, and NK1.1$^+$ CD3$^+$ cells constitute only a small fraction of bulk IEL (~10% [data not shown]).

We have also attempted to identify IEL subpopulations expressing Ly49 receptors, but our flow cytometry data were largely negative (Figure 4.4B), indicating that their expression level and/or the IEL subset endowed with these receptors are too low to be reliably detected by the assays/reagents used here.

Taken together these results demonstrate that all IEL contain small subsets of cells constitutively expressing CD94/NKG2A inhibitory receptors, which may be poised to interact with Qa-1 complexes containing gut leader peptides. In addition, we have identified a new IEL subset, enriched in unconventional IEL populations, which

constitutively expresses the activating NKG2D receptor. This subset is positive for NKG2A, but not the CD94 chain. Accordingly, the cytotoxicity of these NKG2D positive cells may by regulated in the gut epithelium by gut class Ib MHC ligands displayed by neighboring IEC.

Developmental Expression of *H2-Bl* in the Intestine and Thymus

It has been long recognized that expression levels of class I MHC during early development may influence several important processes including suppression of maternal immune mechanisms against paternal alloantigens on fetal cells and thymic education of T cells. It is therefore of considerable interest to determine expression profiles of gut-restricted class Ib *Mhc* during embryonic and early postnatal time periods, when transcriptional activities of the classical class I *Mhc* and β_2m genes are known to be repressed (316).

Intestines and thymuses of $K^{b-/-}D^{b-/-}$ mice ranging in age from embryonic day 18 to 8 postnatal weeks were tested for *H2-Bl* expression by semi-quantitative RT-PCR. *H2-Bl* was clearly detectable in the embryonic day 18 intestine and peaked by postnatal day 7 (Figure 4.6). In the thymus, *H2-Bl* expression was very low in the newborn, increasing through postnatal day 14. Quantitative estimates of the differential expression levels require additional experiments. These results suggest that developmental expression of *H2-Bl* parallels class Ia (310) as well as gut specific genes $Q1^b$ (249) and $Q2^b$ (250). It also documents *H2-Bl*'s low level expression in the newborn thymus,

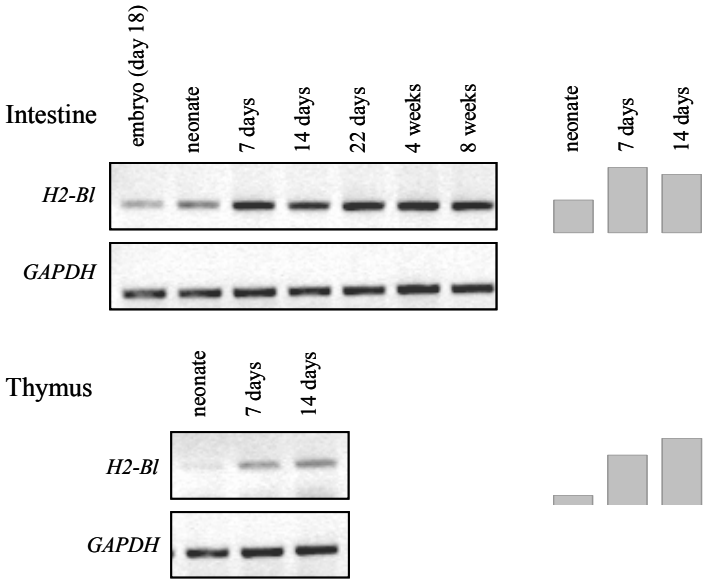

Figure 4.6 Developmental regulation of *H2-Bl* transcription in the small intestine and thymus. Thymic and intestinal cDNA samples of B6.$K^{b-/-}D^{b-/-}$ mice ranging in age from late embryo (~e18) to 8 weeks (postnatal) were subjected to semiquantitative RT-PCR (HotStarTaq®, 28 cycles) with the primers used in Figure 3.1. Bars to the right are signal/GAPDH densitometric representations of the RT-PCR bands shown at left.

where H2-Bl may influence education of T cells, such as IEL, which are known to seed the gut immediately after birth (24).

Immunologically Privileged Tissues Do Not Express Appreciable Levels of Gut-Specific Class Ib *Mhc*

H2-Bl was first identified in a day 3.5 blastocyst cDNA library (264), and transcriptional activity has been detected in the mouse placenta (277), leading to the proposal that *H2-Bl* is a *HLA-G* homolog (264, 277). To evaluate the level of placental

expression of *H2-Bl* and characterize the pregnancy-associated transcription of other gut-specific class Ib *Mhc*, we performed semi-quantitative RT-PCR on cDNA from the uterus and placenta of a late term (embryonic day 18) $K^{b-/-}D^{b-/-}$ mouse along with the uterus, spleen and small intestine of a matching adult virgin animal. Under the conditions of our assay, *H2-Bl* was not detected in the placenta of a late term (embryonic day 18) pregnant mouse, though it was transcribed in the gut tissues of the same day 18 embryo (Figure 4.7A). (Only trace amounts of *H2-Bl* transcripts were detected in day 12 placenta of ICR mice [data not shown].) To confirm this quantitatively, we evaluated the transcription level of *H2-Bl* in tissues of pregnant and virgin $K^{b-/-}D^{b-/-}$ mice by real-time PCR and established that levels of placental H2-Bl mRNA are insignificant compared to the transcriptional activity of this gene in the adult intestine (Figure 4.7B). These experiments unambiguously established that *H2-Bl* is a predominantly gut-restricted gene, and its transcription in the placenta and other tested tissues is below the detection level (<2% of adult gut expression) in our experiments.

As is the case for *H2-Bl*, neither *Q1*, *Tw5* nor *T3* could be detected in the day 18 placenta by semi-quantitative RT-PCR (Figure 4.7A). Of the gut-specific class Ib MHC, only rare *Q2* transcripts were observed in the placenta, but their expression level was in the range of constitutive background *Q2* transcription seen in other adult tissues (Figure 4.7A, (287)). Additional experiments need to be performed to confirm and quantitate these trace amounts of gene activity in individual tissues. Ubiquitously transcribed *T23* and β_2m were detected in all tissues analyzed (Figure 4.7A and 4.7B).

Because H2-Bl has been implicated in inhibiting NK cell mediated cytolysis (277), we sought to determine if its transcription could be detected in other

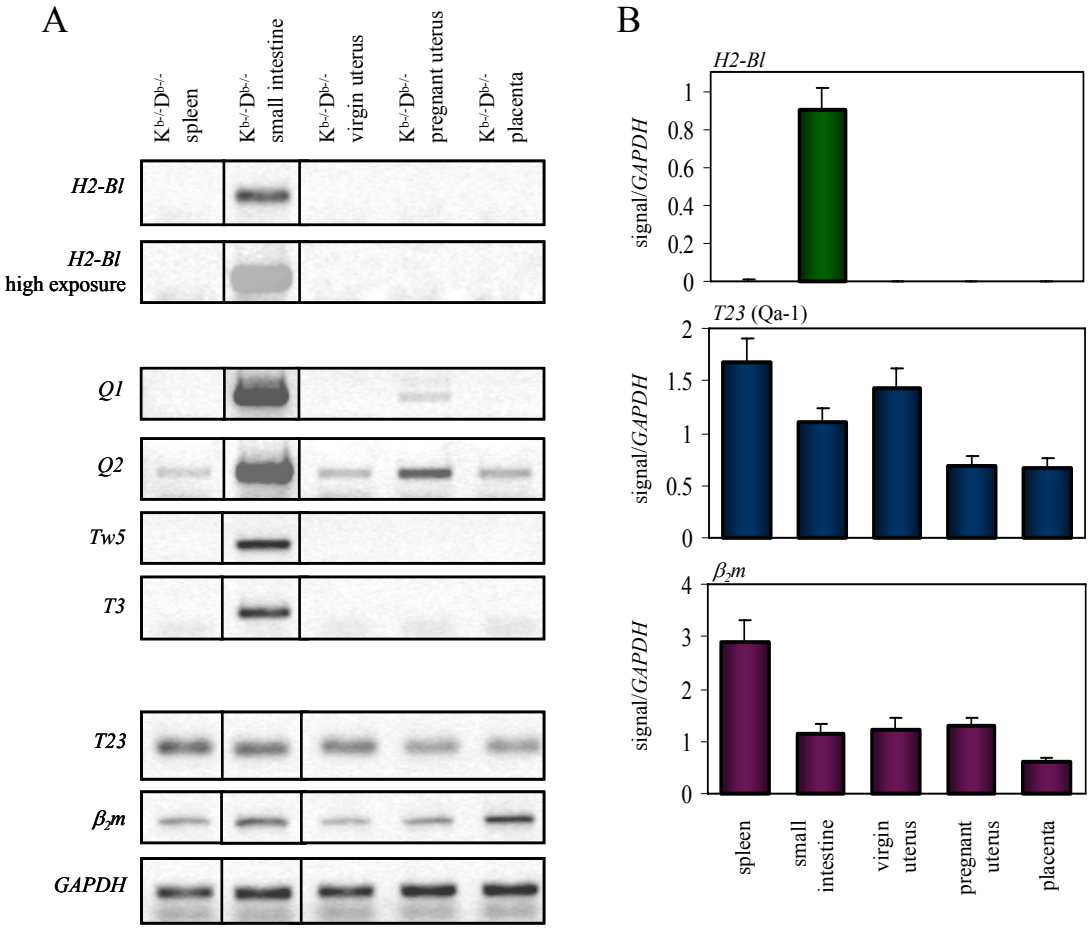

Figure 4.7 Gut-specific class Ib MHC are not transcribed in the late-term placenta. A. Semiquantitative RT-PCR of gut-specific class Ib MHC in pregnancy-associated tissues is compared to small intestine. cDNAs from late stage pregnant and matching virgin female $K^{b-/-}D^{b-/-}$ mice were RT-PCR amplified using HotStarTaq® and the primers in Figures 3.1 and 3.7 . PCR cycle numbers for each primer set were as follows: *GAPDH*, *Qa-1* – 26 cycles; *β₂m*, *H2-Bl*, *Tw5* – 28 cycles; *T3* – 30 cycles; *Q2*, *Q10* – 34 cycles; *Q1* – 36 cycles. cDNA from the small intestine and the spleen served as positive and negative controls, respectively. Ubiquitously transcribed *Qa-1* and *β₂m* were also examined. B. Quantitative PCR of *H2-Bl* in pregnancy-associated tissues. Transcription of *β₂m*, *T23* and all isoforms of *H2-Bl* from the cDNA in A was measured by qPCR (Materials and Methods) using the primers identified in Table 2.3.

immunotolerant tissues. We tested cDNA from the eyes, brain, testes and ovaries of $K^{b-/-}$ $D^{b-/-}$ mice for *H2-Bl* expression by semi-quantitative RT-PCR. We found no appreciable transcription of *H2-Bl* in any of these tissues (Figure 4.8). (Trace *H2-Bl* expression could be detected in the brain, consistent with tissue screening results from a C57BL/6J mouse [Figure 3.1].)

Taken together these data demonstrate that the dominant site of *H2-Bl* and other gut-specific class Ib *Mhc* expression is the small intestine, not the placenta. The specific expression of *H2-Bl* in the intestine, but not other tolerance-associated tissues, suggests a unique role for H2-Bl in this specific immune tolerance-dominated compartment.

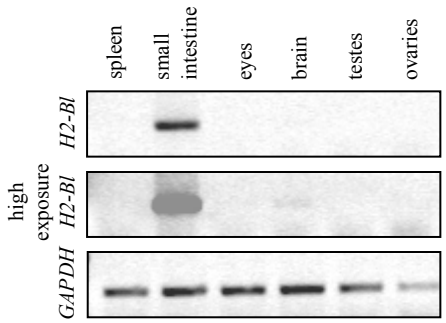

Figure 4.8 Screening of other immune privileged tissues for *H2-Bl* expression. cDNA from the indicated tissues of a $K^{b-/-}D^{b-/-}$ mouse was tested for the presence of *H2-Bl* transcripts by semiquantitative RT-PCR. Reactions were performed using HotStarTaq® (28 cycles with primers *H2-Bl*^{bc} 5'UTR/ex1 F2 and *H2-Bl*^{bc} ex3 R1 for *H2-Bl* and *GAPDH* F2 and *GAPDH* R2 for GAPDH).

H2-Bl Is IFN-γ-Inducible in a Model Hepatoma

Most class I *Mhc* and related genes respond to IFNs and TNF by enhanced transcription, and this inducibility is taken as an indication of their physiological roles in the immune response (317, 318). To determine if *H2-Bl* transcription is regulated by pro-inflammatory signals, we tested a model cell line for upregulation of endogenous *H2-Bl*

transcription in response to IFN-γ. The experiments were performed with liver-derived mouse tumor of *H2*^{bc} origin (258), because, at present, no immortalized gut cells are available. Like the liver (Figure 3.1 and Figure 3.7), the C57L-derived hepatoma Hepa1 expresses very low levels of *H2-Bl* (Figure 4.9). Hepa1 cells were exposed to 20 U/mL IFN-γ or left untreated for 48 hours, and class I *Mhc* upregulation was examined by semi-quantitative RT-PCR. Like the ubiquitously expressed *D*^{b} class Ia and *T23* class Ib *Mhc*, *H2-Bl* expression was significantly (~14 fold) higher in Hepa1 cells treated with IFN-γ. *TAP2* and *tapasin* positive controls were similarly induced by IFN-γ (data not shown). Thus *H2-Bl* expression, like that of all classical and many nonclassical class I *Mhc* (317), can be upregulated in response to IFN-γ, suggesting that the product of this gene participates in immune response pathways.

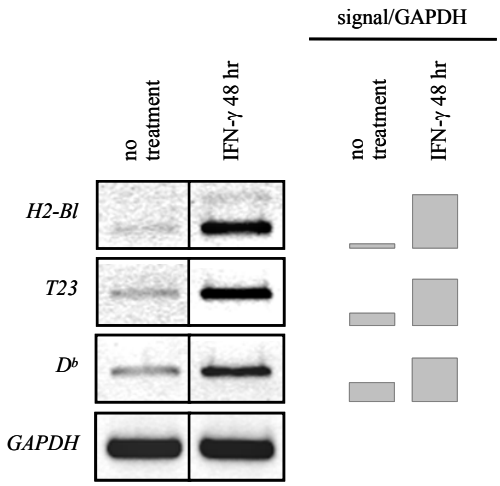

Figure 4.9 *H2-Bl* transcripts are IFN-γ-inducible in a model hepatoma line. Hepa1 tumor cells were cultured with or without 20U/mL IFN-γ for 48 hours, and *H2-Bl*, *D*^{b} and *T23* transcription levels were monitored by semiquantative RT-PCR using HotStarTaq® (*H2-Bl*: 32 cycles with *H2-Bl*^{bc} 5'UTR/ex1 F and *H2-Bl*^{bc} 3' UTR R; *T23*: 32 cycles with *T23*^{b} ex2 F and *T23*^{b} ex3 R; *D*^{b}: 28 cycles with *D*^{b} ex2 F and *D*^{b} ex3 R; *GAPDH*: 28 cycles with *GAPDH* F and *GAPDH* R). All bands were of the correct size and confirmed by sequencing. Small intestine amplification products served as positive controls (not shown). Representative of two experiments.

Promoter Elements of Gut-Specific Class Ib *Mhc* Suggest Unique Regulation

Since the class Ib MHC genes studied here display unique spatial and temporal expression patterns in mouse tissues, we sought to identify the regulatory elements that control the highly restricted transcriptional activity of *H2-Bl*, *Tw5*, *Q1* and *Q2* promoters.

The organization of mouse and human classical class Ia MHC promoters has been well characterized (203, 319-321). Highly conserved promoter elements, such as the CCAAT box, which facilitates proper positioning of the preinitiation complex and RNA polymerase II, the TATA box, involved in recruiting RNA polymerase II holoenzyme to initiate transcription, and the Initiator sequence Inr, which overlaps the transcript inhibition site and interacts with general transcription factors, are all located within the 80-90 nucleotides upstream of the first ATG translation start codon, in the region denoted as the core promoter ((321), Figure 4.10A). The 150-200 bp DNA sequences located 5' of the core promoter, denoted here as the proximal promoter ((321), Figure 4.10A), contain key regulatory elements responsible for ubiquitous expression of class Ia *Mhc* in a variety of tissues (EnhA [Enhancer A], EnhB, X1 and CRE/X2 boxes [in Figure 4.10A, (321)]) and for their inducibility by various cytokines, including type I and II IFN (ISRE [interferon-stimulated response element] binding region and X1/CRE/X2 box) (317, 322-324). Rigorous mutational/functional promoter analyses and biochemical studies of DNA-binding transcription factors have confirmed that basal expression levels and response to hormones and cytokines in class Ia and several studied class Ib genes are primarily encoded by the proximal promoters, though distal 5' flanking sequences may, in some cases, fine-tune their transcriptional activity.

To compare promoters of gut-specific class Ib *Mhc* genes to their class Ia counterparts, the DNA sequences were aligned using the clustalW program (325), and the

A

```
          -360      -350      -340      -330      -320      -310      -300      -290      -280      -270
             :         :         :         :         :         :         :         :         :         :
K^b       AGGACACAGAGAGTCTGGCCTGCGGGTCTCTCCTGGTGTTTTGAGAGTTTCTGGATCAGA--ACTCGGAGACGACAGCACAGGGTTCAGGCAAAGTCTTA
D^bc      GGGTCTCTCCTGG--TGATCTGACAGCTTCTGGGTCAGAACTCGGAGTCACCACGACAAACTGCTCTCTGTCCGCAGTACAGGGTTCAGGCAAAGTCTTG

H2-Bl^bc  TGAAAGAAACTC-TTTCTTTTTCAAGTTGCTT-TTGGTCATGGGGTTTTATCACAGCAATGGAAACCCTCACTAAGACACA-GGTGCACA-AGGGCTTCA
Tw5^bc    TGAAAGAAACCC-TTTCTTCCTCAAGTTGCTT-TTGGTCATGGGGTTTTATCACAGCAATGGAAACCCTCACTAAGACACA-GGTGCACA-AGGGCCTCA
Q1^bc     TGAAATAAACCC-TTTCTTCCTCAAGTTGCTT-TTGGTCATGGGGTCTTATCACAGCAATAGAAACCCTCACTAAGACACA-GCTGCACA-AGGGCCTCA
Q2^bc     TGAAAGAAACCC-TTTCTTTTTCAAGTTGCTT-TTGGTCATGGGGTCTTATCACAGCAATGGAAACCCTCACTAAGACACA-GGTGCACA-AGGGCCTCA
                       ---ISRE---        --C/EBPα---  ---ERG-1---                      -----E1------
                                                     --GATA-1--

T3^b      CTAACCCTGAAGGTTTCCACTCTGA-TTACCACCTGACATTCTGGGCAGGGCTCAG-ATAGAGGATGCTATCTAT-ACACAGGGTTCA-GTGCAGAAGAA
                       --IRF-1---                    --GATA-1---                  -Rev-erbA--     ----

Q10^bc    TTCTGGCTCCCGG--TGTCCTGACAGCTTCTGGGTTAGAACTCGGAGACACCACGACAAACAGCTCTCTGTCCACAGCACATGGTTCAGGAAAAGTCTTA
                     --ER/T3Rα---  --Elk-1---                                                  --C/EBPα--


          -260      -250      -240      -230      -220      -210      -200      -190      -180      -170
             :         :         :         :         :         :         :         :         :         :
                                      Enhancer A
K^b       GTCGCCAGGCAGT-GAGGTCAGGGG-TGGGGAAGCC--CAGGGCTGGGGATTCCCCATCTCCACAGTTTCACTT-CTGCACCTAACCTGGG--TCAGGT-
D^bc      GTTGCCAGGCGGT-GAGGTCAGGGG-TGGGGAAGCC--CAGGGCTGGGGATTCCCCATCTCCTCAGTTTCACTT-CTGCACCTAACCTGGG--TCAGGT-
                   ---------------CLASS IA MULTI-1----------------        ---ISRE---                    --T3R--
                                                                                  ---Myf-3---

H2-Bl^bc  CTCTGCTCCCTGCAGACACCACCCTCTCCTGCAGTT--CAGCTCCTGCCCCTCCCTTGCCCTGGAGCAGCACTA-CTTTATAGCTCCTGGGGATCTGATG
Tw5^bc    CTCTGCTCCCTGCAGACACCACCCTCTCCTGCAGCT--CAGCTCCTGTCCCTCCCTTGCCCTGGAGCAGCACTA-CTTTATAGCTCCTGGGGATCTGATG
Q1^bc     CTCTGTTCCCTGCAGACACCACCCTCTCCTGCAGCT--CAGCTCCTGCCCCTCCCTTGCCCTGGAGCAGCACCA-CTTTATAGCTCCTGGGGATCTGATG
Q2^bc     CTCTGCTCCCTGCAGACTCCACCCTCTCCTGCAGCT--CAGCTCCTGCCCCTCCCTTGCCCTGTAGCAGCACCA-CTTTATAGCTCCTGGGGATCTGATG
          -GATA-1--                                   ---ETF----                                ---AP-2---
                                                                                                   --GATA-1--

T3^b      GGAGTCAGGACAAAGTTCCAAGTCCCGGAAGTGGCTGTCAGGGTCTGAGGCCTGAAGGCGGGGGATTAGGTTGGGCTGTACAGAAC-TATAGTTTCACTT
          ----T3 MULTI-1-------   --Elk-1---                     -WT1/ETF--                          ---ISRE---

Q10^bc    GTCTCCACGCGGT-GAGGTCAGGGG-TTGGGAAGCC--CAGGGCTGAGGACTCCCCATCTCCCCAGTTTCACTT-CTGCTCCTAACCTGGG--CCAGGT-
                   --------------------------Q10 MULTI-1-------------------          ---SRF----    ----ER-
                                                                   ---ISRE---     ----ER----


          -160      -150      -140      -130      -120      -110      -100       -90       -80       -70
             :         :         :         :         :         :         :         :         :         :
                     X1 box    CRE/X2                          Enhancer B                  CAAT box
K^b       --CCTTCTGTCCGG-----ACACTGTTGACGCGCAGTCAGCTCTTACCCCCATTGGGTGGCGCGATCACC----AAGAACCAATCAGTGTC---GCCGCG
D^bc      --CCTTCTGCCGGG-----ACACTGATGACGCGCTGGCAGGTCTCACTATCATTGGGTGGCGAGATT-CC----AGGAGCCAATCAGCGTC---GCCGCG
          ----                -AP-1/c-Jun-                                              ---CP1----
                                ---ATF----

H2-Bl^bc  CCCTCTCTGACCTCCTGAGGTAGCAGGAATTATCTGGCAGGTCTCATCTCCATTGGGTGGCAGGATCCTGGGGAAGGAACCAACCAGCTCCTCATTGGCG
Tw5^bc    CCCTCTCTGACCTCCTGAGGTAGCAGGAATTATCTGGCAGGTCTCCTCTCCATTGGGTGGCAGGATCCTGGGGAAGGAACCAACCAGCTCCTC---CGCG
Q1^bc     CCCTCTCTGACCTCCTGAGGTAGCAGGAATTATCTGGCAGGTC-------CATTGGGTGGCAGGATCCTGGGGAA----CCAACCAGCTACTC---TGTG
Q2^bc     CCCTCTCTGAAC-CCTGAGGTAGCAGGAATTATCTGGCAGGTCTCATTTCCATTGGGTGGCAGGATCCTGGGAAA----CCAACCAGCTCCTCAGCAGCG
            --GUT MULTI-1--      --C/EBPα--                                  ---AP-2---                  ---NF-1
                                                                                 ---PU.1---

T3^b      TTTGCTCTCTGTACCATTGTCA--GATTGTTTTCAAAGGCCTTGCACTCCTGTTGAG-AGCAGGTACTTAGAAGAT---GCAATAAAACTCT---CTGAG
                                                                                 ----T3 MULTI-2-----

Q10^bc    --CATTCGGCTCGGCTCGGACACTGATTGAG-GCTATCAGGTCTCACCCCCAT-GAGTGGCGCGTTCCTG----GGGAACCAACCAGCGTC---GCCGCG
          ------

            -60       -50       -40       -30       -20       -10        +1
             :         :         :         :         :         :         :
          TATA box                     Inr
K^b       GACGCTGGATATAAAGTCCACGCAGCCCGCAGAACTCAGAAGTCGCGAAT-CGCCGACAGGTGCG**ATG**
D^bc      GACGCTGGTTATAAAGTCCACGCAACCCGCGGGACTCAGACACCCGGGAT-CCCAG**ATG**GGGGCG**ATG**

H2-Bl^bc  GGCGCAGGTTATAAAGTCCATGCAGCCCTAGGGCCTCAG**ATG**CCCTGTAT-TCCAA---------**ATG**
Tw5^bc    GGCATTGGTTATAAAGTCCATGCAGCCAGCGGGACTCAGACATCCAGGAT-CCCAG---------**ATG**
Q1^bc     GGCGCTGGTTATAAAGTCCACGCAGCTCGAGGGCCTCAG**ATG**CCCTGTAT-TCCAG---------**ATG**
Q2^bc     GGCGCAGGTTATAAAGTCCATGCAGCCA-AGGGCCTCAG**ATG**CCCTGTAT-CCCAG---------**ATG**
          ---                  ---NF-1----

T3^b      ATTGCAAGTTACAAAGTCCAGGACTTTATACAACTTCAGATTTCCCTAAC**ATG**AGGATAGGGACC**ATG**
           --Oct-1---              --C/EBPβ--
                  --C/EBPα--

Q10^bc    C-CACTGGTTATAAAGTCCACACAGCCCGAGGGACTCAGACGCCCCGGAT-CCCAG**ATG**GGGGCG**ATG**
```

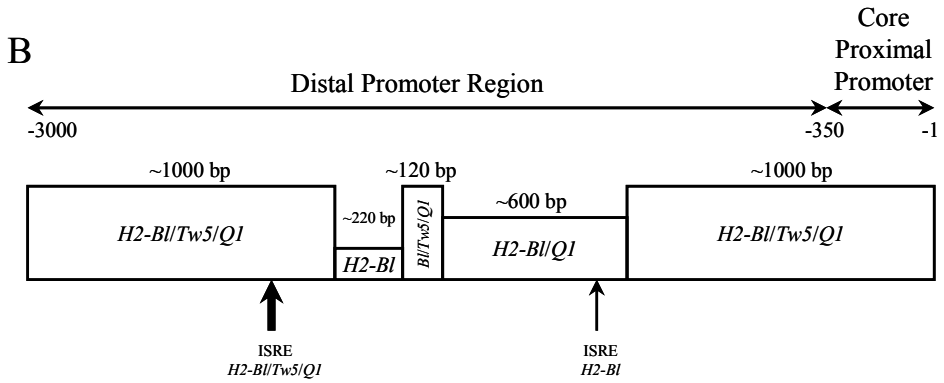

Figure 4.10 Gut-specific class Ib *Mhc* promoters share significant homology with each other and are distinct from those of ubiquitously transcribed and other tissue-specific class I *Mhc*. A. Alignment of K^b, D^b, $H2\text{-}Bl^{bc}$, $Tw5^{bc}$, $Q1^{bc}$, $Q2^{bc}$, $T3^b$ and $Q10^{bc}$ core promoter sequences. ClustalW alignments were performed on sequences from the following sources: K^b – mouse ch17 (34137542-34137200); D^{bc} – AC087217 (4506-4847); $H2\text{-}Bl^{bc}$ – AY518700 (674-1024, with reading frame correction from U21906); $Tw5^{bc}$ – AF532116 (8596-8249); $Q1^{bc}$ – AC087217 (63213-63549); $Q2^{bc}$ – AF111102 (13401-13745), $T3^b$ – mouse ch17 (36327409-36327056); $Q10^{bc}$ – AF111103 (35669-36013). The center portion of transcription factor binding sites, as determined by the AliBaba 2.1 algorithm, are underlined with the putative associating transcription factor underneath. The designation "multi" indicates that multiple transcription factor recognition sequences are present. The transcription factors identified in class Ia MHC sequences are those that are present in both K^b and D^{bc}. Except for those listed in multi sites, all factors are specific to the indicated gene (i.e. not in the K^b/D^{bc} consensus). Class Ia Multi-1: ATF, RAR-α, RXR-β, COUP, USF, RAR-β, ETF, c-Rel, NF-κB, Id2, AP-2α, MBP-1, EBP-1, RelA. Gut Multi-1: RAR-β, ER, CRE-BP1, C/EBPα, COUP, RAR-α1, RXR-β, T3R-β1, REV-ErbA, ARP-1. $Q2^{bc}$ only encodes the COUP binding site of Gut Multi-1. *T3* Multi-1: AP-1, GR, C/EBPα. *T3* Multi-2: Oct-1, C/EBPα. *Q10* Multi-1: c-Jun, CRE-BP1, T3R, T3R-β1, ATF, RAR-α, RXR-β, COUP, USF, RAR-β, NF-κB, C/EBPα, AP-2α, c-Rel, Id2. Transcription factor abbreviations: AP – activator protein; ARP – apolipoprotein repressor protein; ATF – activating transcription factor; C/EBP – CCAAT/enhancer binding protein; COUP – chicken ovalbumin upstream promoter; CRE-BP/CREB – cyclic AMP response element binding protein; ER – estrogen receptor; ETF – epidermal growth factor receptor (EGFR)-specific transcription factor; GATA – GATA-binding protein; GR – glucocorticoid receptor; Id2 – inhibitor of DNA binding 2; IRF – interferon regulatory factor; ISRE – interferon-stimulated response element; MBP – MHC binding protein; NFκB – nuclear factor κB; NF – nuclear factor; Oct-1 – octamer motif binding protein; PU.1 – purine-box binding factor 1; RAR – retinoic acid receptor; RXR – retinoid X receptor; SRF – serum response factor; T3R – thyroid hormone receptor; USF – upstream stimulatory factor; WT – Wilms tumor. B. 5' flanking regions of *H2-Bl*, *Tw5* and *Q1* contain regions of strong homology interspersed by deletions/insertions. ClustalV alignment of core and distal promoter regions of $H2\text{-}Bl^b$

(mouse ch17 [36224168-36221174]), *Tw5*^{bc} (AF532116 [10498-8270]) and *Q1*^{bc} (AC087217 [60753-63549]). Boxes indicate regions of alignment. Small boxes signify a deletion/insertion in the alignment over the indicated region. The location of the putative ISRE in the conserved region of *H2-Bl* (~2.7 kb upstream of ATG), *Tw5* (~2.5 kb upstream of ATG) and *Q1* (~1.9 kb upstream of ATG) is indicated by a thick arrow. The location of an additional ISRE motif in *H2-Bl* (~1130 bp upstream of ATG) is shown with a thin arrow. Significant sequence alignment extends for another 2 kb 5' in all three genes (between *H2-Bl* and *Tw5*: 96%; *H2-Bl* and *Q1*: 89%; *Tw5* and *Q1*: 89%) and for a further 4 kb for *H2-Bl* and *Tw5* (94%).

interaction of putative elements with known transcription factors was predicted using the AliBaba 2.1 algorithm (326). The four sequences corresponding to *H2-Bl*, *Tw5*, *Q1* and *Q2* genes showed significant homology with each other within the core and proximal promoters (Figure 4.10B) as judged by their alignment within these regions. This homology extended for several additional kb for *H2-Bl*/*Tw5*/*Q1* (see legend to Figure 4.10B). In contrast, little sequence similarity was found between the *H2-Bl*/*Tw5*/*Q1*/*Q2* cluster of gut-specific genes and class Ia (*H2-K*^{b} and *H2-D*^{b}), liver specific *Q10*, or a different intestine-restricted promoter, *H2-T3*^{b}, beyond short stretches of DNA within the core promoter. While all the analyzed core promoters contain regions that may function as <u>CCAAT</u>, <u>TATA</u> and <u>Inr</u> elements, they display individual variations. Thus, *H2-Bl*, *Tw5*, *Q1*, *Q2* and *Q10* <u>CCAAT</u> boxes (CCAAC) and *T3* (GCAAT) differ at one position from the canonical CCAAT. It is not known at present whether the canonical <u>CCAAT</u> box in class I *Mhc* genes is required for either basal or inducible transcription, since the class Ia promoter is active in its absence (327). Similarly, T3 carries an alternative <u>TATA</u> box (TACAAA), which nevertheless may bind the same TATA box factor, TCB, as described earlier (328, 329).

In contrast to the similarities found in the core promoter regions, major differences exist between the proximal promoters of gut- and liver-restricted class Ib and class Ia *Mhc* genes (Figure 4.10A). Although the weak EnhB is conserved in *H2-Bl*, *Tw5*, *Q1* and *Q2*, the key regulatory elements defining class Ia ubiquitous and inducible expression (EnhA, X1/CRE/X2 and ISRE sites) are drastically altered. In place of the well characterized class Ia DNA sequences, which interact with factors such as NFκB, CREB/ATF, AP-1, Fra-2 (330, 331), the class Ib 5' sequences contain DNA targets for a completely different set of transcription factors (Figure 4.10A). The latter include unique DNA binding repressors and activators implicated in the control of gene expression in embryo/blastocyst (ETF (332), ERG-1 (333)) and tissue-restricted basal transcription in adults (ARP-1 (334, 335), E-1 (336), AP-2 (337), GATA-1 (338, 339), Rev/ErbA (340)). Most interestingly, the ARP-1 repressor has been shown to bind to regulatory elements in gut-specific genes that restrict expression of reporter genes to the enterocytic lineage and establish crypt-to-villus and duodenal-to-colonic gradients of gene expression in the gut (334, 339). Similarly, C/EBPα boxes, found multiple times in the proximal promoters of gut-specific class Ib *Mhc* genes (repeated three times in *H2-Bl*-related promoters and four times in the *T3* promoter) have been reported in earlier studies to be associated with activation of gene expression in enterocytes (334).

In addition to putative factors that may restrict class Ib expression to gut subcompartments, we noted that class Ib promoters contain sites for interacting with transcription factors that may target their expression to the thymus (Figure 3.7 and Figure 4.6). Indeed, PU.1 was earlier reported as a regulator of gene expression in early myeloid development and in hematopoiesis (341).

Surprisingly, the *T3* promoter and the homologous cluster of other gut-specific promoters share only a few regulatory elements. The exceptions include: GATA-1 sites, which may bind GATA-4-6 factors important for tissue-specific differentiation, including gut enterocytes (338, 339), previously mentioned multiple C/EBPα sites (334) and the Rev/ErbA element, which may silence transcription by binding dominant repressors in multiple tissues (340). This observation suggests that, despite common basal expression patterns in intestinal enterocytes, *T3* and other class Ib *Mhc* studied here, evolved independently of each other to respond to different stimuli and developmental signals.

Within the homologous, gut-specific group of class Ib, *Q2* appears to be most divergent as it fails to align with others in the distal promoter and lacks both ARP-1 and PU-1 sites. Consistent with this, we observed that *Q2* is the most likely of the four to be expressed (albeit at very low levels) outside of the gut/thymus lineages (Figure 4.7A). *Q1* also lacks the PU.1 box and, like *Q2*, has a potential binding site for ERG-1, which regulates developmental steps in murine embryogenesis, including the epithelial-mesenchymal transition (333). This suggests that *Q1* and *Q2*, despite many similarities, are subject to slightly different regulation than *H2-Bl*/*Tw5*.

In addition to factors that may be involved in maintenance of basal expression levels, we sought to identify the candidate regions/factors controlling inducible promoter transcription. One of the most interesting ones in this category is the AP-2 activator, which has no binding sites in class Ia, but is predicted to interact with promoter elements of *H2-Bl*, *Tw5*, *Q1* and *Q2*. This transcription factor is restricted to a subset of tissues, including the gut (337), and has been proposed to act as a “stress-sensor” because it is inducible by p53 and may therefore mediate some of the p53 downstream effects (342).

Similar tumor suppressor activities were attributed to C/EBPα, also represented in *H2-Bl*, *Tw5*, *Q1* and *T3*, which acts to limit mitotic growth and seems to also be involved in responses to injury (343, 344).

In regards to other metabolic sensing elements, it is likely that elimination of EnhA sequences in class Ib promoters resulted in loss of responsiveness to insulin and hydrocortisone (both of which are known to regulate class Ia genes (345, 346)). Instead, the gut-specific class Ib cluster (and liver-specific *Q10*) contain ER (347) and T3R-β1 (348) elements, binding estrogen receptor and thyroid hormone receptor genes, respectively. The presence of these elements suggests that gut class Ib MHC may participate in physiologically regulated responses to some hormones.

It is also of interest that elements responsible for retinoic acid (RA) sensing (RAR-α, RAR-β and RXR-β) were preserved in the *H2-Bl*/*Tw5*/*Q1*/*Q2* cluster, though they are found in a different region of the proximal promoter than those of class Ia (Figure 4.10A). RA triggers specification and/or differentiation during embryonic life, limits growth of stem/progenitor cells and regulates expression of Rae-1 NKG2D ligands (186, 349). Since the intestine is one of the few tissues synthesizing RA during adult life (83), presence of RA sensing elements in multiple *Mhc* genes may be indicative of biological significance of this regulation in class Ia/b expression in the intestine.

Finally, we sought to identify the mechanism responsible for inducibility of *H2-Bl* to IFN-γ (Figure 4.9). The canonical ISRE and X1/CRE/X2 boxes (317, 322-324), present in class Ia, *T3* and *Q10* at ~ -200 to -220 bp are mutated in the gut class Ib proximal promoter. We were, however, able to locate ISRE elements (responsive to both type I and type II IFNs (317)) in distal promoters (at ~ -1200 bp and -2200 bp in *H2-Bl*

and at -2200 in *Tw5* and *Q1*). Thus, we conclude that *H2-Bl* may be inducible by IFNs by the classical JAK-STAT pathways operating via ISRE elements. Additional experiments involving mutational analysis and studies of promoters fused with reporter genes are required to address this hypothesis.

SUMMARY AND DISCUSSION

IEL are critical players in intestinal immune homeostasis, surveying the intestinal epithelium for infection or damage and negotiating immune reactivity and tolerance via T and NK cell receptor triggering. The ligands for these IEL receptors remain largely unknown, but many indirect lines of evidence point to class Ib MHC or class I-related products as the most likely candidates (40, 91, 110-112, 350). Five murine class Ib MHC are known to be transcriptionally restricted to the intestine – *Q1*, *Q2*, *H2-Bl*, *Tw5* and the genes encoding TL (*T3* and *T3-like*). *Q1*, *Q2* and *T3* have been shown to be expressed in IEC, placing them in direct contact with IEL (248-250). In the work described in this chapter, we found that *H2-Bl*, *Tw5* and the *T3-like* putative ortholog of *T3* and *T18* are also specifically expressed in IEC, and all five gut-specific class Ib MHC display cephalocaudal and developmental transcriptional profiles resembling that of several other genes expressed in the enterocyte lineage.

In an effort to characterize potential receptors for these IEC-restricted class Ib MHC, we examined the expression of selective types of T and NK cell receptor transcripts and proteins present on IEL isolated from intestinal sections rich in class Ib MHC transcripts. Using an RT-PCR approach, we detected expression of *CD94*,

NKG2A, *NKG2D* and *Ly49* transcripts in the intestinal sections enriched for both class Ib MHC (this work) and unconventional IEL subsets (195).

The TCR and CD8 phenotype of IEL is imprinted on them during thymic education and/or upon encounter with peripheral antigen challenge. These, in turn, are thought to regulate specificity and reactivity in the intestinal epithelium. Whereas conventional TCR$\alpha\beta^+$ CD8$\alpha\beta^+$ IEL are reminiscent of cytolytic effector memory T cells that acquired specificity for foreign antigen prior to entering the epithelial monolayer, TCR$\alpha\beta^+$ CD8$\alpha\alpha^+$/CD8$^-$ and TCR$\gamma\delta^+$ IEL are proposed to play more of a regulatory role in the intestinal immune response (25). To identify specific IEL subsets that display these receptors, we examined CD8$\alpha\alpha^+$, CD8$\alpha\beta^+$, CD8$^-$ and TCR$\gamma\delta^+$ IEL populations for expression of CD94, NKG2A, NKG2D and Ly49 NK cell receptors. We were particularly interested in CD94/NKG2A expression by IEL since, in human disease, HLA-E expressed on IEC has been shown to suppress the autoimmune response in the gut when engaging this receptor (44). We observed that all conventional and unconventional IEL contained populations co-expressing CD94 and NKG2A (ranging from 2-5%). In addition, we were surprised to detect a phenotypically new fraction of IEL (3-17%) which expressed NKG2A but not CD94 and was enriched in unconventional IEL (>10%). NKG2A has been reported to be dependent on CD94 for its expression on the cell surface (126), and only one other instance of NKG2A expression in the absence of CD94 has been rigorously documented, in transfected COS7 cells (158, 170). Interestingly, we also found that NKG2A$^+$ CD94$^-$ IEL co-express NKG2D, suggesting that these subsets have unique properties that distinguish them from IEL bearing inhibitory CD94/NKG2A homodimers. Little is currently known about the functional

significance of CD94/NKG2A, NKG2A or NKG2D expressed constitutively on IEL, though their low level transcription was previously noted by SAGE from αβ and γδ IEL (81). Only one study has previously attempted to quantitate NKG2A on $CD8^+$ ($CD8\alpha^+$) bulk IEL and, consistent with our data, noted overall low (~14%) positivity among naïve, pooled intestinal lymphocytes (196). Furthermore, the same researchers demonstrated that during model bacterial, viral or tumor challenge, the NKG2A receptor remained uninduced, presumably due to the presence of RA in this environment. Interestingly though, TGF-β, produced by many intestinal cells, is a known inducer of NKG2A (162) and may regulate its expression under a different set of circumstances.

In the human system NK cell receptors play an important role during autoimmune celiac disease, a gluten-induced enteropathy characterized by the presence of gliadin-specific $CD4^+$ T cells in the lamina propria and by a prominent IEL infiltration with a LAK phenotype. Recently it has been found that, in active celiac disease, there is a specific increase of cytotoxic IEL expressing activating NKG2D, which recognizes IL-15-induced class I-like MIC on IEC, as well as CD94 and NKG2A, which have a suppressive regulatory effect on other IEL (44). Thus, these opposing NK cell receptor mediated pathways are turned on during this disregulated immune response in the gut.

Previous studies have demonstrated only low level transcription of Ly49 family members by IEL (81), but more recent data identified a specific subset of unconventional IEL ($TCR\alpha\beta^+$ $CD8\alpha\alpha^+$) that display a relatively high expression of Ly49E and Ly49F orphan NK cell receptors (~23% and ~18%, respectively). These members of the Ly49 family do not bind class Ia or TL (*T3*) tetramers and may therefore be possible candidates for receptor/ligand interactions with gut-specific class Ib MHC (195).

In brief, we have demonstrated here that IEL express NK cell receptors potentially compatible with engaging proximal gut-specific class Ib MHC. Other MHC-associating receptor complexes may also utilize these gut-specific ligands – CD8 and the TCR. *T3*/*T18* encode TL, the gut-specific class Ib MHC protein that associates with CD8αα, inducing cytokine secretion by and inhibiting proliferation of IEL in response to TCR engagement (38). The crystal structure of TL in complex with CD8αα and subsequent mutational studies revealed three amino acids found in TL but not class Ia MHC that are required for TL/CD8αα interaction (351, 352). Q1, Q2, H2-Bl and Tw5 all share two of these three CD8αα-binding residues (Figure 3.2, (351)), raising the possibility that they too might engage CD8αα on proximal IEL.

The TCR$\alpha\beta^+$ CD8$\alpha\alpha^+$ IEL population is unique to the intestine and positively selected by one or more strong agonist class Ib MHC in the thymus (22). Although gut-specific class Ib MHC are almost exclusively expressed in the intestinal epithelium, the home of TCR$\alpha\beta^+$ CD8$\alpha\alpha^+$ IEL, these class Ib MHC can also be detected at low levels in the thymus (this study and unpublished observations), positioning them to direct the thymic development of this unique IEL population.

Gut-specific class Ib MHC may also act as restricting elements for the conventional effector/memory TCR$\alpha\beta^+$ CD8$\alpha\beta^+$ IEL population that migrates into the epithelial layer after being primed in the periphery. Several other class Ib MHC have been shown to restrict CD8$^+$ T cells, including M3 (353), Qa-1 (92) and Qa-2 (354, 355). This would presumably necessitate the expression of these MHC molecules on DC, since IEC do not express co-stimulatory molecules capable of initiating a primary adaptive immune response (356). DC have not been specifically tested for the expression of gut-

restricted class Ib MHC, but given its detectable background expression in most adult tissues, Q2 is a good candidate for APC expression. Q2 is also highly polymorphic, with amino acid substitutions in the peptide binding region on par with class Ia MHC (287). This suggests that Q2 has undergone pathogen-driven positive selection in a manner similar to class Ia MHC, a feature that would be consistent with classical $CD8^+$ T cell responses. Other gut-restricted class Ib MHC may be inducible in DC under inflammatory conditions by cytokines such as IFN-γ.

A most interesting possibility is that gut-specific class Ib MHC act as ligands for γδ T cell receptors on IEL. Very little is known about ligands of the γδ TCR. Only one of them (the class Ib MHC molecule T22) has been characterized structurally to date, and contrary to all other known TCR, which dock on pMHC from above, it engages the T22 heavy chain from the side in a manner similar to antibody/antigen interaction (98, 99). It is not known whether this unusual docking mode is representative of γδ TCR interaction with all its ligands or if it is unique to this very rare population of peripheral γδ T cells. In the gut, $TCR\gamma\delta^+$ IEL predominantly utilize Vγ5 or Vγ1.1 variable regions with diverse junctional sequences (94), likely allowing for recognition of multiple ligands. $TCR\gamma\delta^+$ IEL arise from the thymus in late fetal development (~ embryonic day 16 in the mouse) and seed the gut through adulthood (94). It is still not known if they are educated via positive selection. *Ex vivo* they possess an innate cytotoxicity that does not require signals or antigens from intestinal flora (32). Interestingly, we and others have shown that *Q1*, *Q2* and *H2-Bl* thymic expression begins in the late fetal period ((249, 250), Figure 4.6), and gut-specific class Ib *Mhc* transcription is not differentially regulated in germ-free versus conventional mice (unpublished observations in collaboration with Dr.

L. Hooper). Based on these observations, Q1, Q2, H2-Bl and Tw5 represent possible ligands for TCR$\gamma\delta^+$ IEL.

In the current study we demonstrate that gut-specific class Ib *Mhc* are expressed by IEC where they are available to engage T and NK cell receptors on proximal IEL. Our data suggest that Q1, Q2, H2-Bl and/or Tw5 may act as agonists in the thymus and/or restriction elements for TCRs on effector/memory or regulatory IEL, ligands for IEL-expressed immunoregulatory NK cell receptors and/or stress sensors for γδ IEL in the intestinal epithelium. Future studies need to be undertaken to sort out the receptor/ligand interactions of these unique class Ib MHC in the intestine.

CHAPTER FIVE

Potential Roles of H2-Bl in Qa-1-Mediated Immune Tolerance/Stimulation

BACKGROUND AND RATIONALE

In Chapter Four we demonstrated that gut-specific class Ib MHC are restricted to IEC, positioning them to interact with T and NK cell receptors on neighboring IEL. Among the constitutively expressed IEL receptors is CD94/NKG2A, known to engage the class Ib MHC molecule Qa-1 in association with nonameric peptides derived from the leaders of selected class Ia MHC (170). In the human system it has been reported that some gut γδ T cell populations exert regulatory functions in the intestinal milieu via a pathway involving interaction of CD94/NKG2A with HLA-E on IEC (44). Since murine IEC express only low levels of class Ia MHC (120), we sought to determine if H2-Bl and other tissue-restricted class Ib MHC can supply Qa-1 binding peptides that could impact the immune status of tissue-specific immune effectors in the murine intestine.

Murine Qa-1 and human HLA-E arose independently by convergent evolution to assume key roles in an important innate immunity mechanism that may represent one of the most ancient pathways for self/nonself recognition (127). These ubiquitously expressed class Ib MHC serve as sensors of class I MHC intracellular synthesis. They are ordinarily expressed on healthy cells, but are scarce on virally infected or otherwise diseased cells, which downregulate synthesis of MHC chains.

The murine Qa-1 peptide binding groove is selective in its peptide binding repertoire and is particularly well suited for association with hydrophobic nonamer

peptides, termed Qdm for Qa-1-determinant modifier, derived from the leader sequences of the class Ia MHC molecule D^b (176). Qdm is the single most abundant peptide found in association with Qa-1 in normal cells (in the $H2^b$ haplotype), yet its affinity for Qa-1 is relatively weak (172). This has been proposed to stem from the unusual architecture of the Qa-1 binding cleft, which is also similar to HLA-E. Qdm therefore associates with Qa-1 through several major and minor anchors along its length. Major anchors in the Qa-1 primary amino acid sequence (AMAPRTLLL) are the P1 amino terminus, methionine at P2 and leucine at P9 (173-177). Absence of the P1 residue or non-conservative disruption of either position P2 or P9 residues renders peptide/Qa-1 association undetectable (173-176). Minor anchors, those for which substitutions have been determined to reduce but not entirely abrogate peptide/Qa-1 interaction, are found throughout the peptide at P3, P5, P6 and P7 (175, 176). Thus, Qa-1 can bind peptides differing from Qdm at non-anchor positions, though, in all cases described to date, with reduced affinity.

In addition to a generally weak affinity for its dominant peptide, Qa-1 has several other unusual properties. Though cell surface expression of fully conformed, Qdm-associated Qa-1 is TAP-dependent, unconformed Qa-1, presumably Qdm-free heavy chains, are constitutively displayed at the cell surface in the absence of TAP (172, 357). Additionally, Qa-1 expressed on the cell surface of TAP-deficient cells rapidly binds exogenous Qdm (172). Further, while β_2m is required for Qa-1 heavy chain folding intracellularly, its association with Qdm-independent Qa-1 is poor. This may be caused by endogenous murine β_2m rapidly dissociating from Qa-1 or its exchange with serum β_2m at the cell surface (357). Thus, Qa-1 can be expressed at the cell surface in its fully-

conformed, peptide loaded, β_2m-associated state or, in the absence of a well-fitting associating peptide, in a β_2m-free, unconformed, Qdm receptive state.

We developed a new, physiological assay based upon these features of Qa-1 to test whether class Ib MHC specifically expressed in tolerance-dominated tissues can contribute leader peptides capable of associating with Qa-1. We found that H2-Bl-derived peptide nonamers and Qdm derived from brain-expressed Q5 and liver-specific Q10 can be endogenously processed and presented on the cell surface by Qa-1. Peptides from each of these proteins display a variable requirement for TAP. Additionally, H2-Bl leader peptides from different haplotypes bind Qa-1 with different affinity based on their similarity to Qdm. Our preliminary data suggest that H2-Bl-derived Qdm-like nonamer peptides protect target cells from cytolysis, perhaps better than Qdm. We propose that these features of tissue-specific class Ib MHC broaden the ability of cells in which they are expressed to utilize Qa-1-mediated immune inhibition.

RESULTS

Structural Features of Gut-Specific Qdm-Like Leader Peptides

Though the class Ia genes *H2-D*^{b} and *H2-L*^{d} in *H2*^{b} and *H2*^{d} haplotypes, respectively, encode leader peptides containing the Qdm motif (AMAPRTLLL), the presence of Qdm is not a general feature of class Ia MHC. *H2-K*^{b}, for example, does not encode a leader peptide capable of engaging Qa-1 (358) and many mouse haplotypes do not contain *H2-L* or any other class Ia genes with Qdm leader sequences. For example,

the *H2*^{k} haplotype contains an *H2-D* gene that does not encode Qdm, but rather a Qdm-like peptide (AMVPRTLLL), which does not associate as well with Qa-1 as Qdm (176). In light of this variable Qdm phenotype, we wondered if the Qa-1-mediated NK cell inhibitory pathway might be regulated by class Ib MHC polypeptides, particularly in tolerance-dominated tissues expressing tissue-specific class Ib MHC proteins.

To determine if the sequences of previously sequenced class Ib MHC available in GeneBank encode Qdm or Qdm-like peptides, we aligned the putative first exon translation products (beginning with the first ATG downstream of the transcriptional initiation site (321)) of H2-D^{b} (a known source of Qdm (177)), gut-specific H2-Bl^{b} and H2-Bl^{bc} (which have the same leader sequence), H2-Bl^{q}, Q1^{bc}, Q2^{bc}, Tw5^{bc} and the T3-like protein from the H2^{bc} haplotype, liver-specific Q10 and brain-expressed Q5^{k} by the ClustalW algorithm (325). Two of these sequences, Q10 and Q5^{k}, encode peptides that are an exact match to Qdm (AMAPRTLLL) and include all residues that are critical for Qa-1 association (173-176) (Figure 5.1A). Qdm-like peptides encoded by H2-Bl^{q} (AMAQRTLLL) and H2-Bl$^{b/bc}$ (AMAQRTLFL) differ from Qdm at non-anchor positions, but all 5 major (P2 and P9) and minor (P5, P6 and P7) Qa-1 anchors are preserved. Q2^{bc} (AMALRRLLL) and Q1^{bc} (AMALGRLLL) contain peptide sequences with conserved dominant Qdm anchors but only two out of three and one out of three minor anchors, respectively. The regions over which Tw5^{bc} and T3-like^{bc} aligned with the other leader sequences shared no significant homology with Qdm, containing only one major anchor each (NMRLRRVFR and TMVPGTLLI, respectively). Of the class Ib MHC sequences available for comparison only the leaders of class Ib that are highly expressed in tolerance-associated tissues (Q5 in the brain, Q10 in the liver and H2-Bl, Q1

A

Qdm A M A P R T L L L
1 2 3 4 5 6 7 8 9

B

D^{b}							M	G	A	M	A	P	R	T	L	L	L	L	L	A	A	A	L	A	P	T	Q	T	R	A
$Q5^{k}$							M	W	A	M	A	P	R	T	L	L	L	L	L	A	A	A	L	T	L	T	Q	T	R	A
$Q10^{b}$							M	G	A	M	A	P	R	T	L	L	L	L	L	A	A	A	L	A	P	T	Q	T	Q	A
$H2\text{-}Bl^{q}$	M	P	C	I	P	N	G	A	M	A	Q	R	T	L	L	L	L	L	A	A	A	L	T	M	I	Q	T	R	A
$H2\text{-}Bl^{b/bc}$	M	P	C	I	P	N	G	A	M	A	Q	R	T	L	F	L	L	L	A	A	A	L	T	M	I	E	T	R	A
$Q1^{bc}$	M	P	C	I	P	D	G	A	M	A	L	G	R	L	L	L	L	L	A	A	A	L	T	L	T	K	T	G	A
$Q2^{bc}$	M	P	C	I	P	D	G	A	M	A	L	R	R	L	L	L	L	L	V	A	A	L	K	L	T	E	T	R	A
$Tw5^{bc}$							M	E	N	M	R	L	R	R	V	F	R	V	L	V	A	S	L	T	L	T	E	T	L	A
$T3\text{-}like^{bc}$				M	R	I	G	T	M	V	P	G	T	L	L	I	L	L	A	A	S	Q	V	Q	T	Q	T	C	P	

Figure 5.1 Gut-specific class Ib MHC leader sequences contain peptides similar to Qdm. A. Amino acid sequence of Qa-1-binding Qdm. The Qdm nonamer peptide, as described by Aldrich et al (177), is depicted from N- to C- terminus. Underlined residues are those that correspond to anchors for associating with the peptide binding groove of Qa-1 by various amino acid substitution assays (173-176) and a random peptide library study (176). Top row – anchor positions described by Kraft et al (176). Bottom row – anchor positions described by Kurepa et al (175). B. Qdm-related sequences in class I MHC leader peptides. Predicted amino acid sequences of the leader peptides of indicated class I MHCs aligned by the ClustalW algorithm. Residues that share identity with Qdm are in bold font. Nonamers that are identical to Qdm are darkly shaded. The Qdm-like nonamers containing all anchor residues important for Qa-1 association (see A) are lightly shaded. Circled and boxed "M" are first and second methionines, respectively. Sequences are from the following GeneBank accession numbers: D^{b} – M18523; $Q5^{k}$ – NM_010393; $Q10^{b}$ – NM_010391; $H2\text{-}Bl^{q}$ – submitted; $H2\text{-}Bl^{b}$ – submitted; $H2\text{-}Bl^{bc}$ – submitted; $Q1^{bc}$ – submitted; $Q2^{bc}$ – submitted; $Tw5^{bc}$ – submitted; $T3\text{-}like^{bc}$ – submitted.

and Q2 in the intestine) contained Qdm-like sequences. Thus, we predict that leader peptides from $Q5^{k}$, Q10, $H2\text{-}Bl^{q}$, $H2\text{-}Bl^{b/bc}$ and possibly $Q1^{bc}$ and $Q2^{bc}$ may bind Qa-1 if they are processed into Qdm-like fragments. The corresponding class Ib MHC genes may therefore participate in maintenance of NK/T cell tolerance in the tissues in which they are expressed. Importantly, both canonical as well as alternatively spliced class Ib MHC proteins may potentially contribute Qdm for Qa-1 binding.

The sequence of Qdm in H2-Bl leader peptides represents a special case, in that *H2-Bl* exon 1 encodes two alternative "in frame" ATG start sites, both located 3' of the transcriptional initiation site (321). Only translation from the first ATG will result in the generation of a canonical Qdm-like peptide, while translation from the second ATG will give rise to a truncated octamer missing the first residue of Qdm. To confirm that the *H2-Bl* first ATG is indeed transcribed, and thus potentially translated, we performed RT-PCR on small intestinal cDNA (C57BL/6J mouse) using a reverse primer specific for the H2-Bl 3' UTR (5'-ACT CCA CTA ATC AAC CCT CAG-3') and a forward primer situated over the region downstream of the transcriptional initiation site and four nucleotides 5' of the second ATG (5'-CAG ATG CCC TGT ATT CCA AAT GG-3'). As a negative control, we used a forward primer specific for the H2-Bl promoter (5'-GCG CCG CTC GAG TCT CCT GCA GTT CAG CTC CT-3') and a second reverse primer specific for the 3' end of the gene (5'-AGA GGC GAA TTC TCT AGA TAG GCA TGA CCA CAA-3'). We found that, while the primers designed against the promoter did not amplify a specific product, the primers designed against the region 5' of the second ATG amplified both canonical and major splice variants of *H2-Bl* (data not shown). Thus, *H2-Bl* encodes a transcript capable of producing a nonamer Qdm-like peptide.

Qa-1 Presentation of Qdm-Like Peptides Derived from a Subset of Gut-Specific Class Ib MHC

As previously mentioned, Qdm-like peptides encoded by gut-specific class Ib MHC contain many residues shown to be critical for Qa-1 association. To determine if these peptides could indeed bind Qa-1, we synthesized Qdm-homologous nonamers of each gut-specific class Ib MHC leader sequence as well as the "alternative" octamer H2-Bl^b peptide predicted from translation starting at the downstream ATG. These peptides were then assayed for their association with Qa-1.

Stabilization of β_2m-Associated Qa-1 by Gut-Specific Qdm-Like Peptides

First, we examined if synthetic Qdm-like peptides associate with Qa-1 using an antibody-based "peptide stabilization assay." We developed this assay taking advantage of previously reported properties of Qa-1: 1) Qa-1 presentation of Qdm is TAP-dependent, but cell surface expression of "empty," non-conformed Qa-1 heavy chains occurs in the absence of TAP; 2) Cell surface-expressed Qa-1 is "peptide receptive," and stable Qa-1/peptide complexes can be formed by providing synthetic Qdm peptide exogenously (177); 3) Without Qdm, endogenous β_2m dissociates from Qa-1 at the cell surface; 4) β_2m is required for transport of Qa-1 heavy chains to the cell surface intracellularly (357). Thus, Qdm and TAP-deficient, but β_2m-sufficient cells (such as the B78H1 melanoma described below) can express cell surface Qa-1, but β_2m will not be detectable in association with surface "empty" Qa-1. Model B78H1 cells, which are

monitored for Qa-1/Qdm complex formation in our assay, are devoid of cell surface class I MHC due to transcriptional deficits in multiple class Ia and class Ib genes, as well as *TAP2* and *LMP7* (359). Transfection of exogenous class I heavy chains, such as *T23*-encoding Qa-1, (with or without *TAP2* genes) can result in the cell surface expression of β_2m-associated or β_2m-free class I MHC without the reemergence of endogenous class I (359). Thus, these cells allow us to examine expression of selected class I MHC products in isolation from all other members of the class I MHC-encoded family. In our "indirect" peptide stabilization assay, we used TAP-negative, Qa-1 gene transfected B78H1 cells incubated with exogenous, synthetic Qdm and Qdm-related test peptides. Formation of stable Qa-1/peptide complexes (peptide binding) was monitored serologically via cell surface staining of endogenous mouse β_2m^b.

To ensure the specificity of our Qa-1 expression assay, peptide stabilizations (see Materials and Methods) were performed with Qdm peptides on TAP-negative Qa-1^b transfectants of B78H1 (LS and HeS clones, Figure 5.2). These cells were incubated in the presence of a wide range of concentrations of synthetic Qdm peptides to establish saturation conditions for this assay. Cells were stained with a conformation-specific antibody against mouse β_2m^b (S19.8 antibody) or, as a control, with a conformation-independent antibody produced against a peptide from the α3 domain of Qa-1 (6A8.6F10.1A6 antibody). The Qa-1/Qdm/β_2m stable complexes were then detected by flow cytometry. Cell surface expression of conformed, β_2m-associated Qa-1 was observed at 960 μM and 240 μM Qdm, which indicated Qa-1/Qdm saturation at both concentrations (Figure 5.2). At concentrations between 240 μM and 60 μM Qdm had a titrating effect on the detection of β_2m-associated Qa-1. Qa-1 was not detectable in its

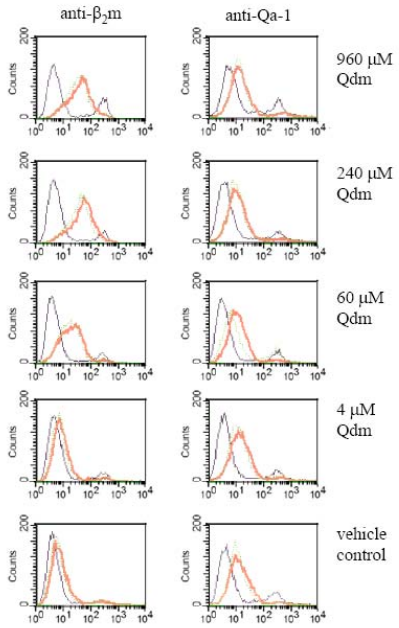

Figure 5.2 Cell surface expression of β_2m serves as a surrogate marker of peptide-stabilized Qa-1. Peptide stabilization of cell surface Qa-1 heavy chain on TAP-negative melanoma cells transfected with the *T23* gene (Qa-1 heavy chain encoding region). Clones LS (thick red line) and HeS (dotted green line) were incubated with the indicated concentration of Qdm or vehicle control (media plus DMSO at the same concentration as the samples containing peptide). Untransfected B78H1 cells served as the negative control for staining (thin black line). Cells were stained with a mouse-specific anti-β_2m^b antibody (S19.8) or the conformation-insensitive anti-Qa-1 antibody specific for a peptide from the α3 domain of Qa-1^b (6A8.6F10.1A6) and subjected to flow cytometry. The specific conditions for the peptide stabilization assay are described in Materials and Methods.

fully conformed, β_2m-associated state at Qdm concentrations below 4 μM. Thus the amount of conformationally stable Qa-1 varies with the concentration of Qdm available

for binding. In sharp contrast, the same cells showed no change in detectable levels of Qa-1 heavy chain cell surface expression when stained with the anti-Qa-1 antibody, which does not discriminate between Qdm-stabilized and unconformed Qa-1, over the entire range of concentrations. This is consistent with previous reports of equivalent Qa-1 cell surface expression in the presence or absence of Qdm as determined by this particular anti-peptide antibody (170, 172). The experiments described above validate our assay and define conditions optimal for detection of Qa-1/Qdm complex formation.

Using the "indirect" peptide stabilization assay just described, we next examined the ability of gut-specific class Ib MHC Qdm-like peptides to associate with Qa-1. Peptide stabilizations were performed with H2-Bl^{q}, H2-Bl$^{b/bc}$, Q1^{bc}, Q2^{bc} and Tw5^{bc} nonamers and the previously described H2-Bl^{b} octamer (277) at the saturating concentrations observed for Qdm (Figure 5.2). The level of Qa-1 stabilization observed with the H2-Bl^{q} nonamer was roughly equivalent to the Qdm control at both concentrations (Figure 5.3). 500 μM of the H2-Bl$^{b/bc}$ nonamer was saturating for Qa-1 stabilization, but at 250 μM the peptide began to exhibit a titrating effect. Q1^{bc}, Q2^{bc}, and Tw5^{bc} nonamers did not stabilize β_2m-associated Qa-1 under the conditions of this assay at either peptide concentration. We were also unable to detect Qa-1 association by the H2-Bl^{b} octamer. These data demonstrate that exogenously applied nonamer, but not octamer peptides of H2-Bl can stabilize β_2m-associated Qa-1 on the cell surface. The H2-Bl^{q}-derived peptide appears to associate with Qa-1 at lower concentrations than the nonamer from H2-Bl$^{b/bc}$, presumably because the H2^{b} and H2^{bc} haplotype peptides differ from Qdm at two positions, while the peptide from the H2^{q} haplotype differs at only one.

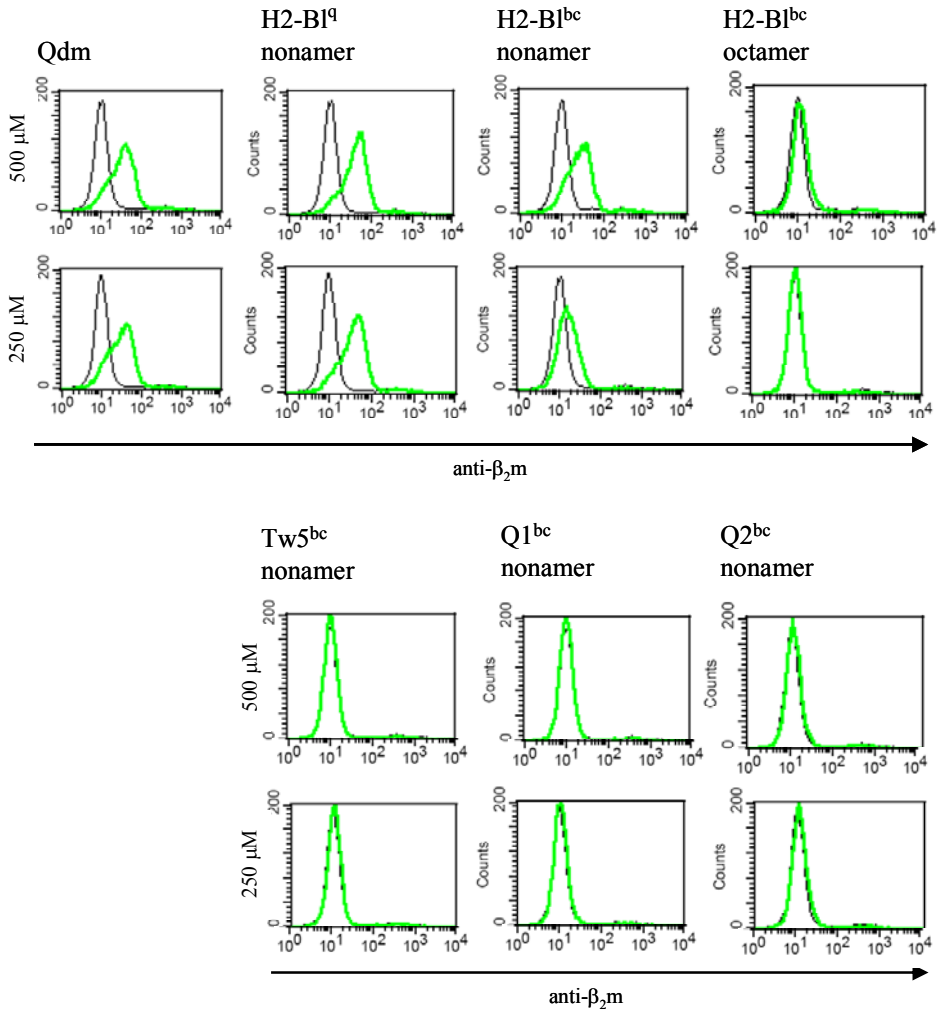

Figure 5.3 Exogenous H2-Bl^q and H2-Bl^{bc} nonamers stabilize β_2m-associated Qa-1^b on the cell surface. TAP-negative melanoma cells, H1Qa-1^b clone LS, (which transcribe the Qa-1 heavy chain, β_2m^b and no other class I MHC heavy chain) were incubated with the indicated concentration of peptide (green lines) or vehicle control (black lines) (see Materials and Methods). Cells were then stained with the anti-β_2m^b antibody S19.8 and analyzed by flow cytometry.

Competition of Qdm and Gut-Specific Qdm-Like Peptides for Qa-1 Association

Our "indirect" stabilization assay demonstrated the association of H2-Bl-derived nonamers with Qa-1 but, as evidenced by the relatively high peptide concentrations required in this assay, was not sensitive enough to detect possible complex formation with other Qa-1-bound gut-specific class Ib leader peptides or the H2-Bl^{b} octamer. The most sensitive of alternative assays, the CTL assay, can detect peptide association with Qa-1 at nM concentrations, but, importantly, it can only recognize Qa-1/peptide complexes that are recognized by Qdm-specific TCR of these CTL (177, 358). We therefore turned to these highly sensitive CTL assays to address whether gut-specific class Ib MHC leader peptides other than the H2-Bl nonamers could associate with Qa-1. The D5D2 anti-Qa-1 CTL clone, developed by Dr. Carla Aldrich, lyses Qa-1-bearing targets in association with several variants of Qdm and some Qdm-divergent sequences (360). It has been used previously to detect binding of synthetic peptide determinants to surface-expressed Qa-1 using chromium release assays (358). Because the CTL clone is Qa-1 restricted, it can be used on targets co-expressing other class Ia/b MHC antigens and still be specific for Qa-1/peptide complexes. Chromium release assays (see Materials and Methods) were performed on the Qa-1-expressing TAP^{-} mouse T cell lymphoma, RMA-S, or Qdm^{-} Qa-1 transfectants of the C1R human lymphoblastoid cell line exogenously loaded with gut-specific class Ib MHC Qdm-like peptides. None of the peptides, except wild type Qdm, was recognized directly by the CTL clone at concentrations ranging from 1 nM to 1 μM (Figure 5.4A). Thus, the class Ib Qdm-like peptides are not sufficiently similar to Qdm (either structurally or electrostatically) to be

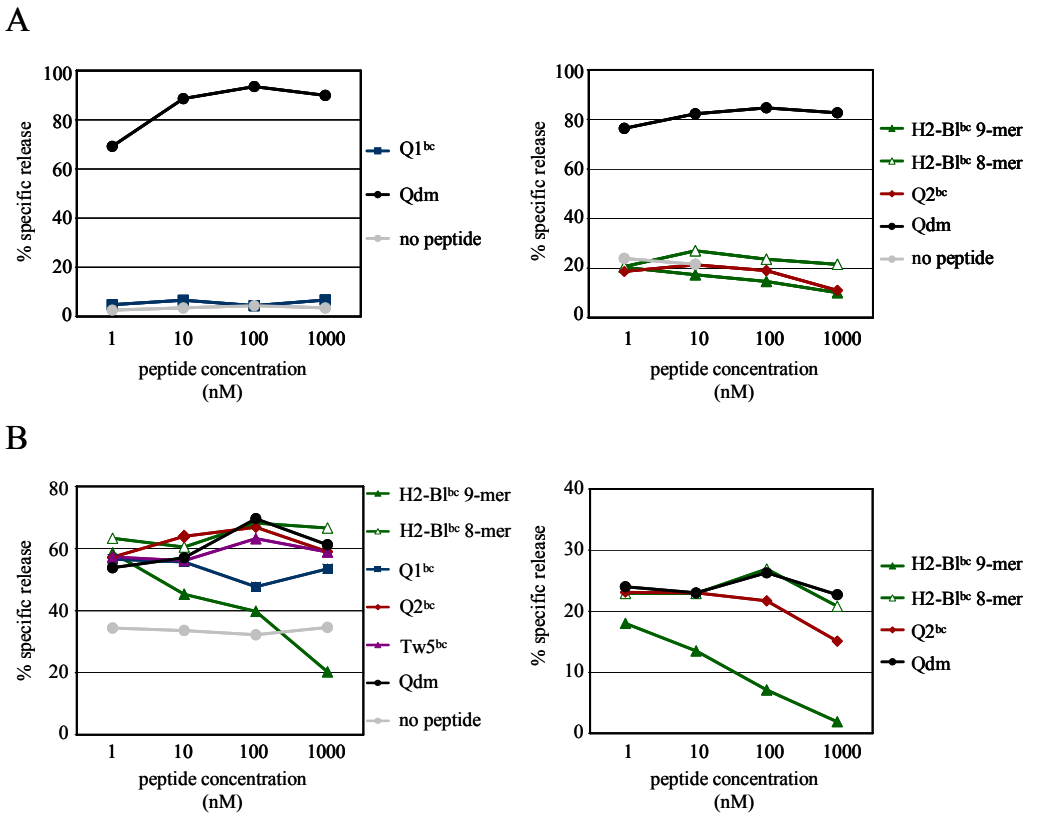

Figure 5.4 High sensitivity assay for the detection of gut-specific class Ib MHC-derived leader peptides in association with Qa-1. A. The Qdm/Qa-1-specific CTL line, D5D2, does not recognize Qa-1^{+} targets incubated with gut-specific class Ib MHC leader peptides. Chromium release assays (see Materials and Methods) performed with D5D2 effectors (177, 358, 360) and target cells consisting of a T23 transfectant of the C1R human lymphoblastoid cell line, J1 ((177), left pane) or the TAP-negative mouse T cell lymphoma RMA-S (right pane) exogenously loaded with the indicated peptide (see Materials and Methods), both at an E:T ratio of 8:1. B. The H2-Bl$^{b/bc}$-derived nonamer peptide can compete with Qdm for Qa-1 association. Chromium release assays performed with D5D2 effectors and J1 (left pane) or RMA-S (right pane) target cells at an E:T ratio of 10:1. Targets were incubated with the indicated peptide and 1 nM Qdm as described in the Materials and Methods and Chun et al (358).

recognized by this Qa-1-restricted, epitope-sensitive CTL clone. We therefore turned to a different strategy and assayed for the ability of gut-specific class Ib MHC Qdm-like peptides to bind to Qa-1 and block Qa-1 access to Qdm, thus inhibiting CTL cytolysis

((358), see Materials and Methods). Using this CTL peptide blocking assay we found that the H2-Bl nonamer, but not the H2-Bl octamer or other tested peptides, inhibited killing of Qdm treated targets at the concentrations of peptide tested here (Figure 5.4B). This pattern of direct and blocking assay results was also seen with a second anti-Qa-1/Qdm CTL clone (39.1D7x, data not shown). At the highest peptide concentrations used in the assay, $Q1^{bc}$ and $Q2^{bc}$ nonamers showed slight CTL inhibition (Figure 5.4B and data not shown [$Q1^{bc}$ with the 39.1D7x clone]), suggesting that these gut-specific class Ib MHC peptides might bind Qa-1 at higher peptide concentrations. However, no such experiments have been performed. The results presented in Figure 5.4 were carried out by our collaborator, Dr. Carla Aldrich, at the Indiana University School of Medicine. Taken together, our results demonstrate that H2-Bl nonamers from $H2^{b}$, $H2^{bc}$ and $H2^{q}$ haplotypes can associate with Qa-1. We have no evidence demonstrating that $Q1^{bc}$, $Q2^{bc}$ or $Tw5^{bc}$ nonamers or the "alternative" H2-Bl^{b} octamer can associate with Qa-1.

Studies of Endogenous Processing and Presentation of Gut-Specific Class Ib MHC Qdm-like Peptides

The Qdm-like sequences of H2-Bl are embedded in the leader peptide encoded by exon 1. Thus, to be presented, the relevant Qdm-like peptide fragment needs to be excised and trimmed by cellular proteases and find its binding partner, Qa-1, in the ER. To address if this process occurs *in vivo*, we designed the following experiment. The strategy was to co-express Qa-1 with tissue-specific class Ib MHC genes (which do not appreciably associate with β_2m on the cell surface under the conditions of this assay [see

Chapter 6]) in a Qdm-deficient model cell line and ask if the presence of tissue-specific class Ib proteins coincides with expression of stable, β_2m-associated Qa-1 complexes on the cell surface.

B78H1 cells expressing Qa-1^b were co-transfected with TAP2 and H2-Bl^q or H2-Bl^{bc} expressed under the human elongation factor 2 promoter in a bicistronic cassette with the puromycin resistance gene, generating H2-Bl, Qa-1 and TAP2 positive cell lines. Transfectants of Q5.1, which encodes canonical Q5^k, Q5.2, which encodes the Q5^k α1α3 variant, Q10.1, which encodes the soluble isoform of Q10, and Q10.3, which encodes the Q10 α3 variant, all of which contain a peptide that is an exact match to Qdm, were also tested.

We found that cells co-expressing Qa-1, TAP and either of the H2-Bl alleles can endogenously process H2-Bl-derived leader peptides and present them on the cell surface via Qa-1 (Figure 5.5, right panes). As expected, the high affinity H2-Bl^q allele stabilizes cell surface Qa-1 better than its lower affinity H2-Bl^{bc} counterpart. Cells co-expressing Qa-1, TAP and Q5^k or Q5^k α1α3 can present Q5-derived leader peptides in the groove of Qa-1. This Qa-1/Qdm interaction is strikingly TAP-independent (Figure 5.5, left panels). Cells co-expressing Qa-1, TAP and Q10 or Q10 α3 initiated from the first ATG codon (and thereby encoding canonical Qdm) can also endogenously process and present Qdm via Qa-1 (Figure 5.5). Both canonical Q10 and the Q10 α3 variant can donate Qdm to Qa-1 despite having different leader/protein junctions. A Q10 α3 protein initiated from the second ATG codon and therefore lacking canonical Qdm does not produce a peptide capable of engaging Qa-1 above background in TAP$^+$ cells, thereby demonstrating the specificity of our assay. In the presence of TAP, an endogenous peptide derived from an

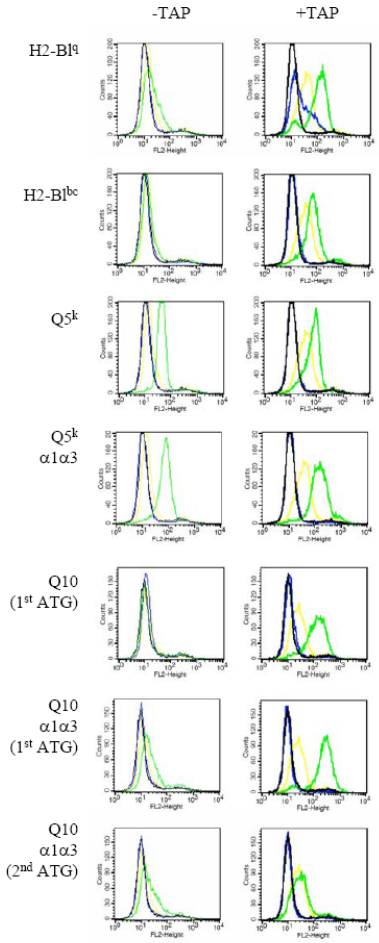
-TAP
+TAP
H2-Bl^{q}
H2-Bl^{bc}
Q5^{k}
Q5^{k} α1α3
Q10 (1st ATG)
Q10 α1α3 (1st ATG)
Q10 α1α3 (2nd ATG)

Figure 5.5 H2-Bl, Q5 and Q10-derived peptides can be endogenously processed and presented by Qa-1. The B78H1 melanoma and its Qa-1^+ transfectant (clone LS) were transfected with the indicated construct with or without co-transfected TAP2. Stable cell lines were treated 48 hours with 20 U/mL IFN-γ and analyzed for cell surface expression of β_2m-associated class I MHC by flow cytometry with anti-$\beta 2m^b$ antibodies. Black line – B78H1 transfected with the empty vector +/- TAP2; blue line – B78H1 transfected with the gene of interest +/- TAP2; yellow line – LS (Qa-1^+ B78H1) transfected with the empty vector +/- TAP2; green line – LS (Qa-1^+ B78H1) transfected with the gene of interest +/- TAP2. Data is representative of three separate experiments on the same cell lines.

unidentified native B78H1 protein associates with Qa-1, giving a background signal against which all test signals were compared (Figure 5.5, right panes, yellow lines).

Assays to Determine if Nonamers Derived from Gut-Specific Class Ib MHC Leader Sequences Can Mediate NK Cell Inhibition

Qdm mediates immunotolerance by associating with Qa-1 and engaging CD94/NKG2A inhibitory receptors on NK cells. To determine if Qdm-like leader peptides derived from gut-specific class Ib MHC can similarly regulate NK cell cytolysis, we performed LAK chromium release assays (see Materials and Methods) on TAP-negative, Qa-1 expressing B78H1 melanoma cells exogenously loaded with synthetic Qdm-like peptides. At saturating concentrations of peptide (see Figure 5.3), we found that the H2-Bl^q-derived nonamer peptide inhibited NK cell cytolysis. In two separate experiments this peptide inhibited killing to a greater extent than Qdm, though the effect was not statistically significant. These preliminary experiments should be repeated, and the study should be extended to include anti-NKG2A blocking assays to determine if any inhibitory effect is mediated through this receptor.

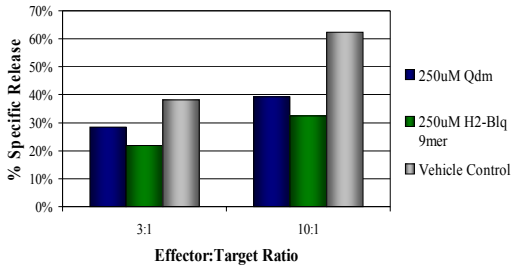

Figure 5.6 Qa-1 associated with the H2-Bl^q-derived Qdm-like nonamer mediates NK cell inhibition. The Qa-1$^+$ transfectant of the B78H1 melanoma (clone LS) was incubated overnight with 250µM of the indicated peptide in cDR10N + 3% DMSO or cDR10N + 3% DMSO alone (vehicle control). Peptide loaded cells were then used as targets in a ^{51}Cr release assay with day 6 aLAKs at the indicated effector to target ratios (see Materials and Methods). Results are representative of two separate experiments.

SUMMARY AND DISCUSSION

Ubiquitously expressed Qa-1 is a class Ib MHC receptor with a highly restricted peptide binding repertoire biased toward hydrophobic ligands (176, 361). In healthy hematopoietic H2^b cells, which express abundant class Ia MHC, Qa-1 associates with a single dominant peptide, termed Qdm (AMAPRTLLL), derived from the leader sequence of the H2-D^b precursor protein. This complex has been shown to serve as a ligand for inhibitory CD94/NKG2A heterodimers, expressed on NK cells, NKT cells and some αβ and γδ T cells (362). When CD94/NKG2A receptors are engaged, they attenuate cytotoxic activity of effector lymphocytes toward Qa-1/Qdm-expressing targets. In cells lacking Qdm, such as virally infected, malignantly transformed, genetically engineered cells or otherwise stressed cells, Qa-1 can bind other protein fragments, including endogenous heat shock protein hsp60 (GMKFDRGYI) (167) and other peptides with

sequences divergent from Qdm (179, 358). In addition, during some bacterial infections, Qa-1 can associate with prokaryotic orthologs of hsp60, termed GroEL (GMQFDRGYL) (167). Interestingly, neither hsp60 nor GroEL bound by Qa-1 in the absence of Qdm inhibits target lysis via CD94/NKG2A (363). Hence, it has been speculated that some peptides may regulate NK or T cell effectors via different sets of receptors and activate, rather than inhibit, immune cells during stress, infection or malignant transformation. Since not all murine haplotypes encode class Ia MHC with canonical Qdm, and many cells in the body express low levels of class Ia MHC (197), we wondered here if there are alternative Qa-1 ligands that may potentiate local tolerance and/or perhaps contribute to rejection of diseased cells in these situations.

We speculated that some members of the class Ib MHC family could contribute to these pathways, particularly in immune privileged organs, or in tissues in which local tolerance/activation is highly regulated and expression of class Ia MHC is limiting. This hypothesis has been put to the test in the current study. We have computationally identified several Qdm and Qdm-like sequences in the leaders of tissue-specific class Ib *Mhc* genes that are highly expressed in the gut (*H2-Bl*), liver (*Q10*) and brain (*Q5*). The experimental portion of this study focused mainly on H2-Bl, restricted to the epithelial cells of the intestine, since earlier work demonstrated that IEC express low levels of class Ia compared to hematopoietic cells (120) and therefore may be vulnerable to constitutively activated cytotoxic IEL that populate the epithelial layer of the gut.

Previous studies of Qa-1/peptide association relied primarily on biochemical assays employing bacterially synthesized soluble Qa-1 heavy chains that were refolded *in vitro*, in the presence of chemically modified, labeled Qdm peptides (172, 174-176). The

Qa-1 binding capacity was then evaluated by competition assays with unlabeled peptides. Furthermore, some assays included chimeric components, such as human β_2m (172, 176) or even the H2-D^b α3 domain substituted for the homologous α3 Qa-1 region in the class Ib heavy chain (173). While many of these assays allowed highly quantitative measurements of Qa-1 ligand binding, they were highly artificial, relying on "surrogate"-variant peptides, *in vitro* conditions for folding and ligand binding and interactions of non-physiological constituents of the class I MHC complex.

We have developed here a new, simple assay, which has similar sensitivity (~20-200 μM range) to the serologically based assay described in Cotterill et al (173), but includes only fully physiological components of the murine Qa-1 complex (Qa-1 displayed on the surface of live cells, stabilized by murine β_2m and unmodified synthetic peptides corresponding to the translated sequences of class Ib exon 1). Using this assay we have conclusively demonstrated that H2-Bl Qdm-like nonamers (AMAQRTLLL) from the H2^q haplotype associate with Qa-1 to a degree similar to that observed with canonical Qdm, while the H2-Bl$^{b/bc}$ variant nonamer (AMAQRTLFL) binds Qa-1 less efficiently under the conditions tested here. This observation was then confirmed by a sensitive CTL blocking assay (358), which also demonstrated that the octameric Qdm-related peptide (MAPRTLFL), translated from the second methionine of H2-Bl exon 1, (Figure 5.1B) as well as other class Ib leader peptides (from Q1, Q2 and Tw5) fail to bind Qa-1. The experimental binding properties of individual peptides tested here are in agreement with earlier mapping studies of anchor positions in Qa-1 ligands (173, 175, 176). Thus, the high affinity Qdm-like peptide from H2-Bl^q differs from canonical Qdm by a single residue at P4 ($Pro_4 \rightarrow Gln_4$) which can tolerate different substitutions without

drastically affecting Qa-1 binding (176). The H2-Bl$^{b/bc}$ peptide differs from Qdm by two substitutions ($Pro_4 \rightarrow Gln_4$ and $Leu_8 \rightarrow Phe_8$), neither of which individually affects Qa-1 binding, but together might contribute to lower affinity of this peptide for the Qa-1 groove. In contrast, the nonbinding peptides Q1, Q2 and Tw5 carry substitutions at residue positions that act as minor or major anchors (173, 175, 176). The nonbinding H2-Bl octamer peptide, which lacks the position 1 residue and in our assays was consistently deficient in Qa-1 association, was also predicted to have this property on the basis of earlier studies (174). The first residue of the Qdm nonamer, like N-terminal residues of most class I peptides, is required for strong, stabilizing contacts between the free amino ends of the peptide and the invariant sites of Qa-1 pocket A (178). This contact is thought to be one of the main stabilizing interactions for peptide-MHC complexes, because synthetic peptide analogs lacking terminal amino groups fail to bind stably to MHC class I molecules (364). Studies with truncated ligands of Qa-1/HLA-E are consistent with these assumptions (174), and the generally weak binding of Qa-1 to Qdm (172) further emphasizes the requirement for full-sized nonamer to stabilize the Qa-1 cleft.

Once bound by Qa-1, Qdm (and potentially Qdm-like peptides) traffic to the cell surface and engage CD94/NKG2A inhibitory receptors on NK cells and some activated T cells. Qdm is required for Qa-1 interaction with the CD94/NKG2A heterodimer. H2-Bl-derived Qdm-like peptides may play one of several roles in this CD94/NKG2A inhibitory pathway, acting as a Qdm surrogate in tolerance-associated tissues, blocking CD94/NKG2A mediated immune inhibition under circumstances of reduced Qdm

availability or increased H2-Bl expression or serving as a recognition element for activating members of the CD94/NKG2 family.

Operating as a Qdm surrogate, the H2-Bl-derived Qdm-like peptide would need to mimic Qdm well enough to successfully engage CD94/NKG2A. Alternatively, acting to block Qdm-mediated tolerance, the H2-Bl nonamer would have to lack Qdm features recognized by the inhibitory heterodimer. Both of these propositions hinge on the $Pro_4 \rightarrow Gln_4$ substitution in H2-Bl^q and possibly the conservative leucine to phenylalanine substitution at P8 in H2-$Bl^{b/bc}$. Lysine substitution at the P8 non-anchor position blocks CD94/NKG2A recognition (176). The crystal structure of human CD94/NKG2A in complex with HLA-E and a peptide derived from the HLA-G signal sequence showed CD94 interaction with P8, though it was poorly matched with the interface chemically and electrostatically (182). Thus a conservative substitution, like the one in H2-$Bl^{b/bc}$, might be tolerated by CD94. While the interaction surface of mouse CD94/NKG2A with Qa-1/Qdm might be quite different than that of its human counterpart, it is interesting to note that the P4 proline is not directly engaged by either CD94 or NKG2A (182). Human CD94/NKG2A can distinguish between subtle differences in peptide conformation, however (181), and a $Pro_4 \rightarrow Gln_4$ substitution would be expected to have conformational consequences distal to the site of the substitution.

The possibility remains that H2-Bl-derived Qdm-like peptides might engage activating, rather than inhibitory subunits of the CD94/NKG2 heterodimer. Most amino acid contacts between the HLA-E associated peptide and human CD94/NKG2A are mediated by CD94. The only exception is the P5 arginine, which protrudes into the cavity formed between CD94 and NKG2A. This has lead to the hypothesis that CD94 is

the major mediator of peptide specificity while the NKG2 subunit determines the outcome of receptor engagement (182). Indeed, the differences between NKG2A and NKG2C reside primarily in the region contacting CD94, not the peptide (181, 182). One difference in peptide association with NKG2A versus NKG2C, however, has been noted (146). A P5 substitution from arginine to lysine brings the affinity of CD94/NKG2C from six times less than to roughly equal that of CD94/NKG2A. This is quite notable given the extremely conservative P5 arginine to lysine substitution. Perhaps, then, a slight change peptide conformation as provided by the proline to glutamine substitution at P4 of the H2-Bl-derived peptide could impact recognition by activating members of the CD94/NKG2 receptor family.

While any of these possible H2-Bl/Qa-1-mediated CD94/NKG2 modes of interaction is formally possible, our preliminary data suggest that the H2-Bl-derived Qdm-like peptide serves as a Qdm surrogate. Indeed, in preliminary experiments performed at saturating peptide concentrations for both Qdm and the H2-Bl Qdm-like nonamer, the H2-Bl-derived peptide appears to protect target cells from lysis better than Qdm. Hence, while the H2-Bl Qdm-like nonamer has a lower affinity for Qa-1 than Qdm, in IEC, where D^b expression is low and H2-Bl transcription is high, the more highly protective H2-Bl peptide may be a major component of the Qa-1 peptide repertoire, perhaps potentiating Qa-1-mediated inhibition in the tolerance-dominated milieu. Similarly, D^b-derived Qdm may be augmented by TAP-independent Q5-derived Qdm in the brain, which is class I MHC^{low}, and by Q10 in the immunotolerance-dominated liver.

Our findings are of interest in view of the results published while the full sequence of H2-Bl exon 1 was still unknown, and our project was underway. The paper by Tajima et al (277) implicated the octamer H2-Bl peptide (assumed at the time to be the only translation product of exon 1) as a ligand for Qa-1 and inhibitor of NK-mediated lysis. Since this paper was published, we have demonstrated that H2-Bl encodes two in-frame ATG codons at its N-terminus, both of which may give rise to Qdm-like peptides. Only one of them, the nonamer, associates with Qa-1 in our assays. We have also demonstrated that the H2-Bl transcription start site is located upstream of the first ATG and, while the accompanying translational start site Kozak sequence is not canonical, it is similar to the translation start site preceding the first ATG of the leader peptide in Qdm-encoding H2-D^b exon 1 (see Figure 4.10). Though we cannot exclude the possibility that the octamer variant peptide associates with Qa-1 very weakly, we believe that the source of the discrepancy between the two studies may have resulted from nonphysiological conditions used for measuring association of Qdm-like peptide with Qa-1 and the use of a serological reagent which does not discriminate between peptide-bound and peptide-empty Qa-1.

In summary, we have observed that the H2-Bl^q nonamer binds to Qa-1 at concentrations similar to Qdm, but its polymorphic variants from H2-$Bl^{b/bc}$ mice have a lower affinity for the Qa-1 groove. This suggests that immune effects associated with the H2-Bl peptide/Qa-1 complex are likely to have variable phenotypes in different mice. The tissue-specific production of Qdm by Q5 and Q10 and Qdm-like peptides by H2-Bl may further diversify CD94/NKG2A-mediated inhibition in these tolerance-dominated

milieus.

CHAPTER SIX

Cell Surface and Endogenous Expression of Gut-Specific Class Ib MHC Isoforms in Transfected Cells

BACKGROUND AND RATIONALE

In the last chapter we investigated the potential of leader peptides derived from tissue-specific H2-Bl, Tw5, Q1, Q2, Q5 and Q10 proteins to bind Qa-1 and mediate NK cell inhibition as a first step in examining the ability of these MHC complexes to mediate immune responses through innate CD94/NKG2 receptors. Another mechanism by which tissue-restricted class Ib MHC have the potential to interface with the innate and/or adaptive immune system is through cell surface expression of canonical and alternatively spliced protein products engaging various receptors (TCRαβ, TCRγδ, NKG2D, Ly49, PIR, etc) on neighboring IEL. In addition to the alternatively spliced isoforms described for H2-Bl in Chapter Three, 3 other murine class Ib expressed in tolerance-dominated tissues – gut-restricted Q1, brain-expressed Q5 and liver-secreted Q10 – encode splicing variants (this thesis and unpublished data from the lab). Importantly, their protein products have not yet been characterized. In this study, we set out to determine if tissue-restricted class Ib MHC transcripts can produce cell surface proteins.

MHC class I and class I-related proteins serve as ligands for many innate and adaptive immune receptors. The dominant known function of the class I MHC family is to present endogenous peptide antigens to $CD8^+$ T cells. Central to the peptide loading process is the transporter associated with antigen processing (TAP), which shuttles

peptides produced in the cytosol into the ER where they are loaded into the groove of β_2m-associated class I MHC. Under inflammatory conditions that are accompanied by production of IFN-γ, various components of the antigen processing and presentation machinery, including TAP, β_2m and immunoproteasome subunits, are upregulated, thus increasing the pool of peptides available for class I MHC presentation and the overall level of class I expression on the cell surface for surveillance by $CD8^+$ T cells.

The major pathway of antigen processing and presentation by class Ia MHC and some ubiquitously expressed class Ib MHC is well understood, but many other class Ib and class I-related MHC have unique mechanisms of antigen association and intracellular trafficking. For example, the only known γδTCR ligand, T22, does not bind peptides and is TAP-independent, but is inducible by IFN-γ. Gut-specific TL, like T22, has a modified peptide binding groove that does not bind peptides and is also displayed on the cell surface in a TAP-independent manner (365). A chimeric Q10 molecule expressing the α1 and α2 domains of Q10 and the α3 and GPI-anchoring domains of Q9 is only partially TAP dependent, though it binds a diverse peptide repertoire (252). CD1d, a class I-related antigen encoded outside of the *Mhc* that is known to restrict iNKT cells, bypasses TAP-dependent antigen processing and enters an endosomal loading pathway to bind glycolipid antigens (366). Aside from Q10 and TL, little is known about the assembly, peptide binding and cell surface expression of tissue-specific class Ib MHC. All previously analyzed class Ib MHC are thought to be β_2m-bound, though some human class I-like molecules, like gut-expressed NKG2D ligands MICA and MICB, are not (367).

In this section we analyzed the expression of multiple, organ-specific class Ib MHC in a model B78H1 melanoma. Specifically, we sought to determine if assembly of canonical, tissue-specific class Ib MHC proteins requires β_2m and TAP-facilitated access to cytoplasmic peptides in a manner similar to classical class I MHC. We also studied if proteins translated from alternatively spliced transcripts are cell surface expressed and therefore accessible to the receptors of immune effector cells. The results of our studies demonstrate that many of the alternatively spliced class Ib studied here are indeed cell surface-expressed. Some of the canonical, gut-specific class Ib transcripts encode surface attached heavy chains associated with endogenous murine β_2m and require TAP for their surface display suggesting that they fold into class Ia-like, peptide loaded trimers.

RESULTS

Tissue-Restricted Class Ib MHC Encode Multiple Alternatively Spliced Isoforms that Are Predicted to Produce Structurally Unique Proteins

In the following paragraphs we will summarize the structural composition of transcripts and proteins generated via alternative splicing from gut-restricted class Ib MHC as well as other class Ib isoforms (Q5 and Q10) expressed in tissues with special immune tolerance status (brain and liver). The structural characteristics of these class Ib MHC variants are presented in Figure 6.1A (transcripts depicted alongside those of placenta-restricted HLA-G) and Figure 6.1B (predicted proteins and their interactions with β_2m and peptides).

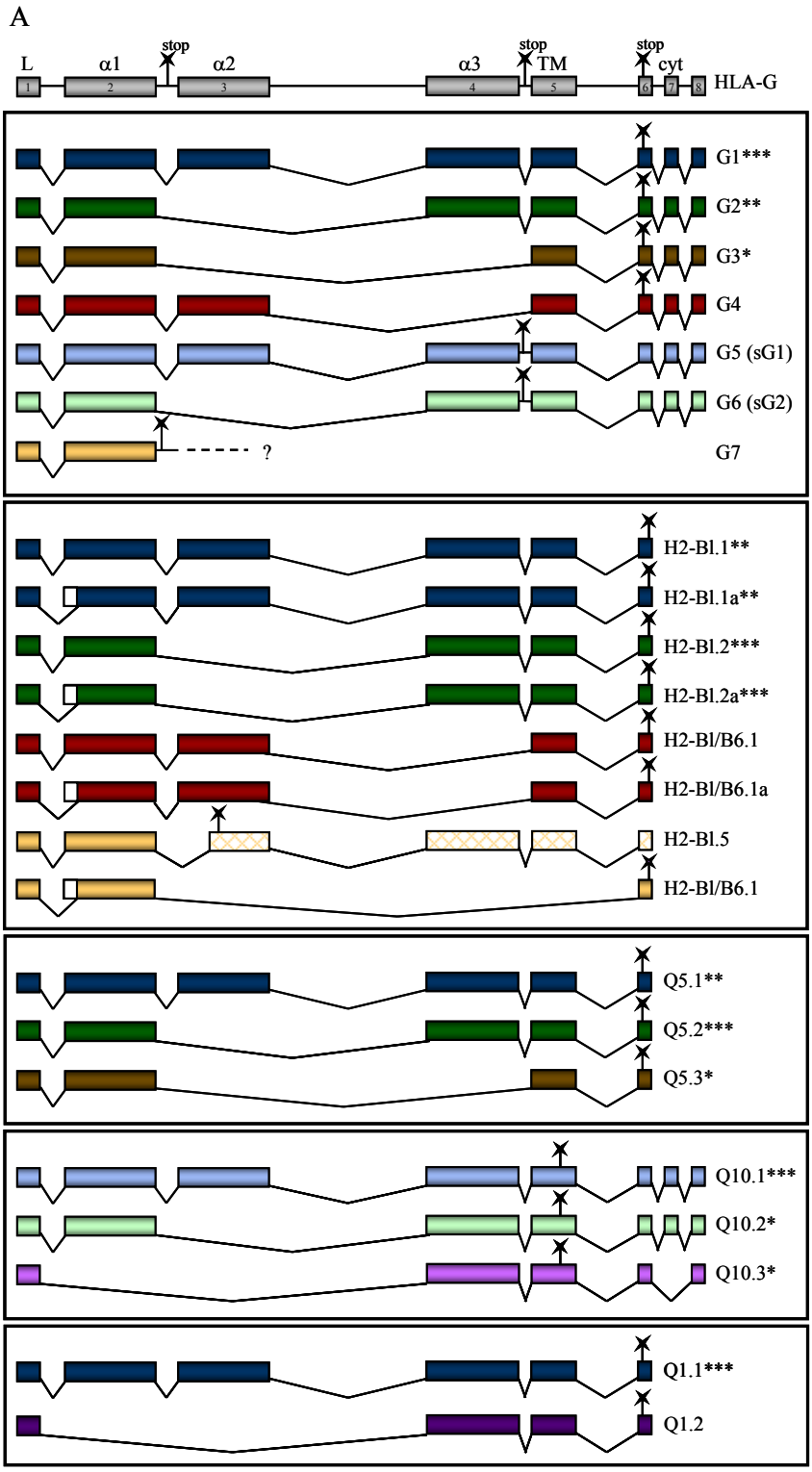
A
L
α1
stop
α2
α3
stop
TM
stop
cyt
HLA-G
1
2
3
4
5
6
7
8
G1***
G2**
G3*
G4
G5 (sG1)
G6 (sG2)
?
G7
H2-Bl.1**
H2-Bl.1a**
H2-Bl.2***
H2-Bl.2a***
H2-Bl/B6.1
H2-Bl/B6.1a
H2-Bl.5
H2-Bl/B6.1
Q5.1**
Q5.2***
Q5.3*
Q10.1***
Q10.2*
Q10.3*
Q1.1***
Q1.2

B

Transcript Name	Protein Name	Predicted Product(s)	Transcript Name	Protein Name	Predicted Product(s)
H2-Bl.1	H2-Bl	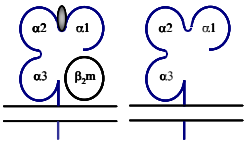	Tw5	Tw5	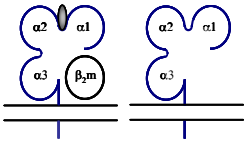
H2-Bl.1a	H2-Bl'	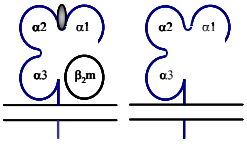	T3	T3	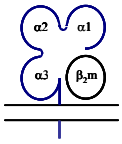
H2-Bl.2	H2-Bl α1α3	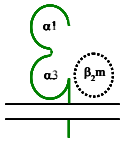	Q5.1	Q5	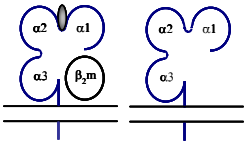
H2-Bl.2a	H2-Bl α1α3'	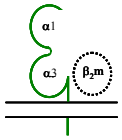			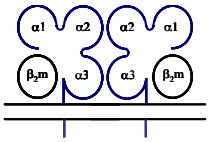
H2-Bl/ B6.1	H2-Bl α1α2	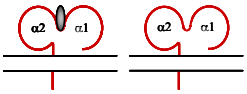	Q5.2	Q5 α1α3	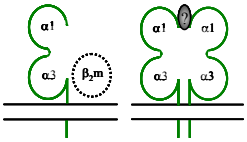
H2-Bl/ B6.1a	H2-Bl α1α2'	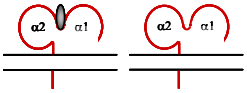	Q5.3	Q5 α1	
Q1.1	Q1	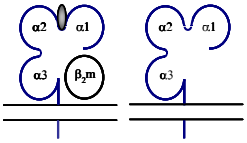	Q10.1	Q10	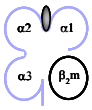
Q1.2	Q1 α3	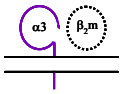	Q10.2	Q10 α1α3	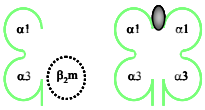
Q2	Q2	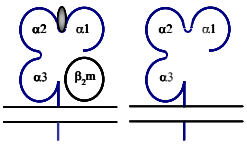	Q10.3	Q10 α3	

Figure 6.1 Tissue-restricted class Ib *Mhc* encode multiple alternatively spliced isoforms. A. Observed isoforms of tissue-restricted class Ib MHC in the mouse as compared to human HLA-G. cDNA from mouse small intestine, liver and brain were assayed for their expression of H2-Bl, Q1, Q2, Tw5, Q10 and Q5 canonical and alternatively spliced transcripts by RT-PCR with primers specific for the 5'UTR and 3'UTR of each gene. PCR products were resolved on an agarose gel, cloned and sequenced. Results are depicted beneath a map of the HLA-G gene and its corresponding alternatively spliced isoforms. Exons are indicated by boxes, introns by lines in between boxes. Most abundant isoform (***); abundant, but not as prevalent as the major isoform (**); detectable on most agarose gels (*); transcribed, but not prevalent (no demarcation). Abundances of H2-Bl are for the $H2^{bc}$ haplotype. Other haplotypes have different abundances, as discussed in Chapter Three. Blue – similar to HLA-G1 (canonical); green – similar to HLA-G2 (missing exon 3); brown – similar to HLA-G3 (missing exons 3 and 4); red – similar to HLA-G4 (missing exon 4); purple – specific to Q1 and Q10; light shades of all colors – soluble form of the respective isoform. Of the minor H2-Bl isoforms, only those that resemble HLA-G transcripts are shown. HLA-G isoforms have been described previously and are depicted here for the purpose of comparison. B. Putative protein products of tissue-restricted class Ib MHC transcripts in the mouse. "'", as in H2-Bl', indicates that the predicted protein lacks the first 11 aa of the α1 domain. Dotted lines in the diagram indicate that the molecule may or may not associate with β_2m. The presence of two predicted protein products for an isoform indicates that both architectures can be envisioned, not necessarily that both exist. Other structures for each isoform are possible, but are not typical of class I and class I-like proteins are therefore not shown.

As reported in Chapter Three, H2-Bl genes from different haplotypes encode several isoforms similar to HLA-G variants, depicted for comparison at the top of Figure 6.1A. The two largest H2-Bl isoforms are the canonically spliced message, H2-Bl.1, and its truncated form, H2-Bl.1a, which differ at the 5' ends of exon 2 by 33 nt (11 aa). Both are predicted to fold into class Ia-like, peptide-binding proteins interacting with β_2m (Chapter Three and Figure 6.1B). The isoform missing exon 3 (H2-Bl.2 and .2a, similar to HLA-G2/G6 transcripts of *HLA-G*) lack the peptide binding groove due to the absence of the α2 domain, and are predicted to be either β_2m-associated or β_2m-free. The H2-Bl/B6.1/.1a transcripts, which lack exon 4 and encode Rae-1-like isoforms (similar to HLA-G4), encode the N-terminal peptide binding domains without α3, and are predicted

to be β_2m-independent. Finally, H2-Bl.5 and H2-Bl/B6.1, similar to G7 of *HLA-G*, encode only the first α1 domain or its N-terminally truncated version and lack peptide binding, β_2m-associating and transmembrane regions. Homologs of the remaining HLA-G-like isoforms (HLA-G3, -G5 or -G6) were not detected among H2-Bl transcripts.

Brain-expressed $Q5^k$ encodes three alternatively isoforms (identified by Sharmila Shanmuganad and Nora Renthal of our laboratory) – Q5.1 (canonical), Q5.2 (lacking α2 and thus devoid of the peptide binding groove but not β_2m-interacting α3) and Q5.3 (containing only the α1 domain), all of which bear similarities to the dominantly expressed HLA-G transcripts HLA-G1, HLA-G2 and HLA-G3, respectively. Liver-restricted Q10 encodes soluble proteins produced by the transcripts Q10.1 (canonical), Q10.2 (similar in external domains to HLA-G2, H2-Bl.2 and Q5.2) and Q10.3 (corresponding to the α3 domain without the N-terminal α1α2) (unpublished observations by Dr. Ming Chen of our laboratory). Due to a stop codon in Q10 exon 5, the protein product of dominantly expressed soluble Q10.1 resembles that of HLA-G5 (soluble G1), while that of the less abundant Q10.2 resembles protein products of HLA-G6 (soluble G2). The soluble α3-encoding Q10.3 isoform has no known homolog among the alternatively spliced transcripts of HLA-G, and is related instead to a membrane bound variant of small intestine-restricted Q1 (Q1.2). Both of these "free" α3 domains preserve major β_2m binding sites (368). While an HLA-G2-like isoform of Q1 was reported in cDNA from a hepatoma cell line (369), the low abundance Q1.2 isoform is the only alternatively spliced message we detected for this gene in normal intestine.

To study if the multiple alternatively spliced transcripts of tissue-specific class Ib MHC in the mouse are expressed at the protein level, we cloned the various isoforms of

gut-restricted H2-Bl, Tw5, Q1, and Q2, liver-specific Q10 and brain-expressed Q5 and placed them under strong mammalian promoters for transfection studies. Q10 and its alternatively spliced isoforms were cloned in our laboratory by Dr. Ming Chen, and Q5 isoforms were prepared in our laboratory by Sharmila Shanmuganad and Nora Renthal.

N-terminally FLAG-tagged Class Ib MHC Can Be Ectopically Expressed in a Model Melanoma

A primary difficulty in studying novel class Ib MHC proteins is the lack of antibodies specific to individual class Ib molecules. In order to investigate the expression profiles of tissue-restricted class Ib MHC proteins we inserted a FLAG epitope tag coding region between exons 1 and 2 (between the leader peptide and N-terminal α1 domain) of the class I cDNA using a strategy first reported in Fulton et al (266) (see Materials and Methods, Figure 2.1). The FLAG-containing class Ib MHC constructs were placed downstream from the strong CMV promoter. Selected hybrid genes encoding FLAG-tagged H2-Bl canonical, H2-Bl α1α3, H2-Bl α1α2, Tw5 and Q2 were transfected into a model B78H1 melanoma, and expression of FLAG-tagged class Ib MHC was evaluated in whole cell lysates by Western blot (Figure 6.2). All FLAG-tagged class Ib MHC proteins migrated in the denaturing agarose gels according to their predicted molecular weight as calculated from their primary amino acid sequence and the number of putative N-linked glycans. In several cases multiple products (bands) were observed, suggesting that differentially glycosylated isoforms (corresponding to distinct steps of protein maturation) were simultaneously present in the transfected cells. The

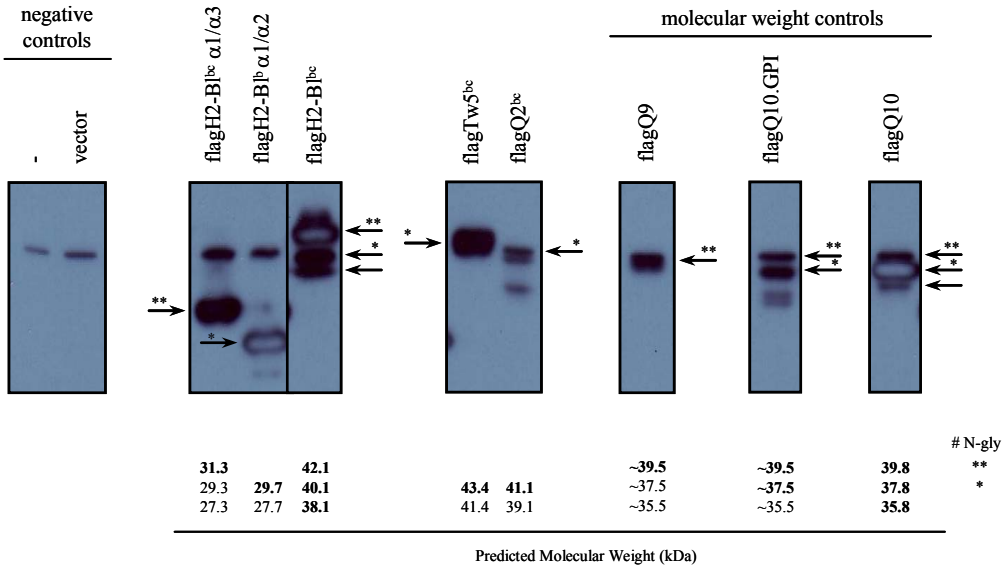

Figure 6.2 N-terminally FLAG-tagged tissue-restricted class Ib MHC encode proteins with predicted glycosylation patterns. TAP-positive B78H1 melanoma cells were transfected with the indicated construct (fConstruct = N-terminally FLAG-tagged construct) under the strong CMV promoter. Whole cell lysates were assayed for expression of FLAG-tagged proteins by Western blot using an anti-flag monoclonal antibody (see Materials and Methods). Q9, Q10 and Q10.GPI encode glycosylated and unglycosylated proteins with known molecular weights and were used to generate a standard curve. This information, along with the predicted molecular weights and glycosylation sites of the protein sequences under study, was used to identify the glycosylation status of class Ib MHC isoforms. Predicted molecular weights for glycosylated and unglycosylated proteins (including the FLAG epitope tag) appear at bottom. Weights in bold font are those observed in this analysis. One N-linked glycan is approximately 2 kDa. The number of N-linked glycans in the observed isoform is denoted by asterisks.

results of this experiment demonstrate that canonical and alternatively spliced isoforms of H2-Bl, Tw5 and Q2 are translated into glycosylated proteins in melanoma cells, and that the FLAG-epitope tag remains associated with the maturing class Ib heavy chain after the leader peptide is co-translationally cleaved.

TAP-Dependence, IFN-γ Inducibility and β_2m Association of Canonically Spliced Gut-Restricted Class Ib MHC

Since the formation of a cell surface expressed class I MHC trimer, consisting of a heavy chain, β_2m and peptide, is a prerequisite for antigen presentation and TCR recognition for all class Ia and some class Ib MHC proteins, we asked if the canonical isoforms of gut-specific class Ib MHC can also fold into similar complexes on the cell surface. To address this question we expressed FLAG-tagged class Ib MHC constructs in our model melanoma cell line, B78H1, in the presence and in the absence of the TAP gene (which regulates access of cytoplasmic peptides to the ER, where class I heavy chains associate with β_2m and form trimers). As mentioned before, this tumor cell line constitutively expresses the soluble β_2m light chain, but is devoid of all known class I transcripts and lacks surface expression of endogenous class Ia/b proteins and surface-associated β_2m. Expression of several components of the class I antigen presentation pathway (including β_2m) is low in B78H1 but can be upregulated by incubation with IFN-γ (359). All the canonical constructs (H2-Bl, Tw5, Q1, Q2, T3-like, soluble Q10, membrane-attached Q10.GPI, Q5 and control class Ia H2-D^b) were assayed after transient or stable transfection, or both, by staining cells with anti-FLAG antibody and/or with anti-β_2m^b antibody (specific for the endogenous murine β_2m^b allele) (Figure 6.3). All β_2m detection data performed with FLAG-tagged and native class Ib MHC were identical, suggesting that the N-terminal FLAG epitope does not interfere with β_2m association.

As evidenced by cell surface expression of the FLAG epitope tag, the heavy chain of H2-Bl^{bc} comes to the cell surface as two populations: TAP-dependent and TAP-independent (Figure 6.3A). Only the TAP-dependent fraction is upregulated by IFN-γ and accompanied by detectable association with β_2m^b. We interpret this result as indicating that unidentified IFN-γ-inducible factors are required to transport/assemble conventionally folded peptide-loaded H2-Bl. Identical results were observed for H2-Bl^q (data not shown). Tw5, the putative H2-Bl paralog, is similarly expressed at the cell surface with TAP-independent and TAP-dependent, IFN-γ-inducible fractions. Variable, but reliable Tw5/β_2m association can be observed in TAP$^+$, IFN-γ treated cells (Figure 6.3B). Taken together, these data suggest that cell surface expression of conformationally stable H2-Bl and Tw5 requires association with a TAP-dependent peptide, but a TAP-independent component of expression provides a steady-state pool of H2-Bl and Tw5 heavy chains at the cell surface which may or may not be associated with β_2m.

In contrast, a constitutively high level of Q2 was observed with the conformation independent anti-FLAG antibody. There was little increase in the expression of the FLAG-tagged Q2 protein in the presence of TAP and IFN-γ (Figure 6.3C). β_2m-associated Q2, on the other hand, showed a distinct TAP-dependence and IFN-γ-inducibility. Thus, conformation-independent (β_2m-free) Q2 cell surface expression seems to be TAP-independent, but TAP-dependent peptide(s) allow for the conformationally stable, β_2m-associated form of Q2 to be expressed at the cell surface in an IFN-γ-inducible manner. This phenotype is reminiscent of Qa-1 properties described in Chapter Five.

A

H2-Bl^{bc}

Transient Transfection

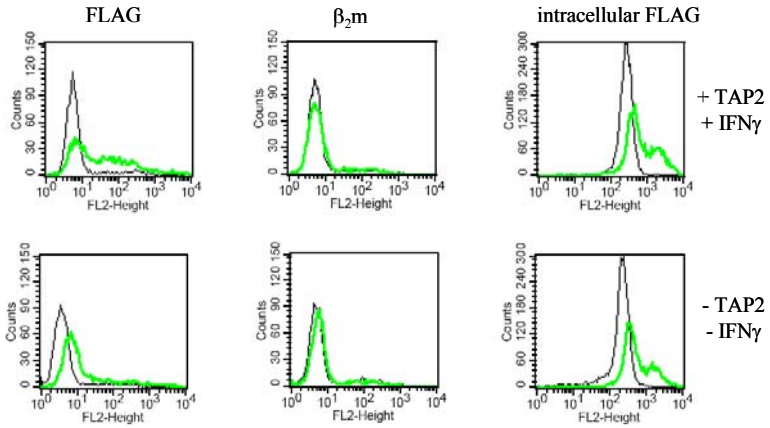

Stable Transfection

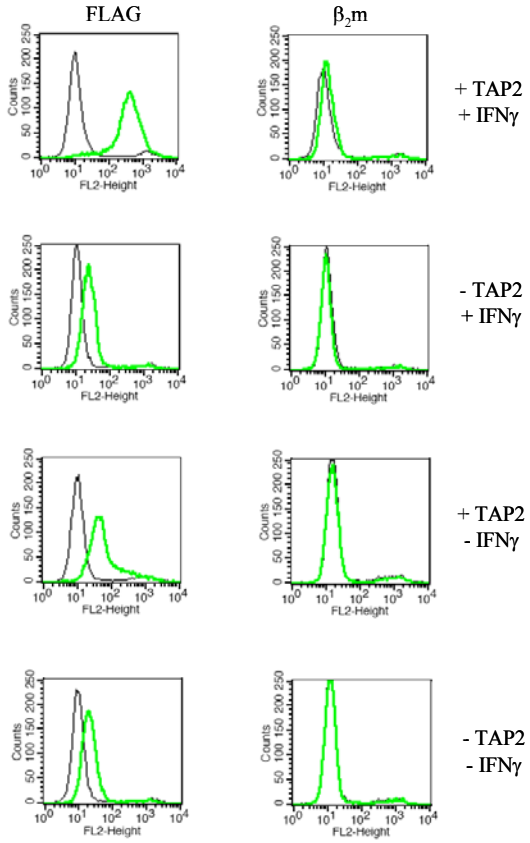

C

Q2^{bc}

Transient Transfection

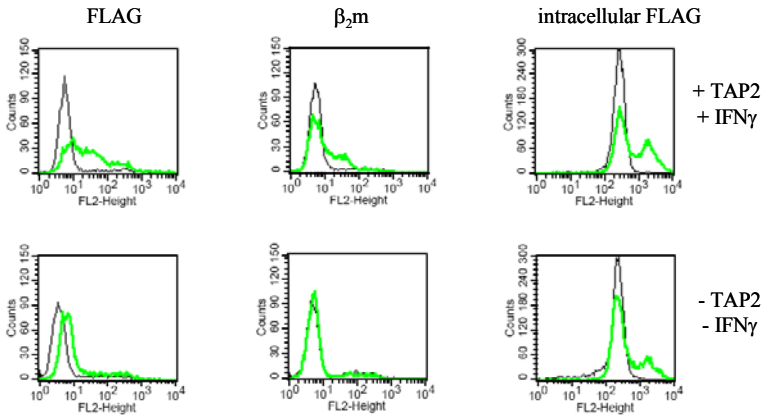

Stable Transfection

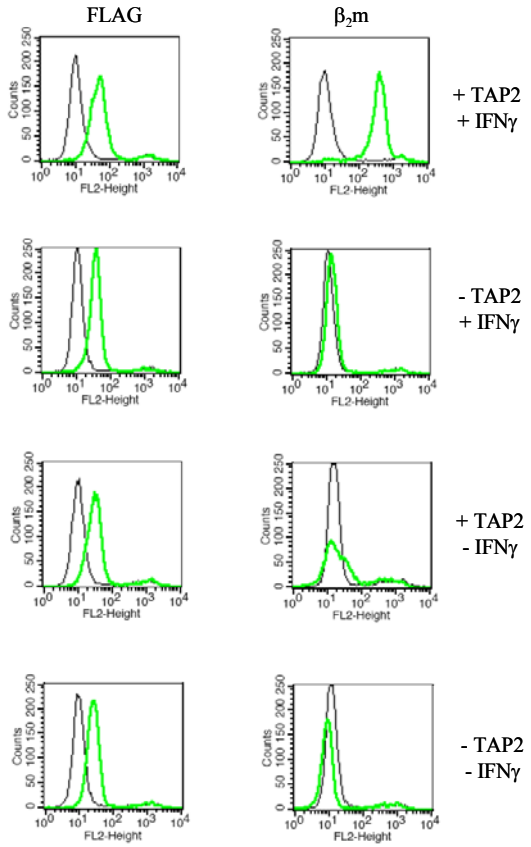

C

Q2^{bc}

Transient Transfection

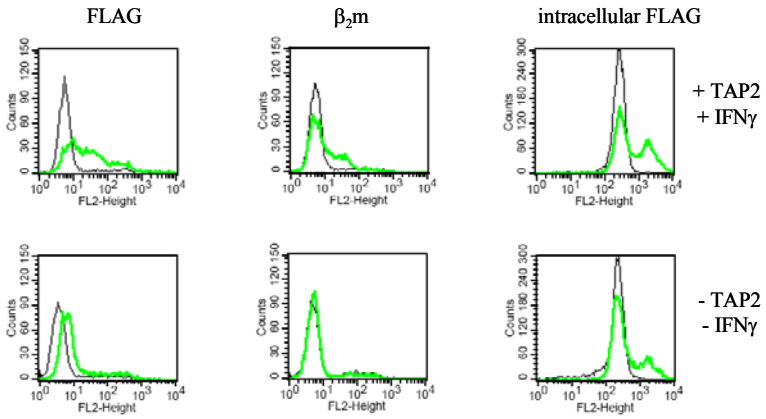

Stable Transfection

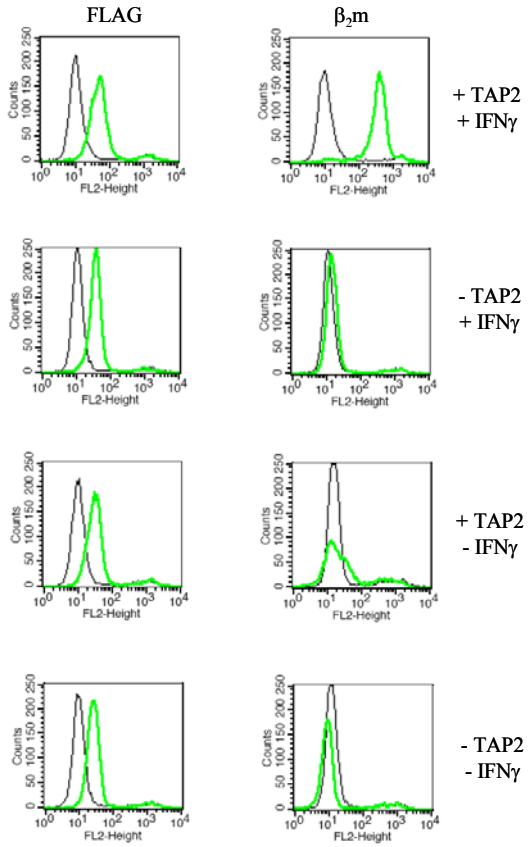

D

Q1^{bc}

Transient Transfection

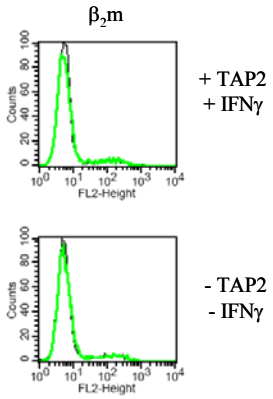

Stable Transfection

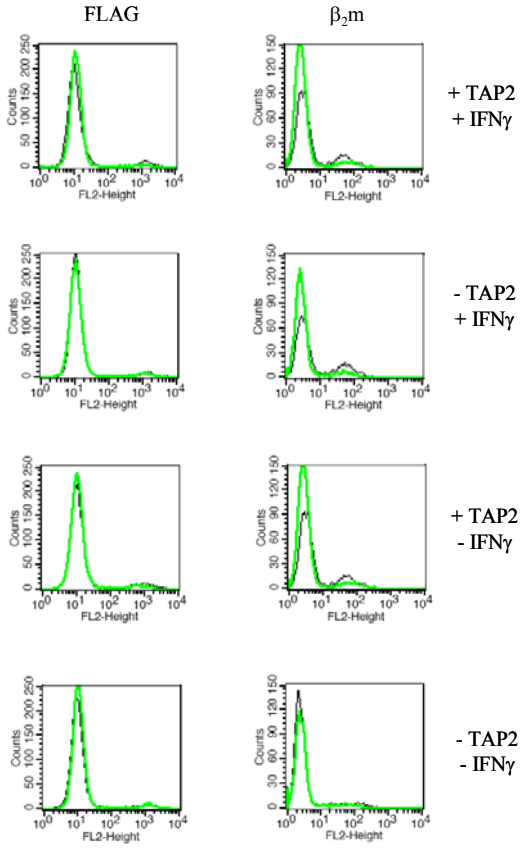

E

T3^{bc}

Transient Transfection

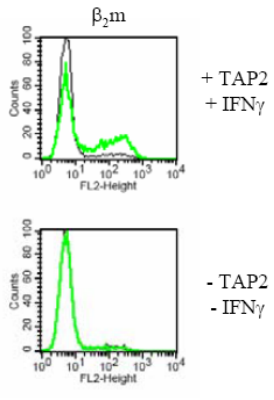

Stable Transfection

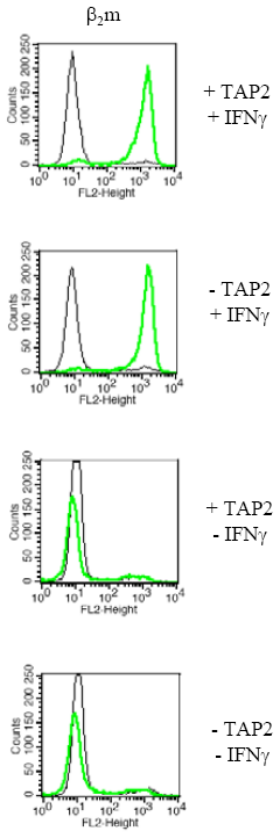

F

Q10

Stable Transfection

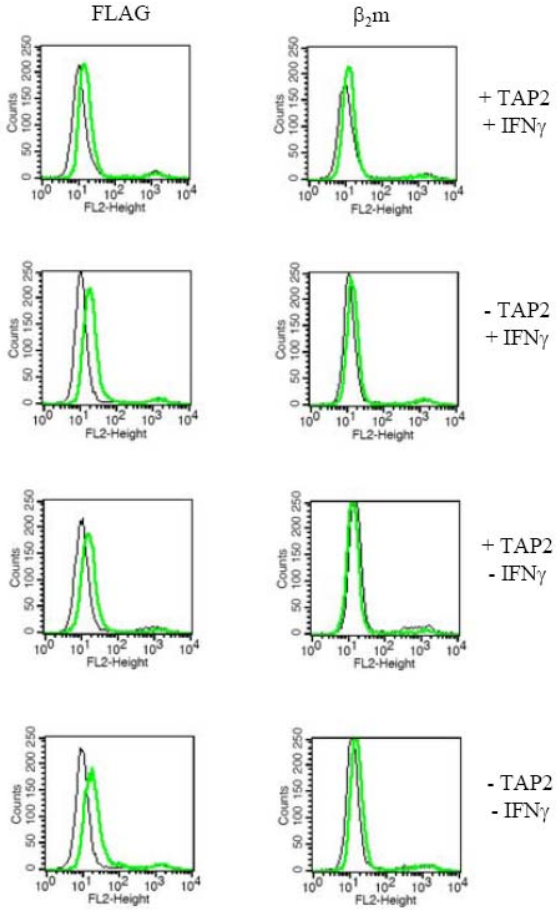

G

Q10.GPI

Transient Transfection

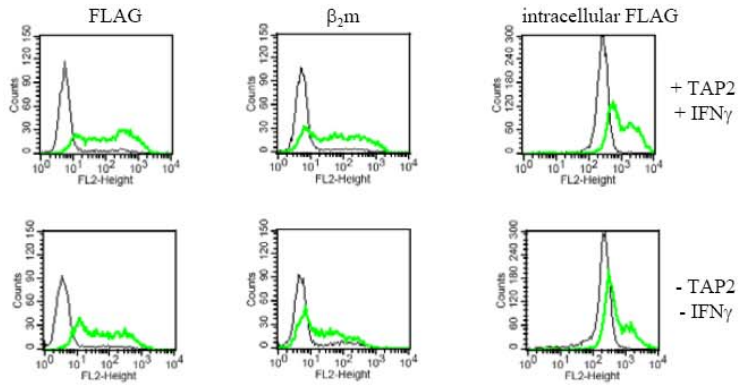

Q10.GPI

Stable Transfection

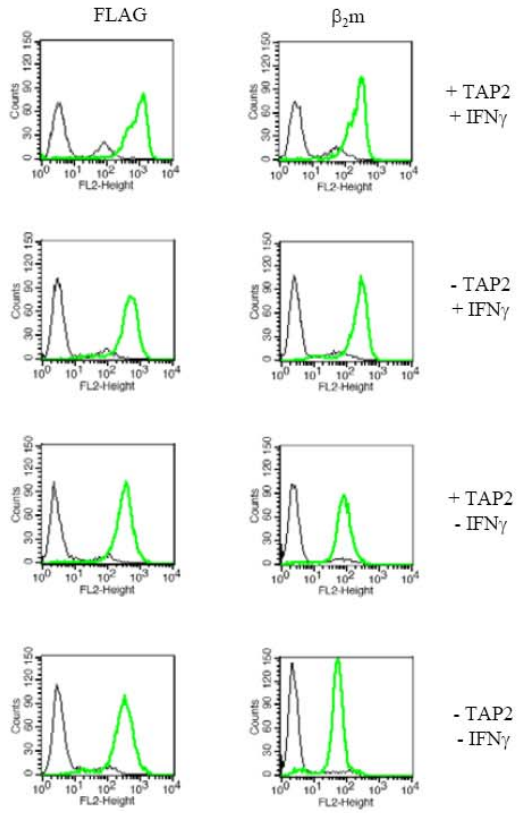

H

$Q5^k$

Stable Transfection

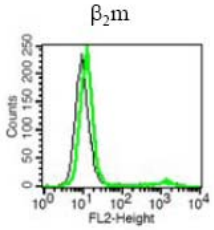

+ TAP2
+ IFNγ

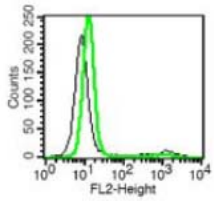

- TAP2
+ IFNγ

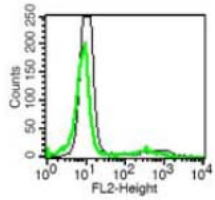

+ TAP2
- IFNγ

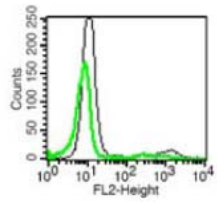

- TAP2
- IFNγ

I

D^{bc}

Stable Transfection

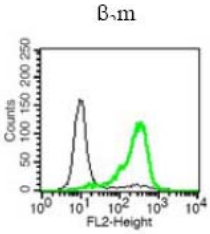

+ TAP2
+ IFNγ

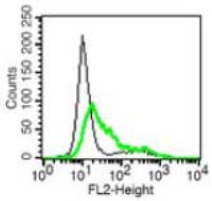

- TAP2
+ IFNγ

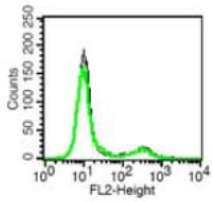

+ TAP2
- IFNγ

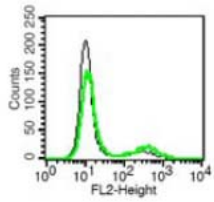

- TAP2
- IFNγ

Figure 6.3 Cell surface expression, β_2m association and IFN-γ induction of canonically spliced, tissue-restricted class Ib MHC. TAP-negative and TAP-positive B78H1 melanoma cells were transfected with the indicated FLAG-tagged construct and assayed for expression of FLAG-tagged and/or β_2m-associated proteins by flow cytometry using polyclonal antibodies against the FLAG epitope or a conformation-dependent anti-mouse β_2m^b antibody. Detection of intracellular FLAG-tagged proteins was performed by first fixing and permeabilizing the cells, then incubating with anti-FLAG antibody. Transient transfections were performed with constructs under the strong CMV promoter (pcDNA3.1N vector) and analyzed 48 hours post-transfection; stable transfectants were generated with constructs under the human EF2α promoter (pEFIRES-P vector) and selected for puromycin resistance for at least 6 weeks before analysis. IFN-γ was applied 24 hours before analysis for transient transfectants and 48 hours before analysis for stable transfectants. Thin black lines represent cells transfected with the empty vector; thick green lines correspond to cells transfected with the indicated construct. To ensure transfection occurred in the transient expression studies, intracellular FLAG was detected by fixing and permeabilizing the cells prior to antibody binding (Transient Transfection, far right panes; see Materials and Methods). Positive expression in the stable transfectants was ensured by expressing the construct 5' to the IRES for the puromycin resistance gene, analyzing multiple clones in each line and repeating the transfection at least once. In all cases, cells expressing the native protein associated with β_2m in the same manner as those expressing the FLAG-tagged construct (data not shown). A. H2-Bl^{bc}. B. Tw5^{bc}. C. Q2^{bc}. D. Q1^{bc}. E. T3^{bc}. F. Q10^{b}. G. Q10.GPI. H. Q5^{k}. I. D^{bc}. Control for TAP-dependence.

Unlike H2-Bl, Tw5 and Q2, Q1 was not detectable in B78H1 transfectants with either anti-FLAG or anti-β_2m^b antibodies (Figure 6.3D). Because lysates of FLAG-Q1 transfected cells were not analyzed by Western, we cannot determine if this is because Q1 is an intracellular protein, or because the N-terminal FLAG epitope tag was cleaved off of the mature protein. Neither the native nor the FLAG-tagged Q1 protein was detectable in association with β_2m in stable transfections.

TL, the product of *H2-T3-like*^{bc} (most similar to *T18* in predicted primary amino acid sequence of the two genes known to encode TL [*T3* and *T18*]; see Chapter Three), was expressed on the cell surface in a TAP-independent manner (Figure 6.3E). This is in agreement with previous reports of TL antigen expression in the absence of TAP (117,

370, 371). In our model melanoma, IFN-γ was required for detectable cell surface expression, because we have monitored it indirectly via its association with β_2m^b. Thus, one or more IFN-γ-inducible chaperone(s), increased β_2m concentration or another IFN-γ-dependent factor involved in TL assembly and transport may be needed to observe the TL heterodimer in this cell line under the conditions of our β_2m-dependent assay. A similar requirement was noted for the H2-D^b control (see below).

Unsurprisingly, wild-type, liver-restricted, soluble Q10 was not expressed appreciably at the cell surface of our transfected model melanoma (Figure 6.3F). Q10 has a truncated transmembrane domain (247, 372), which may allow for the residual membrane attachment detectable in our assay. In a parallel experiment, a chimeric molecule containing the α1, α2 and α3 domains of Q10 and the GPI-membrane anchoring domain of Q9 (Q10.GPI, constructed by Dr. Ming Chen of our laboratory) was expressed very highly at the cell surface (Figure 6.3G). (Q9 is a TAP-dependent class Ib MHC that has been previously expressed in the B78H1 melanoma (256).) The chimeric Q10.GPI is partially TAP-independent, suggesting that soluble Q10 may also be less dependent upon TAP for its expression. This is in agreement with published results obtained previously with a transfected Q10 chimera expressing the α1 and α2 domains of Q10 and the α3 and GPI-anchoring domains of Q9 (252). Q10.GPI is also upregulated by IFN-γ, suggesting that inducible components of the class I antigen processing and presentation machinery influence its assembly in melanoma cells.

$Q5^k$, which is highly transcribed in the brain, was not detectable in association with β_2m at the cell surface under the constitutive EF2α promoter (Figure 6.3H). Unfortunately, a FLAG-tagged variant of Q5 was not available for study due to technical

difficulties in its production, so it is unclear if the Q5 heavy chain is indeed retained intracellularly or reaches the cell surface but dissociates there from endogenous β_2m. Alternatively, it may be transported to the cell surface without β_2m, like MICA (367).

As expected, the class Ia control, H2-D^b, was expressed in the B78H1 melanoma in a TAP-dependent manner in the presence of IFN-γ (Figure 6.3I). Like TL, D^b requires IFN-γ for its detection in the B78H1 melanoma. This is likely reflective of weak β_2m^b association with H2-D^b (373) and/or possibly a requirement for limiting components of the class I MHC assembly machinery.

In summary, H2-Bl and Tw5 can be expressed at the cell surface in a TAP-dependent, IFN-γ inducible manner, though TAP-independent expression is also detectable. Q2 heavy chain expression is largely TAP-independent, though its stable association with β_2m appears to be both TAP and IFN-γ dependent. The *T3-like* gene from the $H2^{bc}$ haplotype is expressed in a manner similar to other TL-encoding class Ib *Mhc* (118). A chimeric, cell surface expressed variant of Q10 is largely TAP-independent but IFN-γ-inducible, suggesting that soluble Q10 may also require components of the antigen processing and presentation machinery. Q1 and Q5 are not detectably β_2m-associated at the cell surface in the B78H1 model melanoma, but whether they are retained intracellularly or cell surface expressed in an at least partially β_2m-free state in this cell line remains unclear.

Cell Surface Expression of Alternatively Spliced Isoforms of Tissue-Restricted Class Ib MHC in Transfected Cells

In addition to the canonically spliced message, several tissue-specific class Ib MHC express alternatively spliced mRNA variants that may produce structurally unique proteins capable of engaging NK cell receptors on NK cells or T cells. It is unknown, however, whether these transcriptional isoforms can produce cell surface associated proteins. We therefore expressed FLAG-tagged class Ib encoding alternatively spliced proteins in our TAP-negative or TAP-transfected melanoma cell lines. Then, as before, we subjected these cells to IFN-γ treatment and assayed for cell surface expression of FLAG and/or β_2m^b by flow cytometry.

Contrary to a previously published report (277), we found that the H2-Bl α1α3 variant, the transcriptionally abundant H2-Bl isoform in the C3H/HeJ and 129/SvJ mouse, is expressed on the cell surface in a TAP- and β_2m-independent manner, as demonstrated by the results of transient transfection and by analysis of stable transfectants (Figure 6.4A). The H2-Bl α1α3' protein, which lacks the first 11 aa of the α1 domain, is similarly expressed in our model melanoma (Figure 6.4B). Structurally related to H2-Bl α1α3, the Q5 α1α3 protein is also cell surface expressed in the absence of TAP and β_2m, but is expressed at a higher level than the H2-Bl variant, at least as judged by the co-expressed FLAG-tag (Figure 6.4C). Similar results were found for the Q5 α1 protein variant (data not shown) and the Q1 α3 variant (Figure 6.4D). Residual β_2m^b association was observed with H2-Bl α1α3, Q5 α1α3 and Q1 α3 isoforms in cells treated with IFN-γ, where the concentration of endogenous β_2m was enhanced. The validity of this effect has not been independently confirmed. Of the alternatively spliced isoforms examined, only the H2-Bl^b α1α2 isoform was not reproducibly detected at the

A

H2-Bl^{bc} $\alpha1\alpha3$

Transient Transfection

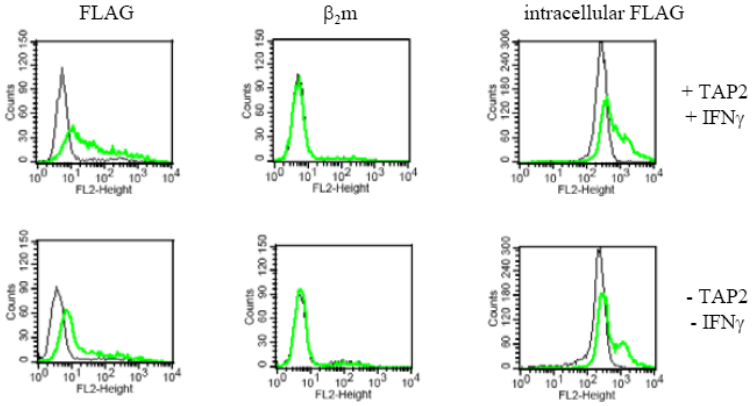

Stable Transfection

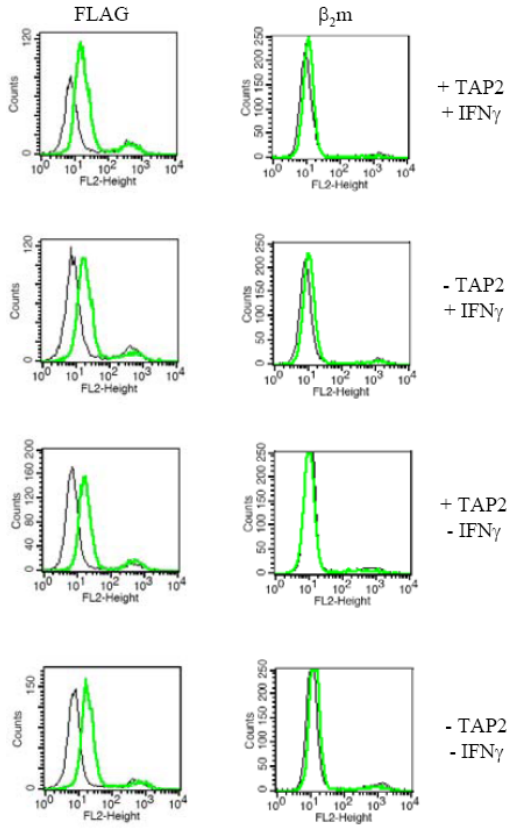

B

H2-Bl^{bc} $\alpha1\alpha3'$

Stable Transfection

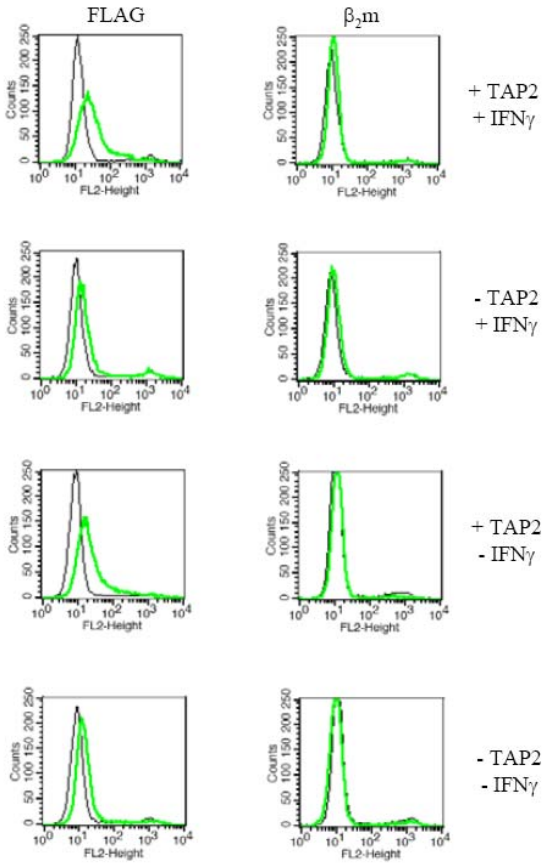

C

$Q5^k$ α1α3

Stable Transfection

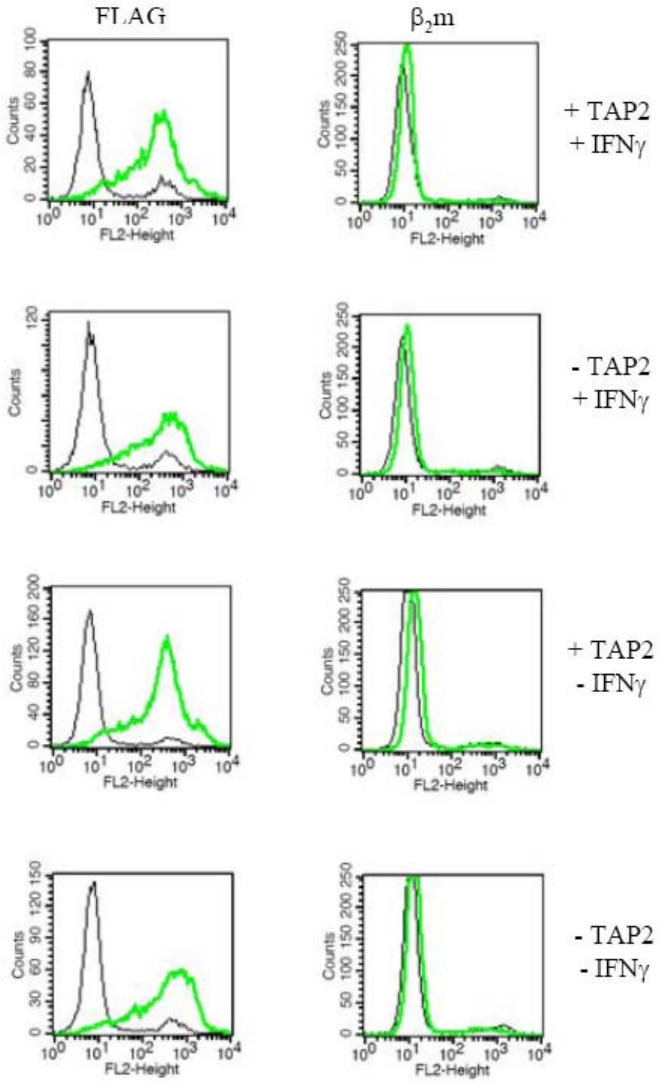

D

Q1^{bc} α3

Stable Transfection

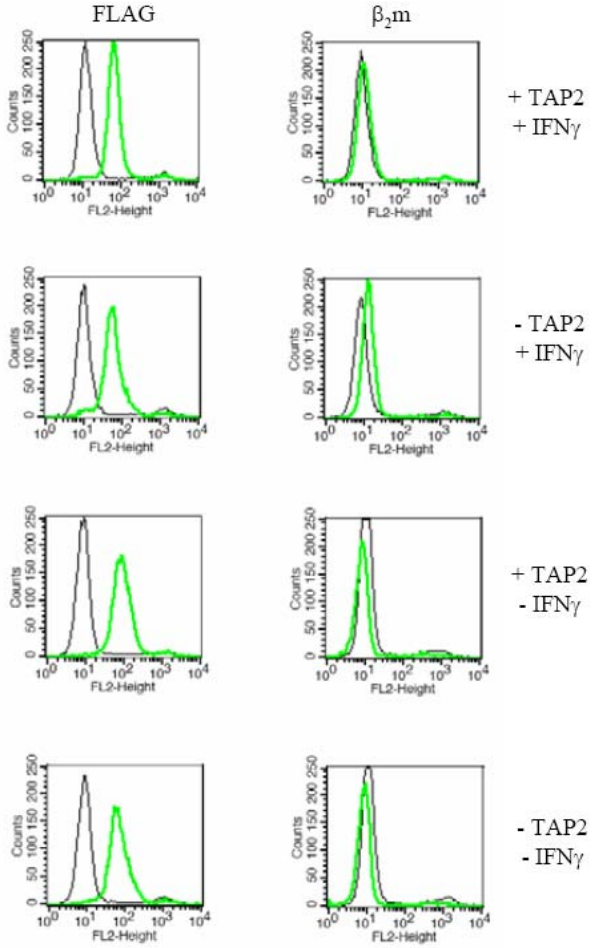

E

H2-Bl^b α1α2

Transient Transfection

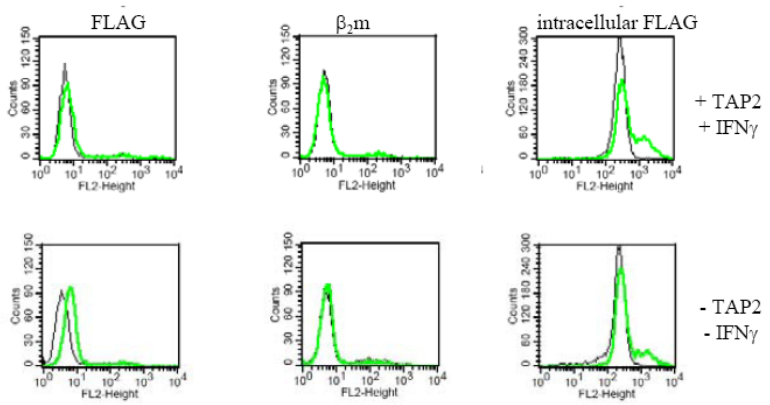

Stable Transfection

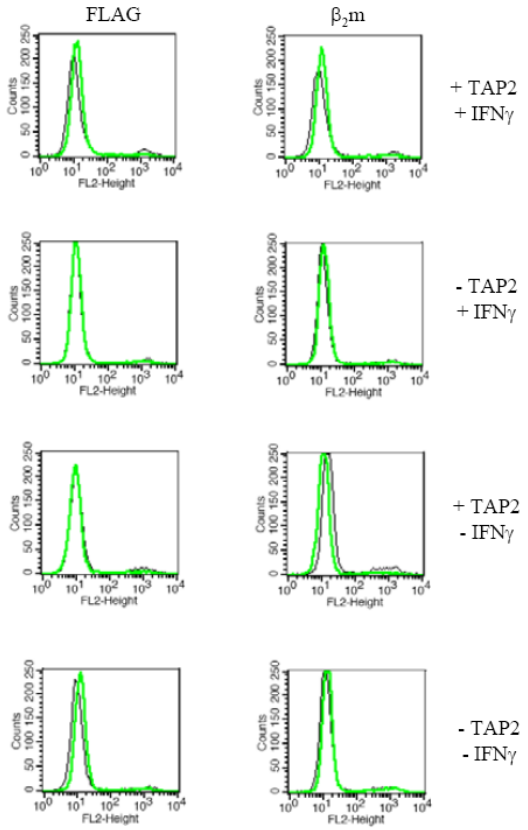

Figure 6.4 Cell surface expression, β_2m association and IFN-γ induction of alternatively spliced, tissue-restricted class Ib MHC. Experimental conditions and figure layout is the same as in Figure 6.3. A. H2-Bl^{bc} α1α3. B. H2-Bl^{bc} α1α3'. C. Q5^{k} α1α3. D. Q1^{bc} α3 E. H2-Bl^{b} α1α2.

cell surface, though it was present intracellularly (Figure 6.4E, top right panel). None of the alternatively spliced isoforms studied here were seen to associate stably with endogenous mouse β_2m^{b} on the cell surface.

Thus, tissue-restricted splicing variants of murine class Ib containing α1α3 domains, the α1 domain alone or the α3 domain alone were shown to reach the cell surface where they may be accessible to lymphocyte receptors.

SUMMARY AND DISCUSSION

Class Ia MHC perform their function in elimination of diseased cells by presenting nonself peptides to T cells. In contrast, some nonclassical members of the class I MHC family, such as gut-specific TL, encoded by *T3* and *T18* paralogous genes in the H2^{d} haplotype, are unable to bind peptides, but can impact the local immune response by engaging CD8αα receptors on IEL, reprogramming their cytokine secretion and effector functions (38). Other class Ib, specifically trophoblast HLA-G, influence innate immunity by providing leader peptides to HLA-E and by engaging ILT receptors on macrophages, etc. In order to address if and how the class Ib MHC proteins studied here may affect the gut milieu it is important to determine if they encode cell surface proteins and to define the structural features of these polypeptides.

We have examined these issues by tagging heavy chains of selected class Ib MHC variants with an N-terminal FLAG epitope and by assessing their stable association with endogenous murine β_2m^b on the surface of the transfected mouse melanoma B78H1. Importantly, anti-FLAG antibodies could stain the heavy chains independently of their conformation, while the anti-$\beta2m^b$ reagent is predicted to detect this subunit incorporated into the correctly folded or "conformed" class I complex. Two of the gut-restricted canonical transcripts, H2-Bl and its putative paralog, Tw5, gave rise to a membrane-bound, FLAG-tagged fraction, which was TAP-dependent, IFN-γ inducible and associated weakly with murine β_2m^b. We propose that H2-Bl and Tw5 class Ib full size proteins fold into conventional structures of MHC trimers associated with TAP-delivered peptides. In addition, both the canonical H2-Bl and Tw5 gave rise to smaller populations of TAP2- and IFN-γ-independent heavy chains that are not detectably associated with murine β_2m^b. In contrast, T3-like full size transcripts (similar in coding capacity to peptide-independent TL, which is synthesized by *T3* and *T18* genes of BALB/c mice (118)) were expressed in association with β_2m^b on the cell surface of IFN-γ-treated TAP-proficient as well as TAP-deficient cells. This phenotype is consistent with our predictions that the groove of this folded MHC, like its TL homologs from BALB/c mice, is devoid of cytosolic peptides. Finally, Q2 has yet another phenotype, resembling in some aspects Qa-1, described in Chapter Five and Robinson et al (357). It expresses a relatively constant level of FLAG-tagged heavy chains in TAP^+ and TAP^- background and is only minimally upregulated by IFN-γ. Its stable association with murine β_2m^b is, however, controlled by TAP expression and is augmented by treatment with IFN-γ. By extrapolating from Qa-1 expression patterns (Chapter Five), we interpret the latter as

indicating that TAP is needed for delivery of peptides that stabilize association of Q2 heavy chains with murine β_2m and that IFN-γ may have multiple contributions in facilitating Q2 display in the cell line in which these studies were performed. These may include formation of appropriate stabilizing peptides (synthesis of the antigens giving rise to these peptides or their processing in the cytoplasm and ER) and/or enhancement in the presentation of these peptides (loading of these peptides due to general enhancement of the components of class I antigen processing and presentation in the ER). It should be emphasized that the model cell line used for our studies is a melanoma tumor, which has been previously demonstrated to have a reduced capacity to assemble class I MHC (359). Thus, even if ectopically expressed H2-K^b (359) and membrane-linked TAP-dependent and independent fractions of Q10 (analyzed here) are, constitutively and independently of IFN-γ, bound to murine β_2m^b, the H2-D^b and T3-like heavy chains require IFN-γ to detect their association with endogenous β_2m^b. A likely explanation for these observations is that H2-D^b and T3-like proteins have a weak association with β_2m^b and, after reaching the cell surface, exchange endogenous β_2m^b for bovine β_2m supplied to the culture medium by fetal calf serum. Indeed, dissociations of endogenous β_2m^b from H2-D^b and its replacement with bovine β_2m have been described previously (373). At present it is not known if cell surface expression of conformed H2-D^b dissociated from all of β_2m^b is stably maintained at the cell surface as a "β_2m-free" isoform or if it is always associated with bovine β_2m (373).

In summary, while we can unambiguously interpret the requirement for TAP expression as a requirement for cytoplasmic peptides during the formation/expression of stable class Ib complexes, we are reluctant to make strong conclusions about association

of β_2m^b with some of the studied MHC populations. We have demonstrated that a fraction of surface expressed canonical H2-Bl, Tw5, Q2 and T3 heavy chains are bound on the cell surface to murine β_2m. The status of those that appear "β_2m-free" needs to be further characterized by alternative approaches. Most interestingly, we have shown here that H2-Bl, Tw5 and Q2 are TAP-dependent and, therefore, likely to associate with peptides. Since the melanoma tumor used here is of neural crest origin, it is likely that the peptides incorporated into these class Ib complexes represent degradation products of common, widely expressed self-proteins rather than epithelial cell-specific antigens. This does not preclude the possibility that in the gut epithelium these class Ib MHC additionally bind constitutively expressed or inducible IEC-specific peptides or microflora/pathogen-derived peptides, endocytosed or synthesized in the IEC cytoplasm or produced upon infection or stress. In addition, our experiments demonstrated that small portions of canonical H2-Bl, Tw5 and Q2 can also reach the cell surface as TAP-independent proteins that are not detectably associated with β_2m. These fractions may exist in peptide-free configurations, or may be loaded with TAP-pathway independent peptides (374).

We have similarly assessed expression properties of major alternatively spliced isoforms of gut-restricted H2-Bl ($\alpha1\alpha3$ and its N-terminally deleted variant) as well as Q1 ($\alpha3$). We also analyzed the brain-expressed Q5 $\alpha1\alpha3$ isoform, which resembles H2-Bl $\alpha1\alpha3$. All these proteins are predicted to be expressed as monomers or monomers associated with β_2m. Alternatively, they may form dimers, composed of two $\alpha1\alpha3$ chains folding like classical MHC as originally proposed for HLA-G (226). All FLAG-tagged $\alpha1\alpha3$ constructs were displayed on the cell surface of melanoma cells in a TAP2 and

IFN-γ independent fashion, as predicted for proteins that no longer require class I MHC antigen processing and presentation components for their surface display. Trace amounts of β_2m^b were observed on the surface of these transfectants in the presence of IFN-γ, suggesting that β_2m may associate with these polypeptides under some circumstances. The Q1 α3 protein was also independent of TAP2 and IFN-γ. As with α1α3 variants, low levels of β_2m was sometimes detectable in association with this isoform in IFN-γ-treated transfectants. In support of this interpretation, it has been reported that a recombinant "free" α3 domain of H2-D^d can bind to β_2m^b and compete for association with the light chain with other class I MHC co-expressed in the same cells (375). If the association of β_2m^b with α1α3 and α3 isoforms indeed occurs, it may act after the proteins have arrived at the cell surface to regulate their conformation or to prevent dimer formation.

The only isoform which we did not conclusively score as surface positive is H2-Bl α1α2. This isoform, resembling stress-inducible Rae-1-like NKG2D ligands (156), was shown to be expressed intracellularly as an appropriately glycosylated polypeptide. In rare experiments we detected it at low levels on the cell surface. Since this has occurred only in transient transfections, it may indicate that stress conditions (such as those inflicted on cells during transfection) are required for its transport to the cell surface.

The results of the experiments described in this chapter demonstrate that the gut-restricted class Ib MHC encode a multitude of cell surface proteins. Some of them (H2-Bl, Tw5 and Q2) are compatible with an assumption that they fold into conventional class I-associated trimers, which may incorporate specialized self or non-self peptides, communicating changes in the cytosolic protein repertoire to the αβ or γδ TCR. Others,

like the T3-like product, appear to represent TL-like, peptide-free dimers that communicate with IEL via α3/CD8αα interactions (254). The most interesting are the apparently β_2m-free alternatively spliced isoforms and constitutively expressed, TAP-independent populations of canonical and Rae-1-like heavy chains that may serve as γδ ligands or structures recognized by NK cell receptors. Their potential interaction with IEL will be discussed in Chapter Seven.

CHAPTER SEVEN

Conclusions and Discussion

In this study we set out to address one of the most fundamental yet elusive questions in IEL biology. *What are the self ligands for unconventional IEL that control their thymic/extrathymic education, maintenance and reactivity in the intestine?* Many lines of evidence from previous studies in the mouse, the most commonly used experimental model for human intestinal immunity, point to class Ib MHC. *What tissue-specific class Ib MHC are found in the gut and can they be expressed at the cell surface where they can engage TCR?* In addition to TCR engagement, class I MHC participate in the immune response by engaging innate immune receptors on NK cells and activated T cells. We therefore also asked: *Do murine IEL express NK cell receptors capable of engaging class I MHC or class I-related molecules?* and *What NK cell receptor-associating products of gut-specific class Ib MHC are expressed in the intestinal epithelium?* In addition to the intestine, many tissues associated with immune tolerance express tissue-restricted class Ib MHC. *Do class Ib MHC specifically expressed in other tolerance-associated or immune privileged sites have properties similar to gut-restricted class Ib MHC?*

SUMMARY OF FINDINGS

We describe here five class Ib MHC – TL, Q1, Q2, H2-Bl and Tw5 – specifically expressed in the intestinal epithelium. The cephalocaudal expression pattern of these

class Ib MHC is similar to other non-immune genes transcribed in intestinal enterocytes. *H2-Bl* can be transcriptionally upregulated in response to an IFN-γ immunological stimulus, and the similarities between the promoters of *H2-Bl* and *Tw5*, *Q1* and *Q2* suggests that the latter genes may be similarly regulated. Most of the canonical gut-specific class Ib MHC proteins characterized here are cell surface expressed in a partially TAP-dependent manner, while protein products from alternatively spliced transcripts of gut-specific class Ib MHC are, for the most part, also cell surface expressed but TAP-independent.

We found that, in addition to the TCR, some IEL express NK cell receptors specific for class I MHC. These include small subsets of conventional and unconventional IEL that are $CD94^{+}$ $NKG2A^{+}$ $NKG2D^{lo/-}$ and a newly described population of $CD94^{-}$ $NKG2A^{+}$ $NKG2D^{+}$ cells. Gut-specific class Ib MHC, in contrast to ubiquitously expressed class Ib MHC, encode a Qdm-like nonamer peptide in their leader sequences. The H2-Bl-derived Qdm-like peptide is processed from the H2-Bl signal sequence, binds Qa-1 and mediates NK cell inhibition, potentially participating in IEL immune responses via CD94/NKG2. Outside of the gut, liver-specific Q10 and brain-expressed Q5 encode canonical Qdm which can be processed from the Q10/Q5 signal sequence in a TAP-independent fashion to associate with Qa-1. Alternatively spliced products of Q10 and Q5 are reminiscent of gut-specific class Ib MHC and pregnancy-associated human HLA-G.

While this study was in progress, Tajima et al reported that canonically spliced H2-Bl was expressed on the cell surface of murine thymoma TAP^{+} RMA transfectants, but not TAP^{-} RMA-S cells (277), and Tanaka et al demonstrated β_2m association with the

H2-Bl heavy chain (376). Tajima et al found no cell surface expression of the α1α3 variant in transfectants of either RMA or RMA-S cells. Using a conformation independent antibody against Qa-1, they reported the upregulation of Qa-1 cell surface expression by both isoforms. They attributed this finding to an octamer peptide derived from the H2-Bl leader peptide based upon subsequent killing assays with Qa-1 and NKG2 blocking antibodies. Oddly, these effects were demonstrated with H2-Bl transfectants of TAP^- RMA-S, a line that would not normally be expected to deliver a Qdm-like peptide to the Qa-1 peptide binding groove, as Qdm itself is TAP-dependent. They saw the same effect in killing assays performed on Qa-1-transfected CHO (Chinese hamster ovary) cells exogenously loaded with 20 μM of the octamer peptide.

As described earlier, our results are consistent with the findings that H2-Bl can be expressed on the cell surface in a TAP-dependent fashion and extended these findings to demonstrate that H2-Bl expression is upregulated by IFN-γ-inducible components of the antigen processing and presenting machinery. Like Tanaka et al (376), we find that H2-Bl associates with β_2m, but only transiently. In contrast with Tajima et al (277), we found that the α1α3 protein variant of H2-Bl is expressed on the cell surface. Possible reasons for this discrepancy are that the RMA tumor cell line used in the previous study lacked the pathway components necessary for expressing the α1α3 variant at the cell surface or that the serological threshold for detection of this protein was below the detection limit of the cell surface biotinylation assay employed. Additionally, in contrast with Tajima et al (277), we do not see Qa-1 association with the H2-Bl octamer peptide either in our flow cytometry or our CTL based assays. It is important to note that the Qa-1-specific, conformation independent antibody used to detect H2-Bl octamer association

with Qa-1 in Tajima et al, cannot discriminate between peptide-bound and peptide-free forms of Qa-1 (Figure 5.2). Since the interpretations of the data in Tajima et al (277) did not take this into account, we believe that our results have corrected the previous report of octamer association with Qa-1. We did see low level TAP-independent Qa-1 association with a Q10-derived peptide lacking the N-terminal alanine of Qdm. This peptide is not necessarily an octamer and may, in fact, be quite longer, since it would not be predicted to enter the proteasome-dependent C-terminal cleavage pathway. There is some precedent for Qa-1 binding unusually long peptides (179), and a C-terminally extended peptide could possibly be accommodated by the unusual Qa-1 F pocket. Thus, the Tajima et al report of Qa-1-mediated NK cell inhibition via a H2-Bl-derived peptide may be the result of a long form of the signal sequence and not the octamer, which we see no evidence of associating with Qa-1.

Importantly, we report here that *H2-Bl* is transcribed at high levels in the adult/fetal intestine, not in the placenta. *H2-Bl* was first detected in blastocysts and placenta by Sipes et al (264) and was proposed on this basis to be a murine functional homolog of HLA-G. This study did not, however, examine expression levels of H2-Bl in the intestine (264). Some differences in H2 haplotype or genetic background may also be to blame, as we have observed miniscule expression of H2-Bl in the placenta of an ICR mouse (unpublished observations), similar to Sipes et al (264). The detected expression was negligible, however, with respect to that of the small intestine. Tajima et al describe low level *H2-Bl* transcription in the placenta of a C57BL/6 mouse using 50 times more RNA than we use to easily detect H2-Bl expression in the small intestine of the same strain of mouse ((277) versus Chapter Three/Materials and Methods). As in Sipes et al,

small intestinal tissues were not tested in the Tajima study. Here, for the first time, we perform quantitative RT-PCR on placental and small intestinal samples from the bc haplotype $K^{b-/-}D^{b-/-}$ mouse and demonstrate that the small intestine is by far the dominant site of H2-Bl transcription. While we cannot preclude the possibility that H2-Bl is expressed by a small portion of placental cells, we conclude that H2-Bl is primarily a gut-restricted class Ib MHC.

HYPOTHETICAL RECEPTOR/LIGAND INTERACTIONS OF TISSUE-SPECIFIC CLASS IB MHC

In the studies detailed in this thesis, we find that canonical isoforms of H2-Bl, Tw5 and Q2 can be expressed on the cell surface in a TAP-dependent, IFN-γ-inducible manner. Protein products of alternatively spliced, tissue-restricted class Ib MHC transcripts (including those from H2-Bl, Q1 and Q5) are also expressed on the cell surface. The tissue-restricted class Ib MHC encode Qdm (Q5 and Q10) and Qdm-like (H2-Bl) nonamer peptides in their leader sequences that can bind Qa-1. Based upon their predicted tertiary structures, cell surface expression and leader peptide association with Qa-1 we predict that the multiple protein products of tissue-restricted class Ib MHC can serve as ligands for a variety of lymphocyte receptors, thus modulating local immune responses.

The predicted tertiary structures, TAP-dependence and IFN-γ-inducibility of H2-Bl, Tw5 and Q2 suggest that they may serve as antigen-presenting restriction elements for TCR on T cells (Figure 7.1). It is predicted that these gut-specific class Ib MHC bind

peptides, as their critical A and F pocket residues are conserved, and they do not contain residues abrogating their peptide binding groove as are found in TL or T10/T22. Hypothetically, candidate TCRαβ$^+$ IEL that may be restricted by gut-specific include conventional TCRαβ$^+$ CD8αβ$^+$ cells. These IEL experience antigen in the periphery and traffic back to the IEL compartment for immediate response to secondary infection (25). Since H2-Bl and Tw5 are not expressed outside of the intestine, Q2 is the most likely TCRαβ$^+$ CD8αβ$^+$ IEL restricting element as it is transcribed in peripheral tissues at low levels (see Chapters Three and Four) and therefore possibly expressed in APCs, a requirement for the initiation of adaptive immunity. Q2 is additionally highly polymorphic in its peptide binding domain (287), suggesting that it has undergone pathogen-induced positive selection in a manner similar to class Ia MHC.

It is particularly attractive to think that H2-Bl, Tw5 and Q2 might be the elusive ligands for TCRαβ$^+$ CD8αα$^+$ IEL (Figure 7.1). These cells are absent in $\beta_2m^{-/-}$ mice, diminished in $TAP^{-/-}$ mice but present in $K^{b-/-}D^{b-/-}$ and $CD1^{-/-}$ mice, suggesting that they are restricted by one or more class Ib MHC that are at least partially TAP-dependent. H2-Bl, Tw5 and Q2 all fit the bill as β_2m associating, gut-specific class Ib MHC with TAP-dependent and TAP-independent expression. These class Ib MHC are also expressed in the thymus (see Chapters Three and Four) where TCRαβ$^+$ CD8αα$^+$ IEL are thought to be selected on self agonists. Finally, H2-Bl, Tw5, Q2 (and Q1, Q10 and Q5) all contain two (glycine at position 197 and aspartic acid at position 198) of the three residues associated with high affinity CD8αα association (351), implying that they, like TL, might regulate CD8αα T cells via this interaction.

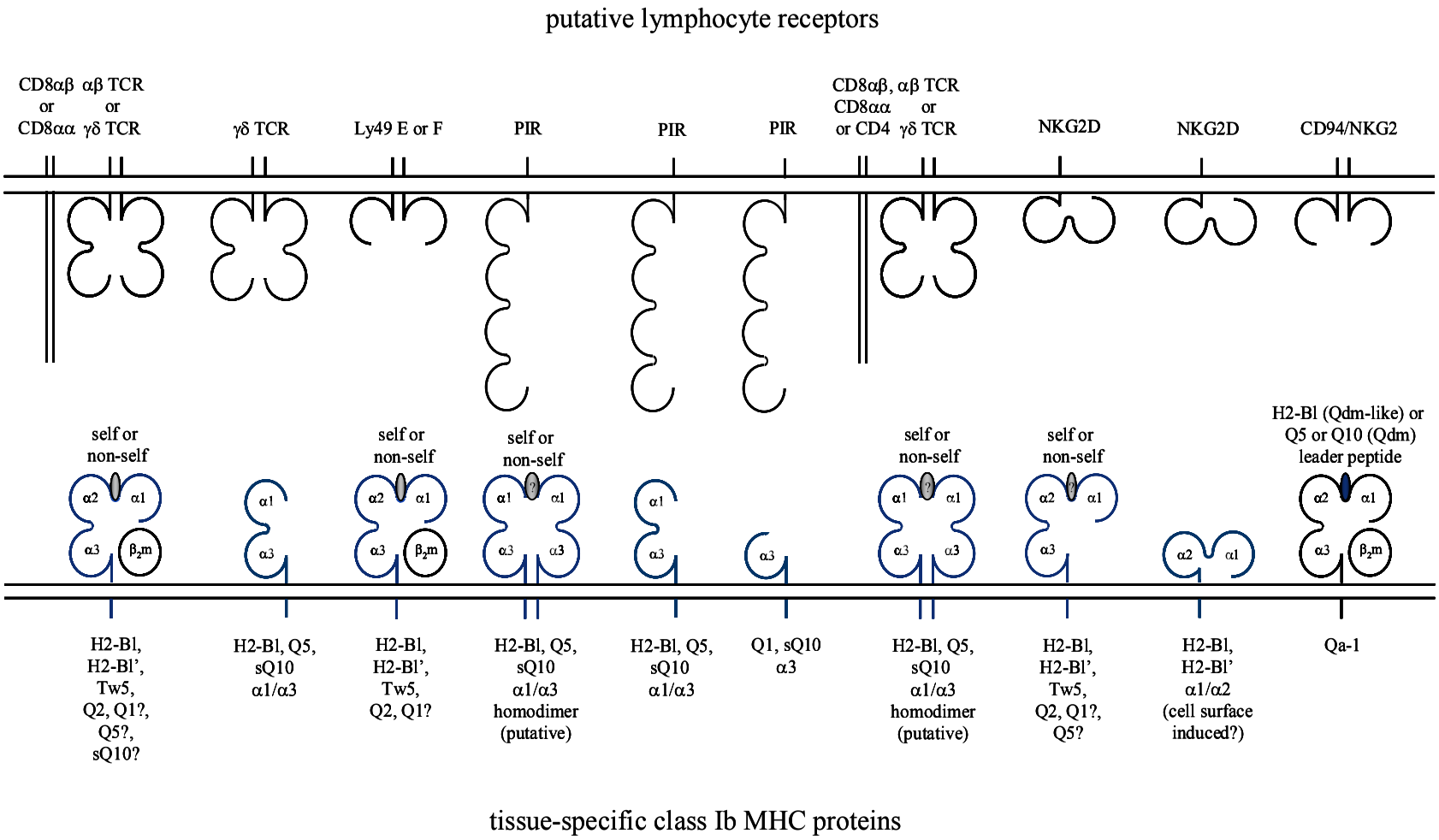
putative lymphocyte receptors
CD8αβ or CD8αα
αβ TCR or γδ TCR
γδ TCR
Ly49 E or F
PIR
PIR
PIR
CD8αβ, CD8αα or CD4
αβ TCR or γδ TCR
NKG2D
NKG2D
CD94/NKG2
self or non-self
self or non-self
self or non-self
self or non-self
self or non-self
H2-Bl (Qdm-like) or Q5 or Q10 (Qdm) leader peptide
α1
α2
α3
β2m
H2-Bl, H2-Bl', Tw5, Q2, Q1?, Q5?, sQ10?
H2-Bl, Q5, sQ10 α1/α3
H2-Bl, H2-Bl', Tw5, Q2, Q1?
H2-Bl, Q5, sQ10 α1/α3 homodimer (putative)
H2-Bl, Q5, sQ10 α1/α3
Q1, sQ10 α3
H2-Bl, Q5, sQ10 α1/α3 homodimer (putative)
H2-Bl, H2-Bl', Tw5, Q2, Q1?, Q5?
H2-Bl, H2-Bl' α1/α2 (cell surface induced?)
Qa-1
tissue-specific class Ib MHC proteins

Figure 7.1 Splicing patterns of tissue-specific class Ib MHC produce multiple putative IEL ligands. Tissue specific class Ib MHC are depicted as theoretical tertiary structures in the bottom portion of the figure, while their putative lymphocyte receptors are depicted on top. It is well established that canonically folded class I MHC can interact with TCR of CD8$\alpha\beta^+$, CD8$\alpha\alpha^+$ and CD4$^+$ T cells and activating and inhibitory Ly49 family members. The α1α3 variant of several tissue-specific class Ib MHC resemble the tertiary structure of a γδTCR ligand (T22) and are depicted here as candidate ligands for the γδTCR. PIRs interact with the α3 +/- β_2m of many class I MHC and are theorized here to bind α3-containing splice variants of tissue-specific class Ib MHC. Though not yet demonstrated to homodimerize, α1α3 variants of H2-Bl, Q5 and Q10 are depicted here in an HLA-G2-like conformation, presenting antigen to CD8$^+$ or CD4$^+$ T cells. NKG2D is a highly promiscuous NK and T cell activating receptor, and is shown here as possibly binding either MIC-like or Rae-like structures of gut-specific class Ib MHC. Finally, tissue-specific class Ib MHC leader peptides associate with Qa-1 and may mediate NK/T cell tolerance or activation by ligating CD94/NKG2 family members.

An intriguing possibility is that gut-specific class Ib MHC serve as ligands for the γδTCR (Figure 7.1). TCRγδ$^+$ T cells account for approximately half of all IEL (42), yet their TCR ligands remain largely undefined. Only one murine class I protein (encoded by paralogous *H2-T10* and *H2-T22* genes) is known to bind a γδ TCR. T22-interacting γδ T cells use a TCR that binds the floor of the interhelical groove in this class Ib MHC (98). Though the crystal structure of the tissue-specific class I MHC α1α3 variant has not been solved, it would be expected to have an exposed partial β-sheet floor overlayed by the α1 helix, similar to T22. Additionally, γδ T cells are present in $\beta_2m^{-/-}$ mice (106), and α1α3 splice variants come to the cell surface independently of β_2m (Chapter Six).

We have demonstrated here that H2-Bl, expressed in IEC, contributes a nonamer peptide derived from its leader sequence to the groove of Qa-1. We have additionally identified a small subset of murine IEL that express the inhibitory CD94/NKG2A homodimer. It therefore seems likely that H2-Bl/Qa-1 can modulate the immune

response of certain IEL via CD94/NKG2 engagement (Figure 7.1). Liver-restricted Q10 and brain-expressed Q5 also encode canonical Qdm in their leader peptides which can be processed from the Q10/Q5 signal sequences and presented in the peptide binding groove of Qa-1. The Q10 α3 leader peptide exhibits some TAP-independence, whereas the Q5 leader peptide can associate with Qa-1 in a complete TAP-independent manner. We therefore postulate that these class Ib MHC participate in local immune tolerance via a Qa-1/CD94/NKG2A-dependent pathway in a manner that allows for TAP-independent presentation of Qdm.

Other possible NK cell receptors for gut-specific class Ib MHC include the orphan Ly49E and Ly49F inhibitory NK cell receptors (Figure 7.1) (195). Expressed on a substantial fraction of TCR$\alpha\beta^+$ CD8$\alpha\alpha^+$ regulatory IEL, these receptors do not react with class Ia MHC, nor do Ly49E$^+$ or Ly49F$^+$ IEL stain with TL or CD1d tetramers (195). Thus the gut-restricted class Ib MHC studied here are excellent candidate ligands for Ly49E and Ly49F receptors on IEL.

While their expression in the intestine has only been demonstrated in humans (377), the PIR family of activating and inhibitory receptors are another set of candidate ligands for tissue-restricted class Ib MHC (Figure 7.1). The best characterized homologs of these molecules, ILT-2 and ILT-4, bind a broad array of class I MHC through the nonpolymorphic β_2m and/or α3 MHC domains. Thus, PIR family members may have the capacity to recognize not only canonical, tissue-restricted class Ib MHC, but also proteins produced from their alternatively spliced isoforms that retain the α3 domain. The protein product of canonically spliced HLA-G1 has been shown to be a high affinity ligand for ILT-2 and ILT-4. HLA-G can homodimerize through a free cysteine in its α2 domain,

increasing its affinity for ILT substantially. Q5, like HLA-G, has two nonstructural cysteines, one in the α1 domain and the other in α2. The α1 cysteine is located 6 aa C-terminal to the homodimerizing cysteine in HLA-G and is positioned on the C-terminal end of the turn going from the peptide binding groove α-helix to the β-floor where it may serve as an α1 domain homodimerizing agent. Thus, canonical Q5 and its α1α3 protein variant may homodimerize and act as high affinity PIR ligands.

No additional cysteines (outside of the four required to form internal disulfide bonds) were observed in any of the other tissue-specific class Ib MHC sequences, indicating that they do not form disulfide-linked homodimers. This may account for the higher cell surface expression seen with Q5 α1α3 than H2-Bl α1α3. It does not, however, preclude the possibility that the α1α3 variants of H2-Bl and Q10 noncovalently associate to form a class II-like structure like what has been proposed for the HLA-G2 α1α3 protein (Figure 7.1). This raises the intriguing possibility that homodimers of H2-Bl, Q5 and/or Q10 α1α3 proteins may participate in a non-canonical class I or class II peptide presentation pathway, serving as ligands for the $CD8^+$ or $CD4^+$ TCR.

The low, variable detection of H2-Bl and Tw5 with β_2m suggests either that their association with the light chain deteriorates at the cell surface, or endogenous β_2m is rapidly exchanged for serum β_2m in the tissue culture medium. It is not clear, however, that a high affinity β_2m/heavy chain interaction is necessary for all class I MHC to achieve a proper fold (378), and ILT-4 can bind HLA-G homodimers that are not associated with β_2m (379). On the other hand, different peptides differentially affect the affinity of the class I/β_2m interaction (380), so the intestinal milieu may provide a set of peptides capable of increasing the affinity of the H2-Bl and Tw5 heavy chains for β_2m.

As another alternative, these class Ib MHC may largely dispense with the β_2m light chain at the cell surface, forming a MICA-like β_2m-free structure (Figure 7.1). Q2 may also form this type of structure when TAP expression is downregulated, as the Q2 heavy chain it is stably expressed at the cell surface independently of β_2m in the absence of TAP2. Human MICA and MICB are NKG2D ligands that are constitutively expressed in the intestinal epithelium and induced in tumors and under conditions of stress. Although they are located within the human *Mhc* region, no known MIC homolog has been discovered in the mouse. Thus it is possible that these gut-specific class Ib MHC may act as MIC functional homologs under certain conditions.

The α1α2 splice variant of H2-Bl resembles the NKG2D ligand Rae-1 (Figure 7.1). While this protein is not expressed on the cell surface under steady state conditions, we see low level cell surface expression in transient transfections, a period of heightened cell stress. Therefore, like Rae-1, H2-Bl α1α2 may come to the cell surface under stress conditions. As additional evidence of such a splice variant coming to the cell surface, we occasionally see low level cell surface expression of a *Q9* (Qa-2) α1α2 variant, though we do not know what contributes to its variably detectable expression (unpublished observations by Terry Coursey of our laboratory). Another alternate NKG2D ligand is the H2-Bl' protein, which lacks the first 11 aa of the α1 β-sheet floor (Figure 7.1). As a precedent for this, ULBP4 splice variants that lack portions of either their α1 or α2 domains are still recognized by NKG2D (381).

NKG2D is a highly promiscuous receptor, binding disparate MHC-like ligands that retain some semblance of the α1α2 fold. Thus several of the gut-specific class Ib MHC studied here may serve as NKG2D ligands. Known NKG2D ligands have been

demonstrated to have different affinities for NKG2D and therefore compete with each other for NKG2D engagement (189, 190, 382). Additionally, NKG2D ligands are differentially expressed in various tissues and are induced under different circumstances (189, 383), theoretically increasing the range of functional outcomes of NKG2D ligand engagement. Thus, expression of the gut-specific class Ib MHC described here may further nuance intestinal immune responses by engaging the NKG2D activating receptor on $CD94^-$ $NKG2A^+$ $NKG2D^+$ IEL. These ligands may be inducible (α1α2) or constitutive (MIC-like) and sequestered on epithelial surfaces that do not interact with $NKG2D^+$ IEL under normal, non-pathogenic circumstances.

This study identifies many class I MHC molecules and variants derived from their alternatively spliced transcripts that are specifically expressed in tolerance-associated tissues. We propose that these molecules modulate local immune responses by serving as ligands for many putative receptors on proximal lymphocytes. The demonstration that any one of these putative receptor/ligand interactions occurs *in vivo* would be a major step forward in understanding the function of tissue-specific lymphocytes and their regulation of immune responses in tolerance-dominated tissues.

THEMES IN TISSUE-SPECIFIC CLASS IB MHC BIOLOGY

A striking feature of many tissue-specific class Ib MHC is their ability to alternatively splice. This suggests that the protein products of alternatively spliced MHC play important roles in tolerance-associated tissues like the placenta (HLA-G [canonical, α1α3 and α1, predominantly]), gut (H2-Bl [canonical and α1α3, predominantly] and Q1

[canonical and α3]), liver (Q10 [soluble canonical, soluble α1α3 and soluble α3]) and brain (Q5 [canonical, α1α3 and α1]). The α1α3 protein is a particularly dominant tissue-specific class Ib MHC. Its specific expression in all of the tolerance-associated tissues studied here and its heightened expression in the brain with respect to all other tissues is strongly suggestive of an immunotolerizing role for this molecule. Another notable splice variant is the α1 molecule, found in both the brain (Q5) and the placenta (HLA-G), two of the classically immune privileged tissues. The α3 protein variant is also interesting from an immune tolerance point of view as it is not only expressed by gut-specific Q1 and liver-specific Q10, but it has also been seen as a tumor-specific isoform of *Q9* (Qa-2, unpublished observations by Jennifer McLean of our laboratory). An artificially isolated α3 domain of D^d has been shown to associate strongly with β_2m and bind the CD8αα TCR co-receptor (368). This could be locus-dependent, as we don't see β_2m association with the α3 protein variant of Q1 or *Q9*-encoded Qa-2. It does not, however, preclude a potential interaction with some PIRs, which recognize the α3 domain of class I MHC in the absence of β_2m.

Another noteworthy feature of all tissue-specific class Ib MHC expressed in the immune tolerance-associated organs that we studied is that they all encode Qdm or Qdm-like sequences in their leader peptides, whereas ubiquitously transcribed class I MHC do not. In the liver (Q10), brain (Q5) and placenta (HLA-G), canonical Qa-1/HLA-E binding peptides are expressed, whereas in the small intestine (H2-Bl) Qdm-like molecules predominate. Placenta and brain express little to no class Ia MHC that might provide a source of HLA-E/Qa-1 associating peptides (197), and small intestinal IEC express reduced levels of Qdm-encoding D^b (120). Thus Qdm and Qdm-like peptides are

available for Qa-1 binding and CD94/NKG2A mediated inhibition in tissues where the classical Qdm/Qa-1 pathway is limited.

We have demonstrated in this study that nonamer peptides derived from the leader sequence of H2-Bl can associate with Qa-1. The functional outcome of this interaction is, however, unclear. The H2-Bl leader peptide differs from Qdm in one to two of its nine residues (depending upon the *Mhc* haplotype; Qdm = AMAPRTLLL; H2-Bl^q = AMAQRTLLL; H2-Bl^{bc} = AMAQRTLFL). In the CD94/NKG2A/HLA-E crystal structure one of these positions directly interacts with CD94 (Leu_8) (146), while the other (Pro_4) is one amino acid removed from the only residue known to affect binding by the NKG2A inhibitory subunit versus the NKG2C activating family member (Arg_5) (146). Since subtle changes in the peptide orientation within the groove have been shown to affect CD94/NKG2A affinity for HLA-E (181), it seems likely that, in addition to the overall lower affinity of the H2-Bl leader peptide for the groove of Qa-1 (see Chapter Five), differences between Qdm and Qdm-like peptides might affect the affinity of the CD94/NKG2A or CD94/NKG2C receptor for Qa-1. As evidence of this, our preliminary data suggest that the H2-Bl-derived Qdm-like nonamer peptide can mediate NK cell inhibition slightly better than Qdm. Thus the H2-Bl Qdm-like peptide may serve a slightly different function than Qdm in the gut, diversifying the functional outcome of CD94/NKG2 ligand engagement in the intestinal milieu.

A common characteristic of many tolerance-associated tissues is the presence of unique lymphocyte populations. Placental tissues interact with dNKs, while the liver is populated by numerous NKT cells, and the gut is home to an immense and diverse population of IEL. We have identified a subset of IEL that is $CD94^+$ $NKG2A^+$ and

another that is CD94^{-} NKG2A^{+} NKG2D^{+}. The function of these cells in health and disease has yet to be explored, but we speculate that, though they are a small body of cells in the larger IEL population, they may expand or elaborate cytokines and/or other regulatory effectors in response to infection or intestinal damage. Thus, this subset of cells may, like the small populations of MAIT (384) and CD8$\alpha\beta^{+}$ TCR$\gamma\delta^{+}$ IEL (92), have a significant effect on local immune responses under certain conditions.

Immune privileged and tolerance-associated tissues face unique immunological challenges and have evolved multiple receptor/ligand interactions to balance immune suppression and activation. Here we describe the expression of an evolutionarily conserved set of MHC-engaging lymphocyte receptors and their putative, rapidly evolving, tissue-restricted class Ib MHC ligands. We believe that "nonclassical," tissue-restricted members of the class I MHC family may be critical components innate and adaptive immune recognition and, perhaps, the key to unlocking many unanswered questions in the study of enigmatic, tissue-specific lymphocyte populations such as IEL.

CHAPTER EIGHT

Future Directions

A primary goal of this thesis was to identify and characterize candidate class Ib MHC that may serve as self ligands for unconventional IEL. We identified several gut-specific class Ib MHC encoding diverse ligands that have the potential to engage a variety of receptors on IEL and extended these findings to examine class Ib MHC restricted to other immune tolerance-associated tissues. Many fundamental questions about IEL and their engagement of gut-restricted class Ib MHC remain as do questions about the function of class Ib MHC restricted to the liver and the brain. The most important of these at this point are: 1) Which class Ib MHC isoforms are recognized by which IEL receptors? 2) Do they support education/selection of IEL? 3) Do they play a role during infections, neoplasia, tissue damage, stress and/or autoimmune conditions?

We felt that the best candidate ligands for the γδ TCR among the molecules we studied here were the β_2m-independent α1α3 variants of H2-Bl and Q5 (though we do not preclude canonically spliced protein products of tissue-restricted class Ib MHC). To determine if γδ IEL recognize α1α3 variants of H2-Bl and/or Q5 (or, for that matter, any of the class Ib MHC products under study) we should attempt to stimulate γδ IEL/PBL proliferation or cytokine induction with our B78H1 transfectants. If positive, these experiments should be performed with γδTCR blocking antibodies to confirm the specificity of the interaction. Next T-T hybridomas derived from TCR$\gamma\delta^+$ IEL or PBL (for Q5) should be generated and tested for recognition of gut-specific class Ib MHC on our melanoma transfectants. Then we could characterize the TCR usage of tissue-

specific class Ib MHC interacting hybridomas. Alternatively, we could generate epitope-tagged, soluble α1α3 molecules to stain TCRγδ$^+$ IEL or PBL. Since it is possible that the binding sites for the anti-γδTCR antibody and the recombinant class Ib MHC would be overlapping, the positively stained T cells could be tested for TCR expression and clonal analysis of TCR genes by RT-PCR. Overlapping binding sites would actually be advantageous since we could then use the antibody to test the specificity of the soluble α1α3 interaction.

We considered H2-Bl, Tw5 and Q2 to be possible self ligands for TCRαβ$^+$ CD8αα$^+$ IEL. To test this hypothesis, single chain transgenic mice (a transgene consisting of the class I MHC heavy chain covalently linked to β_2m, driven by its own promoter on a β_2m$^{-/-}$ background (385)) should be generated and tested for the presence or absence of TCRαβ$^+$ CD8αα$^+$ IEL. If present, these mice could then be used to study the thymic development of unconventional TCRαβ$^+$ CD8αα$^+$ IEL in the presence of one of their natural ligands. Additionally, they could be used to probe the functions of TCRαβ$^+$ CD8αα$^+$ IEL in infection and colitis models. As an alternative, T-T hybridomas derived from TCRαβ$^+$ CD8αα$^+$ IEL could be generated to test for recognition of gut-specific class Ib MHC on our melanoma transfectants.

Q2 was identified as the best candidate among gut-restricted class Ib MHC to serve as a restricting element for conventional TCRαβ$^+$ CD8αβ$^+$ IEL based on its limited but detectable expression outside of the intestine, possibly on APCs. To determine if Q2 can indeed restrict CD8$^+$ T cells, tumor take assays should be performed with GM-CSF-transduced, Q2/TAP transfectants of our model melanoma, B78H1. If Q2 can indeed mediate rejection of these melanoma cells, these studies should be extended to include

mice with specific immunodeficiencies to determine which cell type is primarily responsible for tumor rejection.

To determine if gut-specific class Ib can serve as ligands for Ly49E, Ly49F and/or PIR family members, Ig fusion proteins of these receptors should be generated and tested for binding to our tissue-specific class Ib MHC melanoma transfectants. The same could be done with the existing mNKG2D-Ig fusion protein (156). Additionally, NKG2D association should be tested in the presence/absence of various stress conditions using the melanoma transfectant of our Rae-like H2-Bl α1α2 putative NKG2D ligand.

While we demonstrated that a nonamer peptide derived from the H2-Bl leader sequence can associate with Qa-1, the results of our functional studies were only preliminary. Thus further LAK assays should be performed with peptide stabilized Qa-1 transfectants. Additionally, NKG2A^{+} and NKG2C^{+} LAKs (or experimental equivalents of such lymphocytes expressing these receptors) should be used with or without blocking antibodies to confirm the receptor responsible for the observed killing or protection.

We demonstrated here that among murine IEL in healthy animals are small pools of T cells that are either CD94^{+} NKG2A^{+} NKG2D$^{lo/-}$ or CD94^{-} NKG2A^{+} NKG2D^{+}. These IEL should be tested for *ex vivo* reactivity against gut-specific class Ib MHC transfectants, particularly Qa-1-bearing targets loaded with exogenous H2-Bl nonamer peptides and lines expressing putative NKG2D ligands, in ^{51}Cr release assays. Additionally, it is unknown if these cells can expand and/or produce cytokines in response to infection. Thus, flow cytometry studies should be performed to look at changes in number and/or cytokine production of these unique IEL in response to oral infection (*Salmonella typhimurium*, *Listeria monocytogenes*, rotavirus, etc).

These proposed studies will provide further insight into the interactions of IEL with their putative gut-specific class Ib MHC ligands and the possible functions of other tissue-specific class Ib MHC. Most importantly, they directly address whether gut-specific class Ib MHC participate as the elusive self ligands for the unconventional IEL αβ and/or γδ TCR. This will open the door to understanding the functions of this vast population of lymphocytes that resides at the front lines of intestinal immune defense.

APPENDIX A

Calculation of the Volume of IEL with Respect to IEC

Forward scatter (FSC) is proportional to the cross-sectional area (A) of a cell of radius (r) and volume (V) by some constant (C).

$$FSC_{cell} = CA_{cell}$$

Assuming cells in suspension are approximately spherical,

$$A_{cell} = \pi r_{cell}^2 \quad \text{and} \quad V_{cell} = \frac{4\pi r_{cell}^3}{3}$$

$$FSC_{cell} = C\pi r_{cell}^2 \qquad r_{cell}^3 = \frac{3V_{cell}}{4\pi}$$

$$\frac{FSC_{IEC}}{r_{IEC}^2} = \frac{FSC_{IEL}}{r_{IEL}^2}$$

The average FSC of an IEC is 75, while the average FCS of an IEL is 50, so

$$\frac{75}{r_{IEC}^2} = \frac{50}{r_{IEL}^2}$$

$$r_{IEC}^2 = 1.5r_{IEL}^2$$

$$r_{IEC}^3 = 1.84r_{IEL}^3$$

$$\frac{3V_{IEC}}{4\pi} = 1.84\,\frac{3V_{IEC}}{4\pi}$$

$$V_{IEC} = 1.84V_{IEL}$$

Assuming IEL and IEC have approximately the same concentration of RNA,

$$[RNA]_{IEC} = 1.84[RNA]_{IEL}$$

References

1. Kimball, J. 2008. Kimball's Biology Pages. http://users.rcn.com/jkimball.ma.ultranet/BiologyPages/G/GITract.html.

2. Anderson, A. O. 1990. Structure and organization of the lymphatic system. In *Immunophysiology. The role of cells and cytokines in immunity and inflammation*. J. J. Oppenheim, and E. Shevach, eds. Oxford University Press, New York.

3. Williams, P. L., ed. 1995. *Gray's Anatomy*. Churchill Livingstone, New York.

4. Loeffler, M., A. Birke, D. Winton, and C. Potten. 1993. Somatic mutation, monoclonality and stochastic models of stem cell organization in the intestinal crypt. *J Theor Biol* 160:471-491.

5. Potten, C. S., R. Schofield, and L. G. Lajtha. 1979. A comparison of cell replacement in bone marrow, testis and three regions of surface epithelium. *Biochim Biophys Acta* 560:281-299.

6. Ishikawa, H., T. Naito, T. Iwanaga, H. Takahashi-Iwanaga, M. Suematsu, T. Hibi, and M. Nanno. 2007. Curriculum vitae of intestinal intraepithelial T cells: their developmental and behavioral characteristics. *Immunological reviews* 215:154-165.

7. Mowat, A. M. 2003. Anatomical basis of tolerance and immunity to intestinal antigens. *Nat.Rev.Immunol* 3:331-341.

8. Fagarasan, S., and T. Honjo. 2003. Intestinal IgA synthesis: regulation of front-line body defences. *Nat.Rev.Immunol* 3:63-72.

9. Jarry, A., N. Cerf-Bensussan, N. Brousse, F. Selz, and D. Guy-Grand. 1990. Subsets of CD3+ (T cell receptor alpha/beta or gamma/delta) and CD3- lymphocytes isolated from normal human gut epithelium display phenotypical features different from their counterparts in peripheral blood. *Eur J Immunol* 20:1097-1103.

10. Pavli, P., C. E. Woodhams, W. F. Doe, and D. A. Hume. 1990. Isolation and characterization of antigen-presenting dendritic cells from the mouse intestinal lamina propria. *Immunology* 70:40-47.

11. Spalding, D. M., W. J. Koopman, J. H. Eldridge, J. R. McGhee, and R. M. Steinman. 1983. Accessory cells in murine Peyer's patch. I. Identification and enrichment of a functional dendritic cell. *J Exp Med* 157:1646-1659.

12. Kelsall, B. L., and W. Strober. 1996. The role of dendritic cells in antigen processing in the Peyer's patch. *Ann N Y Acad Sci* 778:47-54.

13. Rescigno, M., M. Urbano, B. Valzasina, M. Francolini, G. Rotta, R. Bonasio, F. Granucci, J. P. Kraehenbuhl, and P. Ricciardi-Castagnoli. 2001. Dendritic cells express tight junction proteins and penetrate gut epithelial monolayers to sample bacteria. *Nature immunology* 2:361-367.

14. Macpherson, A. J., and T. Uhr. 2004. Compartmentalization of the mucosal immune responses to commensal intestinal bacteria. *Ann N Y Acad Sci* 1029:36-43.

15. Iwasaki, A., and B. L. Kelsall. 2001. Unique functions of CD11b+, CD8 alpha+, and double-negative Peyer's patch dendritic cells. *J Immunol* 166:4884-4890.

16. Alpan, O., G. Rudomen, and P. Matzinger. 2001. The role of dendritic cells, B cells, and M cells in gut-oriented immune responses. *J Immunol* 166:4843-4852.

17. Akbari, O., R. H. DeKruyff, and D. T. Umetsu. 2001. Pulmonary dendritic cells producing IL-10 mediate tolerance induced by respiratory exposure to antigen. *Nature immunology* 2:725-731.

18. Stagg, A. J., M. A. Kamm, and S. C. Knight. 2002. Intestinal dendritic cells increase T cell expression of alpha4beta7 integrin. *Eur J Immunol* 32:1445-1454.

19. Mora, J. R., M. R. Bono, N. Manjunath, W. Weninger, L. L. Cavanagh, M. Rosemblatt, and U. H. Von Andrian. 2003. Selective imprinting of gut-homing T cells by Peyer's patch dendritic cells. *Nature* 424:88-93.

20. Johansson-Lindbom, B., M. Svensson, M. A. Wurbel, B. Malissen, G. Marquez, and W. Agace. 2003. Selective generation of gut tropic T cells in gut-associated lymphoid tissue (GALT): requirement for GALT dendritic cells and adjuvant. *J Exp Med* 198:963-969.

21. Khoo, U. Y., I. E. Proctor, and A. J. Macpherson. 1997. CD4+ T cell down-regulation in human intestinal mucosa: evidence for intestinal tolerance to luminal bacterial antigens. *J Immunol* 158:3626-3634.

22. Leishman, A. J., L. Gapin, M. Capone, E. Palmer, H. R. MacDonald, M. Kronenberg, and H. Cheroutre. 2002. Precursors of functional MHC class I- or class II-restricted CD8alphaalpha(+) T cells are positively selected in the thymus by agonist self-peptides. *Immunity* 16:355-364.

23. Cruz, D., B. C. Sydora, K. Hetzel, G. Yakoub, M. Kronenberg, and H. Cheroutre. 1998. An opposite pattern of selection of a single T cell antigen receptor in the thymus and among intraepithelial lymphocytes. *J Exp Med* 188:255-265.

24. Cheroutre, H., and L. Madakamutil. 2004. Acquired and natural memory T cells join forces at the mucosal front line. *Nature reviews* 4:290-300.

25. Cheroutre, H. 2005. IELs: enforcing law and order in the court of the intestinal epithelium. *Immunological reviews* 206:114-131.

26. Penney, L., P. J. Kilshaw, and T. T. MacDonald. 1995. Regional variation in the proliferative rate and lifespan of alpha beta TCR+ and gamma delta TCR+ intraepithelial lymphocytes in the murine small intestine. *Immunology* 86:212-218.

27. Ferguson, A. 1977. Intraepithelial lymphocytes of the small intestine. *Gut* 18:921-937.

28. Rocha, B., P. Vassalli, and D. Guy-Grand. 1991. The V beta repertoire of mouse gut homodimeric alpha CD8+ intraepithelial T cell receptor alpha/beta + lymphocytes reveals a major extrathymic pathway of T cell differentiation. *J Exp Med* 173:483-486.

29. Wang, H. C., and J. R. Klein. 2001. Multiple levels of activation of murine CD8(+) intraepithelial lymphocytes defined by OX40 (CD134) expression: effects on cell-mediated cytotoxicity, IFN-gamma, and IL-10 regulation. *J Immunol* 167:6717-6723.

30. Ibraghimov, A. R., and R. G. Lynch. 1994. Heterogeneity and biased T cell receptor alpha/beta repertoire of mucosal CD8+ cells from murine large intestine: implications for functional state. *J Exp Med* 180:433-444.

31. Sillett, H. K., J. Southgate, P. D. Howdle, and L. K. Trejdosiewicz. 1999. Expression of activation and costimulatory elements by human intestinal intraepithelial lymphocytes. *Scand J Immunol* 50:52-60.

32. Klein, J. R. 2004. T-cell activation in the curious world of the intestinal intraepithelial lymphocyte. *Immunol Res* 30:327-337.

33. Kawaguchi-Miyashita, M., S. Shimada, Y. Matsuoka, M. Ohwaki, and M. Nanno. 2000. Activation of T-cell receptor-gammadelta+ cells in the intestinal epithelia of KN6 transgenic mice. *Immunology* 101:38-45.

34. Viney, J. L., P. J. Kilshaw, and T. T. MacDonald. 1990. Cytotoxic alpha/beta+ and gamma/delta+ T cells in murine intestinal epithelium. *Eur J Immunol* 20:1623-1626.

35. Guy-Grand, D., M. Malassis-Seris, C. Briottet, and P. Vassalli. 1991. Cytotoxic differentiation of mouse gut thymodependent and independent intraepithelial T lymphocytes is induced locally. Correlation between functional assays, presence of perforin and granzyme transcripts, and cytoplasmic granules. *J Exp Med* 173:1549-1552.

36. Ishikawa, H., Y. Li, A. Abeliovich, S. Yamamoto, S. H. Kaufmann, and S. Tonegawa. 1993. Cytotoxic and interferon gamma-producing activities of gamma delta T cells in the mouse intestinal epithelium are strain dependent. *Proc Natl Acad Sci U S A* 90:8204-8208.

37. Kawaguchi, M., M. Nanno, Y. Umesaki, S. Matsumoto, Y. Okada, Z. Cai, T. Shimamura, Y. Matsuoka, M. Ohwaki, and H. Ishikawa. 1993. Cytolytic activity of intestinal intraepithelial lymphocytes in germ-free mice is strain dependent

and determined by T cells expressing gamma delta T-cell antigen receptors. *Proc Natl Acad Sci U S A* 90:8591-8594.

38. Leishman, A. J., O. V. Naidenko, A. Attinger, F. Koning, C. J. Lena, Y. Xiong, H. C. Chang, E. Reinherz, M. Kronenberg, and H. Cheroutre. 2001. T cell responses modulated through interaction between CD8alphaalpha and the nonclassical MHC class I molecule, TL. *Science* 294:1936-1939.

39. Zeissig, S., A. Kaser, S. K. Dougan, E. E. Nieuwenhuis, and R. S. Blumberg. 2007. Role of NKT cells in the digestive system. III. Role of NKT cells in intestinal immunity. *American journal of physiology* 293:G1101-1105.

40. Treiner, E., L. Duban, S. Bahram, M. Radosavljevic, V. Wanner, F. Tilloy, P. Affaticati, S. Gilfillan, and O. Lantz. 2003. Selection of evolutionarily conserved mucosal-associated invariant T cells by MR1. *Nature* 422:164-169.

41. Regnault, A., A. Cumano, P. Vassalli, D. Guy-Grand, and P. Kourilsky. 1994. Oligoclonal repertoire of the CD8 alpha alpha and the CD8 alpha beta TCR-alpha/beta murine intestinal intraepithelial T lymphocytes: evidence for the random emergence of T cells. *J Exp Med* 180:1345-1358.

42. Hayday, A., E. Theodoridis, E. Ramsburg, and J. Shires. 2001. Intraepithelial lymphocytes: exploring the Third Way in immunology. *Nature immunology* 2:997-1003.

43. Arstila, T., T. P. Arstila, S. Calbo, F. Selz, M. Malassis-Seris, P. Vassalli, P. Kourilsky, and D. Guy-Grand. 2000. Identical T cell clones are located within the mouse gut epithelium and lamina propia and circulate in the thoracic duct lymph. *J Exp Med* 191:823-834.

44. Bhagat, G., A. J. Naiyer, J. G. Shah, J. Harper, B. Jabri, T. C. Wang, P. H. Green, and J. S. Manavalan. 2008. Small intestinal CD8+TCRgammadelta+NKG2A+ intraepithelial lymphocytes have attributes of regulatory cells in patients with celiac disease. *J Clin Invest* 118:281-293.

45. Cerf-Bensussan, N., and D. Guy-Grand. 1991. Intestinal intraepithelial lymphocytes. *Gastroenterol Clin North Am* 20:549-576.

46. Suzuki, H., K. I. Jeong, T. Okutani, and K. Doi. 2000. Regional variations in the distribution of small intestinal intraepithelial lymphocytes in three inbred strains of mice. *J Vet Med Sci* 62:881-887.

47. Helgeland, L., J. T. Vaage, B. Rolstad, T. S. Halstensen, T. Midtvedt, and P. Brandtzaeg. 1997. Regional phenotypic specialization of intraepithelial lymphocytes in the rat intestine does not depend on microbial colonization. *Scand J Immunol* 46:349-357.

48. Huleatt, J. W., and L. Lefrancois. 1996. Beta2 integrins and ICAM-1 are involved in establishment of the intestinal mucosal T cell compartment. *Immunity* 5:263-273.

49. Meharra, E. J., M. Schon, D. Hassett, C. Parker, W. Havran, and H. Gardner. 2000. Reduced gut intraepithelial lymphocytes in VLA1 null mice. *Cell Immunol* 201:1-5.

50. Kunkel, E. J., J. J. Campbell, G. Haraldsen, J. Pan, J. Boisvert, A. I. Roberts, E. C. Ebert, M. A. Vierra, S. B. Goodman, M. C. Genovese, A. J. Wardlaw, H. B. Greenberg, C. M. Parker, E. C. Butcher, D. P. Andrew, and W. W. Agace. 2000. Lymphocyte CC chemokine receptor 9 and epithelial thymus-expressed chemokine (TECK) expression distinguish the small intestinal immune compartment: Epithelial expression of tissue-specific chemokines as an organizing principle in regional immunity. *J Exp Med* 192:761-768.

51. Boismenu, R., L. Feng, Y. Y. Xia, J. C. Chang, and W. L. Havran. 1996. Chemokine expression by intraepithelial gamma delta T cells. Implications for the recruitment of inflammatory cells to damaged epithelia. *J Immunol* 157:985-992.

52. Shibahara, T., J. N. Wilcox, T. Couse, and J. L. Madara. 2001. Characterization of epithelial chemoattractants for human intestinal intraepithelial lymphocytes. *Gastroenterology* 120:60-70.

53. Holzmann, B., B. W. McIntyre, and I. L. Weissman. 1989. Identification of a murine Peyer's patch--specific lymphocyte homing receptor as an integrin molecule with an alpha chain homologous to human VLA-4 alpha. *Cell* 56:37-46.

54. Cepek, K. L., S. K. Shaw, C. M. Parker, G. J. Russell, J. S. Morrow, D. L. Rimm, and M. B. Brenner. 1994. Adhesion between epithelial cells and T lymphocytes mediated by E-cadherin and the alpha E beta 7 integrin. *Nature* 372:190-193.

55. Offit, P. A., and K. I. Dudzik. 1989. Rotavirus-specific cytotoxic T lymphocytes appear at the intestinal mucosal surface after rotavirus infection. *J Virol* 63:3507-3512.

56. Dharakul, T., L. Rott, and H. B. Greenberg. 1990. Recovery from chronic rotavirus infection in mice with severe combined immunodeficiency: virus clearance mediated by adoptive transfer of immune CD8+ T lymphocytes. *J Virol* 64:4375-4382.

57. Sydora, B. C., B. D. Jamieson, R. Ahmed, and M. Kronenberg. 1996. Intestinal intraepithelial lymphocytes respond to systemic lymphocytic choriomeningitis virus infection. *Cell Immunol* 167:161-169.

58. Muller, S., M. Buhler-Jungo, and C. Mueller. 2000. Intestinal intraepithelial lymphocytes exert potent protective cytotoxic activity during an acute virus infection. *J Immunol* 164:1986-1994.

59. Masopust, D., J. Jiang, H. Shen, and L. Lefrancois. 2001. Direct analysis of the dynamics of the intestinal mucosa CD8 T cell response to systemic virus infection. *J Immunol* 166:2348-2356.

60. Chardes, T., D. Buzoni-Gatel, A. Lepage, F. Bernard, and D. Bout. 1994. Toxoplasma gondii oral infection induces specific cytotoxic CD8 alpha/beta+ Thy-1+ gut intraepithelial lymphocytes, lytic for parasite-infected enterocytes. *J Immunol* 153:4596-4603.

61. Findly, R. C., S. J. Roberts, and A. C. Hayday. 1993. Dynamic response of murine gut intraepithelial T cells after infection by the coccidian parasite Eimeria. *Eur J Immunol* 23:2557-2564.

62. McDonald, V., H. A. Robinson, J. P. Kelly, and G. J. Bancroft. 1996. Immunity to Cryptosporidium muris infection in mice is expressed through gut CD4+ intraepithelial lymphocytes. *Infection and immunity* 64:2556-2562.

63. Kanwar, S. S., N. K. Ganguly, B. N. Walia, and R. C. Mahajan. 1986. Direct and antibody dependent cell mediated cytotoxicity against Giardia lamblia by splenic and intestinal lymphoid cells in mice. *Gut* 27:73-77.

64. Rose, J. R., M. B. Williams, L. S. Rott, E. C. Butcher, and H. B. Greenberg. 1998. Expression of the mucosal homing receptor alpha4beta7 correlates with the ability of CD8+ memory T cells to clear rotavirus infection. *J Virol* 72:726-730.

65. Pope, C., S. K. Kim, A. Marzo, D. Masopust, K. Williams, J. Jiang, H. Shen, and L. Lefrancois. 2001. Organ-specific regulation of the CD8 T cell response to Listeria monocytogenes infection. *J Immunol* 166:3402-3409.

66. Lepage, A. C., D. Buzoni-Gatel, D. T. Bout, and L. H. Kasper. 1998. Gut-derived intraepithelial lymphocytes induce long term immunity against Toxoplasma gondii. *J Immunol* 161:4902-4908.

67. Blumberg, R. S., C. E. Yockey, G. G. Gross, E. C. Ebert, and S. P. Balk. 1993. Human intestinal intraepithelial lymphocytes are derived from a limited number of T cell clones that utilize multiple V beta T cell receptor genes. *J Immunol* 150:5144-5153.

68. Gross, G. G., V. L. Schwartz, C. Stevens, E. C. Ebert, R. S. Blumberg, and S. P. Balk. 1994. Distribution of dominant T cell receptor beta chains in human intestinal mucosa. *J Exp Med* 180:1337-1344.

69. Van Kerckhove, C., G. J. Russell, K. Deusch, K. Reich, A. K. Bhan, H. DerSimonian, and M. B. Brenner. 1992. Oligoclonality of human intestinal intraepithelial T cells. *J Exp Med* 175:57-63.

70. Camerini, V., C. Panwala, and M. Kronenberg. 1993. Regional specialization of the mucosal immune system. Intraepithelial lymphocytes of the large intestine have a different phenotype and function than those of the small intestine. *J Immunol* 151:1765-1776.

71. Havran, W. L., and J. P. Allison. 1988. Developmentally ordered appearance of thymocytes expressing different T-cell antigen receptors. *Nature* 335:443-445.

72. Maloy, K. J., A. M. Mowat, R. Zamoyska, and I. N. Crispe. 1991. Phenotypic heterogeneity of intraepithelial T lymphocytes from mouse small intestine. *Immunology* 72:555-562.

73. Pennington, D. J., B. Silva-Santos, J. Shires, E. Theodoridis, C. Pollitt, E. L. Wise, R. E. Tigelaar, M. J. Owen, and A. C. Hayday. 2003. The inter-relatedness and interdependence of mouse T cell receptor gammadelta+ and alphabeta+ cells. *Nature immunology* 4:991-998.

74. Klein, J. R. 1986. Ontogeny of the Thy-1-, Lyt-2+ murine intestinal intraepithelial lymphocyte. Characterization of a unique population of thymus-independent cytotoxic effector cells in the intestinal mucosa. *J Exp Med* 164:309-314.

75. Guy-Grand, D., B. Rocha, P. Mintz, M. Malassis-Seris, F. Selz, B. Malissen, and P. Vassalli. 1994. Different use of T cell receptor transducing modules in two populations of gut intraepithelial lymphocytes are related to distinct pathways of T cell differentiation. *J Exp Med* 180:673-679.

76. Ohno, H., S. Ono, N. Hirayama, S. Shimada, and T. Saito. 1994. Preferential usage of the Fc receptor gamma chain in the T cell antigen receptor complex by gamma/delta T cells localized in epithelia. *J Exp Med* 179:365-369.

77. Ohteki, T., and H. R. MacDonald. 1993. Expression of the CD28 costimulatory molecule on subsets of murine intestinal intraepithelial lymphocytes correlates with lineage and responsiveness. *Eur J Immunol* 23:1251-1255.

78. Park, S. Y., H. Arase, K. Wakizaka, N. Hirayama, S. Masaki, S. Sato, J. V. Ravetch, and T. Saito. 1995. Differential contribution of the FcR gamma chain to the surface expression of the T cell receptor among T cells localized in epithelia: analysis of FcR gamma-deficient mice. *Eur J Immunol* 25:2107-2110.

79. Van Houten, N., P. F. Mixter, J. Wolfe, and R. C. Budd. 1993. CD2 expression on murine intestinal intraepithelial lymphocytes is bimodal and defines proliferative capacity. *Int Immunol* 5:665-672.

80. Liu, C. P., R. Ueda, J. She, J. Sancho, B. Wang, G. Weddell, J. Loring, C. Kurahara, E. C. Dudley, A. Hayday, and et al. 1993. Abnormal T cell

development in CD3-zeta-/- mutant mice and identification of a novel T cell population in the intestine. *EMBO J* 12:4863-4875.

81. Shires, J., E. Theodoridis, and A. C. Hayday. 2001. Biological insights into TCRgammadelta+ and TCRalphabeta+ intraepithelial lymphocytes provided by serial analysis of gene expression (SAGE). *Immunity* 15:419-434.

82. Pais, T. F., and R. Appelberg. 2000. Macrophage control of mycobacterial growth induced by picolinic acid is dependent on host cell apoptosis. *J Immunol* 164:389-397.

83. Iwata, M., A. Hirakiyama, Y. Eshima, H. Kagechika, C. Kato, and S. Y. Song. 2004. Retinoic acid imprints gut-homing specificity on T cells. *Immunity* 21:527-538.

84. Jarry, A., C. Bossard, C. Bou-Hanna, D. Masson, E. Espaze, M. G. Denis, and C. L. Laboisse. 2008. Mucosal IL-10 and TGF-beta play crucial roles in preventing LPS-driven, IFN-gamma-mediated epithelial damage in human colon explants. *J Clin Invest* 118:1132-1142.

85. Guy-Grand, D., B. Cuenod-Jabri, M. Malassis-Seris, F. Selz, and P. Vassalli. 1996. Complexity of the mouse gut T cell immune system: identification of two distinct natural killer T cell intraepithelial lineages. *Eur J Immunol* 26:2248-2256.

86. Groh, V., A. Steinle, S. Bauer, and T. Spies. 1998. Recognition of stress-induced MHC molecules by intestinal epithelial gammadelta T cells. *Science* 279:1737-1740.

87. Bahram, S., M. Bresnahan, D. E. Geraghty, and T. Spies. 1994. A Second Lineage of Mammalian Major Histocompatibility Complex Class I Genes. *PNAS* 91:6259-6263.

88. Li, P., S. T. Willie, S. Bauer, D. L. Morris, T. Spies, and R. K. Strong. 1999. Crystal structure of the MHC class I homolog MIC-A, a gammadelta T cell ligand. *Immunity* 10:577-584.

89. Boismenu, R., and W. L. Havran. 1994. Modulation of epithelial cell growth by intraepithelial gamma delta T cells. *Science* 266:1253-1255.

90. Yang, H., P. A. Antony, B. E. Wildhaber, and D. H. Teitelbaum. 2004. Intestinal intraepithelial lymphocyte gamma delta-T cell-derived keratinocyte growth factor modulates epithelial growth in the mouse. *J Immunol* 172:4151-4158.

91. Wingender, G., and M. Kronenberg. 2008. Role of NKT cells in the digestive system. IV. The role of canonical natural killer T cells in mucosal immunity and inflammation. *American journal of physiology* 294:G1-8.

92. Davies, A., S. Lopez-Briones, H. Ong, C. O'Neil-Marshall, F. A. Lemonnier, K. Nagaraju, E. S. Metcalf, and M. J. Soloski. 2004. Infection-induced expansion of a MHC Class Ib-dependent intestinal intraepithelial gammadelta T cell subset. *J Immunol* 172:6828-6837.

93. Bandeira, A., T. Mota-Santos, S. Itohara, S. Degermann, C. Heusser, S. Tonegawa, and A. Coutinho. 1990. Localization of gamma/delta T cells to the intestinal epithelium is independent of normal microbial colonization. *J Exp Med* 172:239-244.

94. Xiong, N., and D. H. Raulet. 2007. Development and selection of gammadelta T cells. *Immunological reviews* 215:15-31.

95. Pereira, P., V. Hermitte, M. P. Lembezat, L. Boucontet, V. Azuara, and K. Grigoriadou. 2000. Developmentally regulated and lineage-specific rearrangement of T cell receptor Valpha/delta gene segments. *Eur J Immunol* 30:1988-1997.

96. Crowley, M. P., A. M. Fahrer, N. Baumgarth, J. Hampl, I. Gutgemann, L. Teyton, and Y. Chien. 2000. A population of murine gammadelta T cells that recognize an inducible MHC class Ib molecule. *Science* 287:314-316.

97. Wingren, C., M. P. Crowley, M. Degano, Y. Chien, and I. A. Wilson. 2000. Crystal structure of a gammadelta T cell receptor ligand T22: a truncated MHC-like fold. *Science* 287:310-314.

98. Adams, E. J., Y. H. Chien, and K. C. Garcia. 2005. Structure of a gammadelta T cell receptor in complex with the nonclassical MHC T22. *Science* 308:227-231.

99. Adams, E. J., P. Strop, S. Shin, Y. H. Chien, and K. C. Garcia. 2008. An autonomous CDR3delta is sufficient for recognition of the nonclassical MHC class I molecules T10 and T22 by gammadelta T cells. *Nature immunology* 9:777-784.

100. Sciammas, R., and J. A. Bluestone. 1998. HSV-1 glycoprotein I-reactive TCR gamma delta cells directly recognize the peptide backbone in a conformationally dependent manner. *J Immunol* 161:5187-5192.

101. Sciammas, R., R. M. Johnson, A. I. Sperling, W. Brady, P. S. Linsley, P. G. Spear, F. W. Fitch, and J. A. Bluestone. 1994. Unique antigen recognition by a herpesvirus-specific TCR-gamma delta cell. *J Immunol* 152:5392-5397.

102. Chen, Z. W. 2005. Immune regulation of gammadelta T cell responses in mycobacterial infections. *Clinical immunology (Orlando, Fla* 116:202-207.

103. Hirsh, M. I., and W. G. Junger. 2008. Roles of Heat Shock Proteins and {gamma}{delta}T cells in Inflammation. *Am. J. Respir. Cell Mol. Biol.*:2008-0090TR.

104. Chen, H., X. He, Z. Wang, D. Wu, H. Zhang, C. Xu, H. He, L. Cui, D. Ba, and W. He. 2008. Identification of human T cell receptor gammadelta-recognized epitopes/proteins via CDR3delta peptide-based immunobiochemical strategy. *The Journal of biological chemistry* 283:12528-12537.

105. Scotet, E., L. O. Martinez, E. Grant, R. Barbaras, P. Jeno, M. Guiraud, B. Monsarrat, X. Saulquin, S. Maillet, J. P. Esteve, F. Lopez, B. Perret, X. Collet, M. Bonneville, and E. Champagne. 2005. Tumor recognition following Vgamma9Vdelta2 T cell receptor interactions with a surface F1-ATPase-related structure and apolipoprotein A-I. *Immunity* 22:71-80.

106. Correa, I., M. Bix, N. S. Liao, M. Zijlstra, R. Jaenisch, and D. Raulet. 1992. Most gamma delta T cells develop normally in beta 2-microglobulin-deficient mice. *Proc Natl Acad Sci U S A* 89:653-657.

107. Lin, T., G. Matsuzaki, H. Kenai, and K. Nomoto. 1994. Progenies of fetal thymocytes are the major source of CD4-CD8+ alpha alpha intestinal intraepithelial lymphocytes early in ontogeny. *Eur J Immunol* 24:1785-1791.

108. Lin, T., G. Matsuzaki, H. Yoshida, H. Kenai, K. Omoto, M. Umesue, C. Singaram, and K. Nomoto. 1996. Thymus ontogeny and the development of TCR alpha beta intestinal intraepithelial lymphocytes. *Cell Immunol* 171:132-139.

109. MacDonald, H. R., and M. P. Mycko. 2007. Development and selection of Valpha l4i NKT cells. *Curr Top Microbiol Immunol* 314:195-212.

110. Fujiura, Y., M. Kawaguchi, Y. Kondo, S. Obana, H. Yamamoto, M. Nanno, and H. Ishikawa. 1996. Development of CD8 alpha alpha+ intestinal intraepithelial T cells in beta 2-microglobulin- and/or TAP1-deficient mice. *J Immunol* 156:2710-2715.

111. Sydora, B. C., L. Brossay, A. Hagenbaugh, M. Kronenberg, and H. Cheroutre. 1996. TAP-independent selection of CD8+ intestinal intraepithelial lymphocytes. *J Immunol* 156:4209-4216.

112. Park, S. H., D. Guy-Grand, F. A. Lemonnier, C. R. Wang, A. Bendelac, and B. Jabri. 1999. Selection and expansion of CD8alpha/alpha(1) T cell receptor alpha/beta(1) intestinal intraepithelial lymphocytes in the absence of both classical major histocompatibility complex class I and nonclassical CD1 molecules. *J Exp Med* 190:885-890.

113. Spies, T., M. Bresnahan, S. Bahram, D. Arnold, G. Blanck, E. Mellins, D. Pious, and R. DeMars. 1990. A gene in the human major histocompatibility complex class II region controlling the class I antigen presentation pathway. *Nature* 348:744-747.

114. Monaco, J. J., S. Cho, and M. Attaya. 1990. Transport protein genes in the murine MHC: possible implications for antigen processing. *Science* 250:1723-1726.

115. Deverson, E. V., I. R. Gow, W. J. Coadwell, J. J. Monaco, G. W. Butcher, and J. C. Howard. 1990. MHC class II region encoding proteins related to the multidrug resistance family of transmembrane transporters. *Nature* 348:738-741.

116. Trowsdale, J., I. Hanson, I. Mockridge, S. Beck, A. Townsend, and A. Kelly. 1990. Sequences encoded in the class II region of the MHC related to the 'ABC' superfamily of transporters. *Nature* 348:741-744.

117. Holcombe, H. R., A. R. Castano, H. Cheroutre, M. Teitell, J. K. Maher, P. A. Peterson, and M. Kronenberg. 1995. Nonclassical behavior of the thymus leukemia antigen: peptide transporter-independent expression of a nonclassical class I molecule. *J Exp Med* 181:1433-1443.

118. Wu, M., L. van Kaer, S. Itohara, and S. Tonegawa. 1991. Highly restricted expression of the thymus leukemia antigens on intestinal epithelial cells. *J Exp Med* 174:213-218.

119. Joyce, S., P. Tabaczewski, R. H. Angeletti, S. G. Nathenson, and I. Stroynowski. 1994. A nonpolymorphic major histocompatibility complex class Ib molecule binds a large array of diverse self-peptides. *J Exp Med* 179:579-588.

120. Ungchusri, T., E. Y. Chiang, G. Brown, M. Chen, P. Tabaczewski, L. Timares, and I. Stroynowski. 2001. Widespread expression of the nonclassical class I Qa-2 antigens in hemopoietic and nonhemopoietic cells. *Immunogenetics* 53:455-467.

121. Das, G., D. S. Gould, M. M. Augustine, G. Fragoso, E. Sciutto, I. Stroynowski, L. Van Kaer, D. J. Schust, H. Ploegh, and C. A. Janeway, Jr. 2000. Qa-2-dependent selection of CD8alpha/alpha T cell receptor alpha/beta(+) cells in murine intestinal intraepithelial lymphocytes. *J Exp Med* 192:1521-1528.

122. Ljunggren, H. G., and K. Karre. 1990. In search of the 'missing self': MHC molecules and NK cell recognition. *Immunol Today* 11:237-244.

123. Bauer, S., V. Groh, J. Wu, A. Steinle, J. H. Phillips, L. L. Lanier, and T. Spies. 1999. Activation of NK cells and T cells by NKG2D, a receptor for stress-inducible MICA. *Science* 285:727-729.

124. Groh, V., R. Rhinehart, H. Secrist, S. Bauer, K. H. Grabstein, and T. Spies. 1999. Broad tumor-associated expression and recognition by tumor-derived gamma delta T cells of MICA and MICB. *Proc Natl Acad Sci U S A* 96:6879-6884.

125. Arase, H., E. S. Mocarski, A. E. Campbell, A. B. Hill, and L. L. Lanier. 2002. Direct recognition of cytomegalovirus by activating and inhibitory NK cell receptors. *Science* 296:1323-1326.

126. Lazetic, S., C. Chang, J. P. Houchins, L. L. Lanier, and J. H. Phillips. 1996. Human natural killer cell receptors involved in MHC class I recognition are disulfide-linked heterodimers of CD94 and NKG2 subunits. *J Immunol* 157:4741-4745.

127. Rodgers, J. R., and R. G. Cook. 2005. MHC class Ib molecules bridge innate and acquired immunity. *Nature reviews* 5:459-471.

128. Le Drean, E., F. Vely, L. Olcese, A. Cambiaggi, S. Guia, G. Krystal, N. Gervois, A. Moretta, F. Jotereau, and E. Vivier. 1998. Inhibition of antigen-induced T cell response and antibody-induced NK cell cytotoxicity by NKG2A: association of NKG2A with SHP-1 and SHP-2 protein-tyrosine phosphatases. *Eur J Immunol* 28:264-276.

129. Lanier, L. L., B. Corliss, J. Wu, and J. H. Phillips. 1998. Association of DAP12 with activating CD94/NKG2C NK cell receptors. *Immunity* 8:693-701.

130. Kaiser, B. K., F. Barahmand-Pour, W. Paulsene, S. Medley, D. E. Geraghty, and R. K. Strong. 2005. Interactions between NKG2x immunoreceptors and HLA-E ligands display overlapping affinities and thermodynamics. *J Immunol* 174:2878-2884.

131. LaBonte, M. L., E. I. Choi, and N. L. Letvin. 2004. Molecular determinants regulating the pairing of NKG2 molecules with CD94 for cell surface heterodimer expression. *J Immunol* 172:6902-6912.

132. Arlettaz, L., J. Villard, C. de Rham, S. Degermann, B. Chapuis, B. Huard, and E. Roosnek. 2004. Activating CD94:NKG2C and inhibitory CD94:NKG2A receptors are expressed by distinct subsets of committed CD8+ TCR alphabeta lymphocytes. *Eur J Immunol* 34:3456-3464.

133. Wu, J., Y. Song, A. B. Bakker, S. Bauer, T. Spies, L. L. Lanier, and J. H. Phillips. 1999. An activating immunoreceptor complex formed by NKG2D and DAP10. *Science* 285:730-732.

134. Borges, L., and D. Cosman. 2000. LIRs/ILTs/MIRs, inhibitory and stimulatory Ig-superfamily receptors expressed in myeloid and lymphoid cells. *Cytokine Growth Factor Rev* 11:209-217.

135. Anfossi, N., J. M. Doisne, M. A. Peyrat, S. Ugolini, O. Bonnaud, D. Bossy, V. Pitard, P. Merville, J. F. Moreau, J. F. Delfraissy, J. Dechanet-Merville, M. Bonneville, A. Venet, and E. Vivier. 2004. Coordinated expression of Ig-like inhibitory MHC class I receptors and acquisition of cytotoxic function in human CD8+ T cells. *J Immunol* 173:7223-7229.

136. Raulet, D. H., W. Held, I. Correa, J. R. Dorfman, M. F. Wu, and L. Corral. 1997. Specificity, tolerance and developmental regulation of natural killer cells defined by expression of class I-specific Ly49 receptors. *Immunological reviews* 155:41-52.

137. Ortaldo, J. R., and H. A. Young. 2005. Mouse Ly49 NK receptors: balancing activation and inhibition. *Mol Immunol* 42:445-450.

138. Natarajan, K., N. Dimasi, J. Wang, R. A. Mariuzza, and D. H. Margulies. 2002. Structure and function of natural killer cell receptors: multiple molecular solutions to self, nonself discrimination. *Annu.Rev.Immunol* 20:853-885.

139. Gardiner, C. M. 2008. Killer cell immunoglobulin-like receptors on NK cells: the how, where and why. *Int J Immunogenet* 35:1-8.

140. Bjorkman, P. J., M. A. Saper, B. Samraoui, W. S. Bennett, J. L. Strominger, and D. C. Wiley. 1987. The foreign antigen binding site and T cell recognition regions of class I histocompatibility antigens. *Nature* 329:512-518.

141. Bjorkman, P. J., M. A. Saper, B. Samraoui, W. S. Bennett, J. L. Strominger, and D. C. Wiley. 1987. Structure of the human class I histocompatibility antigen, HLA-A2. *Nature* 329:506-512.

142. He, X.-l., P. Tabaczewski, J. Ho, I. Stroynowski, and K. C. Garcia. 2001. Promiscuous Antigen Presentation by the Nonclassical MHC Ib Qa-2 Is Enabled by a Shallow, Hydrophobic Groove and Self-Stabilized Peptide Conformation. *Structure* 9:1213-1224.

143. Garboczi, D. N., P. Ghosh, U. Utz, Q. R. Fan, W. E. Biddison, and D. C. Wiley. 1996. Structure of the complex between human T-cell receptor, viral peptide and HLA-A2. *Nature* 384:134-141.

144. Kern, P. S., M. K. Teng, A. Smolyar, J. H. Liu, J. Liu, R. E. Hussey, R. Spoerl, H. C. Chang, E. L. Reinherz, and J. H. Wang. 1998. Structural basis of CD8 coreceptor function revealed by crystallographic analysis of a murine CD8alphaalpha ectodomain fragment in complex with H-2Kb. *Immunity* 9:519-530.

145. Boyington, J. C., S. A. Motyka, P. Schuck, A. G. Brooks, and P. D. Sun. 2000. Crystal structure of an NK cell immunoglobulin-like receptor in complex with its class I MHC ligand. *Nature* 405:537-543.

146. Kaiser, B. K., J. C. Pizarro, J. Kerns, and R. K. Strong. 2008. Structural basis for NKG2A/CD94 recognition of HLA-E. *Proc Natl Acad Sci U S A* 105:6696-6701.

147. Willcox, B. E., L. M. Thomas, and P. J. Bjorkman. 2003. Crystal structure of HLA-A2 bound to LIR-1, a host and viral major histocompatibility complex receptor. *Nature immunology* 4:913-919.

148. Tormo, J., K. Natarajan, D. H. Margulies, and R. A. Mariuzza. 1999. Crystal structure of a lectin-like natural killer cell receptor bound to its MHC class I ligand. *Nature* 402:623-631.

149. Dam, J., R. Guan, K. Natarajan, N. Dimasi, L. K. Chlewicki, D. M. Kranz, P. Schuck, D. H. Margulies, and R. A. Mariuzza. 2003. Variable MHC class I engagement by Ly49 natural killer cell receptors demonstrated by the crystal structure of Ly49C bound to H-2K(b). *Nature immunology* 4:1213-1222.

150. Li, P., G. McDermott, and R. K. Strong. 2002. Crystal structures of RAE-1beta and its complex with the activating immunoreceptor NKG2D. *Immunity* 16:77-86.

151. Radaev, S., B. Rostro, A. G. Brooks, M. Colonna, and P. D. Sun. 2001. Conformational plasticity revealed by the cocrystal structure of NKG2D and its class I MHC-like ligand ULBP3. *Immunity* 15:1039-1049.

152. Li, P., D. L. Morris, B. E. Willcox, A. Steinle, T. Spies, and R. K. Strong. 2001. Complex structure of the activating immunoreceptor NKG2D and its MHC class I-like ligand MICA. *Nature immunology* 2:443-451.

153. Dimasi, N., L. Moretta, and R. Biassoni. 2004. Structure of the Ly49 family of natural killer (NK) cell receptors and their interaction with MHC class I molecules. *Immunol Res* 30:95-104.

154. Treiner, E., and O. Lantz. 2006. CD1d- and MR1-restricted invariant T cells: of mice and men. *Current opinion in immunology* 18:519-526.

155. Diefenbach, A., A. M. Jamieson, S. D. Liu, N. Shastri, and D. H. Raulet. 2000. Ligands for the murine NKG2D receptor: expression by tumor cells and activation of NK cells and macrophages. *Nat.Immunol* 1:119-126.

156. Cerwenka, A., A. B. Bakker, T. McClanahan, J. Wagner, J. Wu, J. H. Phillips, and L. L. Lanier. 2000. Retinoic acid early inducible genes define a ligand family for the activating NKG2D receptor in mice. *Immunity* 12:721-727.

157. Cosman, D., J. Mullberg, C. L. Sutherland, W. Chin, R. Armitage, W. Fanslow, M. Kubin, and N. J. Chalupny. 2001. ULBPs, novel MHC class I-related molecules, bind to CMV glycoprotein UL16 and stimulate NK cytotoxicity through the NKG2D receptor. *Immunity* 14:123-133.

158. Vance, R. E., A. M. Jamieson, and D. H. Raulet. 1999. Recognition of the class Ib molecule Qa-1(b) by putative activating receptors CD94/NKG2C and CD94/NKG2E on mouse natural killer cells. *J Exp Med* 190:1801-1812.

159. Mingari, M. C., C. Vitale, C. Cantoni, R. Bellomo, M. Ponte, F. Schiavetti, S. Bertone, A. Moretta, and L. Moretta. 1997. Interleukin-15-induced maturation of human natural killer cells from early thymic precursors: selective expression of CD94/NKG2-A as the only HLA class I-specific inhibitory receptor. *Eur J Immunol* 27:1374-1380.

160. Mingari, M. C., A. Moretta, and L. Moretta. 1998. Regulation of KIR expression in human T cells: a safety mechanism that may impair protective T-cell responses. *Immunol Today* 19:153-157.

161. Mingari, M. C., M. Ponte, S. Bertone, F. Schiavetti, C. Vitale, R. Bellomo, A. Moretta, and L. Moretta. 1998. HLA class I-specific inhibitory receptors in human T lymphocytes: interleukin 15-induced expression of CD94/NKG2A in superantigen- or alloantigen-activated CD8+ T cells. *Proc Natl Acad Sci U S A* 95:1172-1177.

162. Gunturi, A., R. E. Berg, E. Crossley, S. Murray, and J. Forman. 2005. The role of TCR stimulation and TGF-beta in controlling the expression of CD94/NKG2A receptors on CD8 T cells. *Eur J Immunol* 35:766-775.

163. Endt, J., F. E. McCann, C. R. Almeida, D. Urlaub, R. Leung, D. Pende, D. M. Davis, and C. Watzl. 2007. Inhibitory receptor signals suppress ligation-induced recruitment of NKG2D to GM1-rich membrane domains at the human NK cell immune synapse. *J Immunol* 178:5606-5611.

164. Pende, D., C. Cantoni, P. Rivera, M. Vitale, R. Castriconi, S. Marcenaro, M. Nanni, R. Biassoni, C. Bottino, A. Moretta, and L. Moretta. 2001. Role of NKG2D in tumor cell lysis mediated by human NK cells: cooperation with natural cytotoxicity receptors and capability of recognizing tumors of nonepithelial origin. *Eur J Immunol* 31:1076-1086.

165. Aldrich, C. J., R. Waltrip, E. Hermel, M. Attaya, K. F. Lindahl, J. J. Monaco, and J. Forman. 1992. T cell recognition of QA-1b antigens on cells lacking a functional Tap-2 transporter. *J Immunol* 149:3773-3777.

166. Bai, A., C. J. Aldrich, and J. Forman. 2000. Factors controlling the trafficking and processing of a leader-derived peptide presented by Qa-1. *J Immunol* 165:7025-7034.

167. Davies, A., S. Kalb, B. Liang, C. J. Aldrich, F. A. Lemonnier, H. Jiang, R. Cotter, and M. J. Soloski. 2003. A peptide from heat shock protein 60 is the dominant peptide bound to Qa-1 in the absence of the MHC class Ia leader sequence peptide Qdm. *J Immunol* 170:5027-5033.

168. Wooden, S. L., S. R. Kalb, R. J. Cotter, and M. J. Soloski. 2005. Cutting edge: HLA-E binds a peptide derived from the ATP-binding cassette transporter multidrug resistance-associated protein 7 and inhibits NK cell-mediated lysis. *J Immunol* 175:1383-1387.

169. Bland, F. A., M. K. Lemberg, A. J. McMichael, B. Martoglio, and V. M. Braud. 2003. Requirement of the proteasome for the trimming of signal peptide-derived epitopes presented by the nonclassical major histocompatibility complex class I molecule HLA-E. *The Journal of biological chemistry* 278:33747-33752.

170. Vance, R. E., J. R. Kraft, J. D. Altman, P. E. Jensen, and D. H. Raulet. 1998. Mouse CD94/NKG2A is a natural killer cell receptor for the nonclassical major histocompatibility complex (MHC) class I molecule Qa-1(b). *J Exp Med* 188:1841-1848.

171. Soloski, M. J., A. DeCloux, C. J. Aldrich, and J. Forman. 1995. Structural and functional characteristics of the class IB molecule, Qa-1. *Immunological reviews* 147:67-89.

172. Kambayashi, T., J. R. Kraft-Leavy, J. G. Dauner, B. A. Sullivan, O. Laur, and P. E. Jensen. 2004. The nonclassical MHC class I molecule Qa-1 forms unstable peptide complexes. *J Immunol* 172:1661-1669.

173. Cotterill, L. A., H. J. Stauss, M. M. Millrain, D. J. Pappin, D. Rahman, B. Canas, P. Chandler, A. Stackpoole, E. Simpson, P. J. Robinson, and P. J. Dyson. 1997. Qa-1 interaction and T cell recognition of the Qa-1 determinant modifier peptide. *Eur J Immunol* 27:2123-2132.

174. Kurepa, Z., C. A. Hasemann, and J. Forman. 1998. Qa-1b binds conserved class I leader peptides derived from several mammalian species. *J Exp Med* 188:973-978.

175. Kurepa, Z., and J. Forman. 1997. Peptide binding to the class Ib molecule, Qa-1b. *J Immunol* 158:3244-3251.

176. Kraft, J. R., R. E. Vance, J. Pohl, A. M. Martin, D. H. Raulet, and P. E. Jensen. 2000. Analysis of Qa-1(b) peptide binding specificity and the capacity of CD94/NKG2A to discriminate between Qa-1-peptide complexes. *J Exp Med* 192:613-624.

177. Aldrich, C. J., A. DeCloux, A. S. Woods, R. J. Cotter, M. J. Soloski, and J. Forman. 1994. Identification of a Tap-dependent leader peptide recognized by alloreactive T cells specific for a class Ib antigen. *Cell* 79:649-658.

178. Matsumura, M., D. H. Fremont, P. A. Peterson, and I. A. Wilson. 1992. Emerging principles for the recognition of peptide antigens by MHC class I molecules. *Science* 257:927-934.

179. Tompkins, S. M., J. R. Kraft, C. T. Dao, M. J. Soloski, and P. E. Jensen. 1998. Transporters associated with antigen processing (TAP)-independent presentation of soluble insulin to alpha/beta T cells by the class Ib gene product, Qa-1(b). *J Exp Med* 188:961-971.

180. Tang, X., I. Maricic, N. Purohit, B. Bakamjian, L. M. Reed-Loisel, T. Beeston, P. Jensen, and V. Kumar. 2006. Regulation of immunity by a novel population of Qa-1-restricted CD8alphaalpha+TCRalphabeta+ T cells. *J Immunol* 177:7645-7655.

181. Hoare, H. L., L. C. Sullivan, C. S. Clements, L. K. Ely, T. Beddoe, K. N. Henderson, J. Lin, H. H. Reid, A. G. Brooks, and J. Rossjohn. 2008. Subtle changes in peptide conformation profoundly affect recognition of the non-classical MHC class I molecule HLA-E by the CD94-NKG2 natural killer cell receptors. *J Mol Biol* 377:1297-1303.

182. Petrie, E. J., C. S. Clements, J. Lin, L. C. Sullivan, D. Johnson, T. Huyton, A. Heroux, H. L. Hoare, T. Beddoe, H. H. Reid, M. C. Wilce, A. G. Brooks, and J. Rossjohn. 2008. CD94-NKG2A recognition of human leukocyte antigen (HLA)-E bound to an HLA class I leader sequence. *J Exp Med* 205:725-735.

183. Suemizu, H., M. Radosavljevic, M. Kimura, S. Sadahiro, S. Yoshimura, S. Bahram, and H. Inoko. 2002. A basolateral sorting motif in the MICA cytoplasmic tail. *Proc Natl Acad Sci U S A* 99:2971-2976.

184. Eagle, R. A., and J. Trowsdale. 2007. Promiscuity and the single receptor: NKG2D. *Nature reviews* 7:737-744.

185. Gasser, S., S. Orsulic, E. J. Brown, and D. H. Raulet. 2005. The DNA damage pathway regulates innate immune system ligands of the NKG2D receptor. *Nature* 436:1186-1190.

186. Nomura, M., Z. Zou, T. Joh, Y. Takihara, Y. Matsuda, and K. Shimada. 1996. Genomic structures and characterization of Rae1 family members encoding GPI-

anchored cell surface proteins and expressed predominantly in embryonic mouse brain. *J Biochem.(Tokyo)* 120:987-995.

187. Carayannopoulos, L. N., O. V. Naidenko, D. H. Fremont, and W. M. Yokoyama. 2002. Cutting Edge: Murine UL16-Binding Protein-Like Transcript 1: A Newly Described Transcript Encoding a High-Affinity Ligand for Murine NKG2D. *The Journal of Immunology* 169:4079-4083.

188. Diefenbach, A., J. K. Hsia, M. Y. Hsiung, and D. H. Raulet. 2003. A novel ligand for the NKG2D receptor activates NK cells and macrophages and induces tumor immunity. *Eur J Immunol* 33:381-391.

189. Takada, A., S. Yoshida, M. Kajikawa, Y. Miyatake, U. Tomaru, M. Sakai, H. Chiba, K. Maenaka, D. Kohda, K. Fugo, and M. Kasahara. 2008. Two novel NKG2D ligands of the mouse H60 family with differential expression patterns and binding affinities to NKG2D. *J Immunol* 180:1678-1685.

190. Carayannopoulos, L. N., O. V. Naidenko, J. Kinder, E. L. Ho, D. H. Fremont, and W. M. Yokoyama. 2002. Ligands for murine NKG2D display heterogeneous binding behavior. *Eur J Immunol* 32:597-605.

191. Gianfrani, C., S. Auricchio, and R. Troncone. 2005. Adaptive and innate immune responses in celiac disease. *Immunology letters* 99:141-145.

192. Hue, S., J. J. Mention, R. C. Monteiro, S. Zhang, C. Cellier, J. Schmitz, V. Verkarre, N. Fodil, S. Bahram, N. Cerf-Bensussan, and S. Caillat-Zucman. 2004. A direct role for NKG2D/MICA interaction in villous atrophy during celiac disease. *Immunity* 21:367-377.

193. Meresse, B., S. A. Curran, C. Ciszewski, G. Orbelyan, M. Setty, G. Bhagat, L. Lee, M. Tretiakova, C. Semrad, E. Kistner, R. J. Winchester, V. Braud, L. L. Lanier, D. E. Geraghty, P. H. Green, S. Guandalini, and B. Jabri. 2006. Reprogramming of CTLs into natural killer-like cells in celiac disease. *J Exp Med* 203:1343-1355.

194. Meresse, B., Z. Chen, C. Ciszewski, M. Tretiakova, G. Bhagat, T. N. Krausz, D. H. Raulet, L. L. Lanier, V. Groh, T. Spies, E. C. Ebert, P. H. Green, and B. Jabri. 2004. Coordinated induction by IL15 of a TCR-independent NKG2D signaling

pathway converts CTL into lymphokine-activated killer cells in celiac disease. *Immunity* 21:357-366.

195. Denning, T. L., S. Granger, D. Mucida, R. Graddy, G. Leclercq, W. Zhang, K. Honey, J. P. Rasmussen, H. Cheroutre, A. Y. Rudensky, and M. Kronenberg. 2007. Mouse TCRalphabeta+CD8alphaalpha intraepithelial lymphocytes express genes that down-regulate their antigen reactivity and suppress immune responses. *J Immunol* 178:4230-4239.

196. Laouar, A., M. Manocha, M. Wan, H. Yagita, R. A. van Lier, and N. Manjunath. 2007. Cutting Edge: Distinct NK receptor profiles are imprinted on CD8 T cells in the mucosa and periphery during the same antigen challenge: role of tissue-specific factors. *J Immunol* 178:652-656.

197. Niederkorn, J. Y. 2006. See no evil, hear no evil, do no evil: the lessons of immune privilege. *Nature immunology* 7:354-359.

198. Streilein, J. W. 2003. Ocular immune privilege: therapeutic opportunities from an experiment of nature. *Nature reviews* 3:879-889.

199. Kaplan, H. J., and J. W. Streilein. 1977. Immune response to immunization via the anterior chamber of the eye. I. F. lymphocyte-induced immune deviation. *J Immunol* 118:809-814.

200. Medawar, P. B. 1948. Immunity to homologous grafted skin; the fate of skin homografts transplanted to the brain, to subcutaneous tissue, and to the anterior chamber of the eye. *Br J Exp Pathol* 29:58-69.

201. Abi-Hanna, D., D. Wakefield, and S. Watkins. 1988. HLA antigens in ocular tissues. I. In vivo expression in human eyes. *Transplantation* 45:610-613.

202. Lampson, L. A., and C. A. Fisher. 1984. Weak HLA and beta 2-microglobulin expression of neuronal cell lines can be modulated by interferon. *Proc Natl Acad Sci U S A* 81:6476-6480.

203. Le Bouteiller, P. 1994. HLA class I chromosomal region, genes, and products: facts and questions. *Crit Rev Immunol* 14:89-129.

204. Griffith, T. S., T. Brunner, S. M. Fletcher, D. R. Green, and T. A. Ferguson. 1995. Fas ligand-induced apoptosis as a mechanism of immune privilege. *Science* 270:1189-1192.

205. Stuart, P. M., T. S. Griffith, N. Usui, J. Pepose, X. Yu, and T. A. Ferguson. 1997. CD95 ligand (FasL)-induced apoptosis is necessary for corneal allograft survival. *J Clin Invest* 99:396-402.

206. Yamagami, S., H. Kawashima, T. Tsuru, H. Yamagami, N. Kayagaki, H. Yagita, K. Okumura, and D. S. Gregerson. 1997. Role of Fas-Fas ligand interactions in the immunorejection of allogeneic mouse corneal transplants. *Transplantation* 64:1107-1111.

207. Jerzak, M., and P. Bischof. 2002. Apoptosis in the first trimester human placenta: the role in maintaining immune privilege at the maternal-foetal interface and in the trophoblast remodelling. *Eur J Obstet Gynecol Reprod Biol* 100:138-142.

208. Choi, C., and E. N. Benveniste. 2004. Fas ligand/Fas system in the brain: regulator of immune and apoptotic responses. *Brain Res Brain Res Rev* 44:65-81.

209. Sata, M., T. Suhara, and K. Walsh. 2000. Vascular endothelial cells and smooth muscle cells differ in expression of Fas and Fas ligand and in sensitivity to Fas ligand-induced cell death: implications for vascular disease and therapy. *Arterioscler Thromb Vasc Biol* 20:309-316.

210. Walsh, K., and M. Sata. 1999. Is extravasation a Fas-regulated process? *Mol Med Today* 5:61-67.

211. Lee, H. O., J. M. Herndon, R. Barreiro, T. S. Griffith, and T. A. Ferguson. 2002. TRAIL: a mechanism of tumor surveillance in an immune privileged site. *J Immunol* 169:4739-4744.

212. Phillips, T. A., J. Ni, G. Pan, S. M. Ruben, Y. F. Wei, J. L. Pace, and J. S. Hunt. 1999. TRAIL (Apo-2L) and TRAIL receptors in human placentas: implications for immune privilege. *J Immunol* 162:6053-6059.

213. Wang, S., Z. F. Boonman, H. C. Li, Y. He, M. J. Jager, R. E. Toes, and J. Y. Niederkorn. 2003. Role of TRAIL and IFN-gamma in CD4+ T cell-dependent tumor rejection in the anterior chamber of the eye. *J Immunol* 171:2789-2796.

214. Bora, N. S., C. L. Gobleman, J. P. Atkinson, J. S. Pepose, and H. J. Kaplan. 1993. Differential expression of the complement regulatory proteins in the human eye. *Invest Ophthalmol Vis Sci* 34:3579-3584.

215. Holmes, C. H., K. L. Simpson, H. Okada, N. Okada, S. D. Wainwright, D. F. Purcell, and J. M. Houlihan. 1992. Complement regulatory proteins at the feto-maternal interface during human placental development: distribution of CD59 by comparison with membrane cofactor protein (CD46) and decay accelerating factor (CD55). *Eur J Immunol* 22:1579-1585.

216. Holmes, C. H., K. L. Simpson, S. D. Wainwright, C. G. Tate, J. M. Houlihan, I. H. Sawyer, I. P. Rogers, F. A. Spring, D. J. Anstee, and M. J. Tanner. 1990. Preferential expression of the complement regulatory protein decay accelerating factor at the fetomaternal interface during human pregnancy. *J Immunol* 144:3099-3105.

217. Lass, J. H., E. I. Walter, T. E. Burris, H. E. Grossniklaus, M. I. Roat, D. L. Skelnik, L. Needham, M. Singer, and M. E. Medof. 1990. Expression of two molecular forms of the complement decay-accelerating factor in the eye and lacrimal gland. *Invest Ophthalmol Vis Sci* 31:1136-1148.

218. Sohn, J. H., H. J. Kaplan, H. J. Suk, P. S. Bora, and N. S. Bora. 2000. Chronic low level complement activation within the eye is controlled by intraocular complement regulatory proteins. *Invest Ophthalmol Vis Sci* 41:3492-3502.

219. Sohn, J. H., H. J. Kaplan, H. J. Suk, P. S. Bora, and N. S. Bora. 2000. Complement regulatory activity of normal human intraocular fluid is mediated by MCP, DAF, and CD59. *Invest Ophthalmol Vis Sci* 41:4195-4202.

220. Rooney, I. A., T. J. Oglesby, and J. P. Atkinson. 1993. Complement in human reproduction: activation and control. *Immunol Res* 12:276-294.

221. Xu, C., D. Mao, V. M. Holers, B. Palanca, A. M. Cheng, and H. Molina. 2000. A critical role for murine complement regulator crry in fetomaternal tolerance. *Science* 287:498-501.

222. Harrower, T. P., A. Richards, G. Cruz, L. Copeman, S. B. Dunnett, and R. A. Barker. 2004. Complement regulatory proteins are expressed at low levels in embryonic human, wild type and transgenic porcine neural tissue. *Xenotransplantation* 11:60-71.

223. Singhrao, S. K., J. W. Neal, N. K. Rushmere, B. P. Morgan, and P. Gasque. 1999. Differential expression of individual complement regulators in the brain and choroid plexus. *Laboratory investigation; a journal of technical methods and pathology* 79:1247-1259.

224. Zou, L., N. Sato, B. O. Attuwaybi, and B. C. Kone. 2003. Delayed administration of alpha-melanocyte-stimulating hormone or combined therapy with BAY 11-7085 protects against gut ischemia-reperfusion injury. *Shock* 20:469-475.

225. LeMaoult, J., M. Le Discorde, N. Rouas-Freiss, P. Moreau, C. Menier, J. McCluskey, and E. D. Carosella. 2003. Biology and functions of human leukocyte antigen-G in health and sickness. *Tissue antigens* 62:273-284.

226. Ishitani, A., and D. E. Geraghty. 1992. Alternative splicing of HLA-G transcripts yields proteins with primary structures resembling both class I and class II antigens. *Proc.Natl.Acad.Sci.U.S.A* 89:3947-3951.

227. Kirszenbaum, M., P. Moreau, E. Gluckman, J. Dausset, and E. Carosella. 1994. An alternatively spliced form of HLA-G mRNA in human trophoblasts and evidence for the presence of HLA-G transcript in adult lymphocytes. *Proc.Natl.Acad.Sci.U.S.A* 91:4209-4213.

228. Fujii, T., A. Ishitani, and D. E. Geraghty. 1994. A soluble form of the HLA-G antigen is encoded by a messenger ribonucleic acid containing intron 4. *J Immunol* 153:5516-5524.

229. Moreau, P., E. Carosella, M. Teyssier, S. Prost, E. Gluckman, J. Dausset, and M. Kirszenbaum. 1995. Soluble HLA-G molecule. An alternatively spliced HLA-G

mRNA form candidate to encode it in peripheral blood mononuclear cells and human trophoblasts. *Human immunology* 43:231-236.

230. Paul, P., F. A. Cabestre, E. C. Ibrahim, S. Lefebvre, I. Khalil-Daher, G. Vazeux, R. M. Quiles, F. Bermond, J. Dausset, and E. D. Carosella. 2000. Identification of HLA-G7 as a new splice variant of the HLA-G mRNA and expression of soluble HLA-G5, -G6, and -G7 transcripts in human transfected cells. *Human immunology* 61:1138-1149.

231. Soderstrom, K., B. Corliss, L. L. Lanier, and J. H. Phillips. 1997. CD94/NKG2 is the predominant inhibitory receptor involved in recognition of HLA-G by decidual and peripheral blood NK cells. *J Immunol* 159:1072-1075.

232. King, A., D. S. Allan, M. Bowen, S. J. Powis, S. Joseph, S. Verma, S. E. Hiby, A. J. McMichael, Y. W. Loke, and V. M. Braud. 2000. HLA-E is expressed on trophoblast and interacts with CD94/NKG2 receptors on decidual NK cells. *Eur J Immunol* 30:1623-1631.

233. Ponte, M., C. Cantoni, R. Biassoni, A. Tradori-Cappai, G. Bentivoglio, C. Vitale, S. Bertone, A. Moretta, L. Moretta, and M. C. Mingari. 1999. Inhibitory receptors sensing HLA-G1 molecules in pregnancy: decidua-associated natural killer cells express LIR-1 and CD94/NKG2A and acquire p49, an HLA-G1-specific receptor. *Proc Natl Acad Sci U S A* 96:5674-5679.

234. Eidukaite, A., A. Siaurys, and V. Tamosiunas. 2004. Differential expression of KIR/NKAT2 and CD94 molecules on decidual and peripheral blood CD56bright and CD56dim natural killer cell subsets. *Fertil Steril* 81 Suppl 1:863-868.

235. Kusumi, M., T. Yamashita, T. Fujii, T. Nagamatsu, S. Kozuma, and Y. Taketani. 2006. Expression patterns of lectin-like natural killer receptors, inhibitory CD94/NKG2A, and activating CD94/NKG2C on decidual CD56bright natural killer cells differ from those on peripheral CD56dim natural killer cells. *Journal of reproductive immunology* 70:33-42.

236. Navarro, F., M. Llano, T. Bellon, M. Colonna, D. E. Geraghty, and M. Lopez-Botet. 1999. The ILT2(LIR1) and CD94/NKG2A NK cell receptors respectively recognize HLA-G1 and HLA-E molecules co-expressed on target cells. *Eur J Immunol* 29:277-283.

237. Colonna, M., J. Samaridis, M. Cella, L. Angman, R. L. Allen, C. A. O'Callaghan, R. Dunbar, G. S. Ogg, V. Cerundolo, and A. Rolink. 1998. Human myelomonocytic cells express an inhibitory receptor for classical and nonclassical MHC class I molecules. *J Immunol* 160:3096-3100.

238. Rajagopalan, S., and E. O. Long. 1999. A human histocompatibility leukocyte antigen (HLA)-G-specific receptor expressed on all natural killer cells. *J Exp Med* 189:1093-1100.

239. Shiroishi, M., K. Tsumoto, K. Amano, Y. Shirakihara, M. Colonna, V. M. Braud, D. S. Allan, A. Makadzange, S. Rowland-Jones, B. Willcox, E. Y. Jones, P. A. van der Merwe, I. Kumagai, and K. Maenaka. 2003. Human inhibitory receptors Ig-like transcript 2 (ILT2) and ILT4 compete with CD8 for MHC class I binding and bind preferentially to HLA-G. *Proc Natl Acad Sci U S A* 100:8856-8861.

240. Menier, C., B. Riteau, E. D. Carosella, and N. Rouas-Freiss. 2002. MICA triggering signal for NK cell tumor lysis is counteracted by HLA-G1-mediated inhibitory signal. *Int J Cancer* 100:63-70.

241. Contini, P., M. Ghio, A. Poggi, G. Filaci, F. Indiveri, S. Ferrone, and F. Puppo. 2003. Soluble HLA-A,-B,-C and -G molecules induce apoptosis in T and NK CD8+ cells and inhibit cytotoxic T cell activity through CD8 ligation. *Eur J Immunol* 33:125-134.

242. Horuzsko, A., F. Lenfant, D. H. Munn, and A. L. Mellor. 2001. Maturation of antigen-presenting cells is compromised in HLA-G transgenic mice. *Int Immunol* 13:385-394.

243. Liang, S., B. Baibakov, and A. Horuzsko. 2002. HLA-G inhibits the functions of murine dendritic cells via the PIR-B immune inhibitory receptor. *Eur J Immunol* 32:2418-2426.

244. Liang, S., and A. Horuzsko. 2003. Mobilizing dendritic cells for tolerance by engagement of immune inhibitory receptors for HLA-G. *Human immunology* 64:1025-1032.

245. McIntire, R. H., P. J. Morales, M. G. Petroff, M. Colonna, and J. S. Hunt. 2004. Recombinant HLA-G5 and -G6 drive U937 myelomonocytic cell production of TGF-beta1. *Journal of leukocyte biology* 76:1220-1228.

246. Cosman, D., M. Kress, G. Khoury, and G. Jay. 1982. Tissue-specific expression of an unusual H-2 (class I)-related gene. *Proc Natl Acad Sci U S A* 79:4947-4951.

247. Mellor, A. L., E. H. Weiss, M. Kress, G. Jay, and R. A. Flavell. 1984. A nonpolymorphic class I gene in the murine major histocompatibility complex. *Cell* 36:139-144.

248. Hershberg, R., P. Eghtesady, B. Sydora, K. Brorson, H. Cheroutre, R. Modlin, and M. Kronenberg. 1990. Expression of the thymus leukemia antigen in mouse intestinal epithelium. *Proc Natl Acad Sci U S A* 87:9727-9731.

249. Wang, Q., and L. Flaherty. 1996. Developmental expression of the mouse MHC Q genes. *Eur J Immunogenet* 23:121-127.

250. Wang, Q., J. Geliebter, S. Tonkonogy, and L. Flaherty. 1993. Expression of the Q2 gene of the MHC in thymus and intestinal epithelial cells. *Immunogenetics* 38:370-372.

251. Devlin, J. J., A. M. Lew, R. A. Flavell, and J. E. Coligan. 1985. Secretion of a soluble class I molecule encoded by the Q10 gene of the C57BL/10 mouse. *Embo J* 4:369-374.

252. Zappacosta, F., P. Tabaczewski, K. C. Parker, J. E. Coligan, and I. Stroynowski. 2000. The murine liver-specific nonclassical MHC class I molecule Q10 binds a classical peptide repertoire. *J Immunol* 164:1906-1915.

253. Weiss, E. H. 1987. Molecular biology of the mouse Q region. *Immunol Res* 6:179-191.

254. Weber, D. A., A. Attinger, C. C. Kemball, J. L. Wigal, J. Pohl, Y. Xiong, E. L. Reinherz, H. Cheroutre, M. Kronenberg, and P. E. Jensen. 2002. Peptide-independent folding and CD8 alpha alpha binding by the nonclassical class I molecule, thymic leukemia antigen. *J Immunol* 169:5708-5714.

255. Perarnau, B., M. F. Saron, B. R. San Martin, N. Bervas, H. Ong, M. J. Soloski, A. G. Smith, J. M. Ure, J. E. Gairin, and F. A. Lemonnier. 1999. Single H2Kb, H2Db and double H2KbDb knockout mice: peripheral CD8+ T cell repertoire and anti-lymphocytic choriomeningitis virus cytolytic responses. *Eur J Immunol* 29:1243-1252.

256. Chiang, E. Y., M. Henson, and I. Stroynowski. 2002. The nonclassical major histocompatibility complex molecule Qa-2 protects tumor cells from NK cell- and lymphokine-activated killer cell-mediated cytolysis. *J Immunol* 168:2200-2211.

257. Lo, W. F., C. D. Dunn, H. Ong, E. S. Metcalf, and M. J. Soloski. 2004. Bacterial and host factors involved in the major histocompatibility complex class Ib-restricted presentation of Salmonella Hsp 60: novel pathway. *Infection and immunity* 72:2843-2849.

258. Stroynowski, I., M. Soloski, M. G. Low, and L. Hood. 1987. A single gene encodes soluble and membrane-bound forms of the major histocompatibility Qa-2 antigen: anchoring of the product by a phospholipid tail. *Cell* 50:759-768.

259. Plaut, M., L. M. Lichtenstein, E. Gillespie, and C. S. Henney. 1973. Studies on the mechanism of lymphocyte-mediated cytolysis. IV. Specificity of the histamine receptor on effector T cells. *J Immunol* 111:389-394.

260. Cikes, M., S. Friberg, Jr., and G. Klein. 1973. Progressive loss of H-2 antigens with concomitant increase of cell-surface antigen(s) determined by Moloney leukemia virus in cultured murine lymphomas. *J Natl Cancer Inst* 50:347-362.

261. Karre, K., H. G. Ljunggren, G. Piontek, and R. Kiessling. 1986. Selective rejection of H-2-deficient lymphoma variants suggests alternative immune defence strategy. *Nature* 319:675-678.

262. Hermel, E., C. Smith, and C. J. Aldrich. 2000. Allogeneic responses to the class Ib antigen Qa1: limited T-cell receptor Valpha but not Vbeta chain usage. *Immunogenetics* 51:600-605.

263. Guenet, J. L., and F. Bonhomme. 2003. Wild mice: an ever-increasing contribution to a popular mammalian model. *Trends Genet* 19:24-31.

264. Sipes, S. L., M. V. Medaglia, D. L. Stabley, C. S. DeBruyn, M. S. Alden, V. Catenacci, and C. P. Landel. 1996. A new major histocompatibility complex class I b gene expressed in the mouse blastocyst and placenta. *Immunogenetics* 45:108-120.

265. Bookout, A. L., and D. J. Mangelsdorf. 2003. Quantitative real-time PCR protocol for analysis of nuclear receptor signaling pathways. *Nuclear receptor signaling* 1:e012.

266. Fulton, J. E., E. L. Thacker, L. D. Bacon, and H. D. Hunt. 1995. Functional analysis of avian class I (BFIV) glycoproteins by epitope tagging and mutagenesis in vitro. *Eur J Immunol* 25:2069-2076.

267. Horton, R. M., Z. L. Cai, S. N. Ho, and L. R. Pease. 1990. Gene splicing by overlap extension: tailor-made genes using the polymerase chain reaction. *Biotechniques* 8:528-535.

268. Fritsch, E. F., Sambrook, J., Maniatis, T. 1982. *Molecular Cloning: A Laboratory Manual*. Cold Spring Harbor Laboratory, Cold Spring Harbor.

269. Higgins, D. G., and P. M. Sharp. 1989. Fast and sensitive multiple sequence alignments on a microcomputer. *Comput.Appl.Biosci.* 5:151-153.

270. Jabri, B., N. P. de Serre, C. Cellier, K. Evans, C. Gache, C. Carvalho, J. F. Mougenot, M. Allez, R. Jian, P. Desreumaux, J. F. Colombel, C. Matuchansky, H. Cugnenc, M. Lopez-Botet, E. Vivier, A. Moretta, A. I. Roberts, E. C. Ebert, D. Guy-Grand, N. Brousse, J. Schmitz, and N. Cerf-Bensussan. 2000. Selective expansion of intraepithelial lymphocytes expressing the HLA-E-specific natural killer receptor CD94 in celiac disease. *Gastroenterology* 118:867-879.

271. Roberts, A. I., L. Lee, E. Schwarz, V. Groh, T. Spies, E. C. Ebert, and B. Jabri. 2001. NKG2D receptors induced by IL-15 costimulate CD28-negative effector CTL in the tissue microenvironment. *The Journal of Immunology* 167:5527-5530.

272. van de Wal, Y., N. Corazza, M. Allez, L. F. Mayer, H. Iijima, M. Ryan, S. Cornwall, D. Kaiserlian, R. Hershberg, Y. Koezuka, S. P. Colgan, and R. S. Blumberg. 2003. Delineation of a CD1d-restricted antigen presentation pathway

associated with human and mouse intestinal epithelial cells. *Gastroenterology* 124:1420-1431.

273. Kumanovics, A., T. Takada, and K. F. Lindahl. 2003. Genomic organization of the mammalian MHC. *Annu Rev Immunol* 21:629-657.

274. Radosavljevic, M., and S. Bahram. 2003. In vivo immunogenetics: from MIC to RAET1 loci. *Immunogenetics* 55:1-9.

275. Martin, L. H., F. Calabi, F. A. Lefebvre, C. A. Bilsland, and C. Milstein. 1987. Structure and expression of the human thymocyte antigens CD1a, CD1b, and CD1c. *Proc.Natl.Acad.Sci.U.S.A* 84:9189-9193.

276. Takada, T., A. Kumanovics, C. Amadou, M. Yoshino, E. P. Jones, M. Athanasiou, G. A. Evans, and K. Fischer Lindahl. 2003. Species-specific class I gene expansions formed the telomeric 1 mb of the mouse major histocompatibility complex. *Genome research* 13:589-600.

277. Tajima, A., T. Tanaka, T. Ebata, K. Takeda, A. Kawasaki, J. M. Kelly, P. K. Darcy, R. E. Vance, D. H. Raulet, K. Kinoshita, K. Okumura, M. J. Smyth, and H. Yagita. 2003. Blastocyst MHC, a putative murine homologue of HLA-G, protects TAP-deficient tumor cells from natural killer cell-mediated rejection in vivo. *J Immunol* 171:1715-1721.

278. Jensen, P. E., B. A. Sullivan, L. M. Reed-Loisel, and D. A. Weber. 2004. Qa-1, a nonclassical class I histocompatibility molecule with roles in innate and adaptive immunity. *Immunol Res* 29:81-92.

279. Nakayama, K., S. Tokito, C. Jaulin, C. Delarbre, P. Kourilsky, H. Nakauchi, and G. Gachelin. 1990. Comparative structure of two duplicated T1a class I genes (T10c and 37) of the murine H-2d MHC. Implications on the evolution of the T1a region. *The Journal of Immunology* 144:2400-2408.

280. Hermel, E., A. J. Hart, I. Gunduz, H. Acton, C. Kim, M. Wurth, S. Uddin, C. Smith, K. Fischer Lindahl, and C. J. Aldrich. 2004. Polymorphism and conservation of the genes encoding Qa1 molecules. *Immunogenetics* 56:639-649.

281. Cai, W., W. Cao, L. Wu, G. E. Exley, G. L. Waneck, B. L. Karger, and C. M. Warner. 1996. Sequence and transcription of Qa-2-encoding genes in mouse lymphocytes and blastocysts. *Immunogenetics* 45:97-107.

282. Tine, J. A., A. Walsh, D. Rathbun, L. Leonard, E. K. Wakeland, R. Dilwith, and L. Flaherty. 1990. Genetic polymorphisms of Q region genes from wild-derived mice: implications for Q region evolution. *Immunogenetics* 31:315-325.

283. Badley, J. E., and J. A. Frelinger. 1991. Expression of a MHC non-classical class I gene, Q4, is similar to a classical class I gene, Dp. *Eur J Immunogenet* 18:315-321.

284. Ito, K., L. Van Kaer, M. Bonneville, S. Hsu, D. B. Murphy, and S. Tonegawa. 1990. Recognition of the product of a novel MHC TL region gene (27b) by a mouse gamma delta T cell receptor. *Cell* 62:549-561.

285. Wang, C. R., B. E. Loveland, and K. F. Lindahl. 1991. H-2M3 encodes the MHC class I molecule presenting the maternally transmitted antigen of the mouse. *Cell* 66:335-345.

286. Arepalli, S. R., E. P. Jones, T. K. Howcroft, I. Carlo, C. Wang, K. F. Lindahl, D. S. Singer, and S. Rudikoff. 1998. Characterization of two class I genes from the H2-M region: evidence for a new subfamily. *Immunogenetics* 47:264-271.

287. Cullen, M. K., L. A. Lapierre, K. V. Kesari, and J. Geliebter. 1993. Identification of a recombinogenic major histocompatibility complex Q gene with diverse alleles. *J Exp Med* 177:1803-1807.

288. Trowsdale, J., and P. Parham. 2004. Mini-review: defense strategies and immunity-related genes. *Eur J Immunol* 34:7-17.

289. Hill, A. V. 1998. The immunogenetics of human infectious diseases. *Annu.Rev.Immunol* 16:593-617.

290. Stroynowski, I. 1990. Molecules related to class-I major histocompatibility complex antigens. *Annu Rev Immunol* 8:501-530.

291. Salter, R. D., R. J. Benjamin, P. K. Wesley, S. E. Buxton, T. P. Garrett, C. Clayberger, A. M. Krensky, A. M. Norment, D. R. Littman, and P. Parham. 1990. A binding site for the T-cell co-receptor CD8 on the alpha 3 domain of HLA-A2. *Nature* 345:41-46.

292. Arnaiz-Villena, A., J. Martinez-Laso, M. J. Castro, P. Morales, J. Moscoso, P. Varela, E. Gomez-Casado, and L. M. Allende. 2001. The evolution of the MHC-G gene does not support a functional role for the complete protein. *Immunological reviews* 183:65-75.

293. Ulbrecht, M., S. Maier, V. Hofmeister, C. S. Falk, A. G. Brooks, M. T. McMaster, and E. H. Weiss. 2004. Truncated HLA-G isoforms are retained in the endoplasmic reticulum and insufficiently provide HLA-E ligands. *Human immunology* 65:200-208.

294. Maquat, L. E. 2004. Nonsense-mediated mRNA decay: splicing, translation and mRNP dynamics. *Nat Rev Mol Cell Biol* 5:89-99.

295. Wang, J., Y. F. Chang, J. I. Hamilton, and M. F. Wilkinson. 2002. Nonsense-associated altered splicing: a frame-dependent response distinct from nonsense-mediated decay. *Mol.Cell* 10:951-957.

296. Lizee, G., G. Basha, J. Tiong, J. P. Julien, M. Tian, K. E. Biron, and W. A. Jefferies. 2003. Control of dendritic cell cross-presentation by the major histocompatibility complex class I cytoplasmic domain. *Nature immunology* 4:1065-1073.

297. Hauschka, T. S., Mirand, E. A. 1973. The "Breeder:Ha-(ICR)" Swiss mouse, a multipurpose stock selected for fecundity. In *Perspectives in Cancer Research and Treatment*. G. P. Murphy, ed. Liss, New York. 319-331.

298. Grossberger, D., and P. Parham. 1992. Reptilian class I major histocompatibility complex genes reveal conserved elements in class I structure. *Immunogenetics* 36:166-174.

299. Rammensee, H. G., K. Falk, and O. Rotzschke. 1993. Peptides naturally presented by MHC class I molecules. *Annu.Rev.Immunol* 11:213-244.

300. Madden, D. R., J. C. Gorga, J. L. Strominger, and D. C. Wiley. 1992. The three-dimensional structure of HLA-B27 at 2.1 A resolution suggests a general mechanism for tight peptide binding to MHC. *Cell* 70:1035-1048.

301. Musolf, K., Y. Meyer-Lucht, and S. Sommer. 2004. Evolution of MHC-DRB class II polymorphism in the genus Apodemus and a comparison of DRB sequences within the family Muridae (Mammalia: Rodentia). *Immunogenetics* 56:420-426.

302. Mottonen, J., A. Strand, J. Symersky, R. M. Sweet, D. E. Danley, K. F. Geoghegan, R. D. Gerard, and E. J. Goldsmith. 1992. Structural basis of latency in plasminogen activator inhibitor-1. *Nature* 355:270-273.

303. Zou, Y., and P. Stastny. 2002. Alternatively spliced forms of MICA and MICB lacking exon 3 in a human cell line and evidence of presence of similar RNA in human peripheral blood mononuclear cells. *Immunogenetics* 54:671-674.

304. Riegert, P., V. Wanner, and S. Bahram. 1998. Genomics, isoforms, expression, and phylogeny of the MHC class I-related MR1 gene. *J Immunol* 161:4066-4077.

305. Llano, M., N. Lee, F. Navarro, P. Garcia, J. P. Albar, D. E. Geraghty, and M. Lopez-Botet. 1998. HLA-E-bound peptides influence recognition by inhibitory and triggering CD94/NKG2 receptors: preferential response to an HLA-G-derived nonamer. *Eur.J Immunol* 28:2854-2863.

306. Reik, W., W. Dean, and J. Walter. 2001. Epigenetic reprogramming in mammalian development. *Science* 293:1089-1093.

307. Takai, D., and P. A. Jones. 2002. Comprehensive analysis of CpG islands in human chromosomes 21 and 22. *Proc Natl Acad Sci U S A* 99:3740-3745.

308. Steinle, A., V. Groh, and T. Spies. 1998. Diversification, expression, and gamma delta T cell recognition of evolutionarily distant members of the MIC family of major histocompatibility complex class I-related molecules. *Proc Natl Acad Sci U S A* 95:12510-12515.

309. Apps, R., L. Gardner, and A. Moffett. 2008. A critical look at HLA-G. *Trends Immunol* 29:313-321.

310. Philpott, K. L., S. Rastan, S. Brown, and A. L. Mellor. 1988. Expression of H-2 class I genes in murine extra-embryonic tissues. *Immunology* 64:479-485.

311. Chianale, J., V. Vollrath, A. M. Wielandt, S. Miranda, R. Gonzalez, A. M. Fresno, C. Quintana, S. Gonzalez, L. Andrade, and S. Guzman. 1995. Differences between nuclear run-off and mRNA levels for multidrug resistance gene expression in the cephalocaudal axis of the mouse intestine. *Biochim Biophys Acta* 1264:369-376.

312. Sweetser, D. A., E. H. Birkenmeier, P. C. Hoppe, D. W. McKeel, and J. I. Gordon. 1988. Mechanisms underlying generation of gradients in gene expression within the intestine: an analysis using transgenic mice containing fatty acid binding protein-human growth hormone fusion genes. *Genes Dev* 2:1318-1332.

313. Hadley, G. A., S. T. Bartlett, C. S. Via, E. A. Rostapshova, and S. Moainie. 1997. The epithelial cell-specific integrin, CD103 (alpha E integrin), defines a novel subset of alloreactive CD8+ CTL. *J Immunol* 159:3748-3756.

314. Hooper, L. V., M. H. Wong, A. Thelin, L. Hansson, P. G. Falk, and J. I. Gordon. 2001. Molecular analysis of commensal host-microbial relationships in the intestine. *Science* 291:881-884.

315. Knight, P. A., A. D. Pemberton, K. A. Robertson, D. J. Roy, S. H. Wright, and H. R. Miller. 2004. Expression profiling reveals novel innate and inflammatory responses in the jejunal epithelial compartment during infection with Trichinella spiralis. *Infection and immunity* 72:6076-6086.

316. Morello, D., P. Duprey, A. Israel, and C. Babinet. 1985. Asynchronous regulation of mouse H-2D and beta-2 microglobulin RNA transcripts. *Immunogenetics* 22:441-452.

317. Korber, B., N. Mermod, L. Hood, and I. Stroynowski. 1988. Regulation of gene expression by interferons: control of H-2 promoter responses. *Science* 239:1302-1306.

318. Singer, D. S., and J. E. Maguire. 1990. Regulation of the expression of class I MHC genes. *Crit Rev Immunol* 10:235-257.

319. Tatake, R. J., and R. A. Zeff. 1993. Regulated expression of the major histocompatibility complex class I genes. *Proc Soc Exp Biol Med* 203:405-417.

320. Ting, J. P., and A. S. Baldwin. 1993. Regulation of MHC gene expression. *Current opinion in immunology* 5:8-16.

321. Howcroft, T. K., and D. S. Singer. 2003. Expression of nonclassical MHC class Ib genes: comparison of regulatory elements. *Immunol Res* 27:1-30.

322. Kimura, A., A. Israel, O. Le Bail, and P. Kourilsky. 1986. Detailed analysis of the mouse H-2Kb promoter: enhancer-like sequences and their role in the regulation of class I gene expression. *Cell* 44:261-272.

323. Gobin, S. J., A. Peijnenburg, V. Keijsers, and P. J. van den Elsen. 1997. Site alpha is crucial for two routes of IFN gamma-induced MHC class I transactivation: the ISRE-mediated route and a novel pathway involving CIITA. *Immunity* 6:601-611.

324. Martin, B. K., K. C. Chin, J. C. Olsen, C. A. Skinner, A. Dey, K. Ozato, and J. P. Ting. 1997. Induction of MHC class I expression by the MHC class II transactivator CIITA. *Immunity* 6:591-600.

325. Thompson, J. D., D. G. Higgins, and T. J. Gibson. 1994. CLUSTAL W: improving the sensitivity of progressive multiple sequence alignment through sequence weighting, position-specific gap penalties and weight matrix choice. *Nucleic acids research* 22:4673-4680.

326. Grabe, N. 2002. AliBaba2: context specific identification of transcription factor binding sites. *In Silico Biol* 2:S1-15.

327. Howcroft, T. K., L. A. Palmer, J. Brown, B. Rellahan, F. Kashanchi, J. N. Brady, and D. S. Singer. 1995. HIV Tat represses transcription through Sp1-like elements in the basal promoter. *Immunity* 3:127-138.

328. Zenzie-Gregory, B., A. Khachi, I. P. Garraway, and S. T. Smale. 1993. Mechanism of initiator-mediated transcription: evidence for a functional interaction between the TATA-binding protein and DNA in the absence of a specific recognition sequence. *Molecular and cellular biology* 13:3841-3849.

329. Wiley, S. R., R. J. Kraus, and J. E. Mertz. 1992. Functional binding of the "TATA" box binding component of transcription factor TFIID to the -30 region of TATA-less promoters. *Proc Natl Acad Sci U S A* 89:5814-5818.

330. Giuliani, C., M. Saji, G. Napolitano, L. A. Palmer, S. I. Taniguchi, M. Shong, D. S. Singer, and L. D. Kohn. 1995. Hormonal modulation of major histocompatibility complex class I gene expression involves an enhancer A-binding complex consisting of Fra-2 and the p50 subunit of NF-kappa B. *The Journal of biological chemistry* 270:11453-11462.

331. Soong, T. W., and K. M. Hui. 1992. Locus-specific transcriptional control of HLA genes. *J Immunol* 149:2008-2020.

332. Lee, Y. L., K. F. Lee, J. S. Xu, K. L. Kwok, J. M. Luk, W. M. Lee, and W. S. Yeung. 2003. Embryotrophic factor-3 from human oviductal cells affects the messenger RNA expression of mouse blastocyst. *Biology of reproduction* 68:375-382.

333. Vlaeminck-Guillem, V., S. Carrere, F. Dewitte, D. Stehelin, X. Desbiens, and M. Duterque-Coquillaud. 2000. The Ets family member Erg gene is expressed in mesodermal tissues and neural crests at fundamental steps during mouse embryogenesis. *Mech Dev* 91:331-335.

334. Cohn, S. M., T. C. Simon, K. A. Roth, E. H. Birkenmeier, and J. I. Gordon. 1992. Use of transgenic mice to map cis-acting elements in the intestinal fatty acid binding protein gene (Fabpi) that control its cell lineage-specific and regional patterns of expression along the duodenal-colonic and crypt-villus axes of the gut epithelium. *J Cell Biol* 119:27-44.

335. Rottman, J. N., and J. I. Gordon. 1993. Comparison of the patterns of expression of rat intestinal fatty acid binding protein/human growth hormone fusion genes in cultured intestinal epithelial cell lines and in the gut epithelium of transgenic mice. *The Journal of biological chemistry* 268:11994-12002.

336. Bagheri-Fam, S., F. Barrionuevo, U. Dohrmann, T. Gunther, R. Schule, R. Kemler, M. Mallo, B. Kanzler, and G. Scherer. 2006. Long-range upstream and downstream enhancers control distinct subsets of the complex spatiotemporal Sox9 expression pattern. *Developmental biology* 291:382-397.

337. Schewe, D. M., J. H. Leupold, D. D. Boyd, E. R. Lengyel, H. Wang, K. U. Gruetzner, F. W. Schildberg, K. W. Jauch, and H. Allgayer. 2003. Tumor-specific transcription factor binding to an activator protein-2/Sp1 element of the urokinase-type plasminogen activator receptor promoter in a first large series of resected gastrointestinal cancers. *Clin Cancer Res* 9:2267-2276.

338. Molkentin, J. D. 2000. The zinc finger-containing transcription factors GATA-4, -5, and -6. Ubiquitously expressed regulators of tissue-specific gene expression. *The Journal of biological chemistry* 275:38949-38952.

339. Jacobsen, C. M., N. Narita, M. Bielinska, A. J. Syder, J. I. Gordon, and D. B. Wilson. 2002. Genetic mosaic analysis reveals that GATA-4 is required for proper differentiation of mouse gastric epithelium. *Developmental biology* 241:34-46.

340. Renaud, J. P., J. M. Harris, M. Downes, L. J. Burke, and G. E. Muscat. 2000. Structure-function analysis of the Rev-erbA and RVR ligand-binding domains reveals a large hydrophobic surface that mediates corepressor binding and a ligand cavity occupied by side chains. *Mol Endocrinol* 14:700-717.

341. Dakic, A., L. Wu, and S. L. Nutt. 2007. Is PU.1 a dosage-sensitive regulator of haemopoietic lineage commitment and leukaemogenesis? *Trends Immunol* 28:108-114.

342. Li, H., G. S. Watts, M. M. Oshiro, B. W. Futscher, and F. E. Domann. 2006. AP-2alpha and AP-2gamma are transcriptional targets of p53 in human breast carcinoma cells. *Oncogene* 25:5405-5415.

343. Schuster, M. B., and B. T. Porse. 2006. C/EBPalpha: a tumour suppressor in multiple tissues? *Biochim Biophys Acta* 1766:88-103.

344. Cassel, T. N., and M. Nord. 2003. C/EBP transcription factors in the lung epithelium. *Am J Physiol Lung Cell Mol Physiol* 285:L773-781.

345. Singer, D. S., E. Mozes, S. Kirshner, and L. D. Kohn. 1997. Role of MHC class I molecules in autoimmune disease. *Crit Rev Immunol* 17:463-468.

346. Saji, M., J. Moriarty, T. Ban, L. D. Kohn, and D. S. Singer. 1992. Hormonal regulation of major histocompatibility complex class I genes in rat thyroid FRTL-5 cells: thyroid-stimulating hormone induces a cAMP-mediated decrease in class I expression. *Proc Natl Acad Sci U S A* 89:1944-1948.

347. Pfaffl, M. W., I. G. Lange, and H. H. Meyer. 2003. The gastrointestinal tract as target of steroid hormone action: quantification of steroid receptor mRNA expression (AR, ERalpha, ERbeta and PR) in 10 bovine gastrointestinal tract compartments by kinetic RT-PCR. *J Steroid Biochem Mol Biol* 84:159-166.

348. Yang, Z., and M. L. Privalsky. 2001. Isoform-specific transcriptional regulation by thyroid hormone receptors: hormone-independent activation operates through a steroid receptor mode of co-activator interaction. *Mol Endocrinol* 15:1170-1185.

349. Niederreither, K., and P. Dolle. 2008. Retinoic acid in development: towards an integrated view. *Nature reviews* 9:541-553.

350. Van Kaer, L., M. Wu, Y. Ichikawa, K. Ito, M. Bonneville, S. Ostrand-Rosenberg, D. B. Murphy, and S. Tonegawa. 1991. Recognition of MHC TL gene products by gamma delta T cells. *Immunological reviews* 120:89-115.

351. Attinger, A., L. Devine, Y. Wang-Zhu, D. Martin, J. H. Wang, E. L. Reinherz, M. Kronenberg, H. Cheroutre, and P. Kavathas. 2005. Molecular basis for the high affinity interaction between the thymic leukemia antigen and the CD8alphaalpha molecule. *J Immunol* 174:3501-3507.

352. Liu, Y., Y. Xiong, O. V. Naidenko, J. H. Liu, R. Zhang, A. Joachimiak, M. Kronenberg, H. Cheroutre, E. L. Reinherz, and J. H. Wang. 2003. The crystal structure of a TL/CD8alphaalpha complex at 2.1 A resolution: implications for modulation of T cell activation and memory. *Immunity* 18:205-215.

353. Pamer, E. G., C. R. Wang, L. Flaherty, K. F. Lindahl, and M. J. Bevan. 1992. H-2M3 presents a Listeria monocytogenes peptide to cytotoxic T lymphocytes. *Cell* 70:215-223.

354. Chiang, E. Y., and I. Stroynowski. 2004. A nonclassical MHC class I molecule restricts CTL-mediated rejection of a syngeneic melanoma tumor. *J Immunol* 173:4394-4401.

355. Swanson, P. A., 2nd, C. D. Pack, A. Hadley, C. R. Wang, I. Stroynowski, P. E. Jensen, and A. E. Lukacher. 2008. An MHC class Ib-restricted CD8 T cell response confers antiviral immunity. *J Exp Med* 205:1647-1657.

356. Ponda, P. P., and L. Mayer. 2005. Mucosal epithelium in health and disease. *Curr Mol Med* 5:549-556.

357. Robinson, P. J., P. J. Travers, A. Stackpoole, L. Flaherty, and H. Djaballah. 1998. Maturation of Qa-1b class I molecules requires beta 2-microglobulin but is TAP independent. *J Immunol* 160:3217-3224.

358. Chun, T., C. J. Aldrich, M. E. Baldeon, L. V. Kawczynski, M. J. Soloski, and H. R. Gaskins. 1998. Constitutive and regulated expression of the class IB molecule Qa-1 in pancreatic beta cells. *Immunology* 94:64-71.

359. Chiang, E. Y., M. Henson, and I. Stroynowski. 2003. Correction of defects responsible for impaired Qa-2 class Ib MHC expression on melanoma cells protects mice from tumor growth. *J Immunol* 170:4515-4523.

360. Lowen, L. C., C. J. Aldrich, and J. Forman. 1993. Analysis of T cell receptors specific for recognition of class IB antigens. *J Immunol* 151:6155-6165.

361. Aldrich, C. J., J. R. Rodgers, and R. R. Rich. 1988. Regulation of Qa-1 expression and determinant modification by an H-2D-linked gene, Qdm. *Immunogenetics* 28:334-344.

362. Toyama-Sorimachi, N., Y. Taguchi, H. Yagita, F. Kitamura, A. Kawasaki, S. Koyasu, and H. Karasuyama. 2001. Mouse CD94 participates in Qa-1-mediated self recognition by NK cells and delivers inhibitory signals independent of Ly-49. *J Immunol* 166:3771-3779.

363. Michaelsson, J., C. Teixeira de Matos, A. Achour, L. L. Lanier, K. Karre, and K. Soderstrom. 2002. A signal peptide derived from hsp60 binds HLA-E and interferes with CD94/NKG2A recognition. *J Exp Med* 196:1403-1414.

364. Bouvier, M., and D. C. Wiley. 1994. Importance of peptide amino and carboxyl termini to the stability of MHC class I molecules. *Science* 265:398-402.

365. Weintraub, B. C., M. R. Jackson, and S. M. Hedrick. 1994. Gamma delta T cells can recognize nonclassical MHC in the absence of conventional antigenic peptides. *J Immunol* 153:3051-3058.

366. Roy, K. C., I. Maricic, A. Khurana, T. R. Smith, R. C. Halder, and V. Kumar. 2008. Involvement of secretory and endosomal compartments in presentation of an exogenous self-glycolipid to type II NKT cells. *J Immunol* 180:2942-2950.

367. Groh, V., S. Bahram, S. Bauer, A. Herman, M. Beauchamp, and T. Spies. 1996. Cell stress-regulated human major histocompatibility complex class I gene expressed in gastrointestinal epithelium. *Proc Natl Acad Sci U S A* 93:12445-12450.

368. Whitman, M. C., J. Strohmaier, K. O'Boyle, J. M. Tingem, Y. Wilkinson, J. Goldstein, T. Chen, K. Brorson, M. Brunswick, and S. Kozlowski. 2000. The isolated major histocompatibility complex class I alpha3 domain binds beta2m and CD8alphaalpha dimers. *Mol Immunol* 37:141-149.

369. Dong, L., Q. Ma, and J. P. Whitlock, Jr. 1997. Down-regulation of major histocompatibility complex Q1b gene expression by 2,3,7,8-tetrachlorodibenzo-p-dioxin. *J Biol.Chem.* 272:29614-29619.

370. Tsujimura, K., Y. Obata, S. Iwase, Y. Matsudaira, S. Ozeki, and T. Takahashi. 2000. The epitope detected by cytotoxic T lymphocytes against thymus leukemia (TL) antigen is TAP independent. *Int Immunol* 12:1217-1225.

371. Rodgers, J. R., V. Mehta, and R. G. Cook. 1995. Surface expression of beta 2-microglobulin-associated thymus-leukemia antigen is independent of TAP2. *Eur J Immunol* 25:1001-1007.

372. Kress, M., D. Cosman, G. Khoury, and G. Jay. 1983. Secretion of a transplantation-related antigen. *Cell* 34:189-196.

373. Rock, K. L., S. Gamble, L. Rothstein, and B. Benacerraf. 1991. Reassociation with beta 2-microglobulin is necessary for Db class I major histocompatibility complex binding of an exogenous influenza peptide. *Proc Natl Acad Sci U S A* 88:301-304.

374. Voldby Larsen, M., M. Nielsen, A. Weinzierl, and O. Lund. 2006. TAP-Independent MHC Class I Presentation. *Curr Immunol Rev* 2:233-245.

375. Myers, N. B., E. Wormstall, and T. H. Hansen. 1996. Differences among various class I molecules in competition for beta2m in vivo. *Immunogenetics* 43:384-387.

376. Tanaka, T., T. Ebata, A. Tajima, K. Kinoshita, K. Okumura, and H. Yagita. 2005. Beta2-microglobulin required for cell surface expression of blastocyst MHC. *Biochemical and biophysical research communications* 332:311-317.

377. Wilson, M. D., J. Cheung, D. W. Martindale, S. W. Scherer, and B. F. Koop. 2006. Comparative analysis of the paired immunoglobulin-like receptor (PILR) locus in six mammalian genomes: duplication, conversion, and the birth of new genes. *Physiol Genomics* 27:201-218.

378. Bix, M., and D. Raulet. 1992. Functionally conformed free class I heavy chains exist on the surface of beta 2 microglobulin negative cells. *J Exp Med* 176:829-834.

379. Shiroishi, M., K. Kuroki, L. Rasubala, K. Tsumoto, I. Kumagai, E. Kurimoto, K. Kato, D. Kohda, and K. Maenaka. 2006. Structural basis for recognition of the nonclassical MHC molecule HLA-G by the leukocyte Ig-like receptor B2 (LILRB2/LIR2/ILT4/CD85d). *Proc Natl Acad Sci U S A* 103:16412-16417.

380. Cook, J. R., N. B. Myers, and T. H. Hansen. 1998. Peptide ligand structure influences the exchange of beta2-microglobulin by cell surface Kb. *Mol Immunol* 35:929-934.

381. Cao, W., X. Xi, Z. Wang, L. Dong, Z. Hao, L. Cui, C. Ma, and W. He. 2008. Four novel ULBP splice variants are ligands for human NKG2D. *Int Immunol* 20:981-991.

382. O'Callaghan, C. A., A. Cerwenka, B. E. Willcox, L. L. Lanier, and P. J. Bjorkman. 2001. Molecular competition for NKG2D: H60 and RAE1 compete unequally for NKG2D with dominance of H60. *Immunity* 15:201-211.

383. Bui, J. D., L. N. Carayannopoulos, L. L. Lanier, W. M. Yokoyama, and R. D. Schreiber. 2006. IFN-dependent down-regulation of the NKG2D ligand H60 on tumors. *J Immunol* 176:905-913.

384. Kawachi, I., J. Maldonado, C. Strader, and S. Gilfillan. 2006. MR1-Restricted V{alpha}19i Mucosal-Associated Invariant T Cells Are Innate T Cells in the Gut Lamina Propria That Provide a Rapid and Diverse Cytokine Response. *J. Immunol.* 176:1618-1627.

385. Williams, M. A., and M. J. Bevan. 2005. Cutting edge: a single MHC class Ia is sufficient for CD8 memory T cell differentiation. *J Immunol* 175:2066-2069.